ELECTRICAL TRANSMISSION LINE

Dr. G. Ezhilarasan
Harsh shrivastava

ALEXIS PRESS
JERSEY CITY, USA

ELECTRICAL TRANSMISSION LINE

ELECTRICAL TRANSMISSION LINE

Dr. G. Ezhilarasan

Harsh Shrivastava

ALEXIS PRESS

ALEXIS PRESS

Published by: Alexis Press, LLC, Jersey City, USA
www.alexispress.us

© RESERVED

This book contains information obtained from highly regarded resources.
Copyright for individual contents remains with the authors.
A wide variety of references are listed. Reasonable efforts have been made
to publish reliable data and information, but the author and the publisher
cannot assume responsibility for the validity of
all materials or for the consequences of their use.

No part of this book may be reprinted, reproduced, transmitted,
or utilized in any form by any electronic, mechanical, or other means,
now known or hereinafter invented, including photocopying,
microfilming and recording, or any information storage or retrieval system,
without permission from the publishers.

For permission to photocopy or use material electronically
from this work please access alexispress.us

First Published 2022

A catalogue record for this publication is available from the British Library

Library of Congress Cataloguing in Publication Data

Includes bibliographical references and index.

Electrical Transmission Line by *Dr. G. Ezhilarasan, Harsh Shrivastava*

ISBN 978-1-64532-885-8

CONTENTS

CHAPTER 1

INTRODUCTION TO ELECTRICAL TRANSMISSION LINE

Dr. G. Ezhilarasan, Professor
Faculty of Engineering and Technology, JAIN (Deemed-to-be University), Bengaluru, Karnataka, India
Email id- g.ezhilarasan@jainuniversity.ac.in

A conductor is a material used to physically transport electrical energy from one location to another. It is a crucial part of the underground and overhead electrical transmission and distribution networks. The cost and efficiency affect the conductor of choice. A perfect conductor possesses the qualities listed below.

1. Maximum conductivity is present.
2. It has a strong tensile capacity.
3. It has the lowest specific gravity, or the ratio of weight to volume.
4. Without compromising other aspects, it is least expensive.

Conductor Types:

Early transmission lines often utilized copper conductors, but aluminum conductors have totally replaced copper due to their much cheaper cost and lighter weight when compared to copper conductors of the same resistance. Another benefit is that Aluminum conductors have bigger diameters than Copper conductors with the same resistance. With a bigger diameter, the conductor's surface will have lines of electric flux that are further apart for the same voltage. This results in a smaller voltage gradient at the conductor surface and a decreased propensity to ionize the surrounding atmosphere. Corona is an unfavorable byproduct of ionization[1], [2].

The following are the symbols used to distinguish between several kinds of aluminum conductors:

1. Al Aluminum Conductors (AAC).
2. AAC: Conductors made entirely of aluminum alloy.
3. Aluminum Conductors with Steel Reinforcement ACAR: Alloy-Reinforced Aluminum Conductor

Aluminum alloy conductors have a greater tensile strength than EC grade aluminum conductors or AAC. ACSR has an aluminum core that is encircled by steel strands on both sides. A layer of electrical-conductor-grade aluminum surrounds a core of greater strength aluminum alloy in the ACAR.

ACSR (Aluminum Conductor Steel Reinforced) Aluminum Conductor Steel Reinforced (ACSR) is indeed a concentrically stranded conductor made of a core of galvanized steel wire and one or even more layers comprising hard drawn 1350-H19 aluminum wire. Depending upon the size, the core might be either a single wire or a stranded wire. Additional corrosion protection is offered by applying grease to the core or infusing the whole cable with grease.

Steel wire core was available in Class A, B, or Class C galvanization providing corrosion protection. Depending on the mechanical strength and current carrying capacity required by each application, the percentage of steel and aluminum in an ACSR conductor may be chosen[3], [4].

ACSR conductors have a reputation for being economical, dependable, and having a good strength-to-weight ratio. Aluminum's low weight and superior conductivity are combined with steel's high tensile strength and toughness to create ACSR conductors. Compared to most other forms of overhead conductors, this may provide greater span lengths, lower sag, and higher tensions in line designs.

The addition of the steel strands serves as mechanical reinforcement. ACSR conductors have a reputation for being economical, dependable, and having a good strength-to-weight ratio. ACSR conductors combine the strong tensile strength and durability of steel with the light weight and superior conductivity of aluminum. Compared to most other forms of overhead conductors, this may provide greater span lengths, lower sag, and higher tensions in line designs. The addition of the steel strands serves as mechanical reinforcement. The cross sections up above show some typical stranding. Galvanizing helps to prevent corrosion on steel core wires. For most situations, the typical Class A zinc coating is generally sufficient.

Class B and C galvanized coatings may well be requested for increased protection. The core steel component of the product might have a conductor corrosion resistant inhibitor compound put to it. High tensile strength and better sag qualities are characteristics. Economical design; suited for long-distance distant applications; good amplifying capacity; and good thermal characteristics Low sag, high tensile strength, and high strength to weight[5], [6].

Common Application

Compact Aluminum Conductors, Steel Reinforced (ACSR) are often used for overhead distribution and transmission lines, as well as both transmission and distribution circuits.

Bundled Conductors: There are benefits and drawbacks to using bundle conductors in transmission lines. A bundle conductor is a conductor made up of numerous linked conductor cables. Additionally, bundle conductors will enhance the amount of current carried by the transmission line. Transmission lines have a significant wind load compared to other conductors, which is their principal drawback. Conductor bundle is the arrangement of more than one conductor per phase running in parallel and appropriately distanced from one another as it is used in overhead transmission lines. Sub-conductor is the term used to describe a single conductor inside a bundle. If the circuit only has one wire per phase, the corona at Extra High Voltage (EHV), or voltage exceeding 220 KV, with its ensuing power loss and notably its interference with communication, is considerable. Having two or more conductors per phase close together reduces the High-Voltage Gradient at the conductor inside the EHV region significantly when compared to India's standard of conductor-bundle separation of 450 mm.

The conductors of a three-conductor bundle are often located there at vertices of such an equilateral triangle, whereas those of a four-conductor bundle are typically located at the corners of a square. Unless the conductors inside the bundle are switched around, the current will not split perfectly between them, but this difference has no practical significance. The second key benefit of bundling is less reactance. The effects of corona and reactance are lessened and the reactance is increased by adding more conductors to a bundle. The bundle's higher Geometric Mean Radius (GMR) causes a decrease in reactance[7], [8].

Lines of transmission:

The requirements for the conductors and the geometric configurations of the conductors allow for the determination of the electric parameters of transmission lines (i.e., resistance, inductance, and capacitance).

Transmission Line Resistance

Resistance to D.C. current is given by,

$$R_{dc} = \rho \frac{\ell}{A}$$

Where p is the resistivity at 20° C

e is the length of the conductor A is the cross-sectional area of the conductor

Because of skin effect, the D.C. resistance is different from ac resistance. The ac resistance is referred to as effective resistance, and is found from power loss in the conductor.

$$R = \frac{\text{power loss}}{I^2}$$

The variation of resistance with temperature is linear over the normal temperature range in Figure 1.1.

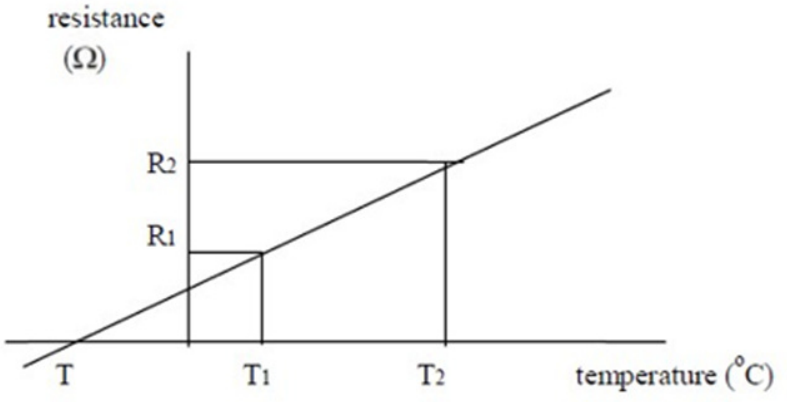

Figure 1.1: ***Illustrates*** **the Graph of Resistance vs Temperature.**

$$\frac{(R_1 - 0)}{(T_1 - T)} = \frac{(R_2 - 0)}{(T_2 - T)}$$

$$R_2 = \frac{T_2 - T}{T_1 - T} R_1$$

Inductive Reactance of a Transmission Line

Transmission lines' inductance is determined per phase. It is made up of the phase conductor's self-inductance and inductances between the electrodes. It comes from:

$$L = 2\times10^{-7} \ln \frac{GMD}{GMR} \quad [H/m]$$

GMR stands for geometric mean radius, which may be found in manufacturer's tables. The geometric mean distance (GMD) (must be calculated for each line configuration)

Radius Geometric Mean: There are magnetic flux lines both within and outside the conductor. GMR is a fictitious radius that, in order to maintain the inductor's self-inductance, substitutes a hollow conductor with a radius equal to GMR for the real conductor. If each phase contains many conductors, the GMR is calculated as follows:

$$GMR = \sqrt[n^2]{(d_{11}d_{12}d_{13}....d_{1n}).(d_{21}.d_{22}....d_{2n})......(d_{n1}.d_{n2}..... \ d_{nn})}$$

D11-GMR1,

d22=GMR2,

Dnn-GMRn

Recall that GMR = r.e -1/4 for a solid conductor, where r is the conductor's radius.

In order to maintain the same mutual inductance of the arrangement, geometric mean distance substitutes a hypothetical mean distance for the real arrangement of conductors,

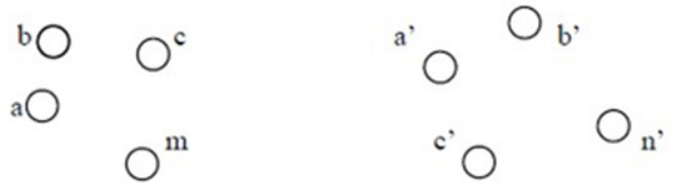

$$GMD = \sqrt[mn]{(D_{aa'}D_{ab'}...D_{an'}).(D_{ba'}D_{bb'}...D_{bn'}).....(D_{ma'}D_{mb'}..... \ D_{mn'})}$$

Two single-phase conductors have an inductance between them:

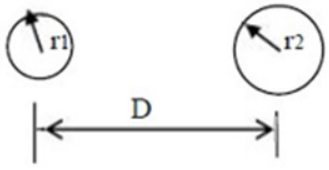

$$L_1 = 2\times10^{-7} \times \ln \frac{D}{r_1'} \qquad L_2 = 2\times10^{-7} \times \ln \frac{D}{r_2'}$$

Where ri' is the conductor's GMR. 1 12' is the conductor's GMR.

The GMD between the conductors is 2 D.

Consequently, the line's overall inductance,

$$L_T = L_1 + L_2 = 2\times10^{-7}\times\left[\ln\frac{D}{r_1'}+\ln\frac{D}{r_2'}\right] = 2\times10^{-7}\times\ln\frac{D^2}{r_1'r_2'} = 2\times10^{-7}\times2\times\frac{1}{2}\times\ln\frac{D^2}{r_1'r_2'}$$

$$L_T = 4\times10^{-7}\times\ln\left[\frac{D^2}{r_1'r_2'}\right]^{1/2} = 4\times10^{-7}\times\ln\frac{D}{\sqrt{r_1'r_2'}}$$

If $r_1 = r_2$, then

$$L_T = 4\times10^{-7}\times\ln\frac{D}{r_1'}$$

Find the GMD, GMR, inductance, and total inductance per metre for two circuits that are connected in parallel, for instance. Three conductors with a radius of 0.25 cm make up one circuit. Two conductors with a 0.5 cm radius make up the second circuit,

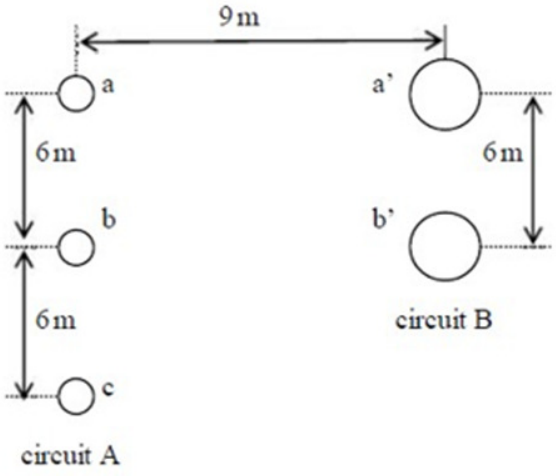

Solution:

m = 3, n' = 2, ∴ m·n' = 6

$$GMD = \sqrt[6]{D_{aa'}D_{ab'}D_{ba'}B_{bb'}D_{ca'}D_{cb'}}$$

Where

=Dbb = 9 m

Dab =Dba = Deb' = √62 +9² = √117 m

Dea√√122 + = 15 m

GMD 10.743 m

Geometric Mean Radius for Circuit A:

$$GMR_A = \sqrt[3^2]{D_{aa}D_{ab}D_{ac}D_{ba}D_{bb}D_{bc}D_{ca}D_{cb}D_{cc}} = \sqrt[9]{\left(0.25\times10^{-2}\times e^{-1/4}\right)^3\times6^4\times12^2} = 0.481\text{m}$$

Geometric Mean Radius for Circuit B:

$$GMR_B = \sqrt[2^2]{D_{a'a'}D_{a'b'}D_{b'b'}D_{b'a'}} = \sqrt[4]{\left(0.5\times10^{-2}\times e^{-1/4}\right)^2\times6^2} = 0.153\text{m}$$

Inductance of circuit A,

$$L_A = 2\times10^{-7}\ln\frac{GMD}{GMR_A} = 2\times10^{-7}\ln\frac{10.743}{0.481} = 6.212\times10^{-7}$$

Inductance of circuit B:

$$L_B = 2\times10^{-7}\ln\frac{GMD}{GMR_B} = 2\times10^{-7}\ln\frac{10.743}{0153} = 8.503\times10^{-7}\quad H/m$$

The total inductance is then

$$L_T = L_A + L_B = 14.715\times10^{-7}\quad H/m$$

Utilizing Tables

Since American manufacturers often provide the cables for power transmission lines, the tables of cable characteristics use the American Standard System of units and provide the inductive reactance in miles.

$$X_L = 2\pi fL = 2\pi f\times2\times10^{-7}\ln\frac{GMD}{GMR}\quad \Omega/m$$

$$X_L = 4\pi f\times10^{-7}\ln\frac{GMD}{GMR}\quad \Omega/m$$

$$X_L = 4\pi f\times10^{-7}\times1609\times\ln\frac{GMD}{GMR}\quad \Omega/\text{mile}$$

$$X_L = 2.022\times10^{-3}\times f\times\ln\frac{GMD}{GMR}\quad \Omega/\text{mile}$$

$$X_L = \underbrace{2.022\times10^{-3}\times f\times\ln\frac{1}{GMR}}_{X_a} + \underbrace{2.022\times10^{-3}\times f\times\ln GMD}_{X_d}\quad \Omega/\text{mile}$$

The inductive reactance at a 1 foot spacing is represented by Xa, and the inductive reactance spacing factor is known as Xd if both GMR and GMD are expressed in feet. Example: Find the single phase, 60 Hz line's inductive reactance per mile. Partridge conductor is used, with conductor centres spaced 20 feet apart.

Thermal Limits and Transmission Line Losses

A transmission line's resistance value directly relates to how much power it loses. The kind and length of the conductor affect the resistance's value. The electricity being provided by the transmission line determines the current in the line.

$$P_R = E_R I_{equiv} \cos\Phi_R \qquad \therefore \qquad I_{equiv} = \frac{P_R}{E_R \cos\Phi_R}$$

From that,

$$P_{loss} = I_{equiv}^2 R = \left(\frac{P_R}{E_R \cos\Phi_R}\right)^2 R$$

Power utilities often work to keep the voltage at the other end consistent. The load attached to the transmission line controls the amount of electricity provided by the line, and the load alone cannot be adjusted. The power factor is the sole variable that can be controlled in the equation above. Power losses will be at their lowest if the power factor can be changed to equal 1. The transmission line's effectiveness is determined by:

$$\eta_{\%} = \frac{P_R}{P_S} \cdot 100\%$$

The material used for conductor insulation affects the thermal limits for both equipment and conductors. Heat is produced by the I2R losses. The conductors and the insulator around them get hotter due to the heat. While certain machinery may be cooled by adding cooling material to the circulation system, other equipment must rely on natural cooling. The insulation will degrade more quickly if the temperature is greater than the recommended value, and at higher temperatures, more rapid damage will happen. As the load increases, the power losses rise. Therefore, the temperature restrictions determine the rated load. A higher temperature results from exceeding the rated load for brief periods of time or by tiny quantities, which shortens the equipment's service life but does not cause it to be destroyed. Many utilities regularly permit equipment overloads for brief periods of time; transformers, for instance, are often overloaded by up to 15% during peak times, which may last just 15 or 30 minutes[7], [9].

Performance of transmission lines of short and medium length.

Routes of Short Transmission

Three kinds of transmission lines are recognised.

1) A short transmission line with a maximum length of 80 kilometers
2) Medium transmission line: This line is between 80 and 160 kilometers long.
3) Long transmission line; it is more than 160 kilometers long.

Power must be sent from one end to the other, regardless of the kind of transmission line. The transmission network will experience some power loss and voltage drop while transporting electricity from one end to the other, much as other electrical systems. Consequently, the efficiency and voltage control of a transmission line may be used to evaluate its performance.

$$\text{Efficiency of transmission line} = \frac{\text{power delivered at receiving end}}{\text{power sent from sending end}} \times 100\ \%$$

Powersentfrom sendingend – linelosses=power deliveredatreceivingend.

A transmission line's voltage regulation measures the change in receive end voltage from a situation of no load to a condition of full load.

$$\%\ \text{regulation} = \frac{\text{no load receiving end voltage} - \text{full load receiving end voltage}}{\text{full load voltage}} \times 100\ \%$$

There will be three fundamental electrical characteristics on every transmission line. The line's conductors will have capacitance, inductance, and resistance. The characteristics are spread evenly throughout the transmission line since it is made up of conductors that are routed from one location to another while being supported by transmission towers. The speed of light used to transfer electrical power through a transmission line is 3X108 metres per second. The electricity operates at 50Hz. The equation shown below may be used to calculate the wave length of the voltage and current of the power.

$$\text{Therefore, } \lambda = \frac{v}{f}$$

$$\lambda = \frac{3X10^8}{50} = 6X10^6 \text{ meters} = 6000 \text{ km.}$$

f.λ=vwhere fispower frequency,&labdaiswavelengthandvis thespeedoflight.

Hencethewavelengthofthetransmittingpowerisquitelongcomparedtothegenerallyusedlinelengt h of transmission line (Figure 1.2).

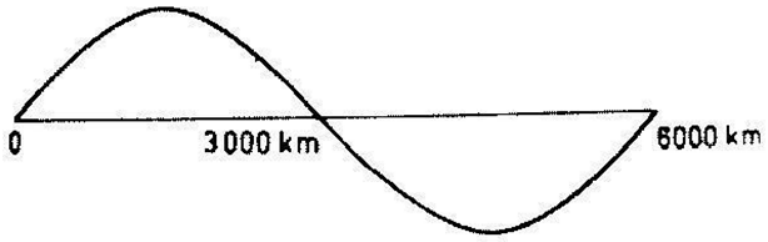

Voltage distribution of 50 Hz supply

Figure 1.2: *Illustrates* the voltage distribution of 50 Hz supply.

Due to this, parameters for transmission lines under 160 km in length are presumed to be lumped together rather than scattered. Electrically short transmission lines are such lines. Once again divided into short and medium transmission lines, these electrically short

transmission lines have a length of up to 80 km (length between 80 and 160 km). In contrast to medium-length transmission lines, where the capacitance is assumed to be lumped in the centre or half of the capacitance may be assumed to be lumped at either end, short transmission lines disregard the capacitive parameter. The parameters are regarded as being dispersed over lines longer than 160 km. We refer to this as a lengthy transmission line.

Parameters ABCD

Power system engineering is primarily concerned with moving electricity as efficiently as possible from one location (such as a generating station) to another, such as a substation or distribution unit. Therefore, it is crucial for power system engineers to use accurate mathematical models. Thus, for the sake of making computations simpler, the complete transmission system may be reduced to a two port network. The figure below depicts the circuit of a two-port network. A two-port network, as its name indicates, has two ports: PQ for input and RS for output. Each port has two terminals that it uses to connect to the outside circuit. It is effectively a two-port or four-terminal circuit since the input port P Q receives supply end current = IS and supply end voltage = VS.

Additionally, there is the Receiving end current (IR) and voltage (VR) that are sent to the output port R S. according to the illustration below. Considering that the circuit parts are linear in nature, the ABCD parameters or the transmission line parameters now offer the connection between the supply and receiving end voltages and currents.

In order to provide the relationship between the transmitting and receiving end parameters,

ABCD parameters by the equations below.VS= AVR+B IR————————————(1)

IS=CVR+ D IR————————————-(2)

Nowinordertodeterminethe ABCDparametersoftransmissionlineletusimposetherequiredcircuit conditions in different cases. ABCDparameters,whenreceivingendisopencircuited in Figure 1.3.

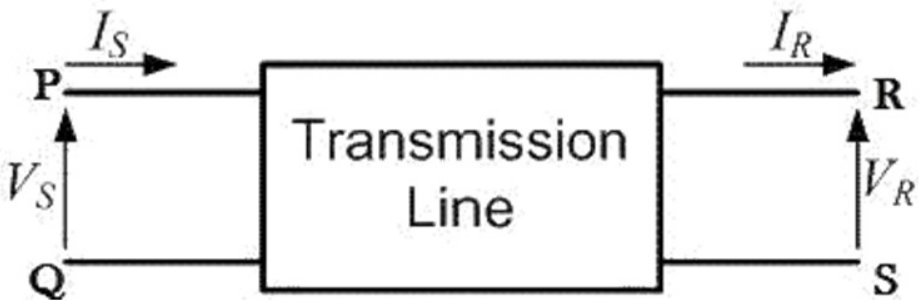

Figure 1.3: ***Illustrates*** **the circuit diagram of ABCD parameters.**

Thereceivingendisopencircuitedmeaningreceivingendcurrent IR=0.Applyingthis condition to

$$V_S = A\,V_R + B\,0 \Rightarrow V_S = A\,V_R + 0$$

$$A = \left.\frac{V_S}{V_R}\right|_{I_R = 0}$$

equation (1)weget.

As a result, it suggests that when we apply the open circuit condition to the ABCD parameters, parameter A is the ratio of the transmitting end voltage to the open circuit

receiving end voltage. A is a dimension-less parameter since it is a voltage to voltage ratio in terms of dimensions.

$$I_S = C\,V_R + D\,0 \Rightarrow I_S = C\,V_R + 0$$

$$C = \left.\frac{I_S}{V_R}\right|_{I_R = 0}$$

Applyingthesameopencircuitconditioni.e IR= 0toequation(2)

This suggests that when we apply the open circuit condition to the ABCD transmission line characteristics, we get parameter C, which is the relationship between the sending end current and the open circuit receiving end voltage. Since C is a ratio of current to voltage in terms of dimensions, its unit is mho.

C = IS VR mho, where C is the open circuit conductance, is the result. ABCDparameterswhenreceivingendisshortcircuited in Figure 1.4.

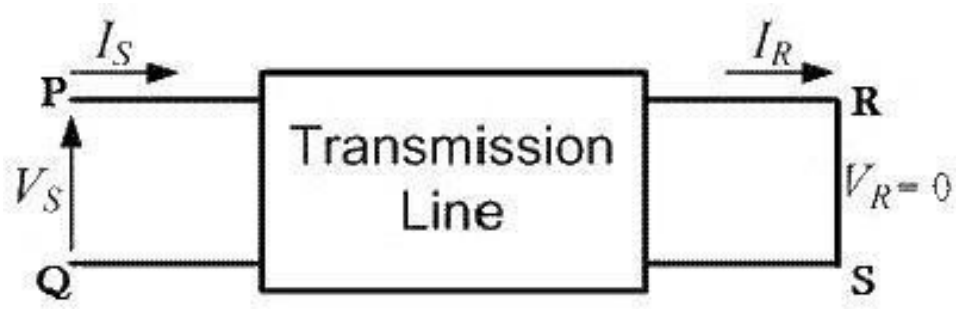

Figure 1.4: *Illustrates* the short circuit of ABCD parameter.

Receivingendisshort circuitedmeaningreceivingend voltageVR=0Applyingthis condition to equation (1)weget:

$$V_S = A\,0 + B\,I_R \Rightarrow V_S = 0 + B\,I_R$$

$$B = \left.\frac{V_S}{I_R}\right|_{V_R = 0}$$

As a result, it suggests that when we apply the short circuit condition to the ABCD parameters, parameter B is the ratio of the transmitting end voltage to the receiving end current under the short circuit. B's unit is because it is a dimensionless ratio of voltage to current. B is the short circuit resistance as a result, and is determined by

B=VS/IRΩ.

Applyingthesame shortcircuitconditioni.eVR=0 toequation(2) we get

$$I_S = C\,0 + D\,I_R \Rightarrow I_S = 0 + D\,I_R$$

$$D = \left.\frac{I_S}{I_R}\right|_{V_R = 0}$$

It follows that when we apply the short circuit condition to the ABCD parameters, we get parameter D, which is the ratio of the sending end current to the receiving end current under short circuit. D is a dimension-less parameter since it is a ratio of current to current in terms of dimensions. ∴ It is possible to tabulate the transmission line's ABCD parameters as:-

Parameter Specification UnitA=VS / VR Voltageratio Unit lessB = VS / IR Shortcircuit resistanceΩ

C= IS/VROpencircuitconductancemho

D=IS/ IRCurrentratio Unitless.

REFERENCES

[1] S. Dian *et al.*, “Integrating Wildfires Propagation Prediction Into Early Warning of Electrical Transmission Line Outages”, *IEEE Access*, 2019, doi: 10.1109/ACCESS.2019.2894141.

[2] E. Lazo, “Localization properties of non-periodic electrical transmission lines”, *Symmetry*. 2019. doi: 10.3390/sym11101257.

[3] F. R. Humire en E. Lazo, “PT -symmetric direct electrical transmission lines: Localization behavior”, *Phys. Rev. E*, 2019, doi: 10.1103/PhysRevE.100.022221.

[4] C. M. Shruthi, A. P. Sudheer, en M. L. Joy, “Dual arm electrical transmission line robot: Motion through straight and jumper cable”, *Automatika*, 2019, doi: 10.1080/00051144.2019.1609256.

[5] A. T. De Hoop en I. E. Lager, “Transient waves along electrical transmission lines. Waves in (1+1)-spacetime”, 2019.

[6] L. A. Alhakim en A. A. Moussa, “The double auxiliary equations method and its application to space-time fractional nonlinear equations”, *J. Ocean Eng. Sci.*, 2019, doi: 10.1016/j.joes.2018.12.002.

[7] *et al.*, “APPLICATION OF NEURAL NETWORKS FOR DETERMINING THE LOCATION OF DAMAGE TO AIR AND CABLE ELECTRICAL TRANSMISSION LINES”, *Min. Equip. Electromechanics*, 2019, doi: 10.26730/1816-4528-2019-4-48-55.

[8] B. A. A, “Closed Electrical Transmission Line as a Ring Waveguide for Interacting Waves of Electron and Phonon Currents”, *J. Energy Conserv.*, 2019, doi: 10.14302/issn.2642-3146.jec-19-3049.

[9] I. Kitta, S. Manjang, I. R. Sahali, en F. Maricar, “Insertion of 275 kV Transmission Line for Improving the Voltage Profile and Efficiency of Electrical Power System”, 2019. doi: 10.1088/1757-899X/676/1/012006.

CHAPTER 2

SHORT TRANSMISSION LINE

Dr. P. Kishore Kumar, Associate Professor
Faculty of Engineering and Technology, Jain (Deemed-to-be University), Bengaluru, Karnataka, India
Email id- k.kishore@jainuniversity.ac.in

Transmission lines smaller than 80 km in length are often referred to as short transmission lines. The equivalent circuit is depicted as follows because for short lengths in Figure 2.1, the shunt capacitive coupling of this type of line is disregarded and other variables like resistance and inductive reactance of these short lines are lumped. Let's draw the vector diagram for this transmission line using the receiving end current Ir as a guide. The transmitting end and receive end voltages, which are represented by s and r, respectively, are at an angle with the reference receiving end current[1], [2].

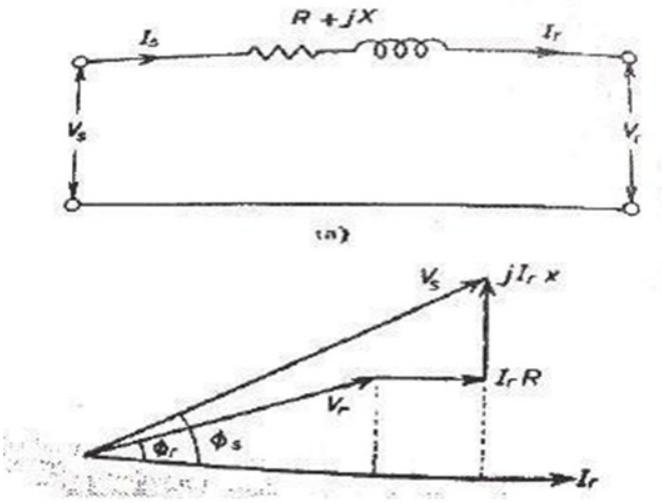

Figure 2.1: ***Illustrates*** **the equivalent circuit of shunt capacitance.**

Astheshuntcapacitanceofthelineisneglected,hencesendingendcurrentandreceivingendcurrent is same, i.e.

Is=Ir.

Nowifweobservethevectordiagramcarefully,wewillget,Vs is approximatelyequal to

Vr + Ir.R.cosφr + Ir.X.sinφr

Thatmeans,

Vs≅Vr+Ir.R.cosφr + Ir.X.sinφrastheitisassumed thatφs≅φr

Because there is no capacitance, the line's current is assumed to be zero when there is no load, hence the receiving end voltage is equal to the transmitting end voltage in this situation. According to voltage regulation teeth.

Here, the short transmission lines per-unit resistance and reactance are denoted by vr and vx. There are typically two input terminals and two output terminals on every electrical network. Any intricate electrical network that we imagine as a black box will have two input terminals and output terminals. Two-port network is the name of this network. The network solution method is made easier by networks with two ports. A two-port network may be mathematically solved using 2 by 2 matrices[3], [4].

$$\% \text{ regulation} = \frac{V_s - V_r}{V_r} X\ 100\ \%$$

$$= \frac{I_r.R.\cos\varphi_r + I_r.X.\sin\varphi_r}{V_r} X\ 100\ \%$$

$$\text{per unit regulation} = \frac{I_r.R}{V_r}\cos\varphi_r + \frac{I_r.X}{V_r}\sin\varphi_r = v_r\cos\varphi_r + v_x\sin\varphi_r$$

$$A = \frac{V_s}{V_r}\Big|_{I_r = 0}$$

A transmission may be seen as a two port network since it is also an electrical network. Thus, a two port transmission line network may be represented as a two by two matrix. The idea of ABCD parameters appears here. The network's voltage and currents may be expressed as,

Vs=AVr +BIr… .....(1)

Is=CVr+DIr…..... (2)

WhereA,B,C andDaredifferentconstantofthenetwork.If weputIr=0 atequation (1), we get. Hence,Aisthevoltageimpressedatthesendingendpervoltatthereceivingendwhenreceivingend is open.It is dimension less.

If weputVr=0atequation(1),we get

$$B = \frac{V_s}{I_r}\Big|_{V_r = 0}$$

When the receiver terminals are shorted out, it means the transmission line impedance is the

$$C = \frac{I_s}{V_r}\Big|_{I_r = 0}$$

cause. Transfer impedance is the name given to this parameter.

Cisthe currentinamperesintothesendingendper voltonopencircuitedreceivingend.Ithasthe dimension of admittance.

D is the transmitting end's current in amps per amp of the shorted receiving end. It has no dimensions.

$$D = \frac{I_s}{I_r}\Big|_{V_r = 0}$$

Now, it is discovered from an analogous circuit that,

Vs=Vr+IrZandIs=IrComparingtheseequations withequation 1and 2we get,

A= 1,B=Z,C=0 andD = 1.Aswe knowthattheconstantA,B, CandD are relatedforpassivenetwork as,

Here, A=1, B=Z,C= 0andD=1

AD− BC=1.

⇒1.1 −Z.0 =1

So the values calculated are correct for short transmission line.Fromaboveequation (1),

Vs=AVr+BIr

WhenIr=0thatmeansreceivingendterminalsisopencircuitedandthenfromtheequation1, we get receivingend voltageat no load

$$V_r' = \frac{V_s}{A}$$

$$\% \text{ voltage regulation} = \frac{V_s / A - V_r}{V_r} X100\ \%$$

Andasperdefinitionofvoltageregulation,

EfficiencyofShortTransmissionLine

$$\% \text{ efficiency } (\mu) = \frac{\text{Power received at receiving end}}{\text{Power delivered at sending end}} X\ 100\ \%$$

$$\% \mu = \frac{\text{Power received at receiving end}}{\text{Power received at receiving end} + 3I_r^2.R} X\ 100\ \%$$

Theefficiencyofshortlineassimpleasefficiencyequationofanyotherelectricalequipment,that means.

Transmission Line, Medium

The term "medium transmission line" normally refers to a transmission line with an effective length of more than 80 km but less than 250 km. Contrary to the situation with short transmission lines, the line length makes it such that admittance Y of the network is taken into account when determining the effective circuit characteristics. For this reason, lumped shunt admittance and lumped impedance in series with the circuit are used in the modelling of a medium-length transmission line. Two distinct models, namely, may be used to describe these lumped transmission line parameters[5], [6].

1) Nominal Π representation.

2) A depiction of nominal T.

Now let's go into a more thorough study of the models listed above.

Representation in terms of a medium transmission line

The lumped series impedance is located in the circuit's centre in a nominal form, while the shunt admittances are located at its ends. The lumped shunt admittance is split into two equal halves, each of which is put at both the transmitting and receiving ends while the complete circuit impedance is situated between them, as can be seen in the network diagram below. The circuit in this configuration mimics the shape of a symbol, and as a result it is referred to as the nominal representation of a medium transmission line. It is mostly utilised for doing load flow analysis and establishing the general circuit characteristics in Figure 2.2.

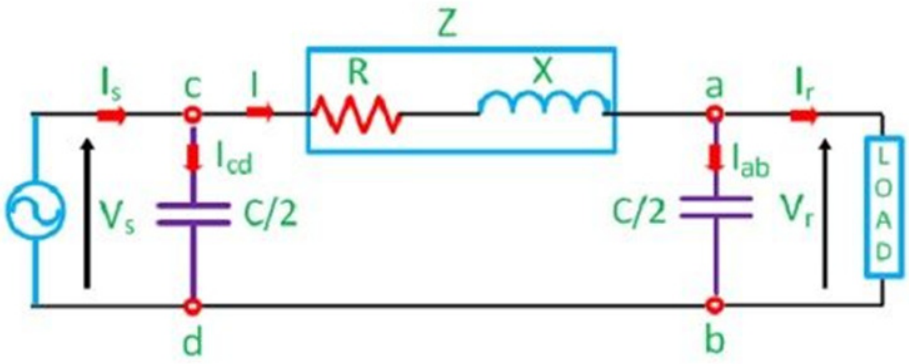

Figure 2.2: The depiction of a medium transmission line.

As we can see, the supply end current is flowing via the supply end, while VS and VR are the corresponding supply and receiving end voltages. The amount of current passing through the circuit's receiving end is known as IR.

The current values passing through the admittances are I1 and I3. I2 represents the current flowing through impedance Z.

NowapplyingKCL,atnodeP,weget.IS= I1+I2 ——————(1)

SimilarlyapplyingKCL,tonodeQ. I2= I3+ IR ——————(2)

Nowsubstitutingequation(2)toequation

(1)IS=I1 +I3+ IR

$$= \frac{Y}{2}V_S + \frac{Y}{2}V_R + I_R \text{-------(3)}$$

NowbyapplyingKVLtothecircuit,VS= VR +ZI2

$$= V_R + Z(V_R\frac{Y}{2} + I_R)$$

$$= (Z\frac{Y}{2} + 1)\, V_R + ZI_R \text{ ----------(4)}$$

Now substituting equation (4) to equation (3), we get.

$$I_s = \frac{Y}{2}[(\frac{Y}{2}Z + 1)V_R + ZI_R] + \frac{Y}{2}V_R + I_R$$

$$= Y(\frac{Y}{4}Z + 1)V_R + (\frac{Y}{2}Z + 1)I_R \text{ ----------(5)}$$

Comparingequation(4) and(5)withthestandard ABCDparameterequationsVS= AVR +B IR

IS=CVR+ D IR

Wederivetheparameters of amedium transmission lineas:

$$A = (\frac{Y}{2}Z + 1)$$

$$B = Z\ \Omega$$

$$C = Y(\frac{Y}{4}Z + 1)$$

$$D = (\frac{Y}{2}Z + 1)$$

An example of a medium transmission system shown in nominal T, The lumped shunt admittance is put in the centre of the nominal T model of a medium transmission line, and the net series impedance is split into two equal halves and placed on each side of the shunt admittance. The circuit that results from this process is known as the notional T network of a medium-length transmission line and is seen in the picture below. It resembles the capital T sign in Figure 2.3.

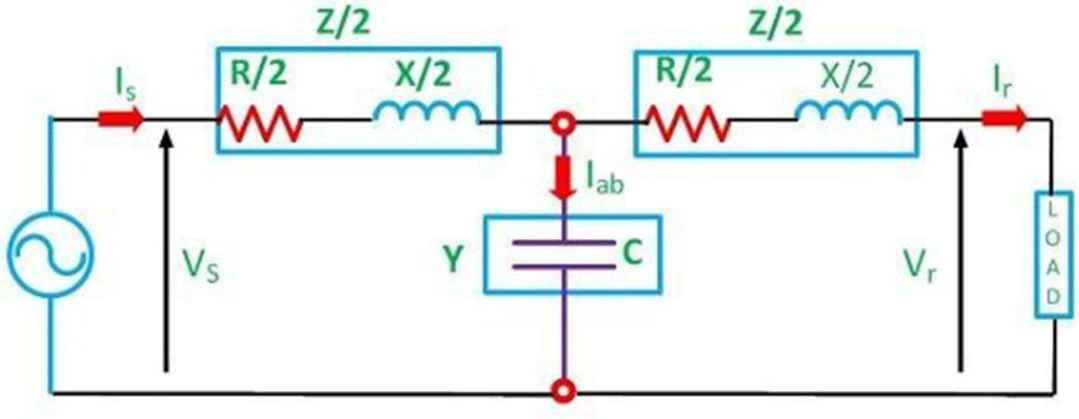

Figure 2.3: ***Illustrates*** **the T representation of a medium transmission line.**

In this instance, is denotes the current flowing through the supply end, while Vs and Vr denote the supply and receiving end voltages, respectively. The circuit's receiving end is where current (Ir) is flowing. Let M serve as the circuit's midway node, and let Vm determine the drop at M. Using KVL on the aforementioned network, we get,

$$\frac{V_S - V_M}{Z/2} = Y V_M + \frac{V_m - V_R}{Z/2}$$

$$\text{Or } V_M = \frac{2(V_S + V_R)}{YZ + 4} \text{ ----------(6)}$$

And the receiving end current

$$\text{Or } I_R = \frac{2(V_M - V_R)}{Z/2} \text{ ----------(7)}$$

Now substituting V_M from equation (6) to (7) we get,

$$\text{Or } I_R = \frac{[(2V_S + V_R)/YZ+4] - V_R}{Z/2}$$

Rearranging the above equation:

$$V_S = (\frac{Y}{2}Z + 1)V_R + Z(\frac{Y}{4}Z + 1)I_R \text{ ----------(8)}$$

Now the sending end current is

Is =YVM+IR ————————(9)

Substituting the value of VM to equation (9)we get,

$$\text{Or } I_S = Y V_R + (\frac{Y}{2}Z + 1)I_R \text{ ----------(10)}$$

AgaincomparingComparingequation(8)and(10)withthestandardABCDparameterequations

VS=AVR+BIRIS=CVR+ D IR

The parameters of the T network of a medium transmission line are

$$A = (\frac{Y}{2}Z + 1)$$

$$B = Z(\frac{Y}{4}Z + 1)\ \Omega$$

$$C = Y \text{ mho}$$

$$D = (\frac{Y}{2}Z + 1)$$

Performance of Long Transmission Lines TRANSMISSION LINE LONG

Long transmission lines are those used for electricity transmission and have effective lengths of at least 250 km. Calculations for such a power transmission's circuit parameters (ABCD parameters) are more complex than they were for short or medium transmission lines. The effective circuit length in this instance is much longer than it was for the previous models (long and medium line), ruling out any approximations that may have been considered in

those cases in Figure 2.4.

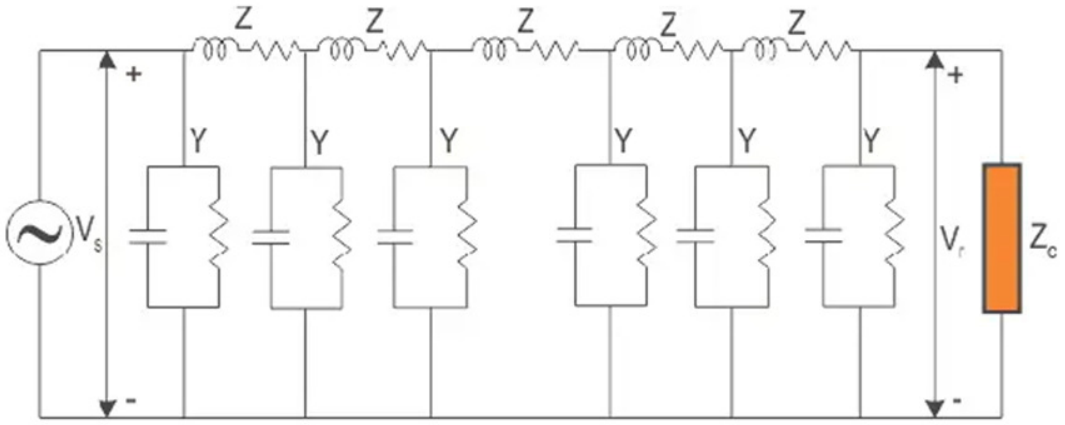

Figure 2.4: *Illustrates* the long transmission line model.

Disregarding the network's shunt admittance, as in a model with a few transmission lines.

Assuming, as was the case with the medium line model, that the circuit impedance and admittance are combined and concentrated at a single point. Instead, we should assume that the circuit impedance and admittance are evenly distributed throughout the whole length of the circuit, as indicated in the figure below, for all practical purposes. For this reason, the calculations of the circuit parameters will be a little more exact, as we shall see below. Let's take into consideration the circuit of the lengthy transmission line as indicated in the Figure 2.5 below for correct modelling to identify circuit characteristics[7], [8].

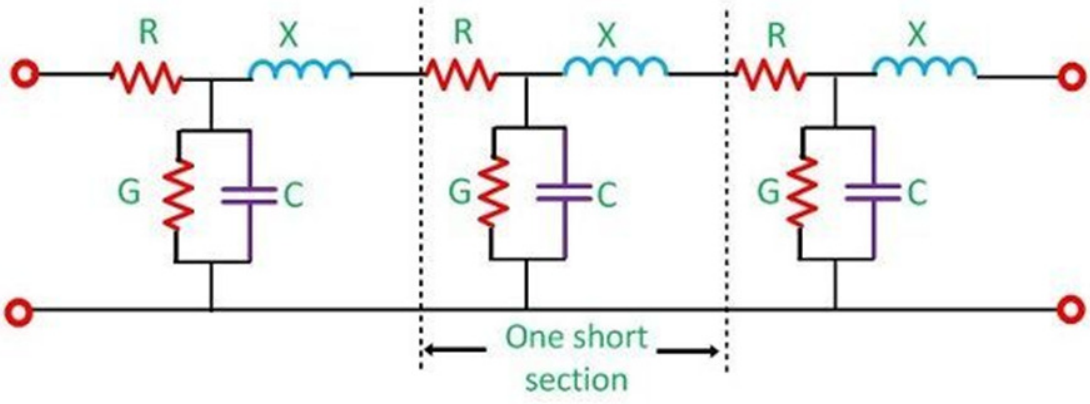

Figure 2.5: *Illustrates* the long transmission line.

In this case, a line with a length of l > 250km is provided with voltage and current of VS and IS, respectively, at the transmitting end, while VR and IR are the voltage and current measurements received at the receiving end. Let's take a look at an element with length x that is infinitely tiny, as indicated in the picture, and placed x distance away from the receiving end. V is the voltage reading immediately before the element x. I = the value that was immediately before to inputting the element x. voltage exiting the element x is given by V+V.

I+ΔI = current leaving the element Δx.ΔV = voltage drop across element Δx.zΔx = series impedence of element ΔxyΔx=shuntadmittanceofelementΔx

WhereZ=zlandY=ylarethevaluesoftotalimpedanceandadmittanceofthelongtransmission line.

The voltage drop across the infinitely small element Δxis given byΔV= IzΔx

OrIz=ΔV/Δx

OrIz=dV/dx————————————(1)

Now to determine the current ΔI, we apply KCL to node A.ΔI=(V+ΔV)yΔx=VyΔx+ΔVyΔx

SincethetermΔVyΔxistheproductof2infinitelysmallvalues, we can ignore it for the sake of easier calculation.

We can write dI/dx = V y ————————(2)Now derevating both sides of eq (1) w.r.t x,d^2V/dx^2=zdI/dx. Now substituting dI/dx=Vy from equation (2)d^2V/dx^2=zyV ord^2V/dx^2–zyV=0————————(3)

The solution of the above second order differential equation is given by.V =A1 $e^{x\sqrt{yz}}$ +A2 $e^{-x\sqrt{yz}}$ ————————(4)

Derivating equation (4)w.r.tox.

dV/dx=√(yz)A1$e^{x\sqrt{yz}}$–√(yz)A2$e^{-x\sqrt{yz}}$————————

(5)Now comparing equation (1) with equation (5)

$$I = \frac{dV}{dx} = \frac{zA_1 e^{x\sqrt{(yz)}}}{\sqrt{(z/y)}} - \frac{zA_1 e^{-x\sqrt{(yz)}}}{\sqrt{(z/y)}} \text{----------(6)}$$

Nowtogofurtherletusdefinethecharacteristicimpedance Zcandpropagationconstantδofalongtransmission lineas

Zc=√(z/y)Ωδ=√(yz)

Thenthevoltageandcurrentequationcanbeexpressedintermsofcharacteristicimpedanceandpropagation constant as

V =A1 $e^{\delta x}$+A2 $e^{-\delta x}$————————(7)

I=A1/Zc$e^{\delta x}$+A2 /Zc$e^{-\delta x}$————————(8)

Now atx=0,V=VR andI=Ir. Substituting the second it iosto equation (7) and (8) respectively. VR =A1 + A2————————(9)

IR= A1/Zc+A2/Zc————————(10)

Solving equation (9) and (10),We get values of A1 and A2 as,

A1=(VR+ZCIR)/2andA1=(VR− ZCIR)

Now applying another extreme condition at x=l, we haveV =VS and I=IS.

Now to determine VS and IS we substitute x by land put the values of A1 and A2 in equation (7) and (8) we get

VS = (VR + ZC IR)$e^{\delta l}$/ 2 + (VR − ZC IR)$e^{-\delta l}$/2 ————————(11)IS= (VR/ZC+IR)$e^{\delta l}$/2–(VR/ZC– IR)$e^{-\delta l}$/2————————(12

By trigonometric and exponential operators we know $\sinh\delta l=(e^{\delta l}-e^{-\delta l})/2$

And $\cosh\delta l=(e^{\delta l}+e^{-\delta l})/2$

∴Equation (11)and(12)can bere-writtenas

VS = VRcoshδl + ZC IR sinhδlIS=(VRsinhδl)/ZC+ IRcoshδl

Thus comparing with the general circuit parameters equation, we get the ABCD parameters of along transmission line as,

C=sinhδl/ZC

A=coshδl

D=cosh δl

B=ZC sinhδl

Surge Impedance: The ratio of the voltage and current amplitudes of a single wave propagating along the line that is, a wave travelling in one direction without reflections in the opposite direction is known as the characteristic impedance or surge impedance of a uniform transmission line (typically written Z0). Characteristic impedance, for a uniform line, is independent of length and is defined by the geometry and materials of the transmission line. **The ohm is the characteristic impedance's SI unit**

A lossless transmission line's characteristic impedance is entirely genuine and devoid of any reactive elements. Such a wire does not lose energy in the process of transmitting energy from a source at one end to the other. The source perceives a transmission line of limited length (lossless or lossy), terminated at one end with an impedance matching the characteristic impedance, as being infinitely long and there are no reflections.

The loading of the surge impedance:

The power load at which the net reactive power is zero is known as the surge impedance loading (SIL) of a line. Therefore, the SIL is the amount of reactive power you would have to supply to balance it out to zero if your transmission line wanted to "absorb" reactive power. You may figure it out by dividing the line-to-line voltage's square by the characteristic impedance of the line. Transmission lines may be seen as a very large number of these combinations connected in series with very modest inductances and capacitances to the ground. Capacitance is used to make up for any voltage loss caused by inductance. If this correction is accurate, you will get surge impedance loading and there won't be any voltage drops for either an infinite length or a finite length that is terminated by this impedance (SIL load). (Assumed loss-less line!) It can be shown that the impedance of this line (Zs) equals sqrt(L/C). The ferranti effect, which causes a voltage increase at the other end, occurs if capacitance compensation is used in excess of what is necessary, which might occur on an empty EHV line. Even though it is presented in numerous books, the topic is always intriguing to debate. A transmission line's associated capacitive reactive power rises immediately as the square of the voltage and is inversely proportional to line capacitance and length[9], [10].

There are two results of capacitance:

The capacitive current of the line passing through the source impedances at the line terminations causes an increase in voltage known as the Ferranti effect. The formula for SIL, or surge impedance loading, is (KV x KV) / Zs, where the units are megawatts. Be careful

that the surge impedance and the surge impedance loading are two completely distinct things, where Zs is the surge impedance.

Wavelength: As indicated in the figure, wavelength is the separation between identical places in subsequent cycles of a waveform signal travelling through space or over a wire in Figure 2.6. This length is often stated in wireless systems in metres, centimetres, or millimetres. When describing the wavelength of infrared, visible light, ultraviolet, and gamma radiation, nanometers (units of 10-9 metre) or Angstrom units are most often used (units of 10-10 meter).

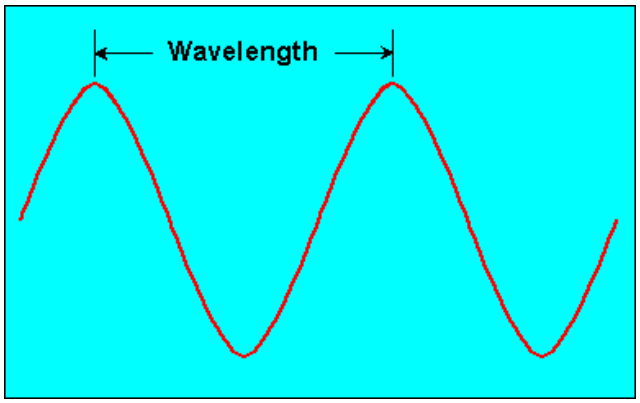

Figure 2.6: *Illustrates* the sine waveform.

Frequency and wavelength have an opposite relationship. The wavelength of a signal decreases with increasing frequency. If the signal's frequency is expressed in megahertz (MHz), and its wavelength is expressed in metres (m), then

$w = 300/f$ and conversely

$f = 300/w$

The Greek letter lambda is occasionally used to denote wavelength.

Speed of Propagation

Velocity of propagation, also known as the speed of the sent signal in relation to the speed of light, is a measurement of how quickly a signal moves across space and time. In computer technology, the speed of transmission across a physical medium, such as a coaxial cable or optical fibre, is referred to as the velocity of propagation of an electrical or electromagnetic signal. Additionally, there is a clear correlation between wavelength and propagation velocity. The speed of propagation is often expressed as a ratio of time to distance or as a fraction of the speed of light.

Ferranti Effect

In all electrical systems, current flows from the area of greater potential to the region of lower potential to make up for the potential difference that occurs in the system, as is known in common practise. Practically speaking, current flows from the source or supply end to the load because the sending end voltage is always greater than the receiving end voltage. But Sir S.Z. Ferranti developed a remarkable theory about medium- or long-distance transmission lines in 1890 that claimed that when a transmission system is operated with little or no load, the receiving end voltage frequently rises above the sending end voltage. This phenomenon is known as the Ferranti effect in the power system.

A transmission line experiences the Ferranti effect

It is possible to think of a lengthy transmission line as having a significant quantity of capacitance and inductance dispersed throughout its whole length. The Ferranti Effect happens when the current pulled by the line's dispersed capacitance is higher than the current drawn by the load at the line's receiving end (during light or no load). This capacitor charging current causes a voltage drop across the transmission system's line inductance, which is in phase with the voltages at the sending end. As we approach closer to the load end of the line, this voltage drop continues growing additively, and as a result, the voltage at the receiving end tends to rise beyond the voltage being supplied, causing the phenomenon known as the Ferranti effect in the power system. With the aid of the phasor diagram below, it is shown. Thus, the transmission line's capacitance and inductance effects both play a role in this specific phenomenon. As a result, the Ferranti effect is minimal for short transmission lines since their inductance is practically thought of as being close to zero. The no load receiving end voltage has been observed to typically be 5% higher than the transmitting end voltage for a 300 Km line running at a frequency of 50 Hz.

Let's now analyse the Ferranti effect using the phasor diagram that was previously shown in Figure 2.7. The reference phasor in this case is Vr, represented by OA.

Thus Vr = Vr (1 + j0)Capacitancecurrent,Ic=jωCVr

NowsendingendvoltageVs =Vr+ resistivedrop+reactivedrop.

=Vr +IcR+ jIcX

=Vr+Ic(R +jX)

=Vr+jωcVr(R+jωL) [sinceX=ωL]

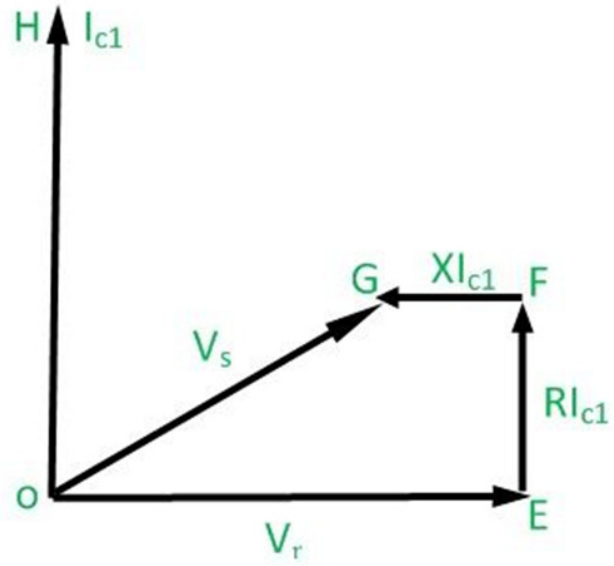

Figure 2.7: ***Illustrates*** **the phasor diagram of Ferranti effect.**

The phasor OC is used to symbolise this.

Now that it has been realistically seen that the line resistance in the case of a long transmission line is negligibly tiny compared to the line reactance, we can assume that the length of the phasor Ic R = 0 and that the increase in voltage is entirely caused by OA - OC = reactive drop in the line.

Now, suppose c0 and L0 are the capacitance and inductance measurements per kilometre of the transmission line, where l is the line's length.

Consequently, capacitive reactance Xc = 1/(l c0)

The average current flowing in a long transmission line is Ic = 1/2 Vr/Xc = 1/2 Vr l c0 because the capacitance is dispersed throughout the whole length of the line.

The line's inductive reactance is now equal to L0 l.

IcX = 1/2Vr l c0 X L0 l is the formula for the increase in voltage caused by line inductance.

Voltage increase= 1/2 Vr2 l 2 c0L0.

It is crystal clear from the aforementioned equation that the rise in voltage at the receiving end is directly proportional to the square of the length of the line. As a result, in the case of a long transmission line, it keeps getting longer and occasionally exceeds the applied sending end voltage, causing the phenomenon known as the Ferranti effect in power systems.

REFERENCES

[1] N. A. Salim, H. Mohamad, Z. M. Yasin, N. F. A. Aziz, en N. A. Rahmat, “Graphical user interface based model for transmission line performance implementation in power system”, *Indones. J. Electr. Eng. Comput. Sci.*, 2019, doi: 10.11591/ijeecs.v16.i1.pp92-100.

[2] N. A. Salim, M. S. Ab Samah, H. Mohamad, Z. M. Yasin, en N. F. Ab Aziz, “Implementation of graphical user interface to observe and examine the frequency and rotor angle stability of a power system due to small disturbances”, *Indones. J. Electr. Eng. Comput. Sci.*, 2019, doi: 10.11591/ijeecs.v17.i2.pp606-614.

[3] J. J. Sánchez-Martínez, M. Pérez-Escribano, en E. Márquez-Segura, “Synthesis of Dual-Band Bandpass Filters With Short-Circuited Multiconductor Transmission Lines and Shunt Open Stubs”, *IEEE Access*, 2019, doi: 10.1109/ACCESS.2018.2886657.

[4] N. Peng, L. Zhou, R. Liang, en H. Xu, “Fault location of transmission lines connecting with short branches based on polarity and arrival time of asynchronously recorded traveling waves”, *Electr. Power Syst. Res.*, 2019, doi: 10.1016/j.epsr.2018.12.022.

[5] X. Che, B. Ip, en Z. Yan, “Field test of multi-hop image sensing network prototype on a city-wide scale”, *Digit. Commun. Networks*, 2019, doi: 10.1016/j.dcan.2017.07.002.

[6] M. Pamula, S. D. Pirade, Y. S. Pirade, en N. Amin, “EVALUASI SETTING RELAI JARAK (DISTANCE RELAY) PADA SALURAN UDARA TEGANGAN TINGGI (SUTT)150 kV ANTARA GARDU INDUK SIDERA-GARDU INDUK TIPO”, *Foristek*, 2019, doi: 10.54757/fs.v9i1.67.

[7] N. N. Shah en S. R. Joshi, “Modal analysis for selection of DFIG-based wind farms for damping and reduction of the risk of SSR”, *IET Energy Syst. Integr.*, 2019, doi: 10.1049/iet-esi.2018.0005.

[8] G. Chaudhary en Y. Jeong, “Wideband Tunable Differential Phase Shifter With Minimized In-Band Phase Deviation Error”, *IEEE Microw. Wirel. Components Lett.*, 2019, doi: 10.1109/LMWC.2019.2920270.

[9] M. Liu, Z. Xiang, P. Ren, en T. Xu, “Quad-mode dual-band bandpass filter based on a stub-loaded circular resonator”, *Eurasip J. Wirel. Commun. Netw.*, 2019, doi: 10.1186/s13638-019-1362-z.

[10] R. Akbar Fauzany, I. G. Dyana Arjana, en C. G. Indra Partha, “ANALISIS RESETTING RELE JARAK AKIBAT UPRATING KONDUKTOR GIS PESANGGARAN - GI SANUR”, *J. SPEKTRUM*, 2019, doi: 10.24843/spektrum.2019.v06.i02.p03.

CHAPTER 3

DESIGN OF TRANSMISSION LINES IN MECHANICAL FORM

Dr. Hannah Jessie Rani R, Assistant Professor
Faculty of Engineering and Technology, Jain (Deemed-to-be University), Bengaluru, Karnataka, India
Email id- jr.hannah@jainuniversity.ac.in

In other words, line conductors must be appropriately insulated from supports. The overhead line conductors should be supported on the poles or towers in such a manner that currents from conductors do not flow to earth via supports. This is accomplished by using insulators to fasten line wires to supports. In order to stop any leakage current from conductors to earth, the insulators act as the essential insulation between line conductors and supports [1], [2]. The following desired qualities should, in general, be present in the insulators:

I Strong mechanical construction to support conductor load, wind load, etc. To prevent leakage currents to ground, insulator materials must have high electrical resistance. Highrelativepermittivityofinsulatormaterialinorderthatdielectricstrengthishigh in Figure 3.1.

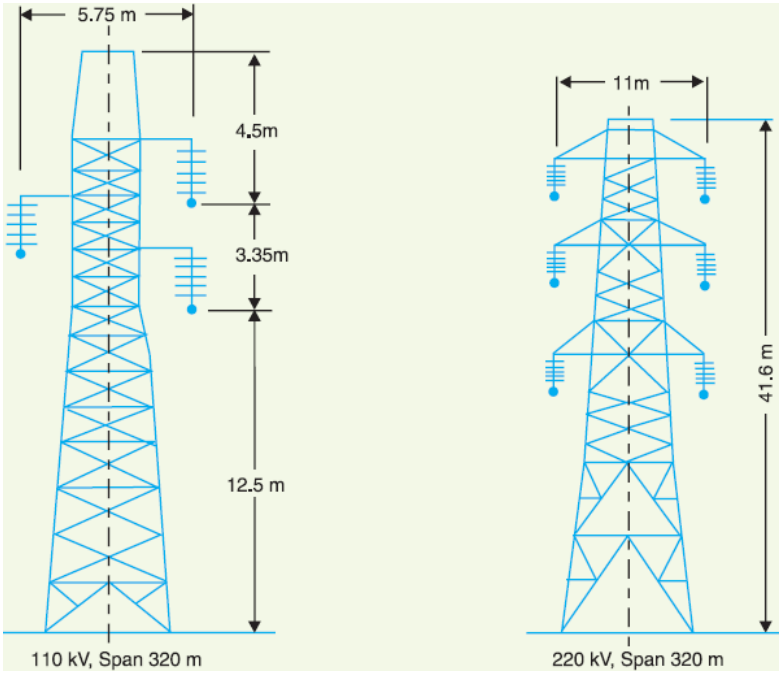

Figure: 3.1: *Illustrates* the permittivity will decrease if the insulator material is porous, has impurities, or has fractures.

High ratio of flashover to puncture strength

Porcelain is the material that is most often used for overhead line insulators, however glass, steatite, and unique composition materials are also sometimes utilised. A combination of kaolin, feldspar, and quartz is fired at a high temperature to create porcelain. It is mechanically more durable than glass, has fewer leakage issues, and is less sensitive to temperature fluctuations.

Different Insulators

The appropriate choice of insulators is crucial to the efficient functioning of an overhead wire. There are many different kinds of insulators, however the pin type, suspension type, strain insulator, and shackle insulator are the most often used varieties [3], [4].

Pin-style insulation: The part section of a pin type insulator. The pin type insulator is attached to the cross-arm on the pole, as the name implies. The conductor is housed in a groove on the insulator's top end. The annealed wire made of the same material as the conductor is used to bind the conductor as it travels through this groove. Electric power transmission and distribution at voltages up to 33 kV employ pin type insulators. The pin type insulators become excessively large and hence uneconomical over working voltage of 33 kV in Figure 3.2.

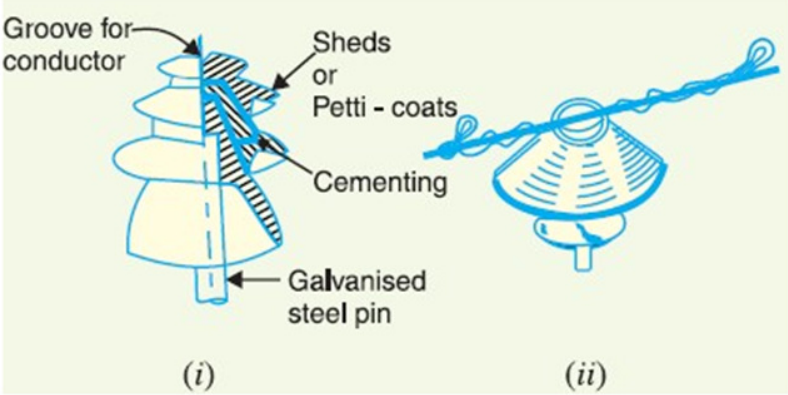

Figure 3.2: ***Illustrates*** **the pin type insulators become too bulky and hence uneconomical.**

Insulator failure causes: To endure mechanical and electrical forces, insulators are necessary. The latter kind, which is mostly brought on by line voltage, may result in the insulator breaking down. Either a flash-over or a perforation might cause the insulator to collapse electrically. When there is a flashover, an arc forms between the line conductor and the insulator pin (i.e., earth), and the discharge jumps over the *air gaps in the shortest possible path. The arcing distance for the insulator (i.e., a + b + c) is shown in Fig. Unless the insulator is destroyed by the intense heat created by the arc, it will continue to function properly in the event of a flash-over. In the event of a puncture, the insulator's body serves as a conduit for the discharge from conductor to pin. When this kind of breakdown occurs, the insulator is irreparably damaged by too much heat. In actuality, enough porcelain thickness is given in the insulator to prevent line voltage penetration [5], [6]. The safety factor, or ratio of puncture strength to flashover voltage,

$$\text{Safety factor of insulator} = \frac{\text{Puncture strength}}{\text{Flash - over voltage}}$$

High safety factor values are preferred so that flash-over occurs before the insulator is penetrated. The safety factor for pin type insulators is around 10. Isolators of the suspension kind. As the operating voltage is raised, the price of pin type insulators rises sharply. As a result, this kind of insulator is not cost-effective over 33 kV. It is standard procedure to utilise the suspension type insulators seen in Fig. at high voltages (>33 kV). They are made up of

many porcelain discs that are linked together in series like a string by metal links. At one end of this string, the conductor is hanged, while the other end is fastened to the tower's crossarm. Each component, such as a disc, is made for low voltage, such as 11 kV. The operating voltage will clearly affect how many discs are connected in series. For instance, six discs will be put on the string in series if the operating voltage is 66 Kv[7], [8].

Advantages

1) For voltages more than 33 kV, suspension type insulators are less expensive than pin type insulators.
2) The suspension type insulator is intended for low voltage, typically 11 kV, in each unit or disc. You may connect the required number of discs in series depending on the operating voltage.
3) Because the damaged disc may be changed with a sound one, the whole string does not become unusable if one of the discs is destroyed.
4) The suspension system allows the line to be more flexible. Because of the connection at the cross arm, the insulator string is free to swing in any direction and may occupy the position with the least amount of mechanical stress.

It is determined to be more acceptable to meet the larger demand by increasing the line voltage rather than by providing an additional set of conductors in cases of increased demand on the transmission line. By adding the requisite number of discs, it is simple to get the extra insulation needed for the elevated voltage in the suspension system. In most cases, steel towers are employed with the suspension type insulators. This configuration offers some lightning protection since the conductors run under the tower's earthed cross-arm.

Isolators under stress

The line is put under more stress when it comes to a dead end, a corner, or a severe bend. Strain insulators are utilised to release the line's excess stress. Shackle insulators are used as strain insulators for low voltage lines (11 kV). As seen in Fig., the strain insulator for high voltage transmission lines is really an assemblage of suspension insulators. In the vertical plane, strain insulator discs are used. In situations when there is very high line tension, such as at lengthy river bridges, two or more strings are utilised in tandem. Insulators in shackles. The shackle insulators were first used as strain insulators. But of days, low voltage distribution lines are commonly installed using them. Both a horizontal and a vertical position may be employed with such insulators. They may be bolted directly to the pole or to the cross arm. A shackle insulator attached to the pole. A soft binding wire is used to attach the conductor in the groove [9], [10].

Distribution Potential over Conduit Insulator String

A series of porcelain discs linked in series by metallic links make up a string of suspension insulators. A three-disc string of suspension insulators is shown in Figure 3.3. Each disc has a porcelain part sandwiched between two metal links. As a result, as seen in Fig., each disc acts as a capacitor C. (ii). This is referred to as self- or mutual capacitance. The charging current would have been the same across all the discs if there had just been mutual capacitance, and as a result, the voltage across each unit would have been the same, or V/3, as shown in Fig (ii). However, in reality, there is also capacitance between each disc's metal fitting and the tower or soil. Shunt capacitance C1 is the name given to this. The charging current is not uniformly distributed throughout the string's discs due to shunt capacitance. As a result, the

voltage across each disc will vary. Of course, the voltage will be highest* on the disc closest to the line conductor, V3 will be much greater than V2 or V1.

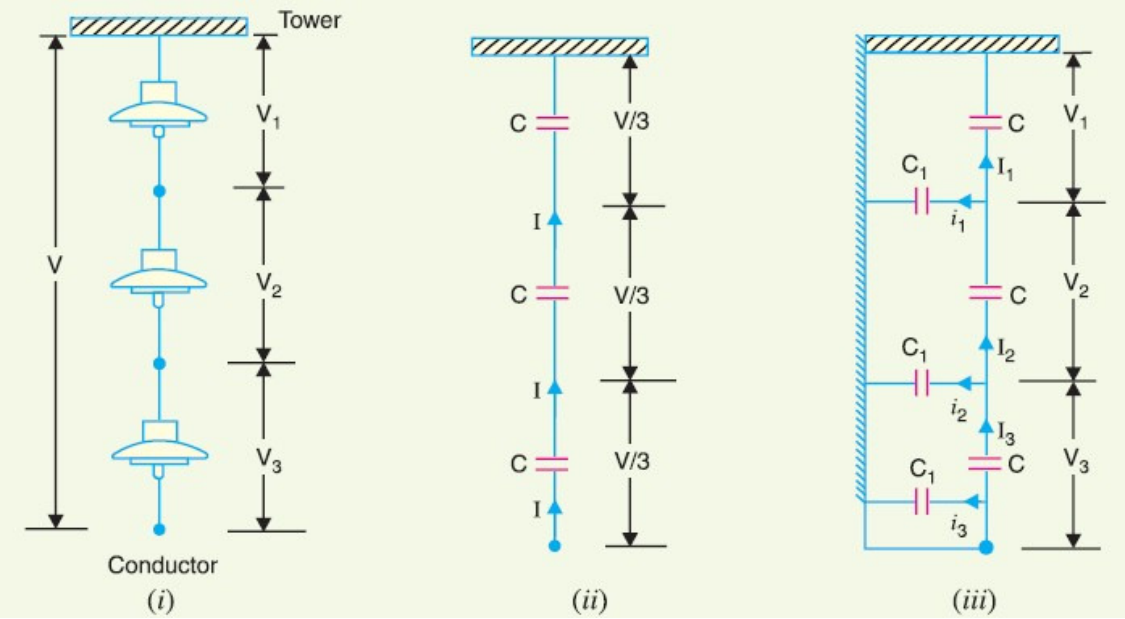

Figure 3.3: ***Illustrates*** **the Conduit Insulator String tower.**

Regarding a string of suspension insulators' probable distribution, the following things should be taken into consideration. Due to the existence of shunt capacitance, the voltage impressed on a string of suspension insulators does not disperse itself evenly over the individual discs. Maximum voltage is present across the disc that is closest to the conductor. The voltage across each disc continues to drop as we get closer to the cross-arm. The device that is closest to the conductor is under the most electrical strain and is thus most prone to puncture. Therefore, it is necessary to establish ways for distributing potential equally across all units. The voltage across each unit would be the same if the voltage impressed across the string were D.C. It is as a result of the inefficiency of insulator capacitances for D.C.

Efficiency in Strings

The voltage delivered across the string of suspension insulators is not evenly spread between different components or discs, as was already mentioned. The potential of the disc closest to the conductor is substantially greater than that of the other discs. The unwanted nature of this uneven potential distribution is often stated in terms of string efficiency. String efficiency, or the ratio of voltage across the whole string to the product of the number of discs and the voltage across the disc closest to the conductor

$$\text{String efficiency} = \frac{\text{Voltage across the string}}{n \times \text{Voltage across disc nearest to conductor}}$$

where n = number of discs in the string.

String efficiency is crucial because it determines how possible distributions are distributed throughout the string. The voltage distribution is more consistent the higher the string efficiency. Therefore, a perfect string efficiency of 100% ensures that the voltage across each

disc is the same. Although 100% string efficiency is unachievable, efforts should be made to get it as near to this number as feasible.

A formulation in Mathematics

The comparable circuit for a string of three discs is shown in Figure 3.4. Let's assume that each disc has a C self-capacitance. Let's further suppose that self-capacitance, denoted by C1, equals some proportion K of shunt capacitance, C. The voltage across each unit, measured from the cross-arm or tower, is V.V2 and V3, respectively, as indicated.

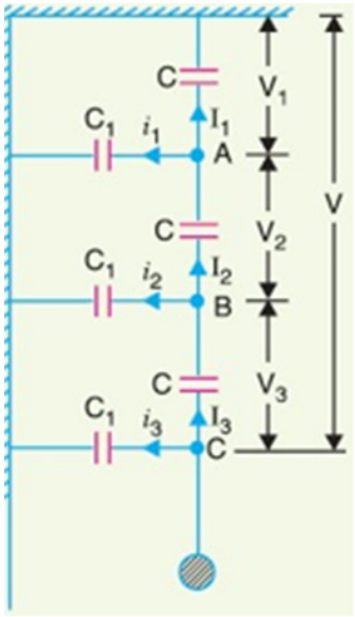

Figure 3.4: *Illustrates* the measurement of cross arm tower.

Applying Kirchhoff's current law to node A, we get,

$$
\begin{aligned}
I_2 &= I_1 + i_1 \\
V_2 \omega C^* &= V_1 \omega C + V_1 \omega C_1 \\
V_2 \omega C &= V_1 \omega C + V_1 \omega K C \\
V_2 &= V_1 (1 + K)
\end{aligned}
$$

Applying Kirchhoff's current law to node B, we get,

$$
\begin{aligned}
I_3 &= I_2 + i_2 \\
V_3 \omega C &= V_2 \omega C + (V_1 + V_2)\, \omega C_1 \dagger \\
V_3 \omega C &= V_2 \omega C + (V_1 + V_2)\, \omega K C \\
V_3 &= V_2 + (V_1 + V_2) K \\
&= K V_1 + V_2 (1 + K) \\
&= K V_1 + V_1 (1 + K)^2 \\
&= V_1 [K + (1 + K)^2] \\
V_3 &= V_1 [1 + 3K + K^2]
\end{aligned}
$$

Voltage between conductor and earth (i.e., tower) is

$$\begin{aligned} V &= V_1 + V_2 + V_3 \\ &= V_1 + V_1(1+K) + V_1(1+3K+K^2) \\ &= V_1(3+4K+K^2) \\ V &= V_1(1+K)(3+K) \end{aligned}$$

From expressions (i), (ii) and (iii), we get,

$$\frac{V_1}{1} = \frac{V_2}{1+K} = \frac{V_3}{1+3K+K^2} = \frac{V}{(1+K)(3+K)}$$

Voltage across top unit, V_1

$$V_1 = \frac{V}{(1+K)(3+K)}$$

$$\text{Voltage across second unit from top, } V_2 = V_1(1+K)$$

$$\text{Voltage across third unit from top, } V_3 = V_1(1+3K+K^2)$$

$$\%\text{age String efficiency} = \frac{\text{Voltage across string}}{n \times \text{Voltage across disc nearest to conductor}} \times 100$$

$$= \frac{V}{3 \times V_3} \times 100$$

The mathematical study mentioned above leads to the following conclusions:

If K = 0•2 (Say), then we have V2 = 1•2 V1 and V3 = 1•64 V1 from exp. This demonstrates unequivocally that the voltage across the disc closest to the conductor is at its greatest, with the voltage across the remaining discs gradually falling as the cross-arm approaches. The voltage across the discs is less uniform and string efficiency decreases as K (= C1/C) increases. As the number of discs in the string rises, so does the voltage distribution disparity. Consequently, a shorter string is more effective than a longer one.

Techniques to Increase String Efficiency

Potential distribution in a line of suspension insulators has been shown above to not be uniform. As the cross arm is reached, the maximum voltage gradually drops and appears across the insulator closest to the line conductor. The collapse of other units will follow if the insulation of the most stressed insulator that is, the one closest to the conductor—breaks down or flashes over. This calls for balancing the potential of the string's numerous components, or improving the string's effectiveness. The many techniques used for this are:

Longer cross-arms are used

String efficiency's worth depends on the value of K, which is the ratio of shunt to mutual capacitance. The string efficiency increases and the voltage distribution becomes more uniform as K decreases in value. Shunt capacitance may be lowered to lower the value of K. Longer cross-arms should be utilised in order to increase the distance between the conductor and the tower in order to minimise shunt capacitance. However, using extremely long cross-arms is not an option because to tower strength and cost restrictions. K = 0•1 is the upper

limit that can be reached by this procedure in real life in Figure 3.5.

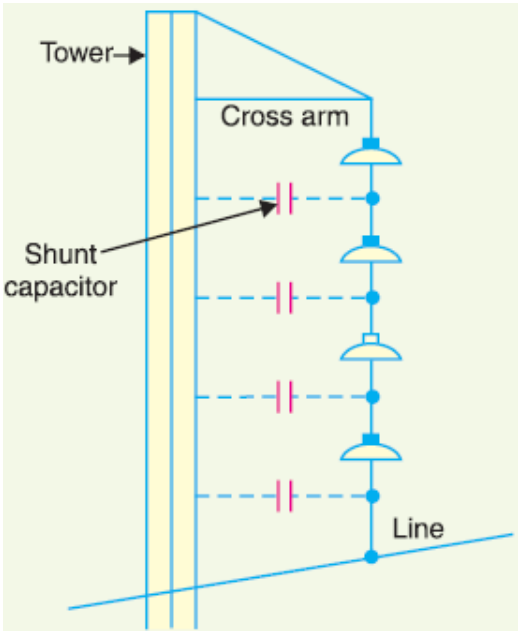

Figure 3.5: *Illustrates* to calculate the cross arm of tower.

Grade the insulators first:

With this technique, insulators of various sizes are selected so that each has a unique capacitance. The insulators are capacitance graded, which means that they are put together in the string such that the top unit has the lowest capacitance, and the capacitance rises steadily until it reaches the bottom unit (i.e., the one closest to the conductor). This technique has the tendency to equalise the potential distribution among the units in the string since voltage is inversely proportional to capacitance. The drawback of this approach is the need of using several insulators of various sizes. However, if normal insulators are used for the majority of the string and bigger units are used for the area close to the line conductor, satisfactory results may be achieved.

Making use of a protective ring

A guard ring, which is a metal ring around the bottom insulator that is electrically linked to the conductor and can be seen in Fig. 1, may be used to equalise the potential across each unit in a string. Capacitance between metal fittings and the line conductor is introduced by the guard ring. Shunt capacitance currents i1, i2, etc. are equivalent to metal fitting line capacitance currents i1, i2, etc. thanks to the guard ring's contouring. As a consequence, each string unit experiences the identical charging current I. As a result, potential will be distributed equally across the units.

Significant Points

The following considerations must be made while addressing string efficiency issues in figure 3.6:

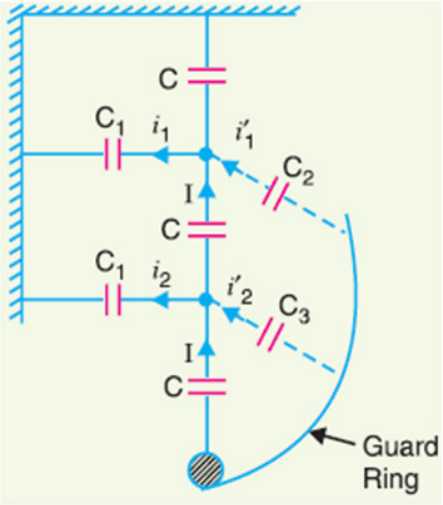

Figure 3.6: *Illustrates* the addressing string efficiency issues.

When a disc is close to a conductor, the maximum voltage is shown across it (i.e., line conductor). In other words, voltage across the string equals voltage between the line and the earth, which is phase voltage. Line Voltage across string = 3 Voltage.

Corona

Electric power transmission essentially entails the mass conveyance of electrical energy from producing units located several miles from major urban areas or consuming centres. This makes long-distance transmission lines essential for efficient power transfer, which unavoidably causes significant system losses. Recently, reducing those has been a big problem for power engineers, and in order to accomplish so, one has to have a thorough grasp of the many kinds of losses that might occur. One of them is the power system's corona effect, which significantly lowers the effectiveness of EHV (extra high voltage lines), on which we will focus.

Power system's corona effect and its causes

Two elements, which are of utmost significance for corona effect here, are as follows:

1) Across the line, an alternating potential difference must be given.

2) The conductor spacing has to be sufficient in relation to the line diameter.

Transmission line with a corona effect

The air around the conductors, which is made up of ions, is exposed to dielectric stress when an alternating current is induced to flow between two conductors of the transmission line whose distance is wide relative to their diameters. Nothing actually happens at low supply end voltages since there isn't enough stress to ionise the outside air. However, when the potential difference is forced to rise over a critical disruptive voltage of roughly 30 kV, the field strength rises and the air around it encounters stress that is strong enough to cause it to be broken up into ions, making the environment conducting. Owing to the passage of these

ions, this causes an electric discharge around the conductors that results in a faint luminous light, a hissing sound, and the release of ozone, which is easily recognised due to its distinctive smell. The corona effect is the name given to the phenomenon of electrical discharge that occurs in transmission lines at high voltages. The light and hissing noise intensify when the voltage across the lines is raised, causing a very significant power loss in the system that has to be taken into consideration.

Corona Effecting Factors

Both the physical characteristics of the environment and the circumstances of the line have an impact on the corona phenomena. The following are the variables that affect corona:

Atmosphere: Corona is impacted by the physical characteristics of the environment since it is created by the ionisation of the air around the conductors. When it is stormy outside, there are more ions than usual, which results in corona occurring at a considerably lower voltage than when it is sunny outside.

Conductor size: The conductors' configuration and shape have an impact on the corona effect. Because of the unevenness of the surface, which lowers the breakdown voltage value, a rough and irregular surface will produce more corona. Because of its uneven surface, a stranded conductor produces more corona than a solid conductor.

Separating conductors: There may not be a corona effect if the distance between the conductors is made extremely great relative to their diameters. This is due to the fact that a greater separation between conductors lowers electro-static forces at the conductor surface, preventing corona formation.

Volts per line: Corona is significantly impacted by line voltage. If it is low, the air around the conductors does not shift, and no corona is produced. Corona is created if the line voltage is high enough to cause electrostatic tensions to occur at the conductor surface that cause the air around the conductor to conduct.

Essential terms

The corona phenomena is crucial to the construction of an overhead transmission line. Consequently, it is beneficial to take into account the following terminology often employed in the investigation of corona effects:

Irreversible critical voltage

It is where corona first appears at phase-neutral voltage. Consider two conductors that are d cm apart and have radii of r cm. Potential gradient at the conductor surface is given by if V is the phase-neutral potential:

Inorderthatcoronaisformed,thevalueofgmustbemadeequaltothebreakdownstrengthof air. The breakdown strength of air at 76 cm pressure and temperature of 25°C is 30 kV/cm(*max*) or 21·2 kV/cm (*r.m.s.*) and is denoted by *go*. If *Vc*is the phase-neutral potentialrequiredunder theseconditions, then,

$$g_o = \frac{V_c}{r \log_e \frac{d}{r}}$$

where g_o = breakdown strength of air at 76 cm of mercury and 25°C
= 30 kV/cm (*max*) or 21·2 kV/cm (*r.m.s.*)

$\therefore$ Critical disruptive voltage, $V_c = g_o r \log_e \frac{d}{r}$

The disruptive voltage expression given above is for standard circumstances, or 76 cm Hg and 25 °C. On the other hand, if these circumstances change, the air density will likewise change, changing the value of go. Air density has a direct relationship with the value of go. Thus, the breakdown strength of air at a temperature of toC and a barometric pressure of b cm of mercury is go where,

δ air density factor= = 3.926 273+t

Under standard conditions, the value of 8 = 1.

Critical disruptive voltage, V =g&r log = d

Correction must also be made for the surface condition of the conductor. This is accounted for by multiplying the above expression by irregularity factor m.

Critical disruptive voltage, V

$$V_c = m_o g_o \delta r \log_e \frac{d}{r} \text{ kV/phase}$$

m_o = 1 for polished conductors
= 0·98 to 0·92 for dirty conductors
= 0·87 to 0·8 for stranded conductors

Visual critical voltage: It is the minimum phase-neutral voltage at which corona glow appears all along the line conductors. It has been seen that in case of parallel conductors, the corona glow does not begin at the disruptive voltage V but at a higher voltage V,, called visual critical voltage. The phase-neutral effective value of visual critical voltage is given by the following empirical formula:

$$V_v = m_v g_o \delta r \left(1 + \frac{0 \cdot 3}{\sqrt{\delta r}}\right) \log_e \frac{d}{r} \text{ kV/phase}$$

Power loss due to corona: Formation of corona is always accompanied by energy loss which is dissipated in the form of light, heat, sound and chemical action. When disruptive voltage is exceeded, the power loss due to corona is given by:

$$P = 242 \cdot 2 \left(\frac{f+25}{\delta}\right) \sqrt{\frac{r}{d}} \left(V - V_c\right)^2 \times 10^{-5} \text{ kW / km / phase}$$

f = supply frequency in Hz
V = phase-neutral voltage (*r.m.s.*)
V_c = disruptive voltage (*r.m.s.*) per phase

Where,

f- $(v - v)^2 \times 10^{-3}$ kW / km / phase P = 242-2 f +25) $\sqrt{}$ - δ

f = supply frequency in Hz

V phase-neutral voltage (r.m.s.). Disruptive voltage (r.m.s.) per phase.

Benefits and Drawbacks of Corona

Corona offers a lot of benefits and drawbacks. The benefits and drawbacks of a high voltage overhead line should be balanced in its proper design.

Advantages

The air around the conductor becomes conducting as a result of corona creation, increasing the conductor's virtual diameter. The electrostatic tensions between the conductors are lessened by the larger diameter.

Transients brought on by surges are lessened by corona.

Disadvantages

Energy is lost when one has corona. This has an impact on the line's transmission effectiveness. The conductor may corrode as a result of ozone's chemical activity, which is created by corona. Since the line's current draw from the corona is nonsinusoidal, the voltage drop in the line also is nonsinusoidal. Inductive interference with nearby communication cables might result from this.

Corona Effect Reduction Techniques

At a working voltage of 33 kV or above, it has been shown that strong corona effects are present. In order to prevent corona on sub-stations or bus-bars rated for 33 kV and greater voltages, careful design should be used. Otherwise, highly charged air might induce flash-over between the phases or in the insulators, severely harming the equipment. The following techniques may be used to lessen corona effects:

By enlarging the conductor: The voltage at which corona develops is increased by increasing conductor size, and as a result, the consequences of corona are greatly diminished. This is one of the explanations for why transmission lines employ ACSR conductors with bigger cross-sectional areas.

By widening the conductor gap: Corona effects may be reduced by reducing the distance between conductors, which raises the voltage at which corona develops. The cost of the supporting structure, such as larger cross arms and supports, may rise significantly if the spacing is raised too much.

Overhead Line Sag:

It is crucial that conductors be under safe strain while building an overhead line. In an effort to save conductor material, if the conductors are stretched too far between the supports, the stress within the conductor may reach hazardous levels, and in certain situations, the conductor may break from too much strain. The conductors are not completely stretched but are permitted to have a dip or sag in order to enable safe strain in them. Sag is the level difference between the lowest point on the conductor and the points of supports.

A conductor is shown hanging between two equally spaced supports in Figure 3.7. The conductors are not completely extended but are permitted to dip. O is the conductor's lowest point, while S is where there is a sag. The following details might be mentioned:

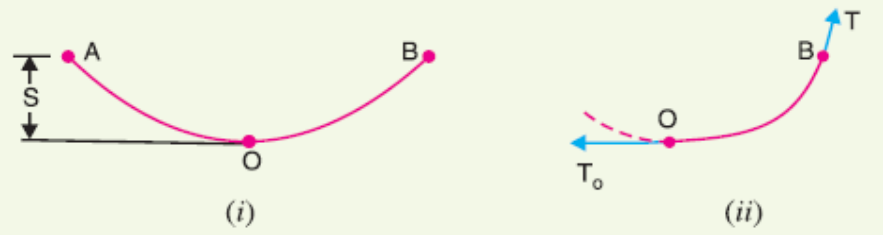

Figure 3.7: A conductor is shown hanging between two equally spaced supports.

The conductor assumes a catenary form when it is hung between two supports at the same height. Sag-span curves, on the other hand, resemble parabolas when the sag is relatively tiny in comparison to the span. Any point of strain on the conductor has tangential effects. As a result, as seen in Figure, tension TO at the lowest point O operates horizontally (ii).

Throughout the whole length of the wire, the horizontal tension component remains constant.

The horizontal tension operating at any point along the wire is about equivalent to the tension at supports. T = TO as a result, where T is the tension at support B.

Tension and conductor sagging: In the mechanical design of overhead wires, this is a crucial factor. In order to limit the amount of conductor material used and prevent the need for additional pole height, the conductor sag should be maintained to a minimum. Low conductor tension is also preferred since it allows for the use of weaker supports and prevents mechanical conductor failure. Low conductor tension and minimal sag, however, are not feasible. The reason for this is because a low tension indicates a loose wire and increased sag, while a low tension indicates a tight wire and low tension. As a result, in reality, a compromise is reached between the two.

Sag Calculation

In an overhead line, the sag should be set up such that the conductor tension is within acceptable bounds. The conductor weight, wind, ice loading, and temperature changes all have an impact on the tension. It is common practise to maintain conductor tension at less than 50% of its maximum tensile strength, which means that the minimum conductor tension safety factor should be 2. The sag and tension of a conductor will now be calculated for both the case of equal and uneven support levels. When the levels of the supports are equal. As shown in Figure 3.8., a conductor is placed between two equilevel supports A and B, with O serving as the lowest point. It is demonstrable that the mid-span will have the lowest point.

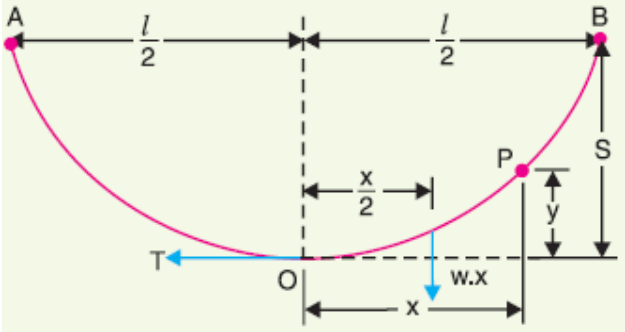

Figure 3.8: a conductor is placed between two equilevel supports A and B, with O serving as the lowest point

Let

l= Lengthofspan

w=Weightperunitlength ofconductor

T=Tension intheconductor.

Conductor point P: The coordinates of point P should be x and y, with the lowest point O serving as the origin. The two forces acting on the section OP of the conductor are, if the curvature is short enough, curved length equal to its horizontal projection (i.e., OP = x):

Theweight *wx*of conductoractingata distance *x*/2 fromo

Thetension *T* actingat*O*.

Equatingthemoments of abovetwo forcesaboutpoint*O*,weget,

$$T y = w x \times \frac{x}{2}$$

or

$$y = \frac{w x^2}{2 T}$$

The maximum dip (sag) is represented by the value of y at either of the supports A and B.

At support A, $x = l/2$ and $y = S$

$$\therefore \quad \text{Sag}, \quad S = \frac{w(l/2)^2}{2T} = \frac{w l^2}{8 T}$$

When the degree of assistance is uneven. We often see conductors hanging between supports at different heights in mountainous locations. A conductor is shown in Fig. hung between two supports A and B that are at various heights. O is the conductor's lowest point.

Let

l=Spanlength

h=Differenceinlevelsbetween twosupports

*x*1 = Distance of support at lower level (*i.e., A*) from *Ox*2 = Distance of support at higher level (*i.e. B*) from *OT*=Tension in theconductor in Figure 3.9.

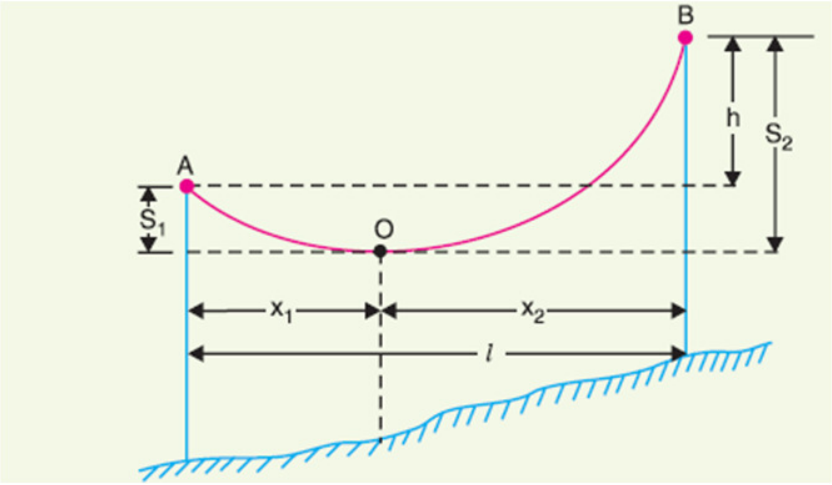

Figure 3.9: ***Illustrates*** **the tension in the conductor.**

Now $S_2 - S_1 = \frac{w}{2T}[x_2^2 - x_1^2] = \frac{w}{2T}(x_2 + x_1)(x_2 - x_1)$

$\therefore$ $S_2 - S_1 = \frac{w\,l}{2T}(x_2 - x_1)$ $[\because x_1 + x_2 = l]$

But $S_2 - S_1 = h$

$\therefore$ $h = \frac{w\,l}{2T}(x_2 - x_1)$

or $x_2 - x_1 = \frac{2\,Th}{w\,l}$ ...(*ii*)

Solving exps. (*i*) and (*ii*), we get,

$$x_1 = \frac{l}{2} - \frac{T\,h}{w\,l}$$

$$x_2 = \frac{l}{2} + \frac{T\,h}{w\,l}$$

S1 and S2 values can be simply determined after x1 and x2 have been discovered.

Impact of ice loading and wind.

Simply under conditions of calm air and at room temperature, when the conductor is only affected by its weight, are the aforementioned sag formulas valid. With reality, a conductor may be coated in ice and experience wind pressure at the same time. The weight of the conductor works vertically upward, while the weight of the ice acts downward. It is expected that the wind's force will act horizontally, or at a right angle to the conductor's projected surface. As a result, the vector sum of the horizontal and vertical forces acting on the conductor, as seen in Figure 3.10.

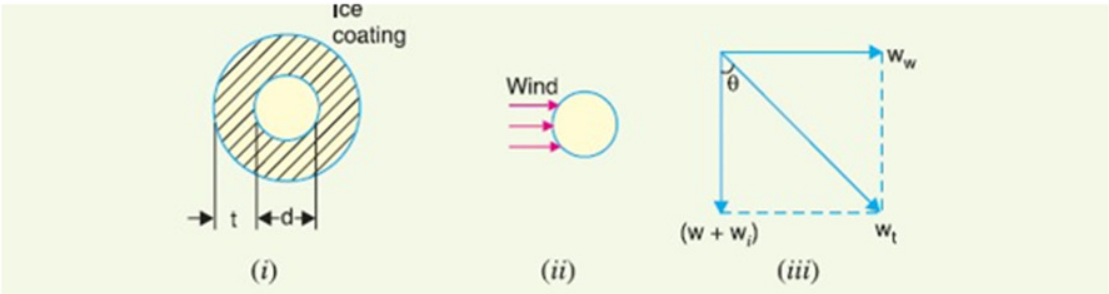

Figure 3.10: ***Illustrates*** **the conductor is the vector sum of horizontal and vertical forces.**

Total weight of conductor per unit length is,

$$w_t = \sqrt{(w + w_i)^2 + (w_w)^2}$$

Where

W = weight of conductor per unit length = conductor material density x volume per unit length

W; = weight of ice per unit length

= density of ice x volume of ice per unit length

π = density of ice x · [(d + 2t)² – d'²³] × 1 4

= density of ice Xπt (d+t)*

W = wind force per unit length Ww

= wind pressure per unit area projected area per unit length

= wind pressure × [(d+ 2t) x 1].

REFERENCES

[1] M. R. M. Asyraf, M. R. Ishak, M. R. Razman, en M. Chandrasekar, "Fundamentals of creep, testing methods and development of test rig for the full-scale crossarm: A review", *J. Teknol.*, 2019, doi: 10.11113/jt.v81.13402.

[2] K. R. McWilliam, A. Ivens, L. J. Morrison, M. R. Mugnier, en K. R. Matthews, "Developmental competence and antigen switch frequency can be uncoupled in Trypanosoma brucei", *Proc. Natl. Acad. Sci. U. S. A.*, 2019, doi: 10.1073/pnas.1912711116.

[3] S. Nam, S. Kang, B. N. Kim, I. H. Jung, en Y. M. Kim, "Post-annealing effect on transparent Mg-Zn aluminate solid solutions fabricated by spark plasma sintering", *J. Eur. Ceram. Soc.*, 2019, doi: 10.1016/j.jeurceramsoc.2019.08.027.

[4] F. Heyroth *et al.*, "Monocrystalline Freestanding Three-Dimensional Yttrium-Iron-Garnet Magnon Nanoresonators", *Phys. Rev. Appl.*, 2019, doi: 10.1103/PhysRevApplied.12.054031.

[5] C. O. Hayes *et al.*, "Low Loss Photodielectric Materials for 5G HS/HF Applications", *Int. Symp. Microelectron.*, 2019, doi: 10.4071/2380-4505-2019.1.000037.

[6] Y. Chen, "Carbon Fiber Composite Core Aluminum Conductor Detection", in *Engineering Energy Aluminum Conductor Composite Core (ACCC) and its Application*, 2019. doi: 10.1016/b978-0-12-815611-7.00003-x.

[7] Z. Luyao, L. Te, Z. Xiaoyu, G. Weiling, W. Zhenguo, en W. Shaohe, "Statistical Analysis of String Fracture and Core Breakdown of Composite Insulators in Zhejiang Province", 2019. doi: 10.1109/iSPEC48194.2019.8974954.

[8] A. Smirnov, N. Popova, E. Nikonenko, N. Ababkov, K. Knyaz'Kov, en N. Koneva, "Impact of modulated current welding on structural-phase state of 0.12 C-18Cr-10Ni-1 Ti-Fe austenitic steel", 2019. doi: 10.1063/1.5132207.

[9] Y. Yulita, "PENGARUH HARGA, STORE ATMOSPHERE, PROMOSI PENJUALAN DAN LOKASI TERHADAP IMPLUSE BUYING KENTUCKY FRIED CHICKEN (KFC) RAMAYANA PLAZA ANDALAS PADANG", *J. Wind Eng. Ind. Aerodyn.*, 2019.

[10] Syafrudin, "PERANCANGAN SISTEM PENYIRAMAN OTOMATIS TANAMAN BAWANG MERAH DENGAN METODE FUZZY SUGENO BERBASIS ARDUINO UNO", *Peranc. Sist. PENYIRAMAN OTOMATIS Tanam. BAWANG MERAH DENGAN Metod. FUZZY SUGENO Berbas. ARDUINO UNO*, 2019.

CHAPTER 4

BASICS OF CABLES USED IN TRANSMISSION LINE

Dr. P. Kishore Kumar, Associate Professor
Faculty of Engineering and Technology, Jain (Deemed-To-Be University), Bengaluru, Karnataka, India
Email Id- k.kishore@jainuniversity.ac.in

A cable buried underground basically consists of one or more conductors that are insulated properly, encased in a protective cover. Despite the fact that there are many different kinds of cables, the working voltage and service needs will determine which type of cable is utilised. In general, a cable has to meet the following conditions:

1) High conductivity tinned stranded copper or aluminium should be utilised as the conductor in cables. The purpose of stranding is to make the conductor more flexible and able to carry more current.
2) The conductor size has to be such that the cable can carry the appropriate load current without overheating and with a voltage drop that doesn't go above what is allowed.
3) For a high level of safety and dependability at the voltage for which it is intended, the cable's insulation must have the right thickness.
4) The cable has to have enough mechanical protection so that it can resist the rigorous handling it will experience while being laid.
5) The materials used to make cables should be completely chemically and physically stable all throughout[1], [2].

Cable construction

The overall layout of a 3-conductor wire is shown in Fig. The different elements are: I Conductors or Cores. Depending on the kind of service it is designed for, a cable may contain one or multiple cores (conductors). The 3-conductor wire in Fig., for instance, is utilised for 3-phase service. To provide the cable flexibility, the conductors, which are typically stranded and constructed of tinned copper or aluminium,

Insulation: Each core or conductor has a layer of insulation that is an appropriate thickness, the thickness of which depends on the voltage that the cable must be able to withstand. Impregnated paper, varnished cambric, or rubber mineral compound are some of the materials that are often used as insulation.

Metallic covering: A metallic coating of lead or aluminium is put over the insulation to protect the cable from moisture, gases, or other harmful liquids (acids or alkalies) in the soil and environment, as illustrated in Figure 4.1.

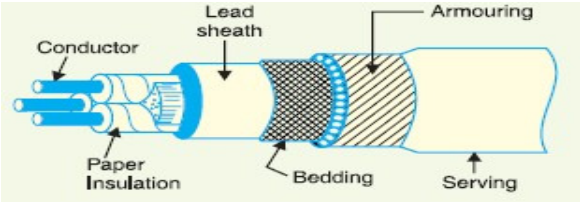

Figure 4.1: ***Illustrates*** **a metallic sheath of lead or aluminium is provided over the insulation.**

Bedding: A layer of bedding made of a fibrous substance like jute or hessian tape is put over the metallic sheath. Bedding serves to shield the metallic sheath from corrosive damage and mechanical harm from armoring.

Armouring: Armoring is put over the mattress and consists of one or two layers of steel tape or galvanised wire. Its function is to shield the cable from mechanical damage while it is being laid and handled. For certain cables, armoring may not be necessary.

Serving: A layer of fibrous material (like jute) resembling bedding is placed on top of the armoring to protect it from atmospheric conditions. Serving is what is meant here. It would not be out of place to emphasise that bedding, armouring, and serving are solely applied to the cables in order to protect the metallic sheath from mechanical damage and the conductor insulation[3], [4].

Cable Insulating Materials

The properties of the insulation used have a significant impact on how well a cable functions. Therefore, it is crucial to choose the right insulating material for cables. The following qualities should, in general, be present in the insulating materials used in cables:

1) High insulation resistance to prevent current leakage.
2) High dielectric strength to prevent cable electrical breakdown.
3) High mechanical toughness to sustain manipulation of cables mechanically.

It should not collect moisture from the air or the soil since it is non-hygroscopic. Moisture has a tendency to decrease insulation resistance and speed up wire deterioration. If the insulating substance is hygroscopic, a waterproof covering, such as a lead sheath, must be applied.

Non-inflammable

Low price to make the subsurface system an attractive option.

Acid and alkali inert to prevent any chemical activity. None of the insulating materials has every one of the qualities listed above. Therefore, the usage of an insulating material relies on the function for which the cable is intended as well as the desired level of insulation quality. Rubber, vulcanised India rubber, impregnated paper, varnished cambric, and polyvinyl chloride are the main insulating materials used in cables[5], [6].

Rubber: Rubber may be made from oil-based materials or the milky sap of tropical plants. It has an insulating resistivity of 1017 cm, a relative permittivity that ranges between 2 and 3, and a dielectric strength of roughly 30 kV/mm. Aside from the fact that pure rubber immediately absorbs moisture, its maximum safe temperature is only approximately 38 degrees Celsius, it is fragile and easily damaged by harsh handling, and it ages when exposed

to light. As a result, rubber that is pure cannot be utilised as insulation.

Vulcanized India Rubber (V.I.R.): It is made by combining mineral stuff, such as zine oxide, red lead, etc., with pure rubber and 3-5% sulphur. The thusly created composite is next rolled into thin sheets and separated into strips. The conductor is then covered with the rubber compound, which has been heated to a temperature of around 150oC. The whole process is known as vulcanization, and the final product is referred to as vulcanised India rubber. India rubber that has been vulcanised is more durable, wear-resistant, and mechanically strong than pure rubber. Due to the fact that sulphur interacts with copper extremely fast, cables with VIR insulation have tinned copper conductors as a result. In most cases, low and intermediate voltage cables employ VIR insulation.

Paper with an impurity: It comprises of paper that has been chemically pulped from wood chips and saturated with a substance like paraffin or napthenic material. The rubber insulation has practically been replaced by this form of insulation. This is due to its benefits of being inexpensive, having low capacitance, having a strong dielectric, and having excellent insulation resistance. The sole drawback is that paper is hygroscopic, meaning that even when saturated with the right substance, it will still absorb moisture and reduce the cable's insulating resistance. Paper insulated wires are always given some kind of protective covering and are never left unprotected because of this. Its ends are momentarily sealed with wax or tar if it must be left idle on the installation site. Paper insulated cables are utilised in locations with few joints in the cable path because they have a propensity to absorb moisture. For instance, they may be utilised successfully for low-voltage distribution in crowded regions where joints are often only present at the terminal device. VIR cables, on the other hand, will be more affordable and robust than paper insulated cables for smaller installations when the lengths are short and couplings are needed in many locations.

Cambric with a varnish: It is a cotton fabric that has been varnished and impregnated. Empire tape is another term for this kind of insulation. To allow for the sliding of one turn over another when the cable is bent, the cambric is applied to the conductor as a tape that has been covered with petroleum jelly compound. Due to the hygroscopic nature of varnished cambric, such cables are constantly covered with metal. Its permittivity ranges from 2.5 to 3.8 and its dielectric strength is around 4 kV/mm. 5. Vinyl chloride polymer (PVC). This insulation is made of a synthetic substance. It is produced when acetylene is polymerized and comes in the form of a white powder. This material is combined with certain substances known as plasticizers, which are liquids with high boiling points, to produce it as cable insulation. The plasticizer creates a gell and turns the substance plastic across the required temperature range. High insulating resistance, strong dielectric strength, and mechanical durability across a broad temperature range are all characteristics of polyvinyl chloride. It is virtually inert to several alkalies and acids and inert to oxygen. Because of this, this form of insulation is favoured over VIR in harsh environments like cement or chemical factories. PVC insulated cables are often used for low and medium home lighting and electricity installations since the mechanical qualities of PVC (such as elasticity, etc.) are not as excellent as those of rubber[7], [8].

Cable classification

According to I the kind of insulating material used in their construction and (ii) the voltage for which they are designed, cables for subterranean service may be categorised in two different ways. However, the latter form of categorization, which categorises cables into the following classes, is commonly preferred in Figure 4.2:

1) Low-tension cables (L.T.) are up to 1000 volts;
2) High-tension cables (H.T.) are up to 11,000 volts;
3) Super-tension cables (S.T.) are between 22 and 33 kvolts (iv)
4) Extra high-tension (EHT) cables, ranging in voltage from 33 to 66 kV (v)
5) Wires with a higher supervoltage than 132 Kv

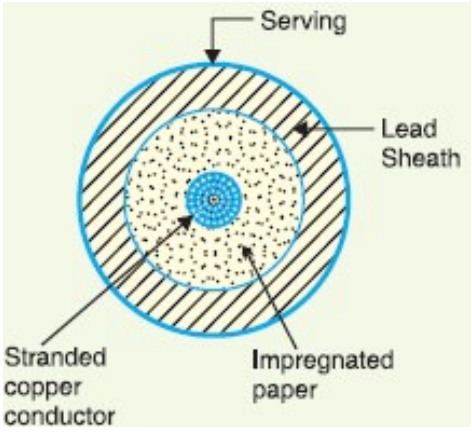

Figure 4.2: ***Illustrates*** **the cable inner structure of which contained impregnated paper.**

Depending on the service type it is designed for, a cable may contain one core or more. It might have one core, two cores, three cores, four cores, etc. Depending on the operating voltage and load requirement, either three-core cables or three-single-core cables may be utilised for a three-phase service. A single-core low tension cable's fabrication details are shown in Fig. Because the strains that emerge in the cable at low voltages (up to 6600 V) are often modest, the cable has an ordinary structure. It has a single, circular core made of tinned stranded copper (or aluminium) that is surrounded by layers of impregnated paper for insulation. A lead sheath covers the insulation, preventing moisture from penetrating the inside. There is a general serving of blended fibrous substance (jute, etc.) to prevent corrosion of the lead sheath. Due to the high sheath losses they are susceptible to, single-core cables are often not armoured. Single-core cables' main benefits are their ease of production and accessibility to bigger copper sections[9]–[11].

3-Phase Service Cables

In reality, 3-phase power delivery often necessitates subterranean lines. Three core cables or three single core cables may be utilised for the purpose. Due to financial considerations, 3-core cable (i.e., multi-core construction) is chosen at voltages up to 66 kV. However, 3-core cables get excessively big and cumbersome for voltages beyond 66 kV, thus single-core cables are utilised instead. For 3-phase service, the following kinds of cables are often employed in Figure 4.3:

1. Belted cables up to an 11 kV rating.
2. Cables with screens — 22 kV to 66 kV
3. Beyond 66 kV pressure cables

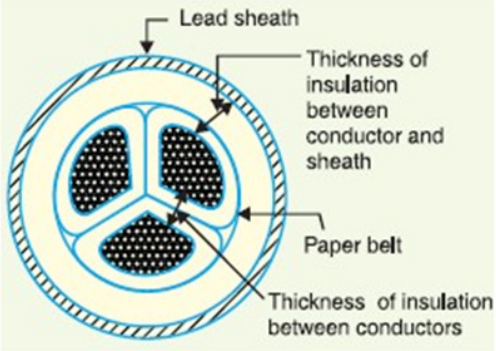

Figure 4.3: *Illustrates* the 3 phase cable lead sheath thickness.

Belted cables: Although these cables are designed to handle voltages up to 11 kV, under exceptional circumstances, their usage may be increased to 22 kV. A 3-core belted cable's fabrication details are shown in Figure 4.4. A layer of impregnated paper separates the cores from one another. The grouped insulated cores are wrapped in a second layer of impregnated paper tape, known as paper belt. To give the cable a circular cross section, the space between the insulated cores is filled with fibre insulating material (jute, etc.). To effectively use the available space, the cores are often stranded and may have an irregular form. Lead sheath is used to coat the belt in order to shield the cable from mechanical harm and moisture intrusion. A serving or more layers of armour are placed on top of the lead sheath (not shown in the figure0). As the electrostatic pressures created in cables for these voltages are more or less radial, that is, across the insulation, the belted type design is only appropriate for low and medium voltages. However, tangential stresses also play a significant role at high voltages (over 22 kV). Along the layers of paper insulation, these stresses operate. Tangential strains create leakage current along the layers of paper insulation because the insulation resistance of paper is fairly low along the layers. Local heating brought on by the leakage current raises the possibility of insulation collapse at any time. Screened cables are utilised to get around this problem, conducting leakage currents to ground via metallic screens.

Cable screens: These cables are designed to operate at voltages up to 33 kV, but under some circumstances, their usage may be increased to 66 kV. Htype cables and S.L type cables are the two main categories of screened cables.

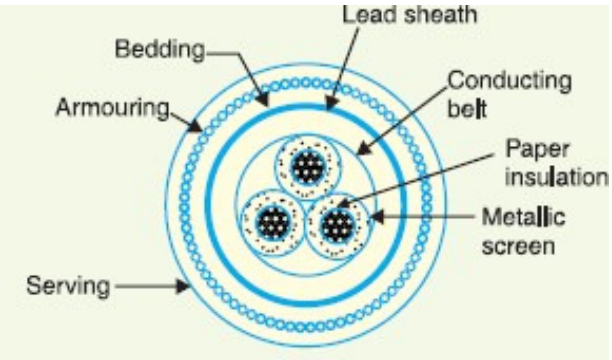

Figure 4.4: *Illustrates* the 33kv 3 phase structure of cable.

H-type cables: H. Hochstadter is the inventor of this sort of cable, therefore the name. The construction characteristics of a typical 3-core, H-type cable are shown in Fig. Layers of impregnated paper cover each core to act as insulation. Each core's insulation is protected by

a metallic screen, which is typically made of perforated aluminium foil. Metal screens are in touch with one another because of how the cores are put out. The three cores are encircled by an extra conducting belt (copper-woven fabric tape). The lead sheath, sleeping, armouring, and serving continue as normal even when the cable lacks an insulating belt. Each core screen's electrical connection to the conducting belt and the lead sheath may easily be seen. Due to the fact that all four screens one conducting belt and three core screens—as well as the lead sheath are at earth potential, the electrical strains are only radial, which lowers dielectric losses.

H-type cables are said to have two main benefits

First off, the metallic screens' holes help the cable to be completely impregnated with compound, removing any chance of air pockets or voids (vacuous spaces) in the dielectric. If there are vacancies, they tend to lower the cable's breakdown strength and may seriously harm the paper insulation. Second, the metallic screens improve the cable's ability to dissipate heat.

Type S.L. cables: The construction specifics for a 3-core *S.L. (separate lead) type cable are shown in Fig. Although essentially an H-type cable, each insulation core's screen is protected by its own lead sheath. There is merely armouring and serving offered; there is no overall lead sheath. Two things set S.L. type cables apart from H-type cables. First off, the distinct sheaths reduce the likelihood of core-to-core breakage. Second, the removal of the overall lead sheath makes cable bending simpler. The three lead sheaths of S.L. cable have three times as many leads as H-cable, but they are significantly thinner, requiring more attention during manufacturing in Figure 4.5.

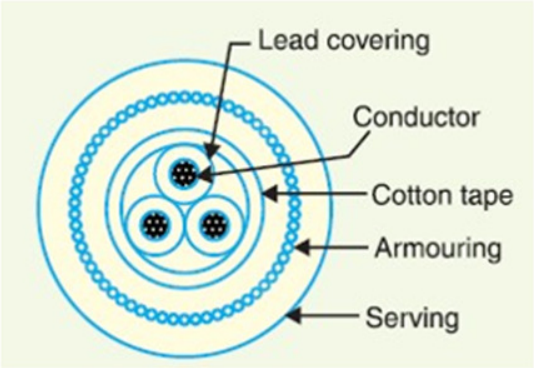

Figure 4.5: *Illustrates* the core diagram of S.L. types of cable.

Solid type pressure cables are problematic for voltages over 66 kV because there is a risk of insulation breakage because to the existence of voids. Pressure cables are utilised when the operating voltages are higher than 66 kV. These cables are known as pressure cables because the gaps in them are filled by raising the compound's pressure. Oil-filled cables and gas pressure cables are the two most often utilised forms of pressure cables.

Resistance to Insulation in Single-Core Cables

In order to stop leakage current, the cable conductor is equipped with an adequate thickness of insulating material. Radial current leakage travels through the insulator. Insulation resistance of the cable refers to the resistance provided by insulation to leakage current.

The cable's insulation resistance has to be quite strong for successful functioning. Consider

the single-core cable shown in Fig. with a conductor radius of r1 and an interior sheath radius of r2. Let l be the cable's length and be the insulation's resistance.

Consider an extremely thin layer of insulation with a radius of x and a thickness of dx. Leakage current tends to travel along a length of dx, and the area of the X-section that this flow is offered is 2πx l.

Insulation resistance of the layer being considered,

$$= \rho \frac{dx}{2\pi x l}$$

Insulation resistance of the whole cable is,

$$R = \int_{r_1}^{r_2} \rho \frac{dx}{2\pi x l} = \frac{\rho}{2\pi l} \int_{r_1}^{r_2} \frac{1}{x} dx$$

$$R = \frac{\rho}{2\pi l} \log_e \frac{r_2}{r_1}$$

This demonstrates that a cable's insulation resistance is inversely correlated with its length. In other words, the insulation resistance of a cable reduces as its length grows and vice versa.

Single-Core Cable Capacitance

One may compare a single-core wire to two very long co-axial cylinders. The inner cylinder of the cable, which represents the conductor (or core), is represented by a lead sheath that is at earth potential. Consider a single core cable that has an inner sheath diameter of D and a conductor diameter of D. Let Q coulombs represent the charge per axial metre of the cable, and let represent the permittivity of the insulation material positioned between the core and the lead sheath. Naturally, * = 0 r, where r is the insulation's relative permittivity in Figure 4.6. Consideracylinderofradius*x*metresandaxiallength1metre.Thesurfaceareaofthiscylinderis

=2π*x*×1 =2 π *x*m2

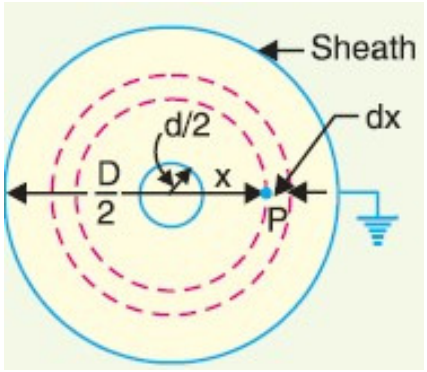

Figure 4.6: ***Illustrates*** **to consideracylinderofradius*x*metresandaxiallength1metres.**

∴ Electric flux density at any point *P* on the considered cylinder is

$$D_x = \frac{Q}{2\pi x} \text{ C/m}^2$$

Electric intensity at point *P*, $E_x = \frac{D_x}{\varepsilon} = \frac{Q}{2\pi x \varepsilon} = \frac{Q}{2\pi x \varepsilon_0 \varepsilon_r}$ volts/m

Ex dx is the amount of labour required to move a unit positive charge from point P across a distance dx in the direction of the electric field. As a result, the potential difference V between the conductor and sheath, which represents the work done in transferring a unit positive charge, is given by:

$$V = \int_{d/2}^{D/2} E_x dx = \int_{d/2}^{D/2} \frac{Q}{2\pi x \varepsilon_0 \varepsilon_r} dx = \frac{Q}{2\pi \varepsilon_0 \varepsilon_r} \log_e \frac{D}{d}$$

Capacitance of the cable is

$$C = \frac{Q}{V} = \frac{Q}{\frac{Q}{2\pi \varepsilon_0 \varepsilon_r} \log_e \frac{D}{d}} \text{ F/m}$$

$$V = \int_{d/2}^{D/2} E_x dx = \int_{d/2}^{D/2} \frac{Q}{2\pi x \varepsilon_0 \varepsilon_r} dx = \frac{Q}{2\pi \varepsilon_0 \varepsilon_r} \log_e \frac{D}{d}$$

Capacitance of the cable is

$$C = \frac{Q}{V} = \frac{Q}{\frac{Q}{2\pi \varepsilon_0 \varepsilon_r} \log_e \frac{D}{d}} \text{ F/m}$$

$$= \frac{2\pi \varepsilon_o \varepsilon_r}{\log_e (D/d)} \text{ F/m}$$

$$= \frac{2\pi \times 8{\cdot}854 \times 10^{-12} \times \varepsilon_r}{2{\cdot}303 \log_{10} (D/d)} \text{ F/m}$$

Dielectricstressinasinglecorecable:

The electric intensity at any distance x from the center of cable O is given by (Figure 4.7),

Ex = [Q / 2πε0εr] (1 / x) volt / meter

Where

ε0 = Absolute Permittivity = 8.854 × 10 – 12 Farad / meter

εr = Relative Permittivity

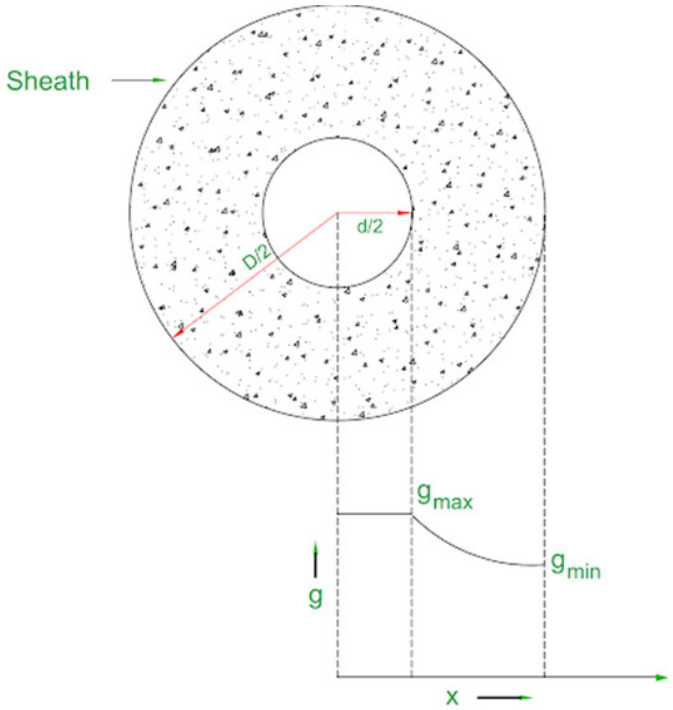

Figure 4.7: Dielectric stress in a single core

Electrostatic pressures are applied to a cable's insulation while it is in use. Dielectric stress is the term for this. Any point in a cable where there is dielectric stress affects the potential gradient (or *electric intensity) there in Figure 4.8.

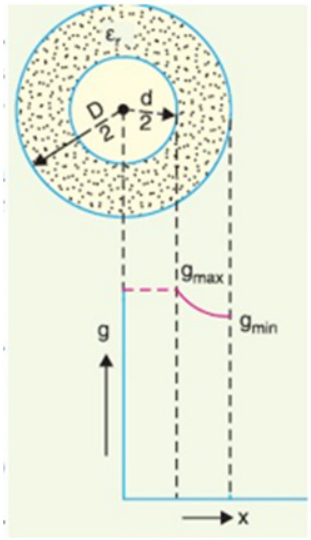

Figure 4.8: *Illustrates* the dielectric stress affects the potential gradient

Consider a single core cable with core diameter d and internal sheath diameter D. As proved in Art 11.8, the electric intensity at a point x metres from the centre of the cable is

$$E_x = \frac{Q}{2\pi \varepsilon_o \varepsilon_r x} \text{ volts/m}$$

By definition, electric intensity is equal to potential gradient. There- fore, potential gradient g at a point x metres from the centre of cable is,

$$g = E_x$$

$$g = \frac{Q}{2\pi\varepsilon_o\varepsilon_r x} \text{ volts/m}$$

As proved, potential difference V between conductor and sheath is,

$$V = \frac{Q}{2\pi\varepsilon_o\varepsilon_r}\log_e\frac{D}{d} \text{ volts}$$

$$Q = \frac{2\pi\varepsilon_o\varepsilon_r V}{\log_e\frac{D}{d}}$$

Substituting the value of Q from exp. (ii) in exp. (i), we get,

$$g = \frac{\frac{2\pi\varepsilon_o\varepsilon_r V}{\log_e D/d}}{2\pi\varepsilon_o\varepsilon_r x} = \frac{V}{x\log_e\frac{D}{d}} \text{ volts/m}$$

The fluctuation in stress in the dielectric. It is obvious that the dielectric stress is greatest near the conductor surface and that it continuously decreases the more we are from the conductor. It should be remembered that maximal stress plays a crucial role in cable design. For instance, the insulation employed must have a dielectric strength of at least 5 kV/mm if a cable is to be operated at a voltage where the *maximum stress is 5 kV/mm; otherwise, cable breakage would become unavoidable. The potential gradient changes inversely with the distance x. As a result, the potential gradient will be at its highest when x is at its lowest value, that is, at x = d/2 or at the conductor's surface. The potential gradient, however, will be at its lowest point at x = D/2 or the sheath surface.

The greatest possible gradient is,

$$g_{max} = \frac{2V}{d\log_e\frac{D}{d}} \text{ volts/m}$$

Minimum potential gradient is,

$$g_{min} = \frac{2V}{D\log_e\frac{D}{d}} \text{ volts/m}$$

GradingofCables

The process of achieving uniform electrostatic stress in the dielectric of cables is known as gradingofcables:

Electrostatic stress in a single core cable has previously been shown to peak (gmax) near the conductor surface and gradually decrease as we travel towards the sheath. Gmax, or the electrostatic stress at the conductor surface, determines the maximum voltage that may be supplied to a cable safely. A homogeneous dielectric cable must have dielectric strength greater than gmax in order to function safely. If a high strength dielectric is utilised for a cable, it is only effective close to the conductor where stress is greatest. However, the electrostatic tension reduces as we go away from the conductor, causing the dielectric to be

too strong. There are two reasons why an uneven stress distribution in a cable is bad. First, a larger cable is needed since the insulation has to be thicker. Second, it can cause insulation to break down. A consistent stress distribution in cables is required to address the aforementioned drawbacks. This may be done by dispersing the stress such that the outer layers of the dielectric experience an increase in its value. This is referred to as cable grading. The two primary techniques for grading cables are as follows:

1) Grading of capacitance
2) Grade intersheath
3) Grading of Capacitance

Capacitance grading is the method of employing layers of various dielectrics to achieve uniformity in the dielectric stress. A composite dielectric is used in lieu of the homogeneous dielectric in capacitance grading. The relative permittivity r of each layer in the composite dielectric is inversely proportional to its distance from the centre thanks to the use of numerous layers of varied dielectrics. At every point in the dielectric under these circumstances, the potential gradient's value is *constant and independent of the location's distance from the centre. In other words, the cable's dielectric stress is uniform throughout, and the grading is perfect. However, the usage of an unlimited number of dielectrics is required for optimal grading, which is not practical. In actual usage, two or three dielectrics are utilised, with the one with the greatest permittivity being used next to the core, in decreasing order of permittivity. A nice explanation of the capacitance grading may be found in Figure 4.9. There are three different types of dielectrics, each with a different outer diameter (d1, d2, and D) and relative permittivity (1, 2, and 3).

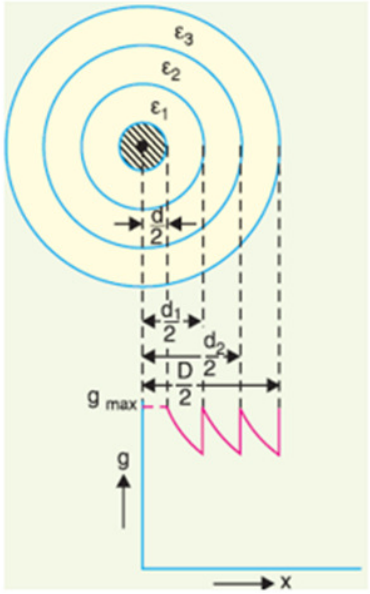

Figure 4.9: the explanation of the capacitance grading.

If the permittivity's are such that Ɛ>Ɛ> £3 and the three dielectric are worked at the same maximum stress, then,

$$\frac{1}{\varepsilon_1 d} = \frac{1}{\varepsilon_2 d_1} = \frac{1\dagger}{\varepsilon_3 d_2}$$

$$\varepsilon_1 d = \varepsilon_2 d_1 = \varepsilon_3 d_2$$

Potential difference across the inner layer is,

$$V_1 = \int_{d/2}^{d_1/2} g\,dx = \int_{d/2}^{d_1/2} \frac{Q}{2\pi\varepsilon_0\varepsilon_1 x}dx$$

$$= \frac{Q}{2\pi\varepsilon_0\varepsilon_1}\log_e\frac{d_1}{d} = \frac{g_{max}}{2} d\log_e\frac{d_1}{d}\left[\because \frac{Q}{2\pi\varepsilon_0\varepsilon_1} = {}^{*}\frac{g_{max}}{2} d\right]$$

Similarly, potential across second layer (V) and third layer (V3) is given by ;

$$V_2 = \frac{g_{max}}{2} d_1 \log_e\frac{d_2}{d_1}$$

$$V_3 = \frac{g_{max}}{2} d_2 \log_e\frac{D}{d_2}$$

Total p.d. between core and earthed sheath is V = V₁+ V₂+ V3 d = Emax dlog, 4+d, 108, +d, 108, 2 2 log.

$$V = V_1 + V_2 + V_3$$

$$= \frac{g_{max}}{2}\left[d\log_e\frac{d_1}{d} + d_1\log_e\frac{d_2}{d_1} + d_2\log_e\frac{D}{d_2}\right]$$

If the cable had homogeneous dielectric, then, for the same values of d, D and gmax the permissible potential difference between core and earthed sheath would have been

$$V' = \frac{g_{max}}{2} d\log_e\frac{D}{d}$$

Evidently, V> V', i.e., a graded cable may be operated at a higher potential than a non-graded cable for a given dimension of the cable. Alternatively, graded cable will be smaller than non-graded cable with the same safe potential. It's possible to remark the following:

(i) All of the voltages in the aforementioned expressions should be considered as peak values rather than r.m.s. values since the permitted values of gmax are peak values.

(ii) In the event where the maximum stress in the three dielectrics differs,

$$V = \frac{g_{1max}}{2} d\log_e\frac{d_1}{d} + \frac{g_{2max}}{2} d_1\log_e\frac{d_2}{d_1} + \frac{g_{3max}}{2} d_2\log_e\frac{D}{d_2}$$

This method's main drawback is the scarcity of high-grade, reasonably priced dielectrics with permittivity ranges that match the specifications.

The Inters Health Scale

A homogenous dielectric is employed in this technique of cable grading, however it is separated into different layers by sandwiching metallic inter sheaths between the core and lead sheath. The intersheaths are maintained at acceptable potentials, which are situated halfway between the core potential and the earth potential. This configuration enhances the voltage distribution in the cable's dielectric, resulting in a more uniform potential gradient. Consider a cable with a d-diameter core and a d-diameter lead sheath. Assume that a homogeneous dielectric is filled with two inter sheaths that are d1 and d2 in diameter and kept at certain set potentials. Let V1 be the voltage between the core and intersheath 1, V2 be the voltage between intersheath 1 and 2, and V3 be the voltage between intersheath 2 and the outer lead sheath. Each sheath may be thought of as a uniform single core cable since there is a distinct potential difference between the inner and outer layers of each inter sheath. Maximum stress between core and inter sheath 1 has shown that,

$$g_{1max} = \frac{V_1}{\frac{d}{2}\log_e \frac{d_1}{d}}$$

$$g_{2max} = \frac{V_2}{\frac{d_1}{2}\log_e \frac{d_2}{d_1}}$$

$$g_{3max} = \frac{V_3}{\frac{d_2}{2}\log_e \frac{D}{d_2}}$$

Since the dielectric is homogeneous, the maximum stress in each layer is the same i.e.,

$$g_{1max} = g_{2max} = g_{3max} = g_{max} \text{ (say)}$$

$$\frac{V_1}{\frac{d}{2}\log_e \frac{d_1}{d}} = \frac{V_2}{\frac{d_1}{2}\log_e \frac{d_2}{d_1}} = \frac{V_3}{\frac{d_2}{2}\log_e \frac{D}{d_2}}$$

As the cable behaves like three capacitors in series, therefore, all the potentials are in phase i.e. Voltage between conductor and earthed lead sheath is

$V = V_1+V_2+V3$

Inters health rating has three main drawbacks. Fixing the sheath potentials is difficult, to start with. Second, there is a chance that the intersheaths will be harmed during installation and transit, which might lead to localized concentrations of the potential gradient. Thirdly, significant losses from charging currents occur in the intersheaths. Intersheaths grading is seldom employed because of these factors in Figure 4.10.

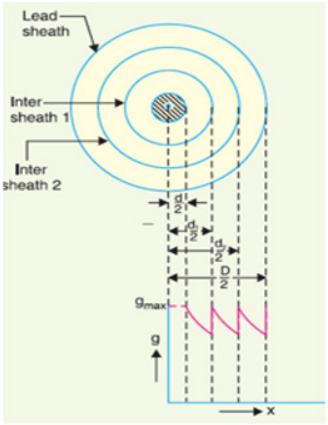

Figure 4.10: The inter-sheaths grading is rarely used.

REFERENCES

[1] M. A. Shokry, A. Khamlichi, F. Garnacho, J. M. Malo, en F. Alvarez, "Detection and localization of defects in cable sheath of cross-bonding configuration by sheath currents", *IEEE Trans. Power Deliv.*, 2019, doi: 10.1109/TPWRD.2019.2903329.

[2] M. Asif, H. Y. Lee, U. A. Khan, K. H. Park, en B. W. Lee, "Analysis of Transient Behavior of Mixed High Voltage DC Transmission Line under Lightning Strikes", *IEEE Access*, 2019, doi: 10.1109/ACCESS.2018.2889828.

[3] V. T. Rathod, "A review of electric impedance matching techniques for piezoelectric sensors, actuators and transducers", *Electronics (Switzerland)*. 2019. doi: 10.3390/electronics8020169.

[4] S. Adhe Putri, A. asni B, en A. fitri Saiful rahman, "Perancangan Prototype Mesin Pembersih kabel transmisi listrik berbasis internet", *J. Tek. Elektro Uniba (JTE UNIBA)*, 2019, doi: 10.36277/jteuniba.v4i1.48.

[5] F. Lv, P. Zhang, Z. Tang, Y. Yue, en K. Yang, "A guidedwave transducer with sprayed magnetostrictive powder coating for monitoring of aluminum conductor steel-reinforced cables", *Sensors (Switzerland)*, 2019, doi: 10.3390/s19071550.

[6] X. Liu, Y. Hu, en M. Cai, "Free vibration analysis of transmission lines based on the dynamic stiffness method", *R. Soc. Open Sci.*, 2019, doi: 10.1098/rsos.181354.

[7] Z. Pan, J. Yang, X. B. Cheng, en R. Chen, "A Low-Impedance Transmission Line Transformer Based on the Multicore Coaxial Transmission Line", *IEEE Trans. Plasma Sci.*, 2019, doi: 10.1109/TPS.2019.2907550.

[8] "Soft Computing Methods for Fault Detection in Power Transmission Lines", *Int. J. Eng. Adv. Technol.*, 2019, doi: 10.35940/ijeat.a1047.1291s319.

[9] C. Z. Fu, W. R. Si, L. Quan, en J. Yang, "Numerical study of heat transfer in trefoil buried cable with fluidized thermal backfill and laying parameter optimization", *Math. Probl. Eng.*, 2019, doi: 10.1155/2019/4741871.

[10] L. I. Iuferev, D. V. Ermolenko, en O. A. Roshchin, “Electrical energy transmission systems at elevated frequency”, *Int. J. Innov. Technol. Explor. Eng.*, 2019, doi: 10.35940/ijitee.G6227.0881019.

[11] C. Pothisarn en C. Jettanasen, “The study on wavelet coefficient behavior of simultaneous fault on the hybrid between overhead and underground distribution system”, *Int. J. Smart Grid Clean Energy*, 2019, doi: 10.12720/sgce.8.3.367-371.

CHAPTER 5

CABLE CAPACITANCE

B. Spoorthi, Assistant Professor
Faculty of Engineering and Technology, Jain (Deemed-To-Be University), Bengaluru, Karnataka, India
Email Id- spoorthi.b@jainuniversity.ac.in

Because conductors in cables are closer to one another and the earthed sheath and are separated by a dielectric with a permittivity substantially higher than that of air, the capacitance of a cable system is far more significant than that of an overhead line. A system of capacitances in a three-core, belted cable used for a three-phase system is seen in Fig. Electrostatic fields are established in the cable as seen in Figure 5.1. Because there is a potential difference between adjacent pairs of conducts as well as between each conductor and the sheath (i). As shown in Fig., these electrostatic forces result in conductor-earth capacitances Ce and core-core capacitances Cc (ii). The sheath creating the star point separates the three Ce from the three Cc, which are joined in a star rather than a delta manner[1], [2].

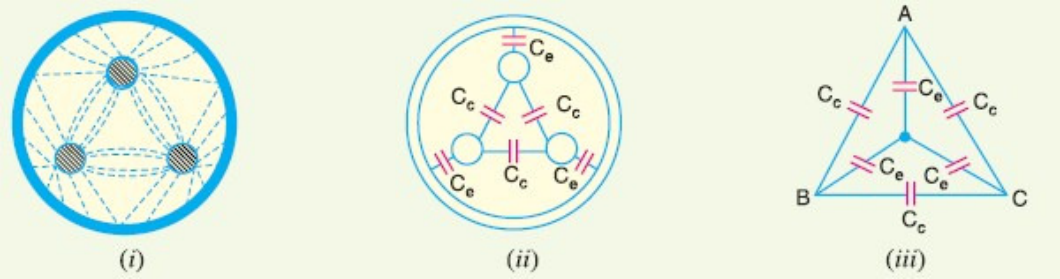

Figure 5.1: the potential difference between adjacent pairs of conducts

They lay of a belted cable makes it reasonable to assume equality of each *Cc* and each *Ce*. The threedelta connected capacitances*Cc*[See Figure 5.2(*i*)] can be converted into equivalent star connectedcapacitances as shown in Figure 5.2 (*ii*). It can be easily *shown that equivalent star capacitance *Ceq*isequaltothree timesthe deltacapacitance*Cci.e.Ceq*=3*Cc*.

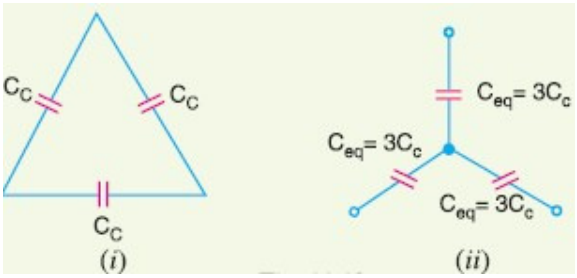

Figure 5.2: *Illustrates* the equivalent star connectedcapacitances.

The system of capacitances shown in Figure 5.3(*ii*) reduces to the equivalent circuit shown in Figure 5.3 (*i*).There fore, the who lecable is equivalent to three star-connected capacitor seach of capacitance

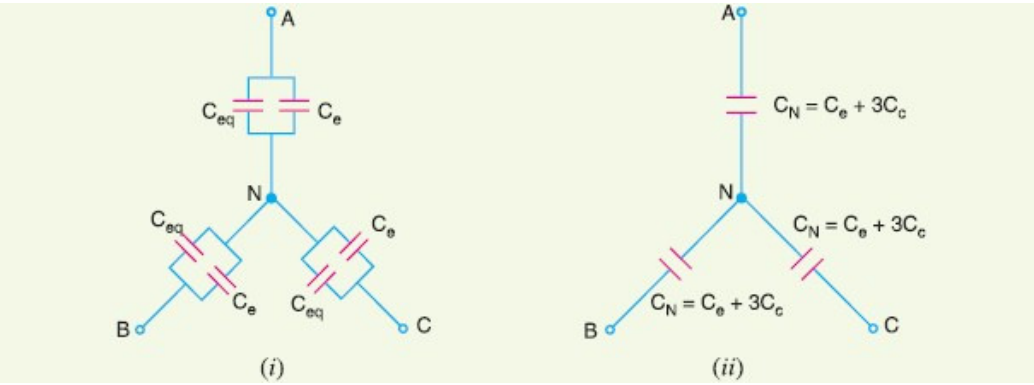

Figure 5.3: *Illustrates* system of capacitances.

$$C_N = C_e + C_{eq}$$
$$= C_e + 3C_c$$

If V_{ph} is the phase voltage, then charging current I_C is given by ;

$$I_C = \frac{V_{ph}}{\text{Capacitive reactance per phase}}$$
$$= 2\pi f V_{ph} C_N$$
$$= 2\pi f V_{ph} (C_e + 3C_c)$$

Measurements ofCeandCc

Although core-core capacitance *Cc* and core-earth capacitance *Ce* can be obtained from the empiricalformulas for belted cables, their values can also be determined by measurements. For this purpose,thefollowingtwomeasurementsarerequired. Inthefirstmeasurement,thethreecoresarebunchedtogether(*i.e*.commoned)andthecapacitance is measured between the bunched cores and the sheath. The bunching eliminates all thethree capacitors *Cc*, leaving the three capacitors *Ce*in parallel. Therefore, if *C*1is the measuredcapacitance,thistestyields:

$$C_1 = 3\,C_e$$

or

$$C_e = \frac{C_1}{3}$$

Knowingthevalueof *C*1,thevalueof*Ce*canbedetermined.

Inthesecondmeasurement,twocoresarebunchedwiththesheathandcapacitanceismeasuredbetweenthemandthe thirdcore.Thistestyields2*Cc*+ *Ce*. If*C*2isthemeasuredcapacitance,then,*C*2 = 2*Cc*+ *Ce*.

Since the value of Ce is known from the first test and C2 has been discovered experimentally, the value of Cc may also be established. It should be noted that another test may directly determine the value of CN (= Ce + 3Cc) if that value is needed. In this test, the third core is left free or attached to the sheath while the capacitance between the first two cores or lines is measured. This eliminates one of the capacitors *Ce* so that if *C*3 is themeasured capacitance,then, Transient Overvoltages on Transmission Lines (Travelling Waves on Power Systems)[3], [4].

$$C_3 = C_c + \frac{C_c}{2} + \frac{C_e}{2}$$
$$= \frac{1}{2}(C_e + 3C_c)$$
$$= \frac{1}{2} C_N$$

An electrostatic flux is produced together with the construction of a potential difference between the conductors of an overhead transmission line, while a magnetic field is produced when current flows through the conductor. While the inductances are connected in series with the line, the electrostatic fields are really generated by a number of shunt capacitors. Figure 5.4 shows the part of the line next to the generator.

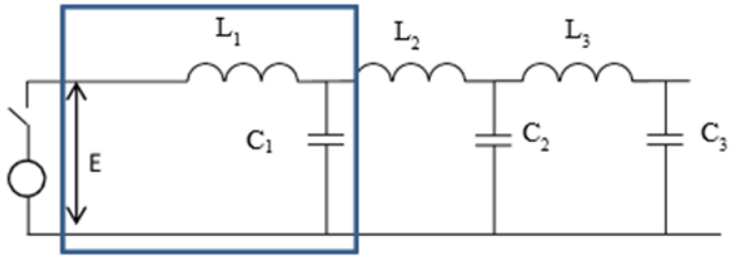

Figure 5.4: ***Illustrates*** **the line adjacent to the generator.**

By shutting the switch, allow the voltage E to be supplied abruptly to the circuit. In these circumstances, the capacitance C1 requires a significant initial charging current, hence the whole voltage will initially be utilised to drive a charging current through the circuit comprised of L1 and C1 connected in series, the farther away from the generator, the longer it will take for the full line voltage E to be established after the switch is closed. As the charge on C1 builds up, its voltage will rise, and this voltage will start to charge C2 by driving a current through the inductance L2. It is also obvious that current and voltage are closely related, and that each voltage phenomena has a corresponding current phenomenon. The progressive development of the line voltage may be attributed to a voltage wave moving from the generator to the far end, and the accompanying current wave will be caused by the line capacitances gradually being charged[5], [6].

The impact of 60 Hz alternate voltage

Due to the very fast propagation velocity, the voltage E has been assumed to be constant in the treatment above. In actuality, this assumption is often sufficient. For the majority of lines, the impulse would have travelled the whole distance before enough time had passed for the 60 Hz voltage to noticeably shift. By the conclusion of the first cycle, the initial impulse will have travelled a distance of (3 108)/60, or 5 106 metres, assuming that the actual value of v is 3 108 m/sec. This suggests that the line would need to be 5000 km long in order to carry the whole voltage distribution for one cycle. Such a long line is not conceivable[7], [8].

The Line with Open Circuits

Allow for a quick switchover of a source of constant voltage E on a line that is open-circuited at the other end. When this happens, a rectangular voltage wave with amplitude E and its corresponding current wave with amplitude I = E/Zc would move with velocity v in the direction of the open end while disregarding the influence of line resistance and potential conductance to earth. Depicts the circumstances just as the waves reach the open end, with the whole line at voltage E and carrying current I. Since the current at the open end must inevitably become zero, the magnetic field's stored energy must be released in some manner. Since resistance and conductance have not been taken into account in the situation at hand, this energy can only be utilised to generate an equivalent quantity of electrostatic field. In the event that this is carried out, the voltage at the point will be raised by an amount e such that the energy obtained by the electrostatic field (0.5Cv2) is equal to the energy lost by the electromagnetic field (0.5LI2), making the total voltage at the open end 2E. Thus, the open end of the line may be thought of as the source of a second voltage wave with amplitude E and velocity v that travels back to the source. The state of affairs on the line will be in which the incoming and reflected voltage waves are superposed at some point after the original wave arrives at the open end. This results in a step in the voltage wave, which will move back towards the source with a velocity v. Since no current may go through the open circuit, the doubling of the voltage at the open end must be accompanied by the disappearance of the current. This is the same as when a reflected current wave with a negative sign is created, as shown in Figure 5.5.

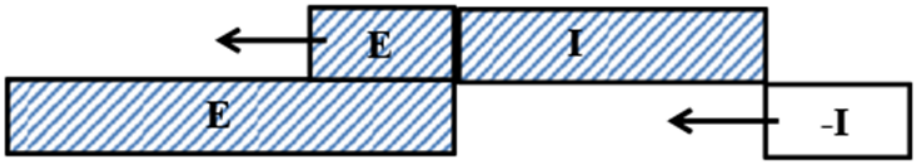

Figure 5.5: ***Illustrates*** **the establishment of a reflected current wave of negative sign.**

Attheinstantthereflectedwavesreachtheend G,thedistributionalongthewholelinewillbeavoltageo f 2E and a current of zero as in Figure 5.6.

Figure 5.6: ***Illustrates*** **thedistributionalongthewholelinewillbeavoltageof 2E and a current of zero.**

If the source holds the voltage at G to the value E, then there must be a reflected voltage of -E and an accompanying current wave of -I. When they have moved a short distance down the line, the circumstances will resemble those in Figure 5.7.

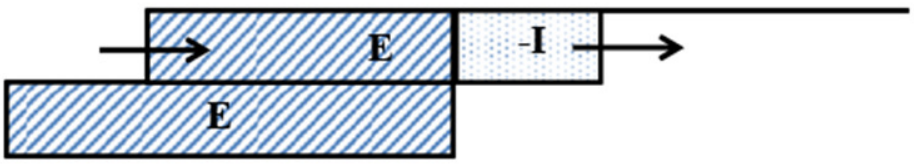

Figure 5.7: ***Illustrates*** **the voltage is held by the source to the value E.**

Voltage E and current -I will be present down the line when they reach the open end. When these reflected waves reach the end G, they will have eliminated both the voltage and current distributions, returning the line briefly to its initial condition. The reflected waves as a result of this will be -E and +I. After then, the cycle above is repeated[7], [8].

The Circuit-Breaking Line

In this situation, the voltage at the far end of the line must by necessity be zero, causing electrostatic energy to be transformed into electromagnetic energy when each component of the voltage wave reaches the end. As a result, the voltage is reflected with a sign reversal while the current is reflected with no sign change, causing the current to increase to 2I on the first reflection phases that the phenomena goes through. The class of specialized electrical devices known as linear electric motors converts' electrical energy directly into mechanical energy of translator motion. A linear-motion load may be driven by linear electric motors without the need of intermediary gears, screws, or crank shafts. The following categories apply to linear electric motors:

1) Synchronous motors, such as reluctance and stepping motors.
2) DC motors.
3) Induction motors.
4) Oscillating motors.
5) Hybrid motors.

DC linear motor applications are few. The most widely used are linear induction motors (LIMs) and linear synchronous motors (LSMs), which are commercially produced in a number of nations and have a wide range of uses. Cutting a rotary motor along its radius from the shaft's axis to the stator core's outer surface and rolling it out flat yields a linear motor.

Synchronous linear motors

Basic constructions and geometries

The mechanical motion of an LSM is synchronised with the magnetic field, meaning that it moves at the same speed as the moving magnetic field. The action of a travelling magnetic field created by a polyphase winding and a collection of magnetic poles N, S,..., N, S or a variable resistance ferromagnetic rail may produce the push (propulsion force) (LSMs with AC armature windings), Magnetic field generated via electrically switched DC windings, a collection of magnetic poles (N, S,..., N, S), or a ferromagnetic rail with changing reluctance (linear stepping or switched reluctance motors) in Figure 5.8.

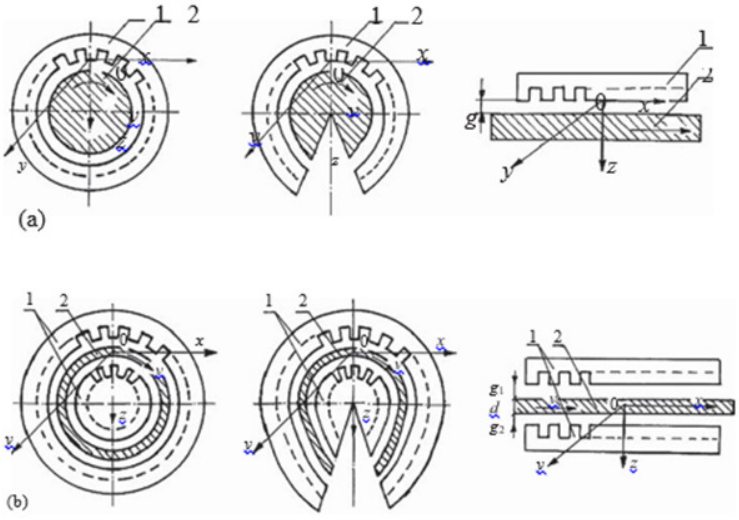

Figure 5.8: Evolutionofarotaryinductionmotor:(a)solid-rotorinductionmotorintoaflat,single-sidedLIM and(b)hollow-rotorinductionmotorintoaflatdouble-sidedLIM.1,primary;2,secondary.

The armature or forcer is the component that generates the moving magnetic field. The component that generates the DC magnetic flux or variable reluctance is referred to as the variable reluctance platen, salient-pole rail, reaction rail, or field excitation system (if the excitation system is present). The labels main and secondary are better avoided since they are only appropriate for transformers or LIMs. An LSM may operate regardless of which component is mobile and which is fixed. It is customary for AC polyphase synchronous motors to have DC electromagnetic excitation. These motors' propulsion force is divided into two parts: (1) a synchronous component caused by the travelling magnetic field and DC current magnetic flux, and (2) a variable component caused by the travelling magnetic field and d- and q-axis reluctance (reluctance component). PMs are often used in lieu of DC electromagnets, with the exception of LSMs for magnetically levitated vehicles. Two categories of PM brushless LSMs are distinguishable:

PM LSMs that generate a travelling magnetic field from sinusoidal input current waveforms. PM DC linear brushless motors (LBMs) with position feedback, where the input waveforms of the rectangular or trapezoidal current are accurately synced with the speed and position of the moving component. Both kinds of LSMs have the same magnetic and electric circuit construction. LSMs may be created as tubular or flat motors in Figure 5.10. An absolute position sensor typically provides data on the location of the moving component in DC brushless motors. This control method translates a mechanical commutation seen in DC commutator motors into an electronic commutation (Figure 5.9). Thus, DC brushless motors are defined as those having square (trapezoidal) current waveforms. The difference between the d- and q-axes reluctances and the moving magnetic field may provide the reluctance component of the thrust in place of DC or PM excitation. A motor like this is known as an AC variable reluctance LSM. Making conspicuous ferro-magnetic poles with ferromagnetic and non-ferromagnetic materials or with anisotropic ferromagnetic materials would result in different reluctances in the d- and q-axes. LBM operation may be seen as a unique instance of LSM operation in Figure 5.10.

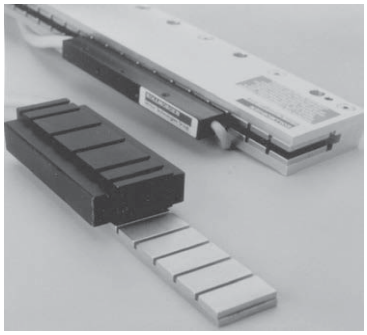

Figure 5.9: The Flatthree-phasePMlinearmotors.

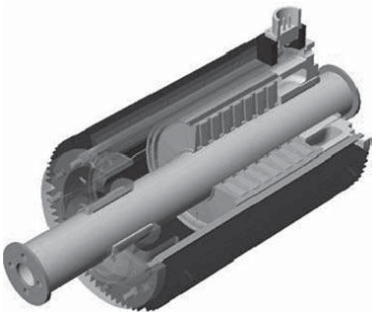

Figure 5.10: *Illustrates* the Tubular PMLSM. Moving rod (reactionrail) contains circular PMs.

The moving part's speed v in LSMs that operate on the travelling magnetic field principle is equal to the travelling magnetic field's synchronous speed vs, which is only dependent on the input frequency f (angular input frequency = 2f) and pole pitch. It is independent of 2p the number of poles. The usable force (thrust) Fx, like that of any other linear-motion electrical machine, is inversely proportional to the speed v = vs and directly proportional to the output power Pout in Figure 5.11,

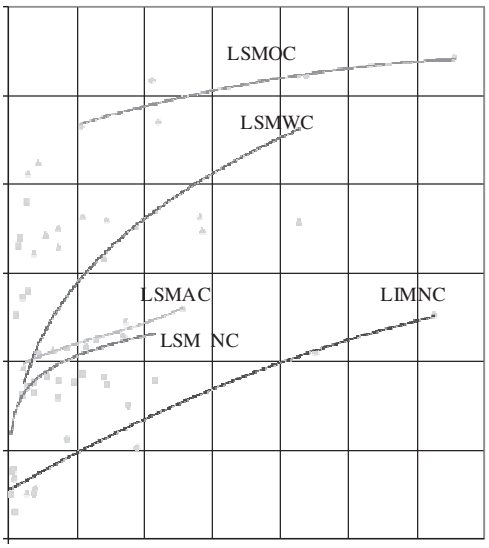

Figure 5.11: *Illustrates* the Comparisonofthrustdensityforsingle-sidedLIMsandLSMs.AC,aircooling;NC,naturalcool-ing;OC,oilcooling;WC,watercooling.

For industrial automation systems, direct electromechanical drives with LSMs are capable of accelerating up to 360 m/s2 and reaching speeds more than 600 m/min, or 36 km/h. The thrust density of LSMs is greater than that of LIMs, measured as thrust per active surface (2pLi), where Li is the effective width of the stack. The poly-phase (often three-phase) armature winding may be produced as a coreless (air-cored) winding layer, concentrated-parameter coils, or spread in slots. For small travel lengths (less than 10 m), such as industrial transportation or automation systems, PMs are the most often used field excitation methods. A lengthy PM train would be costly. High-speed passenger transportation systems based on the magnetic levitation concept use electromagnetic excitation (maglev). The German Transrapid system makes use of stationary slotted armatures and steel core excitation electromagnets placed on vehicles. Japanese MLX001 test train sets use stationary three-phase air-cored armature windings and onboard superconducting (SC) air-cored electromagnets (Yamanashi Maglev Test Line)[9], [10].

Classification

According on whether they are flat (planar) or tubular, LSMs may be categorised (cylindrical). Iron cored or air cored; single- or double-sided; slotted or pristine; transverse flux or longitudinal flux. The aforementioned topologies are feasible for almost all excitation system types. Excitation systems for LSMs based on the travelling magnetic field theory include the following:

1) Passive reaction rail with saliency and neither PMs nor windings.
2) PMs in the reaction rail.
3) PMs in the armature (passive reaction rail).
4) Electromagnetic excitation system (with winding).

Either linear stepping motors or linear switching reluctance motors are developed for LSMs with electronically switched DC armature windings.

REFERENCES

[1] G. Levačić, I. Uglešić, B. Jurišić, en B. Filipović-Grčić, "Influence of cables on power transmission network frequency response", *Teh. Vjesn.*, 2019, doi: 10.17559/TV-20171201102402.

[2] C. Gettings en C. C. Speake, "A method for reducing the adverse effects of stray-capacitance on capacitive sensor circuits", *Rev. Sci. Instrum.*, 2019, doi: 10.1063/1.5080016.

[3] A. V. Gusenkov, V. D. Lebedev, A. M. Sokolov, T. E. Shadrikov, A. Tankoy, en A. A. Dyachkov, "A Study of the Characteristics of Two-Wire High-Voltage Cables for Increased-Frequency Electrical Systems", *Russ. Electr. Eng.*, 2019, doi: 10.3103/S1068371219080054.

[4] M. Batalovic, H. Zildzo, H. Matoruga, M. Matoruga, en S. Berberovic, "Detection of defect presence inside the insulation of cable accessories through changes in cable capacitance", 2019. doi: 10.1109/icat47117.2019.8938874.

[5] I. Oualid, S. Flazi, F. Miloua, en N. Naoui, "Computing Coaxial Cable Capacitance through a DC and AC Power Supply", 2019. doi: 10.1109/CAGRE.2019.8713297.

[6] V. Grando Sirtoli, V. Coelho Vincence, en P. Bertemes-Filho, “Mirrored enhanced Howland current source with feedback control”, *Rev. Sci. Instrum.*, 2019, doi: 10.1063/1.5079872.

[7] J. Joseph, S. Mohan, en S. T. Krishnan, “Numerical modelling, simulation and experimental validation of partial discharge in cross-linked polyethylene cables”, *IET Sci. Meas. Technol.*, 2019, doi: 10.1049/iet-smt.2018.5248.

[8] J. Dai, S. S. Hagen, en D. C. Ludois, “High-Efficiency Multiphase Capacitive Power Transfer in Sliding Carriages with Closed-Loop Burst-Mode Current Control”, *IEEE J. Emerg. Sel. Top. Power Electron.*, 2019, doi: 10.1109/JESTPE.2018.2845385.

[9] E. S. S. A. Said, E. S. A. E. A. Othman, M. R. Ezz-Eldin, H. G. A. M. Taha, en W. A. E. El-Kattan, “Modification of cable insulation characteristics using nanocomposites for the nuclear power plant”, *Nucl. Radiat. Saf.*, 2019, doi: 10.32918/nrs.2019.3(83).09.

[10] K. Higashikawa *et al.*, “Dynamic performance analysis of long-distance power transmission system with DC superconducting cable from large photovoltaic generation”, *IEEE Trans. Appl. Supercond.*, 2019, doi: 10.1109/TASC.2019.2903390.

CHAPTER 6

ARMATURE REACTION OF RAIL PM MOTORS

Dr. G. Ezhilarasan, Professor
Faculty of Engineering and Technology, Jain (Deemed-To-Be University), Bengaluru, Karnataka, India
Email Id- g.ezhilarasan@jainuniversity.ac.in

It displays a single-sided flat LSM with surface PMs and slots for the armature winding. A comparable motor with buried-type PMs is shown in Figure 6.1. In the surface arrangement of PMs, the reaction rail's yoke (back iron) is ferromagnetic, and the magnetization of the PMs is in the normal direction (perpendicular to the active surface) in Figure 6.2. The yoke is not ferromagnetic, for instance, it is constructed of aluminium, and the buried PMs are magnetized in the direction of the moving magnetic field (Al). If not, the linkage flux would be larger than the bottom leakage flux. In rotary machines with buried-type PM rotors, where the shaft must also be non-ferromagnetic, the same result is seen[1], [2].

The so-called Halbach array of PMs also generates greater magnetic flux density and is closer to the sinusoids than a regular PM array while without requiring any ferromagnetic yoke in Figure 6.3. The magnetization vector should rotate as a function of distance along the Halbach array, according to the main idea behind it. The provision of a damper for a PM LSM is advised. In the pole shoe slots of a rotary synchronous motor is a cage damper winding in Figure 6.4. Electric currents are generated in damper circuits when the speed is not synchronised. Asynchronous beginning is possible because to the influence of the armature magnetic field and damper currents, which also assist the system recover to synchronous operation when the speed changes in Figure 6.5. A damper circuit also lessens the magnetic field that travels backward in Table 6.1. It would be somewhat challenging to equip PMs with a cage winding such that the damper of PM LSMs takes the shape of solid steel pole shoes or an Al cover. Additionally, fragile PMs may be shielded from mechanical harm using aluminium covers or steel pole shoes in Table 6.2.

Skewed PM assembly may help to lessen the detent force, which is the attraction force between PMs and the armature ferromagnetic teeth, force ripple, and certain higher-space harmonics. Skewed PMs may be set up in a single row[3]–[5].

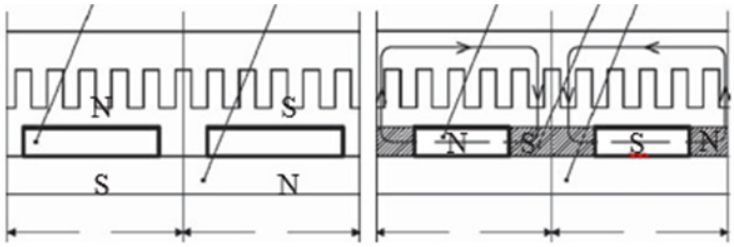

Figure 6.1: ***Illustrates*** **the Single-sided flat PM LSMs with slotted armature core and (a) surface PMs and (b) buried PMs. 1, PM; 2, mild steel pole; 3, yoke.**

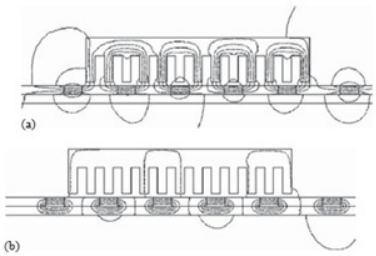

Figure 6.2: ***Illustrates*** **the Magnetic flux distribution in the longitudinal sections of buried-type PM LSMs: (a) non-ferromagnetic yoke and (b) ferromagnetic yoke (back iron).**

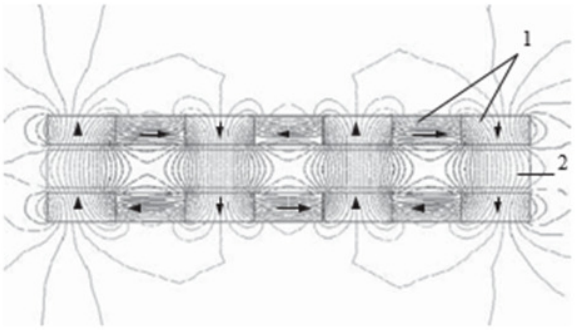

Figure 6.3: ***Illustrates*** **the Double-sided LSM with Halbach array of PMs. 1, PMs;2, coreless armature winding.**

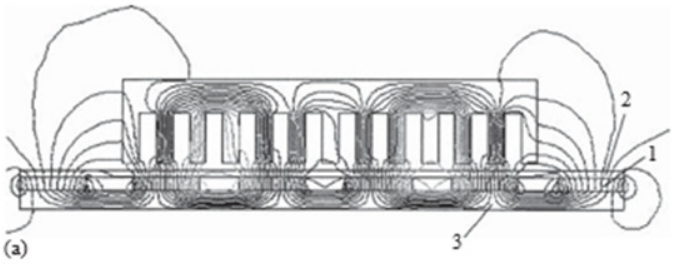

Figure 6.4: ***Illustrates*** **the Dampersofsurface-typePMLSMs:(a)Alcover(shield)and(b)solidsteelpoleshoes.1,PM; 2,damper;3,yoke.**

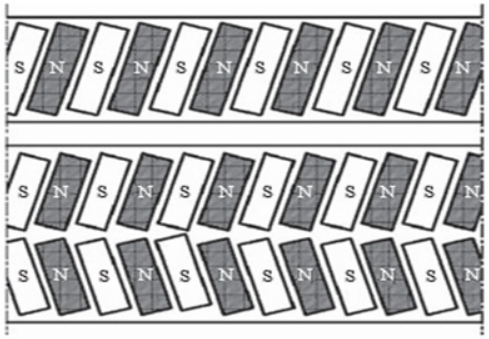

Figure 6.5: ***Illustrates*** **the Skewed PMs in flat LSMs: (a) one row and (b) two rows.**

Table 6.1: *Illustrates* the FlatThree-Phase,Single-SidedPMLBMswithNaturalCoolingSystemsManufactured.

Parameter	**LCD-T-1**	**LCD-T-2-P**	**LCD-T-3-P**	**LCD-T-4-P**
Continuousthrustat25°C,N	163	245	327	490
Continuouscurrentat25°C,A	4.2	6.3	8.5	12.7
Continuousthrustat125°C,N	139	208	277	416
Continuouscurrentat125°C,A	3.6	5.4	7.2	10.8
Peakthrust(0.25s),N	303	455	606	909
Peakcurrent(0.25s),A	9.2	13.8	18.4	27.6
Peakforce(1.0s),N	248	373	497	745
Peakcurrent(1.0s),A	7.3	11.0	14.7	22.0
Continuouspowerlossesat125°C,W	58	87	115	173
Armatureconstant,k_E,Vs/m	12.9			
Thrustconstant(threephases),k_F,N/A	38.6			
Resistanceperphaseat25°C,Ω	3.2	2.2	1.6	1.1
Inductance,mH	14.3	9.5	7.1	4.8
PMpolepitch,mm	23.45			
Maximumwindingtemperature,°C	125			
Armatureassemblymass,kg	1.8	2.4	3.6	4.8
PMassemblymass,kg/m	6.4			
Normalattractiveforce,N	1036	1555	2073	3109

The specifications of flat, single-sided PM LBMs made by Anorad are shown in Table together with motors made by Kollmorgen. The temperature of the armature winding is 25°C, 125°C, or 130°C for the thrust, current, resistance, and power loss. The equation defining the electromotive force (EMF) (induced voltage) stimulated by PMs without the armature response, denoted by the electromotive force constants kE in Tables 6.2 for sinusoidal operation i.

Table 6.2: *Illustrates* the FlatThree-Phase,Single-SidedPMLBMswithNaturalCoolingSystemsManufacturedbyKollmorgen.

Parameter	IC11-030	IC11-050	IC11-100	IC11-200
Continuousthrustat130°C,N	150	275	600	1260

Continuouscurrentat130°C,A	4.0	4.4	4.8	5.0
Peakthrust,N	300	500	1000	2000
Peakcurrent,A	7.9	7.9	7.9	7.9
Continuouspowerlossesat130°C,W	64	106	210	418
Armatureconstant,at25°C,k_E,Vs/m	30.9	51.4	102.8	205.7
Thrustconstant(threephases)at25°C,k_F,N/A	37.8	62.9	125.9	251.9
Resistance,linetoline,at25°C,Ω	1.9	2.6	4.4	8.0
Inductance,linetoline,mH	17.3	27.8	54.1	106.6
Electricaltimeconstant,ms	8.9	10.5	12.3	13.4
Thermalresistancewindingtoexternalstructure,°C/W	1.64	0.99	0.50	0.25
Maximumwindingtemperature,°C	130			
Armatureassemblymass,kg	2.0	3.2	6.2	12.2
PMassemblymass,kg/m	5.5	7.6	12.8	26.9
Normalattractiveforce,N	1440	2430	4900	9850

Thethrustconstant$k_F$inisdefinedaccordingtothesimplifiedequationforthedevelopedelectromagnetic thrust,i.e.

$F_d k_F I_a \cos\theta$

For an LSM that is sinusoidally stimulated, has equal reluctances in the d- and q-axes, and has an angle of 0° (cos = 1) between the armature current Ia and the q-axis. The electromagnetic thrust generated by the LSM is then calculated by multiplying the thrust constant kF by the armature current Ia.Two external armature systems and one internal excitation system, or one internal armature system and two external excitation systems, make up double-sided, flat PM LSMs (Figure 6.6). A linear Gramme's armature winding may be employed in the second scenario[6], [7].

The main winding is evenly distributed over a smooth armature core or absent altogether in slotless motors. Spotless PM LSMs are detent force-free motors that have minimal torque ripple and can outperform slotted LSMs in terms of efficiency at high input frequencies in Table 6.3. However, a bigger non-ferromagnetic air gap necessitates more PM material, and this results in a lower thrust density (thrust per mass or volume) than slotted motors. Given the synchronous reactance, the input current is greater.

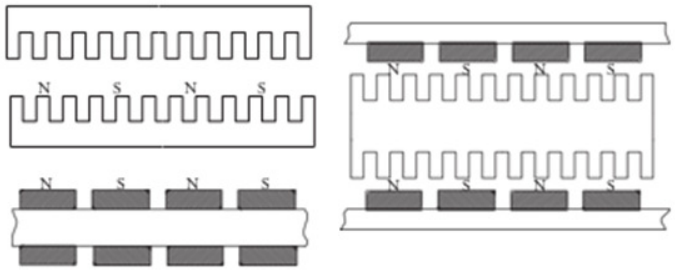

Figure 6.6: *Illustrates* the Double-sidedflatPMLSMswith(a)twoexternalarmaturesystemsand(b)oneinternalarmature system.

Table 6.3: *Illustrates* the SlottedversusSpotlessLSMs.

Quantity	**SlottedLSM**	**SlotlessLSM**
Higherthrustdensity	X	
Higherefficiencyinthelowerspeedrange	X	
Higherefficiencyinthehigherspeedrange Lowerinputcurrent	X	x
LessPMmaterial	X	
Lowerwindingcost		x
Lowerthrustpulsations		x
Loweracousticnoise		x

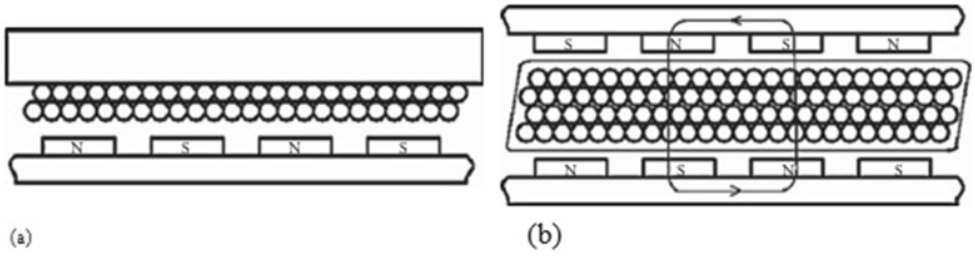

Figure 6.7: The flatslotlessPMLSMs:(a)single-sidedwitharmaturecoreand(b)double-sidedwithinnerair- coredarmaturewinding.

Due to the lack of teeth, in the d- and q-axes, might decline to a low undesirable value. A single-sided flat slotless motor with an armature core is shown in Figure 6.7, and a double-sided slotless motor with an inner air-cored armature winding.Performance characteristics for double-sided PM LBMs from Trilogy Systems Corporation, Webster, with an inner three-phase air-cored armature winding are listed in the Table 6.4.

Table 6.4: *Illustrates* the Flat Double-Sided PM LBMs with Inner Three-Phase Air-Cored Series-Coil Armature Winding Manufactured by Trilogy Systems Corporation, Webster, TX

Parameter	310-2	310-4	310-6
Continuousthrust,N	111.2	209.1	314.9
Continuouspower for sinusoidal operation, W	87	152	230
Peakthrust,N Peakpower,W	356 900	712 1800	1068 2700
Peak/continuouscurrent,A	10.0/2.8	10.0/2.6	10.0/2.6
Thrustconstant$k_F$forsinusoidaloperation,N/A	40.0	80.0	120.0
Thrust constant $k_F$for trapezoidal operation with Hallsensors,N/A	35.1	72.5	109.5
Resistanceperphase,Ω	8.6	17.2	25.8
Inductance±0.5mH	6.0	12.0	18.0
Heatdissipationconstantfornaturalcooling,W/°C	1.10	2.01	3.01
Heatdissipationconstantforforcedaircooling,W/°C	1.30	2.40	3.55
Heatdissipationconstantforliquidcooling,W/°C	1.54	2.85	4.21
Numberofpoles	2	4	6
Coillength,mm	142.2	264.2	386.1
Coilmass,kg	0.55	1.03	1.53
MassofPMexcitationsystems,kg/m	12.67or8.38		

A tubular (cylindrical) LSM may be created by rotating a flat LSM along an axis parallel to the moving magnetic field, or parallel to the direction of thrust (Figure 6.8). Another design option for a tubular PM LSM is a double-sided or slotless motor. Sulzer Electronics AG, Zurich, Switzerland, makes tubular single-sided LSMs LinMoT®* with a sliding internal PM excitation mechanism and a fixed external armature (Table 6.5). A hard metal cylinder containing all of the active motor's bearing, position sensors, and electronics has been used.

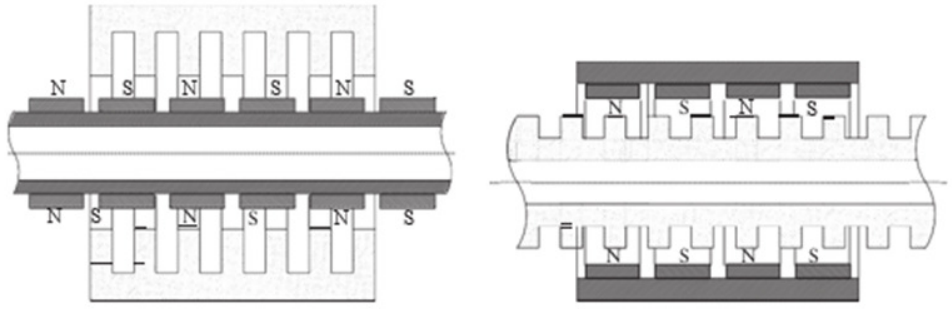

(a) (b)

Figure 6.8: *Illustrates* the Single-sidedslottedtubularPMLSMs:(a)withexternalarmaturesystemand(b)withexternal excitationsystem.

Table 6.5: *Illustrates* the DataofTubularLSMsLinMot®Manufactured

Parameter	P0123×80	P0123×160	P0137×120	P0137×240
Numberofphases	2			
PMs	NdFeB			
Maximumstroke,m	0.210	0.340	1.400	1.460
Maximumforce,N	33	60	122	204
Maximumacceleration,m/s^2	280	350	247	268
Maximumspeed,m/s	2.4	4.2	4.0	3.1
Stator(armature)length,m	0.177	0.257	0.227	0.347
Statorouterdiameter,mm	23	23	37	37
Statormass,kg	0.265	0.450	0.740	1.385
Sliderdiameter,mm	12	12	20	20
Maximumtemperatureofthearmaturewinding,°C	90			

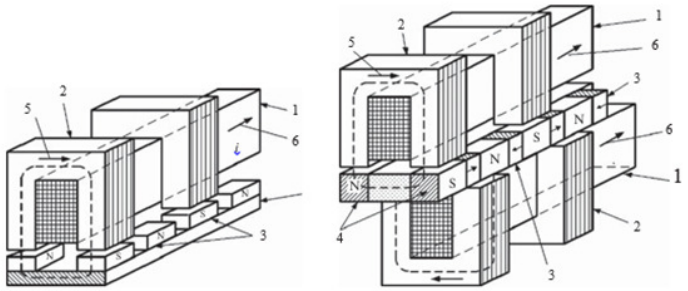

Figure 6.9: *Illustrates* the TransversefluxPMLSM:(a)single-sidedand(b)double-sided.1,armaturewinding;2,armature laminatedcore;3,PM;4,backferromagneticcore;5,magneticflux;6,armaturecurrent.

All of the aforementioned PM LSMs have longitudinal magnetic flux, which has lines that are parallel to the moving magnetic field's direction. As transverse magnetic flux motors, LSMs may also be created using magnetic flux lines that are parallel to the direction of the moving field. A single-sided transverse flux LSM with two rows of PMs. An excitation system for two pole flux is produced by two parallel PMs. Transverse flux motors can be configured on both sides, although doing so is difficult and costly[8], [9].

REFERENCES

[1] O. Font *et al.*, "Origin and speciation of major and trace PM elements in the barcelona subway system", *Transp. Res. Part D Transp. Environ.*, 2019, doi: 10.1016/j.trd.2019.03.007.

[2] L. Kang, Y. Chen, W. Hao, Y. Yang, en Q. Zhang, "Multi-physics Field Analysis of Traction PMSM for Shunting Locomotive", 2019. doi: 10.1109/ICEMS.2019.8922514.

[3] W. Zhang, G. Wu, Z. Rao, J. Zheng, en D. Luo, "Predictive power control of novel n*3-phase pm energy storage motor for urban rail transit", *Energies*, 2020, doi: 10.3390/en13071578.

[4] S. Nategh *et al.*, "A Review on Different Aspects of Traction Motor Design for Railway Applications", *IEEE Trans. Ind. Appl.*, 2020, doi: 10.1109/TIA.2020.2968414.

[5] "Proton Motor units for rail milling train, UPS system in road tunnels", *Fuel Cells Bull.*, 2020, doi: 10.1016/s1464-2859(20)30567-8.

[6] R. Septiana, "Makna Denotasi, Konotasi Dan Mitos Dalam Film Kein", *J. Wind Eng. Ind. Aerodyn.*, 2019.

[7] B. kamil and laila puspita Utami Pratiwi, "PENGARUH MODEL PEMBELAJARAN EXPERIENTIAL LEARNING DI DUKUNG METODE EXAMPLE NON EXAMPLE PADA KEMAMPUAN BERPIKIR KRITIS PESERTA DIDIK DI SMA NEGERI 1 SIMPANG AGUNG Skripsi", *J. Wind Eng. Ind. Aerodyn.*, 2019.

[8] P. K. Padang, "Peraturan Daerah Kota Padang Nomor 6 Tahun 2019 tentang Rencana Pembangunan Jangka Menengah Daerah (RPJMD) Kota Padang Tahun 2019-2024", *J. Wind Eng. Ind. Aerodyn.*, 2019.

[9] M. Ulva, "Gambaran Karakteristik Kecelakaan Lalu Lintas di Kota Makassar Tahun 2014-2018", *J. Wind Eng. Ind. Aerodyn.*, 2019.

CHAPTER 7

PASSIVE REACTION RAIL OF PERMANENTMOTORS

Dr. P. Kishore Kumar, Associate Professor
Faculty of Engineering and Technology, Jain (Deemed-To-Be University), Bengaluru, Karnataka, India
Email Id- k.kishore@jainuniversity.ac.in

The substantial quantity of PM material required to design the excitation mechanism is a disadvantage of PM LSMs. Rare-earth PMs cost a lot; hence they are often asked for. The cost of the reaction rail without assembly works out to US$ 1300 for 1 m if a small PM LSM, for example, uses 10 kg of NdFeB per 1 m of the reaction rail and 1 kilogramme of good-quality NdFeB costs US$ 130. For instance, fares at this level cannot be accepted in passenger transportation systems. Applying the PM excitation system to the short armature, which magnetises the long reaction rail and generates magnetic poles in it, is a more affordable option. The homopolar LSM is a name for this kind of linear motor. The homopolar LSM is a double-sided AC linear motor that is described in and is made up of two polyphase armature systems that are mechanically and magnetically coupled by a ferromagnetic U-type yoke. A standard slotted linear motor stack, a polyphase armature winding, and PMs positioned between the stack and the U-type yoke make up each armature. The armature stack is larger than in a traditional steel-cored LSM because the armature and excitation systems are merged. Electromagnets may also be used in lieu of the PMs. Passive is the variable reluctance response rail. By utilising ferromagnetic (solid or laminated) cubes spaced apart by a nonferromagnetic substance, the saliency is produced. The armature PMs use the air gap to magnetise the reaction rail poles. The thrust is produced by the reaction rail's salient poles and the travelling magnetic field of the polyphase armature winding. A homopolar LSM of this kind has been suggested for the Swissmetro's maglev trains[1], [2]. The double-sided arrangement may be further simplified to create the single-sided PM LSM in Table 7.1.

PM Flux-Switching the linear motor

Strong linear motors are needed for large gantry systems and machining centres, ideally with reaction rails that are PM-free in Figure 7.2. The class of the so-called Siemens 1FN6 PM LSMs with a magnet-free reaction rail in Figure 7.1.

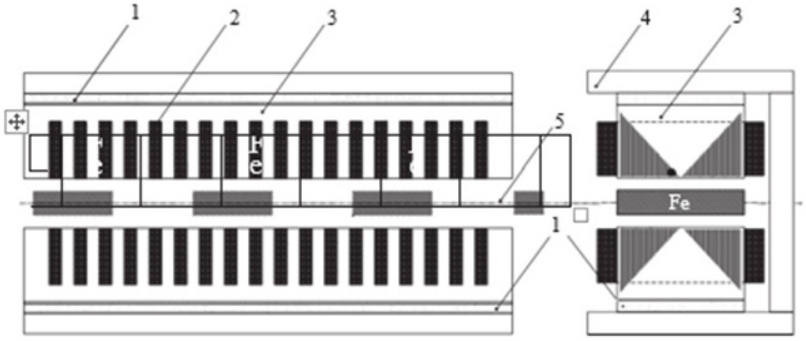

Figure 7.1: ***Illustrates*****double-**

sidedhomopolarPMLSMwithpassivereactionrail.1,PM;2,armaturewinding;

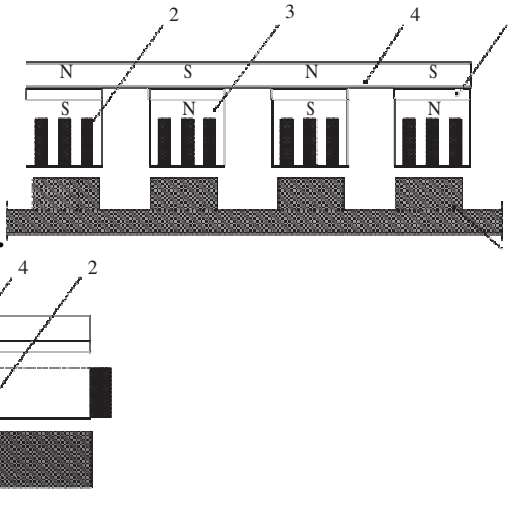

3,armaturestack;4,yoke;5,reactionrail.

Figure 7.2: ***Illustrates*** **the Single-sidedPMLSMwithapassivereactionrail.1,PM;2,armaturewinding;3,armaturestack; 4,yoke;5,ferromagneticreactionrail.**

Table 7.1:*Illustrates* the SpecificationsofIFN6PMLSMsManufacturedbySiemens,Erlangen,Germany

ArmatureUnit	RatedThrustN	Max.ThrustN	Max. Speed atRated Thrustm/min	Max. Speed atMax. Thrustm/min	RatedCurrentA	Max.CurrentA
1FN6008-1LC17	235–350	900	263	103	1.7–2.6	9.0
1FN6008-1LC37	235–350	900	541	224	3.5–5.3	18.0
1FN6016-1LC30	470–710	1800	419	176	5.4–8.0	28.0
1FN6016-1LC17	935–1400	3590	263	101	7.0–10.5	36.0
1FN6024-1LC12	705–1060	2690	176	69	3.5–5.3	18.0
1FN6024-1LC20	705–1060	2690	277	114	5.4–8.0	28.0
1FN6024-1LG10	2110–3170	8080	172	62	10.5–16.0	54.0
1FN6024-1LG17	2110–3170	8080	270	102	16.2–24.3	84.0

PM devices that switch flux are known as such. The armature system has the following specifications: air cooling, IP23 protection level, F insulation class, line voltage range of 400–480 V, rated thrust of 235–2110 N, maximum speed at rated thrust of 170–540 m/min (Table 34.6), overload capacity of 3.8 of rated thrust, and modular construction. External encoders and Siemens Sinamics or Simodrive solid-state converters are used to power these LSMs. According to Siemens, for light-duty machine tool, machine accessory, and material handling applications, these new LSMs deliver thrust forces and velocities equal to competing classical counterparts in Figure 7.3.

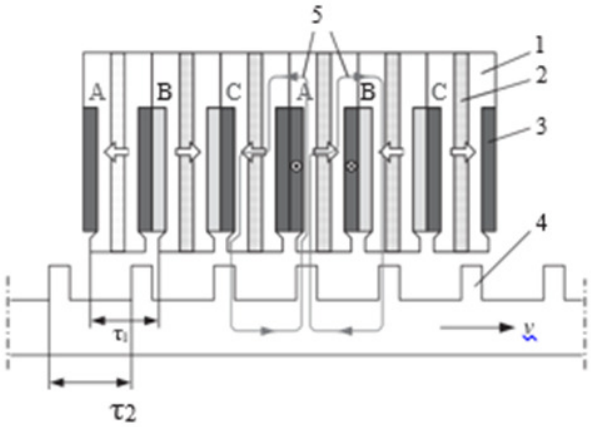

Figure 7.3: ***Illustrates*** **the Construction of flux-switching LSM with PM-free reaction rail. 1, laminated armature core; 2, PM; 3, armature coil (phase C); 4, toothed passive steel reaction rail; 5, linkage magnetic flux (phase A is on).**

The magnet-free reaction rail requires no special installation techniques and does not have the same safety requirements as conventional PM reaction rails. There is no issue with ferrous chips and other trash being drawn to these portions in the absence of PMs. Installing a wiper or brush on the slide's moving component makes maintenance a breeze[3], [4].

The flux-switching LSM is made up of a response rail part with teeth that is not magnetic and an armature section with coils and PMs. The main design novelty is an LSM in which PMs and specific windings for each phase are laminated right into the armature core. Along with the periodic movement of the reaction rail, the linkage flux in the armature winding varies in both magnitude and polarity. By switching the three-phase armature currents in accordance with a predetermined algorithm, the magnetic flux between the armature core and steel reaction rail is managed. The passive response rail is significantly easier to make and is made of milled steel with poles (teeth).

Motors that Use Electromagnetic Excitation

The salient-pole rotor of a rotary synchronous motor and the electromagnetic excitation system of an LSM are similar. A flat single-sided LSM with conspicuous ferromagnetic poles and a DC field excitation coil is seen in Figure 7.4. Solid steel, laminated steel, or sintered powder are all acceptable materials for the poles and pole shoes. DC current may be given via brushes and contact bars, inductive power transfer (IPT) systems, linear transformers, or linear brushless exciters if the electromagnetic excitation system is integrated with the moving component[5], [6].

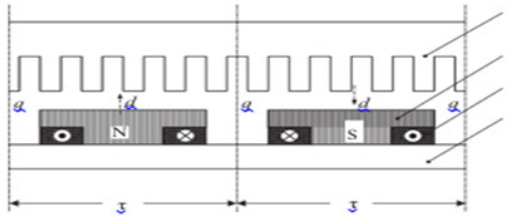

Figure 7.4: ***Illustrates*** **the Electromagneticexcitationsystemofaflatsingle-sidediron-coredLSM.1,salientpole;2,DC excitationwinding;3,ferromagneticrail(yoke);4,armaturesystem.**

Superconducting Excitation System for Motors

The ferromagnetic core electromagnets that provide the excitation flux in large-power LSMs may be swapped out with coreless SC electromagnets. There is no need to employ the armature ferromagnetic core since the magnetic flux density generated by the SC electro-magnet exceeds the saturation magnetic flux density of the best laminated alloys (Bsat 2.4 T for cobalt alloy). The whole core of an LSM with a SC field excitation system is made of air.Air-cored LSMs with SC excitation systems power the experimental maglev trains on the Yamanashi Maglev Test Line (YMTL) in Yamanashi Prefecture, Japan, which is located west of Tokyo.

Motors with Linear Induction

LIMs have the greatest potential for usage in transportation systems, from electrical traction on tiny passenger or material supply vehicles (used in airports, exhibits, electrohighways, and elevators) through pallet and wafer transportation, belt conveyors, bulk material transportation systems, etc. The second significant setting for LIM applications is in business, namely in manufacturing processes (machine tools, hammers, presses, mills, separators, automated manufacturing systems, strip tensioners, textile shuttles, index tables, turntables, disc saws for wood, sliding doors, robots, etc.).

LIMs can be crucial in industrial research and testing as well. Some examples include the high acceleration of model aircraft in aerodynamic tunnels, the high acceleration of vessels in laboratory pools, the propulsion of mixers, shakers, and vibrators, and the adjusting of x-y tables and instruments. LIMs may also be used in offices and consumer electronics (such as sound and vision devices, knitting machines, and curtains) (transportation of documents, letters, and cash). About 50 examples of LIM applications in use or in the implementation process may be found in the Handbook of Linear Motor Applications [21], which was published in Japan in 1986.

Basic constructions and geometries

A cage rotor induction motor or a winding rotor induction motor may both be cut in the same manner to produce a LIM. The rotor becomes the secondary and the stator the main. The secondary of a LIM may be made simpler by employing a solid steel core and a high-conductivity non-ferromagnetic plate in place of the cage (ladder) or slip-ring winding (Al or Cu). The ferromagnetic core functions as a conductor for both the magnetic flux and the electric current, while the non-ferromagnetic plate is a secondary electric circuit with scattered characteristics. From the perspective of the operating principle, it makes no difference whether the main or secondary portion is moving. Thus, a solid rotor induction motor may produce a flat, single-sided LIM, while a hollow-rotor induction motor with

wound exterior and internal stator can produce a flat, double-sided LIM. The secondary ferromagnetic core is not required in a double-sided LIM because the magnetic flux created by one of the primary windings is closed off by the core of the second primary unit after passing through the air gaps and non-ferromagnetic secondary[7], [8].

Theoretically, the air gap magnetic flux density of a double-sided LIM with primary windings distributed over two cores is double that of a single-sided LIM stimulating the same MMF. Therefore, assuming the same size, the thrust of such a motor is four times larger. The output characteristics of a double-sided LIM with laminated secondary back iron are the same as those for a single-sided LIM with just one main core wrapped. Due to the secondary's typical nonferromagnetic nature, double-sided LIMs have the essential benefit of eliminating the customary attractive force between the primary and secondary. Primary cores for flat LIMs may be made up of a series of cores stacked in parallel at the proper spacing and magnetically coupled by extra yokes that run perpendicular to the direction of the travelling field. It is feasible to apply two windings, often multiphase windings with perpendicular conductors, to a magnetic circuit created in this fashion, as illustrated in Figure 7.5. The secondary may be shifted in two perpendicular directions and positioned at any location in the x-y plane by adjusting the current in each winding. Both single-sided and double-sided machines may be constructed for a flat LIM with two degrees of freedom (DOFs).

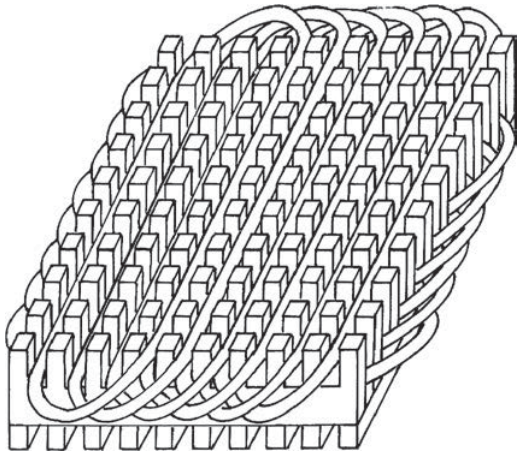

Figure 7.6: *Illustrates* theprimaryofaflatLIMwithtwoDOFs.

A tubular motor may be created by rotating a flat, single-sided or double-sided LIM around an axis parallel to the direction of the travelling magnetic field, or, more specifically, parallel to the direction of the push (Figure 7.7). Similar to a flat LIM, a tubular (cylindrical) LIM may have a square or rectangular cross section and be constructed as both single-sided and double-sided devices in Figure 7.8.

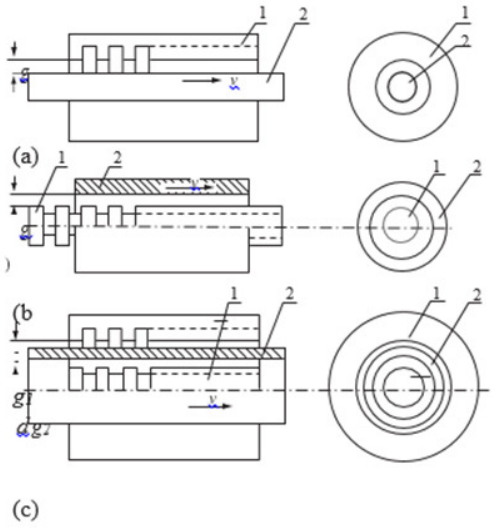

Figure 7.7: *Illustrates* the TubularLIMs:(a)single-sidedwithanexternalshortprimary,(b)single-sidedwithanexternal shortsecondary,and(c)double-sidedwithshortprimary.1,primary;2,secondary.

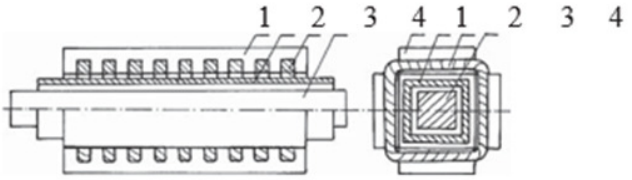

Figure 7.8: *Illustrates* the Tubular,double-sidedLIMwithasquarecrosssection:1,primary;2,secondary;3,primarycoil; 4,internalcore.

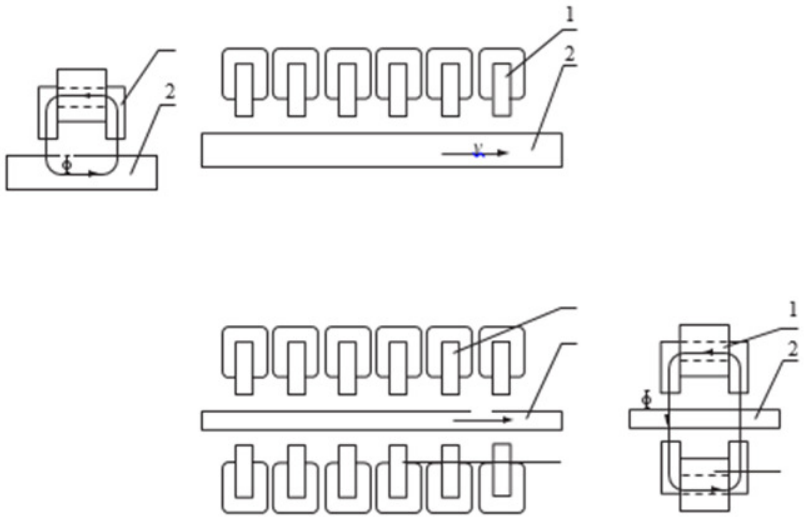

Figure 7.9: *Illustrates* the FlatLIMwithtransversemagneticfluxandsalientpoles:(a)single-sidedand(b)double-sided. 1,primary;2,secondary.

Regarding the length of the secondary in relation to the length of the primary in configurations other than that in Figure 7.9.All of the aforementioned LIMs are longitudinal magnetic flux motors, meaning that the lines of magnetic flux are parallel to the direction of the moving magnetic field and are located in a plane. Additionally, a LIM may be built to produce magnetic flux lines that are parallel to the moving field's direction. It is claimed that these motors contain transverse magnetic flux. The main benefit of a transverse magnetic flux LIM over a longitudinal magnetic flux LIM is the reduction in the amount of magnetising current required owing to the shorter magnetic flux routes. Lower thrust is a severe disadvantage. There is often a main winding of focused coils on salient poles in a flat LIM with transverse magnetic flux[9].

With transverse flux, a flat, one-sided LIM may generate both thrust and electrodynamic suspension. Construction places the secondary in electrodynamic suspension while the main magnetic field propels and stabilises it laterally. The main magnetic circuit is made up of two rows of E-shaped laminations. The short secondary is fashioned like a boat out of a light aluminium alloy. The boat's lateral sides are 60 degrees slant towards the active surface. Maximum lateral stability and normal repelling force are both provided by this form. The LIMs may be categorised into the following categories based on their geometry:

Flat and tubular; single- and double-sided; moveable primary or secondary; movable primary or secondary; single- and double-sided; short primary and short secondary; longitudinal and transverse magnetic flux.

1) Wheel-on-rail vehicle propulsion
2) The following criteria should be met by contemporary electrical traction systems:
3) Significant computerization and automation

Independent of adhesion, which is primarily influenced by environment and weather, propulsion and braking are possible.Low noise level, sometimes less than 70 dB (A). Able to handle slopes of at least 6% and bends with a radius of curvature less than 20 m; High dependability; No contamination of the environment or terrain. By developing communal transportation systems that can be adopted without having an impact on a densely populated city, the congestion issues of large cities should be resolved. For instance, the historical core of many Italian towns has hardly changed since the Renaissance. A large railway might be an entirely incorrect solution and have a significant influence on city development. A light railway, or people mover, with a capacity of 10,000–20,000 passengers per hour, might serve as a sufficient substitute for conventional transportation networks and integrate existing rail networks.

The use of LIMs as propulsion devices allows for the fulfilment of all the before listed conditions. In most cases, new tracks are not necessary when replacing electrical rotary motors with linear motors in traction drives (electric locomotives); just the tracks' adaptation to linear drives is needed. The best LIMs are single-sided LIMs, since their natural attractive force may improve the adhesion of wheels and rails. There is a 10 to 15 mm air gap. The motor vehicle typically has two LIMs with short primaries arranged in series (Table 7.2). The solid back iron and an Al cap make up the double-layer secondary, which is situated between the rails. Along the track are cables for electrical energy distribution to the vehicle as well as, rather often, collectors for computer connection with the vehicle. Variable-voltage, variable-frequency (VVVF) voltage-source inverters provide power to three-phase LIMs. Wheel-on-rail vehicles may be more flexible thanks to a linear propulsion system, which also reduces noise on curves and wear on the wheels and rails.

Due to the technical challenges of removing faults brought on by bends in the secondary with main cores on each side, double-sided LIMs (Figure 7.11 c and d) have only found a very limited use. In double-sided LIMs, maintaining a uniformly narrow and small air gap is more challenging than in single-sided LIMs. The LIM-driven wheel-on-rail vehicles are designed for low speeds, or below 100 km/h, and for short routes, or below 50 km (urban transit systems and short-distance trains). Currently, LIM-driven trains run in Toronto and Vancouver, British Columbia, Canada; Detroit, Michigan; Tokyo, Japan; Osaka, Japan; and Kuala Lumpur, Malaysia (Figure 7.10);.

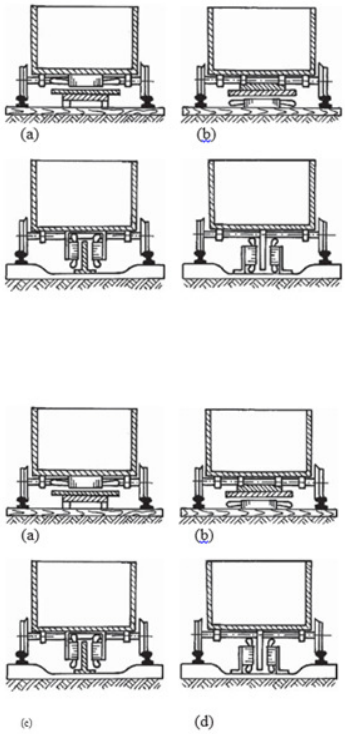

Figure 7.10: ***Illustrates*** **the LIM-driven wheel-on-rail cars: (a) single-sided LIM with short primary mounted on the undercarriage, (b) single-sided LIM with short secondary mounted on the undercarriage, (c) double-sided LIM with short primary mounted on the undercarriage, and (d) double-sided LIM with short secondary mounted on the undercarriage.**

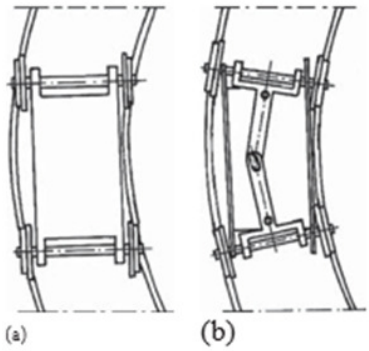

Figure 7.11: ***Illustrates*** **the undercarriage of a wheel-on-rail vehicle: (a) rotary motor propulsion and (b) LIM propulsion.**

Table 7.2: ***Illustrates*** **the DesignDataofSingle-Sided,Three-PhaseLIMsforPropulsionofVehicles.**

Quantity	**JLMDR**	**ICTS**	**LIMKU**	**CIGGT**	**GEC**	**Unit**
Pullout thrust at frequency giveninthe following, F_x	12.5	9.0	3.5	1.7	0.7	kN
Inputfrequency,f	20.0	40.0	25.0	40.0	60.0	Hz
Ratedphasecurrent,V_1	275.0	465.0	130.0	200.0	200.0	A
Number of poles, $2p$	8	6	4	6	4	—
Number of turns perphase, N_1	128	96	128	108	48	—
Equivalent diameter of conductor, d_1	—	8.93	5.28	1.115	8.1	mm
Number of parallel conductors	—	1	—	19	1	—
Effective width of primary core, L_i	0.23	0.216	0.29	0.101	0.1715	m
Polepitch, τ	0.27	0.2868	0.30	0.25	0.20	m
Length of single end connection, l_e	—	0.3483	—	0.2955	0.3685	m
Coilpitch, w_c	0.225	0.1673	0.25	0.1944	0.1555	m
Airgap,g	15.0	12.6	12.0	15.0	18.2	mm
Number of slots, z_1 (z_1□)	96(106)	72(79)	48(58)	54(61)	36(43)	—
Width of slot, b_{11}	—	15.6	17.0	15.0	13.08	mm
Width of slot opening, b_{14}	—	15.6	—	10.44	13.08	mm
Depth of slot, h_{11}	—	53.0	38.0	34.21	61.47	mm
Height of yoke, h_{1y}	—	43.6	39.3	71.63	50.0	mm
Conductivity of back iron at 20°C, σ_{Fe}	—	4.46	9.52	4.46	5.12	$\times 10^6$S/m
Conductivity of Alcapat 20°C,σ_{Al}	—	30.0	30.3	32.3	21.5	$\times 10^6$S/m
Width of back iron, w	0.3	0.24	0.3	0.111	0.1715	m
Thickness of backiron, h_{sec}	19.0	12.5	25.0	25.4	47.4	mm

ThicknessofAlcap,d	5.0	4.5	5.0	4.5(2.5)	3.2	mm
ThicknessofAlcapbehindFecore,t_{ov}	5.0	17.0	5.0	12.7	3.2	mm
Width of Al cap	0.30	0.32	0.40	0.201	0.2985	m

Reluctance-variable motors

The building of a linear reluctance motor (LRM) or variable reluctance LSM with no DC excitation winding is the most basic. The ratio of d-axis permeance to q-axis permeance is low, hence the thrust of such a motor would be minimal. Utilizing flux barriers or steel laminations may result in improved performance. Any non-ferromagnetic substance is suitable for the construction of flux barriers. Steel laminations must be orientated to provide high permeance for the d-axis magnetic flux if high permeance in the d-axis and low permeance in the q-axis are to be achieved.

Table 7.3 *Illustrates* how to arrange steel laminations to achieve various reluctances in the d- and q-axes using a variable reluctance platen with flux barriers. Segments that are equivalent in length to the pole pitch may be used to construct the platen. Each section is made up of electro technical sheet-cut semicircular lamellas. The section is made stiff and durable using a filler, such as epoxy resin. A platen of any desired length may be created by joining the segments.

Table 7.3: *Illustrates* the DesignDataofDouble-Sided,Three-PhaseLIMsforPropulsionofVehicles.

Maximumthrustatinputfrequency,F_x,giveninthefollowing	0.85	16.68	kN
Inputfrequency,f	60.0	173.0	Hz
Inputphase current, I_1	200.0	2000.0	A
Numberofpoles,2p	4	10	—
Numberof turns perphase, N_1	144	100	—
Diameterofconductor,d_1	0.75	1.10	mm
Effectivewidthofprimarycore,L_i	0.0869	0.254	m
Polepitch,τ	0.1795	0.3556	m
Coilpitch,w_c	0.05	0.05	m
Numberofslots,z_1(z_1□)	36(45)	150(160)	—
Widthofslot,b_{11}	13.7	16.0	mm
Widthofslotopening,b_{14}	13.7	—	mm
Depthofslot,h_1	63.0	—	mm
Heightofyoke,h_{1y}	23.9	—	mm

Widthoftooth,c_1	20.0	7.7	mm
Resultantairgap,$2g+d$	38.1	38.075	mm
Airgap,g	2×12.7	2×11.1	mm
Thicknessofsecondary,d	12.7	15.875(hollow)	mm
EffectivethicknessofAlsecondary	12.7	7.2	mm
Widthofsecondary,w	≥0.3046	—	m
ConductivityofAlcapat20°C,σ_{Al}	≈24.34	≈24.0	$\times 10^6$S/m

Steady-state motors

A concentrated armature wrapped on salient poles and either a variable reluctance platen or PM excitation rail are features of a linear stepping motor. The thrust is produced by the interaction of the PM flux and the active platen's armature magnetic flux, or by the salient ferromagnetic poles and armature magnetic flux (variable reluctance platen). There is no position feedback with stepping motors in 7.12.

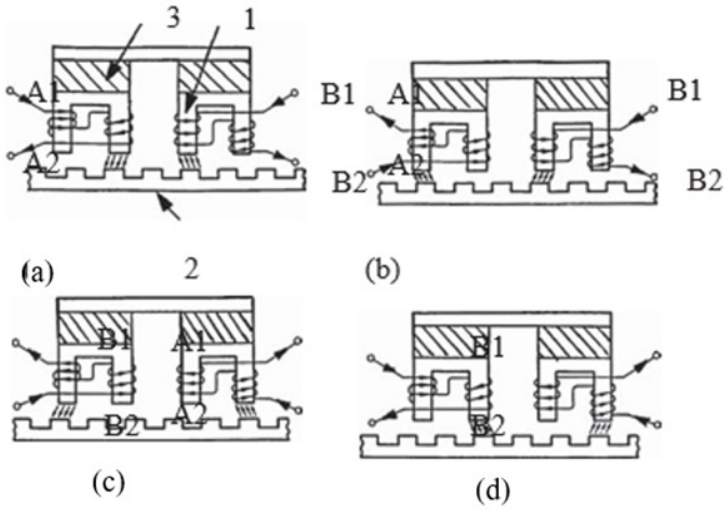

Figure 7.12: ***Illustrates*** **thePrincipleofoperationofanHLSM:(a)initialposition,(b)1/4toothpitchdisplacementofthe forcer,(c)2/4toothpitchdisplacement,and(d)3/4toothpitchdisplacement.1,forcer;2,platen;3,PM.**

Only hybrid stepping linear motors (PM, winding, and variable reluctance air gap) have so far found use in real world applications. The hybrid linear stepping motor (HLSM) is made up of two components: the forcer (also known as the slider) and the variable reluctance platen. They are both composed of high-permeability steel and have uniform teeth. This is an early version of the Sawyer linear motor, often known as the HLSM. Two concentrated-

parameter windings and two rare-earth magnets make up the forcer, which is the moving component. The tooth pitch on the platen and the forcer are the same. The tooth pitches on the forcer poles, however, are separated by 1/4 or 1/2 pitch between each pole. With this configuration, the winding may regulate the PM flux at any value between minimum and maximum, lining up the forcer and the platen for maximum permeance. Similar to a rotary stepping motor, the HLSM is supplied with two-phase currents that are 90 degrees out of phase. Per each complete step, the forcer travels 1/4 of a tooth pitch.

A powerful air flow created by an air compressor maintains a tiny air gap between the two components. Depending on how many phases are activated, the average air pressure ranges from 300 to 400 kPa. Table 7.4 contains information about HLSM specifications. At rated current provided to the motor, the holding force is the amount of outside force necessary to dislodge the force from its rest position. The greatest variation from the correct location in the length of each step is measured by the step-to-step accuracy.

Table 7.4: *Illustrates* the DataofHLSMsManufacturedbyTokyoAircraftInstrumentCo.,Ltd.,Tokyo,Japan.

Parameter	LP02-20A	LP04-20A	LP04-30A	LP60-20A
Driver	Bipolarchopper			
Voltage,V	24DC			
Resolution,mm	0.2	0.4	0.4	0.423
Holdingforce,N	20	20	29.5	20
Step-to-stepaccuracy,mm	±0.03			
Cumulativeaccuracy,mm	±0.2			
Maximum start–stop speed, mm/s	60	120	120	127
Maximumspeed,mm/s	400	600	500	600
Maximumloadmass,kg	3.0	3.0	5.0	3.0
Effectivestroke,mm	330	300	360	310
Mass,kg	1.4	1.2	2.8	1.4

For full-step and microstepping drives, this number varies. The fastest possible speed that may be utilised to start or stop a motor without ramping without causing it to lose synchronism or steps is known as the maximum start-stop speed. The fastest linear speed that can be reached without the motor stopping or losing synchronism is the maximum speed. The maximum load mass is the most permissible mass that may be used to push the forcer against the scale without causing mechanical harm. The position increment achieved when the currents are transferred from one winding to the next winding is known as the full-step resolution. This is the normal resolution that full-step drives can achieve, and it solely depends on the design of the motor. The position increment achieved when the full-step resolution is electronically halved by balancing the currents in the two windings is known as the microstepping resolution. In comparison to the full-step resolution, this resolution is often 10-250 times smaller [13]. High precision and quick acceleration positioning systems are

recognised as having a great use for HLSMs. Smooth operation may be achieved with a typical resolution of a few hundred steps/mm using a microprocessor-controlled microstepping mode. These types of motors are becoming more and more popular in applications like factory automation, high speed positioning, computer peripherals, facsimile machines, numerically controlled machine tools, automated medical equipment, automated laboratory equipment, and welding robots due to benefits like high efficiency, high throughput, mechanical simplicity, high reliability, precise open-loop operation, and low system inertia.

This motor is particularly well suited for computer-controlled material handling applications, machine tools, printers, plotters, and other devices where high positioning precision and repeatability are critical issues in Table 7.5.In order to achieve the x-y motion (two DOFs) in a single plane, two or four forcers positioned at a 90° angle must be employed, as well as a specific grooved platen (a "waffle plate").Specifications for the x-y HLSMs made by Santa Clarita, California-based Normag Northern Magnetics in Figure 7.13

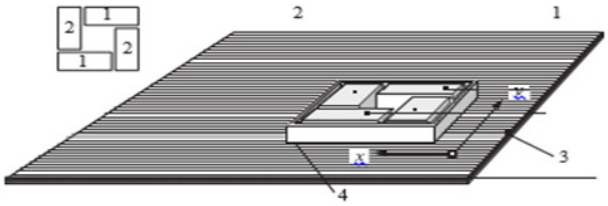

Figure 7.13: *Illustrates* the HLSM with a four-unit forcer to obtain the x–y motion: 1, forcers for the x-direction; 2, forcers for the y-direction; 3, platen; 4, air pressure.

Table 7.5: Dataof*x–y*HLSMs Manufactured by Normag Northern Magnetics, Inc., Santa Clarita, CA

Parameter	4XY0602-2-0	4XY2002-2-0	4XY2004-2-0	4XY2504-2-0
Numberofforcerunitsperaxis	1	1	2	2
Numberofphases	2	2	2(4)	2(4)
Staticthrust,N	13.3	40.0	98.0	133.0
Thrustat1m/s,N	11.1	31.1	71.2	98.0
Normalattractiveforce,N	160.0	400.0	1440.0	1800.0
Resistanceperphase,Ω	2.9	3.3	1.6	1.9
Inductanceperphase,mH	1.5	4.0	2.0	2.3
Inputphase current,A	2.0	2.0	4.0	4.0
Airgap,mm	0.02			
Maximumtemperature,°C	110			
Mass,kg	3.2	0.72	2.0	1.5
Repeatability,mm	0.00254			
Resolution,mm	0.00254			

Bearingtype	Air		

REFERENCES

[1] O. Le Chapelain, S. Jadoui, Y. Boulaftali, en B. Ho-Tin-Noé, "The reversed passive Arthus reaction as a model for investigating the mechanisms of inflammation-associated hemostasis", *Platelets*. 2020. doi: 10.1080/09537104.2020.1732325.

[2] S. Nakajima *et al.*, "Activation of the reward system ameliorates passive cutaneous anaphylactic reaction in mice", *Allergy: European Journal of Allergy and Clinical Immunology*. 2020. doi: 10.1111/all.14442.

[3] N. F. Bte, H. M. Naim, en A. A. A. Ibrahim, "The study of affective value in educational video production style using kansei engineering method", *Int. J. Inf. Educ. Technol.*, 2020, doi: 10.18178/ijiet.2020.10.8.1426.

[4] C. K. Owuamalam en A. S. Matos, "When Might Heterosexual Men Be Passive or Compassionate Toward Gay Victims of Hate Crime? Integrating the Bystander and Social Loafing Explanations", *Arch. Sex. Behav.*, 2020, doi: 10.1007/s10508-019-01592-y.

[5] W. Ishikawa en S. Sato, "Mechanical C–C Bond Formation by Laser Driven Shock Wave", *ChemPhysChem*, 2020, doi: 10.1002/cphc.202000563.

[6] A. Shamsabadi, A. Dasmeh, A. Nojoumi, K. M. Rollins, en E. Taciroglu, "Lateral Capacity Model for Backfills Reacting against Skew-Angled Abutments under Seismic Loading", *J. Geotech. Geoenvironmental Eng.*, 2020, doi: 10.1061/(asce)gt.1943-5606.0002183.

[7] M. Schlafly en K. B. Reed, "Novel passive ankle-foot prosthesis mimics able-bodied ankle angles and ground reaction forces", *Clin. Biomech.*, 2020, doi: 10.1016/j.clinbiomech.2019.12.016.

[8] M. Safarabadi, H. Izi, J. Haghshenas, en H. K. Kelardeh, "Design of micro-vibration isolation system for a remote-sensing satellite payload using viscoelastic materials", *Eng. Solid Mech.*, 2020, doi: 10.5267/j.esm.2019.8.003.

[9] M. Rocca en A. Cavallo, "Wired actions: Anticipatory kinematic interference during a dyadic sequential motor interaction task.", *J. Exp. Psychol. Gen.*, 2020, doi: 10.1037/xge0001003.

CHAPTER 8

MOTORS WITH SWITCHED RELUCTANCE

Dr. V. Pushparajesh, Professor
Faculty of Engineering and Technology, JAIN (Deemed-to-be University), Bengaluru, Karnataka, India
Email id- v.pushparajesh@jainuniversity.ac.in

A stepping motor with a changeable reluctance platen and a linear switching reluctance motor have comparable topologies. Additionally, position sensors are included. The input current's on and off times are coordinated with the movement of the moving component. The turn-on and turn-off instants have a significant impact on the thrust. The speed of the moving component in a linear stepping or linear switched reluctance motor is, where the pole pitch of the reaction rail is, and fsw is the fundamental switching frequency in one armature phase winding. In a rotary stepping or switching reluctance motor, fsw equals 2prn, where n is the rotational speed in rev/s and 2pr is the number of rotor poles[1], [2].A polyphase winding on the armature and a doubly salient magnetic circuit are features of a linear switching reluctance motor. Transverse and longitudinal flux designs. The design limitations of linear AC motors (minimum speed restricted by lowest practical pole pitch) do not apply to linear switching reluctance motors, which provide accurate speed and position control of linear motion at low speeds in Figure 8.1.

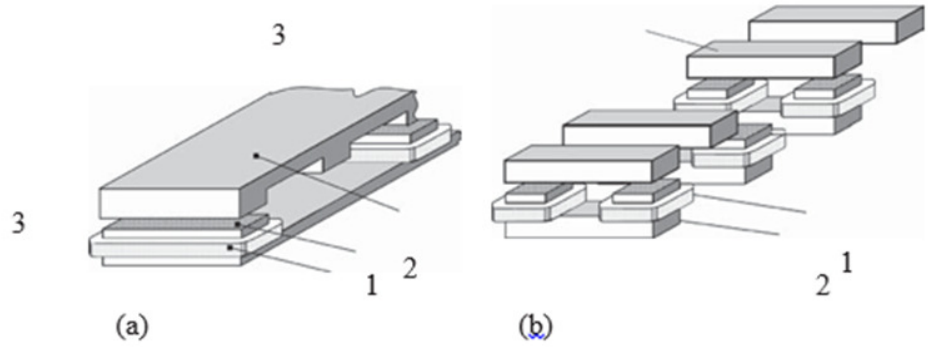

Figure 8.1: *Illustrates* **the linearswitchedreluctancemotorconfigurations:(a)longitudinalfluxdesignand(b)transverse fluxdesign.1,armaturewinding;2,armaturestack;3,plate.**

Stages of Linear Positioning

Modern improved precision linear positioning relies heavily on linear motors. Systems for linear precision positioning may be divided into closed-loop servo systems with LSMs, LBMs, or LIMs and open-loop systems with HLSMs. Al, steel, ceramic, or granite plates are used to create fixed bases. It offers a flat, accurate base that is sturdy, on which all stationary positioning components may be fastened. Using mounting screws, the stage's base is fastened to the host system[3], [4].

All movable positioning elements may fit on the moving table. The moving table's mass should be as low as possible to obtain maximum acceleration, and often, Al is utilised as a lightweight material. To secure the payload to the mounting table, the moving table must

include a number of mounting holes. The moving table is precisely guided by linear bearing rails. There must be at least one bearing rail. Each rail is equipped with a linear ball bearing or an air bearing. A response rail (PM excitation system) is installed in the base between the rails and a linear motor's armature is attached to a moving table (in Figure 8.2).

To get exact control of the table's location, velocity, and acceleration, a linear encoder is required.

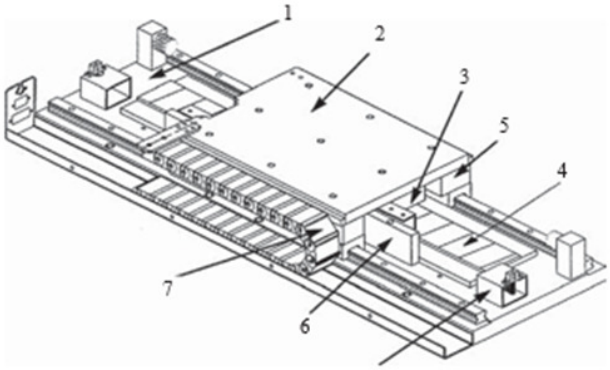

Figure 8.2: *Illustrates* the Linear positioning stage driven by PM LBM. 1, base; 2, moving table; 3, armature of LBM; 4, PMs; 5, linear bearing; 6, encoder; 7, cable carrier; 8, limit switch.

Over travel prevention and initial homing are provided by noncontact limit switches mounted to the base. Electrical wires are accommodated and routed via a cable carrier between the stationary connection box fastened to the base and the movable table. A linear precision stage powered by an HLSM has a similar design. It features a variable reluctance platen rather than PMs in the space between the bearing rails. In addition to the electrical wires, HLSMs often need an air hose to connect the air bearings to the compressor. Electronic assembly, quality control, laser cutting, optical scan, water jet cutting, gantry systems (x, y, and z stages), colour printers, plotters, and Cartesian coordinate robots all employ linear positioning stages[5], [6].

Planning for Transmission Systems

A generating system, a transmission system, a sub transmission system, and a distribution system may all be thought of as parts of an electrical power system. The bulk power supply, sometimes referred to as the generating and transmission systems, is thought to be transferred to the end client via the sub transmission and distribution networks. A high-voltage network, typically 138–765 kV alternating current, is used for bulk power transmission. This network is used to link power plants to electrical utility systems and to carry electricity from the plants to large load centres. The ANSI Standard C-84 of the American National Standards Institute, which specifies the typical transmission voltages. The term "sub transmission" refers to a lower voltage network, typically between 34.5 to 115 kV,that links distribution and bulk power substations. Extra-high voltages are those that fall within the range of 345-765 kV. (EHVs). A highly extensive system design is required by the EHV systems. The sequence of processes that make up the design of an EHV line. While voltages exceeding 765 kV are regarded as ultrahigh voltages, high-voltage transmission lines up to 230 kV may be constructed using very straightforward and standardised designs (UHVs). UHV systems are now in the research and development phases at voltage levels of 1000, 110, 1500, and 2250 kV. Transmission line lengths, technological advancements, and the cost of electricity in the

service regions of regional reliability councils (based on 1968 constant dollars). In the past, technical advancements that were reflected in operational efficiency and economies of scale caused the cost of electrical energy to decline.

Currently Used Transmission System Planning Methods

The goal of transmission system planning, as noted above, is to identify the timing and kind of additional transmission facilities needed to provide appropriate transmission network capability to handle future generating capacity expansions and load-flow needs. A functional block diagram of an ordinary transmission system planning procedure. For each year in a long-term (15–20-year) planning horizon, this procedure may be repeated with less and less depth. The main goal is to reduce the long-term capital and operational expenses associated with delivering an appropriate degree of system dependability while taking into account the environment and other pertinent factors. Planning for transmission may take into account both current and future service regions. The planning process begins with the development of load estimates for the system as a whole, for each area, and for each significant existing and future substation. Next, specific solutions that meet the new load circumstances are found. Both steady-state and contingency scenarios are used to evaluate the performance of the system. The transmission expansion logic diagram. The major goal is to discover any possible issues, such as inappropriate voltage circumstances, facility overloads, declining dependability, or any transmission system failure to fulfil performance standards. Following the analytical phase, the planner creates alternative plans or scenarios that, in addition to preventing the anticipated issues, will also best achieve the long-term goals of system dependability and economics. Studies of load-flow under both regular operations and emergency situations are used to evaluate the efficacy of the alternative strategies. The utilities' current load-flow programmes enable the automatic calculation of currents, voltages, real power flows, and reactive power flows while taking into account the specified generation schedules, the voltage-regulating capacity of generators, transformers, synchronous condensers, and net interchange among interconnected systems. The planner may accomplish to create a cost-effective system that satisfies the operational and design requirements by altering the placement, size, and number of transmission lines. The planner analyses the system behavior under fault situations after selecting the ideal system design through load-flow studies[7], [8].

The two main goals of short-circuit studies are to (1) establish the relay specifications and settings to detect the fault and trigger the circuit breaker to operate when the current flowing through it exceeds the maximum permissible current, and (2) establish the relay requirements and settings to enable the disconnected equipment to successfully clear the fault from the system. The short-circuit studies may also be used to design grounding systems, compute electromechanical forces impacting system facilities, and predict voltages under faulted situations that influence insulation coordination and lightning arrester applications. Finally, the planner conducts stability assessments to ensure that the system will continue to be stable even in the event of a serious defect or disruption. Here, the transient behavior of the power system after a disturbance is referred to as the stability analysis. Transient stability analysis is a category that fits this. The capacity of the system to sustain synchronous functioning after a disturbance, often a fault state, is referred to as transient stability. The generators, which are linked to one another by a transmission network, will go out with respect to one another and cease to function in synchronism unless the fault state is quickly corrected by circuit breakers. As a result, the power system will become unstable as enormous currents start to flow across the network, oscillating shifting power from one generator to another. As a result, the protective relays will notice these high currents and trigger the network's circuit breakers

to open, cutting off the power completely. The initial swing of the rotor angles is often regarded as a reliable sign of how stable the power system is still. Therefore, transient stability may be achieved by simulating the initial few seconds after a disruption[7], [9].

The system is simulated for anywhere between a few seconds and several minutes, as opposed to the steady-state stability study, which is characterised as long-term changes in system frequency and power transfers that result in complete blackouts. The planner may investigate the system's transient and steady-state stabilities using a variety of computer programmes. A transient stability programme typically uses the data—in the form of beginning voltages and power flows—provided by a load-flow programme as the input and modifies the system to that required for the transient stability analysis. A common measure of stability margin is the critical switching time, which is the amount of time that a malfunctioning system component must be tripped to ensure stability. For a variety of failure kinds and locations, the crucial switching times are determined. The resulting minimum needed clearing time is compared to the actual running times of the relays and circuit breakers. The planner may think about altering the network design, the characteristics of the turbine-generator, or maybe the control equipment if the relays and circuit breakers are unable to react quickly enough to maintain stable operation.

Transmission System Planning Models

The planning and design of transmission systems in the past relied heavily on the planner's prior expertise and were very intuitive. The planner has access to a wide range of analysis and synthesis tools nowadays. These tools may be used for design and planning tasks such transmission network expansion planning, transmission route identification and selection, network analysis, and reliability analysis.

Selection and Identification of Transmission Routes

A typical transmission route (corridor) selection process is shown in Figure. Safety, engineering and technology, system planning, institutional, economics, environmental, and aesthetic considerations are the limiting elements that have an impact on the process. The planner chooses the best transmission route today based on his understanding of the system, the findings of the system analysis, and the availability of rights of way. Two computer programmes, Power and Transthetics, have recently been created to help the planner with the identification and selection of transmission routes. The Power computer software may be used to find different kinds of corridors in addition to transmission line corridors. While the Transthetics computer application was created especially for electrical utilities to find and choose suitable transmission line paths and acquire the requisite rights of way in Figure 8.3.

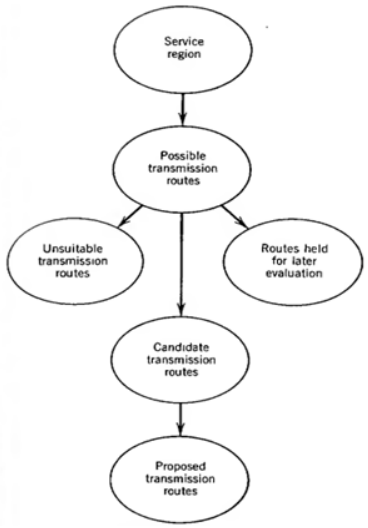

Figure 8.3: ***Illustrates*** **a typical transmission route (corridor) selection procedure.**

Planning For Transmission System Expansion

To analyse the performance of various transmission system options today, the system planner mainly employs tools like load-flow, stability, and short-circuit programmes. To choose the best system, some utilities, however, also utilise what are known as automated expansion models. The optimal system is the one that minimises an objective function (performance function) subject to constraints. This is an optimality claim in the mathematical sense. The automated expansion models may generally be divided into three fundamental groups: algorithmic models. Models for single-stage optimization. Models for time-phased optimization.

Historical Models

The main benefit of heuristic models is interactive planning, which allows the system planner to watch the growth process and influence it in the desired direction. Heuristic models include the following features, in order: (1) simple model and logic; (2) user involvement; and (3) families of practicable, close to ideal plans. While the mathematical programming models include the following traits: (1) no user input; (2) fixed model via programme formulation; (3) precise logic or limitation set j specification; and (4) a single "global" solution. In contrast to mathematical models, the heuristic models may be thought of as being constructed to order. Some assist in simulating the use of analytical tools by system planners, such load-flow programmes and reliability analyses [6], by simulating the planning process using automated design logic. The traditional publication by Garver [7] offers an approach that combines optimization methods with heuristic reasoning for circuit selection. The most efficient way to transmit power from the generator to the load without overloading any circuits is what the suggested approach does. In a heuristic method, the computer software automatically provides the planner with the optimal circuit addition or exchange at each step of the synthesis process. The planner has the option of accepting it or making the desired changes. More details on heuristic models are provided.

Models for Single-Stage Optimization

The optimal network growth from one stage to the next may be determined using the single-stage or single-state (or so-called static) optimization models. However, they omit to mention the expansion's timeframe. They may not provide the best answer for the overall growth

pattern over a time horizon, even while they offer the best option for year-by-year expansion. The linear programming, integer programming, and gradient search methods are some of the mathematical programming approaches utilised in single-state optimization models.

Program linearly: A mathematical method known as linear programming (LP) may be used to reduce or maximise an objective function, a given linear function with linear restrictions on the variables. Z is the value that has to be optimised, and the objective function has the linear form Z=tctXl (1.1) 1=1. Z is the overall cost that has to be reduced (in expansion studies). The ct are the expenses related to one unit of xr, and the xt are n unknown quantities. The ct may take either a positive or negative value, however the xt must be configured to only take positive values. The unknowns' potential values are restricted by the constraints, which must be a linear combination of the unknowns. The limitations take the shape of aux,

$$\sum a_{ji} x_i = , \geq , \leq b_j \qquad x_i \geq 0$$

$$\begin{aligned} a_{11}x_1 + a_{12}x_2 + \cdots + a_{1n}x_n &= , \geq , \leq b_1 \\ a_{21}x_1 + a_{22}x_2 + \cdots + a_{2n}x_n &= , \geq , \leq b_2 \\ a_{m1}x_1 + a_{m2}x_2 + \cdots + a_{mn}x_n &= , \geq , \leq b_m \\ x_1 \geq 0,\ x_2 \geq 0, \ldots, x_n &\geq 0 \end{aligned}$$

$$j = 1, 2, \ldots, m,\ i = 1, 2, \ldots, n$$

When there are m restrictions, any number of which may be equal or unequal. Furthermore, the quantity of constraints, w, may be larger, lower, or equal to the quantity of unknowns, n. The coefficients of the unknowns, an i9, must be constants and may either be positive, negative, or zero. Constants that may be positive, negative, or zero are the b j. The limitations specify an area in n-dimensional space where solutions are feasible. The point in this space whose xt values decrease or maximise the objective function Z is the best solution. The results are often accurate and beneficial. The approach makes it easier to see capacity gaps and identify areas where additional circuits could be added to reduce overloads. The goal function is calculated by adding the circuit lengths (guide numbers) and the amount of power they carry. Here, power flows are computed using a network model with a linear loss function that is akin to a transportation model. This model does not employ Kirchhoff's voltage law to define flows; instead, it uses Kirchhoff's current law, which states that at each bus, the total of all flows in and out must equal zero. Instead, the approach relies on guiding potentials to prevent overloading of traditional circuits. The flow model, however, also employs overflow routes, through which power may flow if necessary, to pinpoint the locations of circuit additions. When there are no overload pathways left, the networks are enlarged one circuit at a time, eliminating the path with the biggest overload. After the network extension is complete, the system is typically evaluated using an AC load-flow algorithm. As previously indicated, the procedure is also heuristic since determining the guide numbers requires a lot of judgement. It approaches the issue more firmly as an optimization problem, however.

Arithmetic Programming

The class of linear programming problems known as "integer programming" are those in which some or all of the decision variables must be integers. For instance, a binary variable may be added to each line to indicate whether it is picked or not in the LP programme shown in equations in order to convert it into an integer programme.

$$x_i = 1 \quad \text{if line } i \text{ is selected}$$
$$x_i = 0 \quad \text{if line } i \text{ is not selected}$$

Therefore,

$$\text{Minimize } Z = \sum_{i=1}^{n} c_i x_i$$

subject to

$$\sum_{i=1}^{n} a_{ji} x_i \leq b_j \qquad x_i = 0, 1$$

where $j = 1, 2, \ldots, m$ $i = 1, 2, \ldots, n$.

Since a line component is either added to the network or not, integer programming often works better for the transmission expansion issue than linear programming because it recognises the problem's discrete character. A pure integer programme is one in which all variables must have integer values between 0 and 1. A mixed-integer programme is one that limits some of the variables to take integer values while allowing others to accept continuous (fractional) values. Integer programming was used to solve the transmission expansion issue. For the most effective planning of electricity networks, mixed-integer programming was adopted. Proposed techniques that focus the search on a small number of new additions that are most likely to fulfil all requirements by combining sensitivity and screening processes. In order to identify the overcrowded lines and determine the line flow sensitivities to changes in admittances in all transmission corridors, it begins with a dc load-flow solution. It uses a screening procedure to identify unproductive corridors in order to decrease the dimension of the integer programming problem in terms of the number of variables and, therefore, the computing time. The ensuing issue is then resolved using the branch-and-bound method. Only discrete increments of capacity are added in accordance with the optimum capacity cost curves. Until all limits are met, the procedure is repeated as many as required.

Models for Time-Phased Optimization

The scheduling of new installations across a specified time horizon is not taken into consideration by the single-stage transmission network expansion models. Because of this, Garver notes that "a way of identifying a succession of annual transmission plans which result in the lowest revenue needs across time but which may be greater in cost than truly required in any one specific year" is necessary. When comparing alternative network expansion plans, a time-phased (trough-time, or multistate, or so-called dynamic) optimization model may take inflation, borrowing rates, and annual operational costs into account.

The optimization techniques for dynamic programming and integer programming have both been utilised to address the time-phased network expansion models. By breaking up a particular time horizon into several yearly subperiods, integer programming has been used. In order to establish the capacity, placement, and timing of new facilities according to stated limitations, the objective function in terms of current worth of a cost function is minimised. Problems with network growth have been addressed using dynamic programming by creating a set of network configurations for each year (stage). Only workable proposals (states) that adhere to the established constraints are approved. According to the author, however, "the dynamic programming approach has ordered the search so that just a small number of evaluations were required to locate the lowest cost expansion. However, the

dynamic programming approach alone cannot create new plans (states); rather, it merely optimally connects preexisting states.

REFERENCES

[1] A. Asok Kumar, G. R. Bindu, E. Cherian, en M. L. Parvathy, "Energy Saving and Economic Analysis of Switched Reluctance Motor in Agricultural Applications", *Technol. Econ. Smart Grids Sustain. Energy*, 2020, doi: 10.1007/s40866-019-0075-z.

[2] I. Tariq, R. Muzzammel, U. Alqasmi, en A. Raza, "Artificial Neural Network-Based Control of Switched Reluctance Motor for Torque Ripple Reduction", *Math. Probl. Eng.*, 2020, doi: 10.1155/2020/9812715.

[3] J. A. Sanchez, P. Andrada, B. Blanque, en M. Torrent, "Predictive Maintenance Plan for Switched Reluctance Motor Drives", *IEEE Lat. Am. Trans.*, 2020, doi: 10.1109/TLA.2020.9049463.

[4] S. Wang, Z. Hu, en X. Cui, "Research on Novel Direct Instantaneous Torque Control Strategy for Switched Reluctance Motor", *IEEE Access*, 2020, doi: 10.1109/ACCESS.2020.2986393.

[5] A. Rezig, W. Boudendouna, A. Djerdir, en A. N'Diaye, "Investigation of optimal control for vibration and noise reduction in-wheel switched reluctance motor used in electric vehicle", *Math. Comput. Simul.*, 2020, doi: 10.1016/j.matcom.2019.05.016.

[6] X. Zhao, A. Xu, en W. Zhang, "Research on DTC system with variable flux for switched reluctance motor", *CES Trans. Electr. Mach. Syst.*, 2020, doi: 10.23919/tems.2017.7961342.

[7] D. Bajpai*, V. K. Jogi *, en M. K. Nigam, "Torque Enhancement of Switched Reluctance Motor with Teethed Stator Pole", *Int. J. Innov. Technol. Explor. Eng.*, 2020, doi: 10.35940/ijitee.e2575.039520.

[8] S. Hosseini en Y. Alinejad-Beromi, "Noise reduction in switched reluctance motor by modifying the structures", *IET Electr. Power Appl.*, 2020, doi: 10.1049/iet-epa.2020.0081.

[9] X. Sun, K. DIao, G. Lei, Y. Guo, en J. Zhu, "Real-Time HIL Emulation for a Segmented-Rotor Switched Reluctance Motor Using a New Magnetic Equivalent Circuit", *IEEE Trans. Power Electron.*, 2020, doi: 10.1109/TPEL.2019.2933664.

.

CHAPTER 9

TRANSMISSION SYSTEM PLANNING

MukthaEti, Assistant Professor
Faculty of Engineering and Technology, Jain (Deemed-To-Be University), Bengaluru, Karnataka, India
Email Id- muktha.eti@jainuniversity.ac.in

We've spoken about a few of the methods that utility sector system planning engineers have used in the past and now to develop transmission networks. Additionally, the planning for the transmission system's influencing aspects have been examined. This section's goal is to evaluate the potential implications of current trends on the planning process going forward. The planning of the transmission system in the 1980s will be significantly impacted by a number of economic considerations. Inflation is #1 on the list. Inflation will continue to play a significant role due to energy shortages, the expense of switching energy sources, environmental concerns, and significant governmental deficits. The rising cost of raising finance will be the second significant economic driver. Government will strive to lower the money supply as long as inflation keeps the dollar's actual worth from rising. As a result, there will be more competition to attract the cash required for power system expansions. The third element that has to be taken into account is the growing difficulties in raising customer rates. This "inertia" of rate hikes is caused in part by inflation as well as the effects of consumer advocacy organisations making consumers more sensitive to rate increases. Extrapolations of current techniques must be made in order to make predictions about the transmission system planning approaches of the future. There is little chance that the fundamental network analysis methods will be enhanced in the foreseeable future. To take advantage of the new techniques that technology has made feasible, it is envisaged that the superstructure that underpins these algorithms and the problem-solving environment employed by the system designer would alter dramatically. Before delving into the specifics of these anticipated changes, it is necessary to consider how transmission system planning is evolving. Construction, expansion, and modification costs for transmission lines will rise due to the aforementioned economic factors. Therefore, it is crucial that each transmission system design be as economical as feasible. This implies that from the first day of operation to the planned time horizon, the system must be ideal from a variety of angles. In order to save capital cost, satisfy performance objectives, and reduce losses, components must be phased in and out of the system together with correct load growth forecasts. Economics is the most influential factor influencing the development of the utility sector, therefore any new ideas are unlikely to be embraced for their own reason. Only if these innovations lower the cost of any activity or produce something valuable for the economy that was previously unavailable for similar prices will they be embraced. It is necessary to evaluate their adoption on this basis when making predictions about which methods or technologies may eventually replace the ones we now use. Planning tools that are implemented on a digital computer and deal with transmission systems in terms of networks are the anticipated advancements that meet these characteristics. One would be tempted to think that these planning tools would be suitable for use in the 1980s by industry. By comparing the tendencies that were deemed to be prevalent throughout this era with those that ruled over the period in which the tools were built, it can be observed that this is not likely to be the case[1], [2].

New Planning Instruments

There are two types of tools to be taken into consideration: network design tools and network analysis tools. The context in which they are utilised will change dramatically, while the analytic tools themselves may become more effective but are not anticipated to undergo any significant modifications. The following part will cover this setting. However, it is anticipated that the design tools would advance the most since greater planning can have a big influence on the utilities sector. The outcomes of this development will exhibit the traits listed below:

1. Using programming techniques from operations research, network architecture will be optimised in terms of a variety of criteria.

2. The administration of the transmission system, which will be overseen by engineers utilising a computer system created for such management tasks, will include other aspects outside network architecture.

3. Trial networks may be created using so-called network editors; these digital designs are then sent to sophisticated simulation tools to see whether the proposed network fulfils performance and load growth requirements[3], [4].

The Computer's Fundamental Function in Transmission System Design

It is common knowledge that transmission system designers have long relied on computers to carry out the time-consuming calculations required for system analysis. But it wasn't until recently that technology gave planners the tools they needed to properly adopt a "systems approach" to the overall design and analysis. The creation of such an approach will keep planners busy in the 1980s and play a crucial role in helping them overcome the issues previously covered, according to the chapter's main premise.

Systems-Based Method

Even though the result of one programme may be utilised as the input of another, a collection of computer programmes employed to address a designer's analytical issues does not automatically make for an effective problem-solving system. Examining the sorts of information needed and its sources is the first step in the systems approach to the creation of a practical tool for the designer. The assumption is that when choices are made and new information is gathered, the design process moves on to the next step. It is observed that the human engineer must assess the data produced and include his own contributions at various times. The last step is to show the findings for usage and save them for future use. The systems approach attempts to automate as much of the planning process as feasible using this paradigm, making sure that all information transformations are carried out as effectively as possible. This information flow is shown in one way[5], [6].

Basics of Power Measurement

Electrical power measurements are critical parameters that need accuracy. Accurate measurements are necessary for the regular functioning of electrical power systems. Consequently, a wide variety of measures and measuring tools are related to electrical power systems. The parts that follow will go through the basics of measurement. The metric system of measuring is now used by the majority of countries in the globe. In order to assess the viability and economics of switching the country to the metric measuring system, the National Bureau of Standards in the United States started a study in 1968. This conversion isn't finished yet. The kilogramme and the metre serve as the basis for the decimal

measurements that make up the metric system. Despite the fact that the metric system is fairly straightforward, several nations have been sluggish to embrace it. Because a full switchover of measuring systems calls for a complicated set of activities, the United States has been one of these reticent nations.

Measuring instruments

Although they have a big impact on our lives, units of measurement are often taken for granted. Nearly everything we interact with on a daily basis is quantified using some kind of unit. For instance, we may measure the time of day, the length of a day, and the quantity of food we consume during a meal using such units. Although units of measurement have been around for a while, they are today more defined than they were centuries before. The majority of units of measurement are based on physical science rules. For instance, the speed of light is used to measure distance, while the length of certain atomic vibrations is used to measure time. The measuring standards we use have a significant impact on contemporary technologies. All nations in the globe must recognise measuring units. There must be a means to compare standard measuring units used in various nations. For worldwide marketing as well as for business, industry, and science in general, standard units of length, mass, and time are essential. The inch, foot, and pound are only a few examples of the units employed by the English system of units, which has long been in use in the United States. The metric system, which uses measurements like kilometres, centimetres, and grammes, is used in a large number of other nations. The International System of Units, or SI, is another name for the metric system. Despite the fact that there are clear numerical links between the English and SI systems of measurement, many find it challenging to switch between the two. Either the English or the SI systems become habitual. Since both measurement methods are in use, this chapter will acquaint you with both systems as well as the unit conversion process. Appendix C's conversion tables should be useful. The SI system of measuring, which was adopted in 1960, provides a number of benefits over the English system. It is a decimal system that employs elements like volts, watts, and grammes that are often utilised in commerce and industry[7], [8]. The SI system is also easily applicable worldwide. However, there are situations when using other units is more practical. The seven units that make up the SI system of units are listed in Table 9.1. From the basic units, further units are created, as illustrated in Table 9.2.

Table 9.1: *Illustrates* the Base Units of the SE System.

Measurement Quantity	*Unit*	*Symbol*
Length	meter	m
Mass	kilogram	kg
Time	second	s
Electric current	ampere	A
Temperature	kelvin	K
Luminous Intensity	candela	cd
Amount of substance	mole	mol

Table 9.2: *Illustrates* the Derived Units of the SI System.

Measurement Quantity	*Unit*	*Symbol*
Electric capacitance	farad	F
Electric charge	coulomb	C
Electric conductance	siemen	S
Electric potential	volt	V
Electric resistance	ohm	Ω
Energy	joule	J
Force	newton	N
Frequency	hertz	Hz
Illumination	lux	lx
Inductance	henry	H
Luminous intensity	lumen	lm
Magnetic flux	weber	Wb
Magnetic flux density	tesla	T
Power	watt	W
Pressure	pascal	Pa

Basics of Power Systems

The study of electrical power is one of the most important branches of electrical expertise. The enormous demand for electrical power in our nation is met by complex systems. We must continually worry about the effective functioning of our power generation and power conversion systems due to our enormous power requirements. The characteristics of electrical power generation systems, power transmission systems, power conversion systems, and power control systems are covered in this textbook. This section also includes an overview of electrical power measuring systems. Jigsaw puzzles have been used by humans as a kind of amusement for many years. An image may be created by correctly assembling the several distinct pieces that make up a jigsaw puzzle. The final product then utilises each component in a certain way. Without a sample image, it might be difficult to see the completed puzzle when one is first starting. If a complicated topic like electrical power is analysed in terms of its discrete components, understanding it presents a challenge somewhat like to the jigsaw puzzle. The function that a discrete component performs in the functioning of a complex system is also difficult to ascertain in this situation. As a result, it becomes highly helpful to have a representation of the whole system broken down into its component elements. The "grand picture" in the study of electrical power will be the system idea. In this method, a system will first be broken down into a number of crucial building components. This will make it clearer what function each block serves in the overall system's functioning. The discrete component action associated with each block becomes increasingly important after the position of each block has been determined. This strategy should help to clarify how some of the "parts" of electronic systems interact with one another[9], [10].

Functions of Basic Systems

A system is often understood to be an arrangement of components that work together to create a whole. There are several different electrical systems in use today. Each system differs from other systems in a variety of specific ways, or characteristics. But more significantly, each system has a similar set of components. All systems rely on these components in the same fundamental way. The different system components are referred to as energy source, transmission route, control, load, and indication. Every component of a fundamental system serves a particular purpose in the overall performance of the system. When a thorough examination of the system is required, this job has utmost importance. For certain block functions, hundreds or even thousands of discrete components may be required.

No matter how complicated the system is, each block has to fulfil its purpose for the system to work. Understanding these functions and where they are located in a whole system is a significant step towards comprehending how the system works. A system's energy source transforms energy from one form into another that is more useful. The basic forms of energy are heat, light, sound, chemical, nuclear, and mechanical energy. Prior to usage in an operating system, a major energy source often undergoes an energy transition in Figure 9.1.

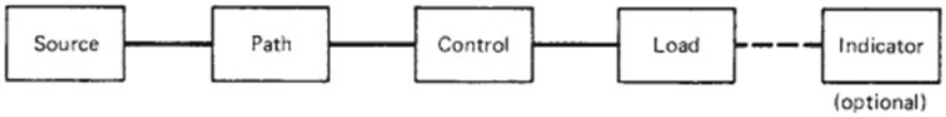

Figure 9.1: *Illustrates* each block of a basic system has a specific role to play in the overall operation of the system.

A system's transmission route is a little bit easier to do than other system operations. Simply said, this component of the system offers an energy transmission channel. The energy source is the first stop, and the load is reached after moving through the system. This channel between the source and the load might sometimes be a single electrical conductor, light beam, or other medium. In other systems, the source and the load could be connected via a supply line. There may be a supply line connecting the source and the load in certain systems, as well as a return line connecting the load to the source. Within a comprehensive system, there could also be a number of other alternative or support pathways. These pathways may be linked in parallel to a large number of unrelated devices or in series to a number of tiny load devices. The control portion of a system is by far its most intricate component. Control is done in its most basic form when a system is switched on or off. This kind of control might occur anywhere between the source and the load device. This procedure is sometimes referred to as having "complete control." A system may also use some kind of partial control in addition to this sort of control. Other than a on or off status, partial control often results in some form of operational change in the system. Changes made possible by partial control include adjustments to electric current or light intensity. A system's load is a particular portion, or a group of related parts, intended to carry out some kind of task. When energy undergoes a transition or change, work takes place. Some of the typical kinds of work performed by a load device are heat, light, chemical activity, sound, and mechanical motion. Typically, the load device uses a significant amount of the energy generated by the source while it is in operation. Due to its clear job function, the load is often the component of the system that stands out the most. A system's indicator is basically designed to show certain operating conditions at different locations all across the system. While the indicator is an optional component in certain systems, it is a necessary component in others for the system to function. In the latter scenario, system changes and actions are often crucial and reliant on certain indicator readings. This application is referred to as a "operational indication". To establish various operational values, test indicators are also required. The indicator serves this purpose by being momentarily connected to the system in order to take measurements. Typical tools used in this role include test lights, metres, oscilloscopes, chart recorders, and digital display equipment.

Structure Stability

Energy balance and the capacity to provide enough restorative forces to offset system disruptions are two issues with network stability. The machines in the system exchange power with one another to keep pace with one another and maintain a single global frequency as a consequence of minor system faults. By naturally adjusting the system voltage levels and

the common system frequency, a balance between the total mechanical power/energy input and the electrical power/energy output is maintained. There are three stable regimes: (a) Steady state stability refers to the system's capacity to maintain synchronism in the face of small shocks or gradually forming system changes, such as a progressive rise in load when the 24-hour maximum demand is approached. (b) Transient stability is concerned with how a system behaves after a rapid change in the amount of demand on it, such as one that may be caused by a defect, the sudden loss of generation or a connecting line, or the sudden connection of extra load. The transitory phase lasts for about one second. Power system design must take into account the behaviour of the system throughout this time. (c) The behaviour of the system between transient behaviour and the steady state area is referred to as dynamic stability. Dynamic stability studies, for instance, might examine the operation of turbine governors, fuel and steam flows, load shedding and the recovery of motor loads, among other things. Another idea for a stability issue is how induction motors react to system disturbances and motor startup. It has nothing to do particularly with the system's capacity to maintain synchronism.

The power-to-load angle property

$$P = UI\cos\phi \text{ (per phase)}$$

Also for the vector triangles it is true that:

$$E\sin\theta = IX\cos\phi$$

Substitute for I:

$$P = \frac{U\cos\phi \times E\sin\theta}{X\cos\phi} = \frac{UE\sin\theta}{X}$$

Therefore, the electrical power output is inversely proportional to the machine reactance but directly proportional to the internal voltage of the generator (E) and the system voltage (U) (X). Only the load angle determines the power output when (U), (E), and (X) are maintained constant. A group of charts plotting power output against load angle to illustrate this. A load angle of 90° is finally obtained as primary mover power rises. Beyond this threshold, mechanical input power must be further increased since the output of electrical power will decrease. The machine is believed to become unstable as a result of the excess input power acting to accelerate it even further. Losing synchronism with the rest of the system is the practically unavoidable result. A machine may now genuinely function at a load angle larger than 90° thanks to quick-acting contemporary automated voltage regulators (AVRs). If the load angle increases (E) more quickly than the AVR:

$$\frac{\mathrm{d}E}{\mathrm{d}t} > \frac{\mathrm{d}\theta}{\mathrm{d}t}$$

Once stability is achieved, it can be maintained up to a theoretical maximum of around 130°. Because the synchronous machine may go through stages when it alternately acts as a generator and then as a motor, this loss of synchronism is important. Power surges entering and exiting the machine, which may be many times the equipment's rating, would subject the device to very high electrical and mechanical strains in Figure 9.2.

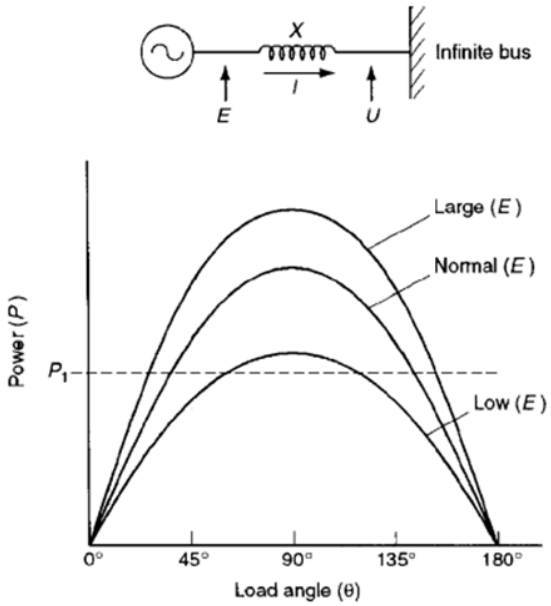

Figure 9.2: *Illustrates* the Power/load angle relationship.

When out-of-synchronism problems are ultimately detected, generator overcurrent relay protection will separate the generator from the system. Before this occurs, additional network components may trip out as a result of the power surge, and the whole system may crash. In order to maintain synchronism for all anticipated modes of system operation, disruptions, and outages, it is important to ensure that the right design and operational procedures are adopted.

Operating chart for a generator

The generating operating chart provides an illustration of the impact of a generator's maximum steady power output. This is effectively an expansion of the vector diagrams in Figure 9.3, where the value of internal voltage (E) and load angle () are displayed for every MW or MVAr loading situation. The circles on the operating chart stand in for constant values of (E), and the load angle is shown for an a priori operating point. The theoretical stability limit is represented by the operating locations when the load angle is 90°. Operation outside of the theoretical stability limit corresponds to load angles greater than 90 degrees and is forbidden. One of the limits that the operating point must fall inside is the theoretical stability limit.

1. The maximum permissible stator current, shown on the chart as an arc of maximum MVA loading, forms one of the other limits.

2. The chart displays the maximum permitted field excitation current as an arc at the associated maximum internal voltage (E).

3. The power limit of the primary mover may be represented by a vertical line of maximum power. The limits of the generator's various operating ranges are defined by whichever of the aforementioned restrictions applies first. Operation at any position along the theoretical stability limit line would be very undesirable in a real-world setting. A desire for increased power production at a load angle of 90° causes the generator to become unstable. A realistic stability limit is often included into the operating chart so that stability can always be maintained for operation at any point along this line with an increased power output of up to a specified percentage of rated power. The practical stability limit is shown for a 10%

increase in power above the output's rated value. The stabilising impact of the AVR is shown by the dotted line beyond the theoretical stability limit with a load angle of 90°.

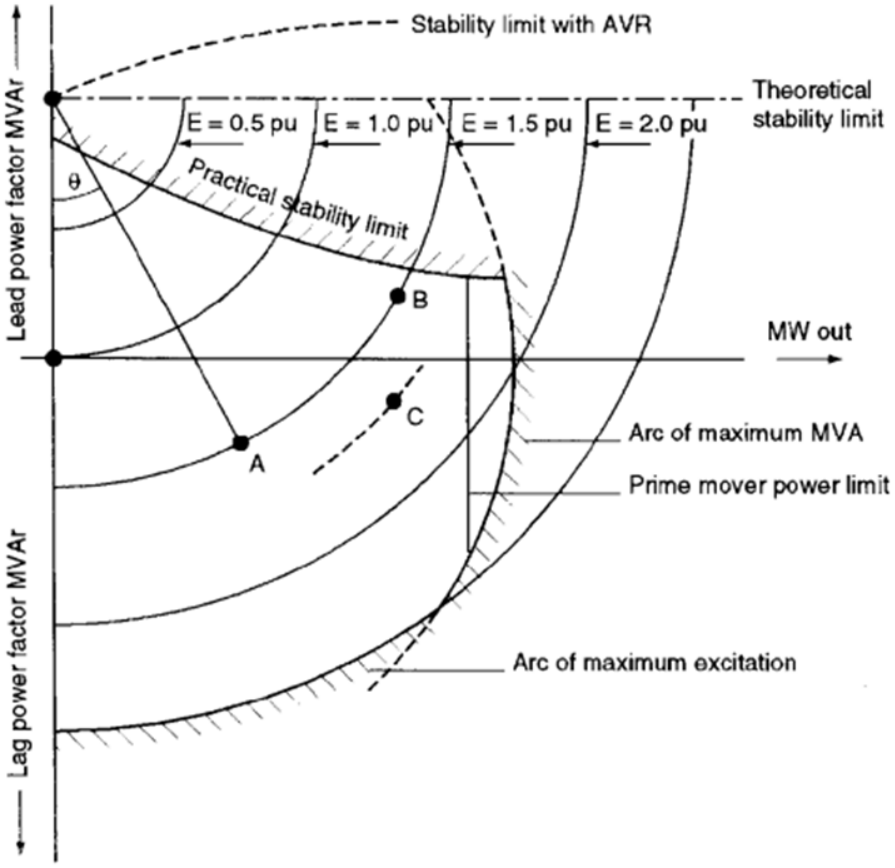

Figure 9.3: ***Illustrates*** **the practical stability limit is shown for a power increase of 10% of rated power output.**

Regulators of voltage automatically (AVRs)

For all circumstances of electrical output, the AVR typically maintains a constant generator terminal voltage. In actuality, this is accomplished by altering the machine's excitation, and consequently (E), in response to any changes in terminal voltage. The infinite bus maintains the terminal voltage constant in the straightforward system of one generator powering an infinite bulbar. In this instance, changes in excitation result in adjustments to the machine's reactive power MVAr loading. In more realistic setups, the machine's output at least somewhat affects the generator's terminal voltage. When the electrical load increases, the terminal voltage decreases, and the AVR responds by boosting the internal voltage (E). On the circle of constant internal voltage (E) on the generator operating chart, an increase in power output from the starting point A would result in a new operating point B if there were no human or automated adjustments (E). The operating point becomes closer to the stability limit when the power output is increased in this way. The new operating point would be at C if, concurrently with the increase in power, there is a rise in (E) owing to the action of the AVR. The AVR may be seen of as functioning to maintain steady state stability since its primary function is to keep the operating point far away from the stability limit.

It can be demonstrated from steady state stability in industrial facilities that when generators provide capacitive loads, their steady state stability limitations are reached. The issue of

steady state stability is unlikely to arise since industrial facilities typically run at trailing power factors. The likelihood of a leading power factor situation is important and has to be looked into when power factor adjustment is utilised or when synchronous motors are involved. Think about the 21 kV distribution plan for the Channel Tunnel. This comprises of 50 km long 21 kV cross-linked polyethylene (XLPE) cables that span between England and France beneath the English Channel. In the very rare event that both the UK National Grid and the French National Grid supplies go down at the same time, standby generation is intended to keep vital services running. The single-line diagram's 3 MVAr reactor is utilised to offset the capacitive impact of the 21 kV cable system. The system is initially separated from the malfunctioning Grid supply. Before turning on the cable network, the generators are first run up and first put into the reactor. The Channel Tunnel control centre then uses a remote control to activate the critical loads (ventilation, drainage pumping, lighting, and control and communications plant).

An illustration using physical principles

The capacity of every component of the network to maintain synchrony after a sudden change in operating circumstances is known as transient stability. The three phase failure is often the most severe rapid shift, although network switching, electrical system load applications, mechanical drive power to the generator, and other abrupt changes may all cause system instability. Typically, this instability is seen as a systemic issue with the energy balance. The loaded spring analogy is a helpful tool to assist with situational visualisation. The following is the general energy equation:

$$\text{Mechanical energy} = \text{Electrical energy} \pm \text{Kinetic energy (energy of motion)} + \text{Losses}$$

When changes are gradual under steady state circumstances, the system's kinetic energy is unaffected. The machine cannot instantly provide energy from its prime mover or absorb energy from the electrical supply if there is a sudden disruption to the machine (fault or load change). The most frequent reason for instability in a generator system is a problem near to the terminals, which abruptly prohibits the energy of the machine from being delivered to the system. The machine's kinetic energy and speed fluctuations are where the surplus or shortfall of energy must go or originate from. As an example, a motor will give more mechanical load from its kinetic energy and slow down if it is unexpectedly requested to do so. The process of slowing down will overshoot (go too far) and be followed by an increase in speed, approaching the new load situation oscillatorily much like the loaded spring. A spring with stiffness S will expand by a distance x until the stiffness force Sx Mg, or the mass's weight, is applied. The system's kinetic energy won't be affected. The spring is like the machine, and the spring's extension is like the load angle on the machine. When a spring is loaded over its elastic limit, a loaded machine has steady state instability. A machine can only be unstable in relation to a reference (another machine or an infinite busbar that it is linked to) with which it may exchange restorative forces and energy. A machine cannot be unstable in isolation. An unattached spring cannot be expanded in the analogy; it can only be loaded against a restraint mass (its attachment). Consider the spring analogy situation, where the transitory state is represented by the spring being abruptly loaded by a mass M. The system's kinetic energy is now disrupted, and the weight will cause the spring to extend over its usual length in the direction of x where xx. Until the mass's initial kinetic energy is transformed into strain energy in the spring, the mass M goes past x to x:

$$\frac{1}{2}MV^2 = \frac{1}{2}S(\Delta x' - \Delta x)^2$$

There is an overrun when the weight briefly rests at x because the spring has now accelerated the mass higher beyond x after absorbing the weight's kinetic energy into its strain energy. Eventually, the mass oscillates to settle into its fixed position. It should be noted that the spring is capable of supporting a weight that, if put on it, would force it to stretch over its elastic limit before stopping the weight's downward motion. Similar to transitory instability, this in Figure 9.4.

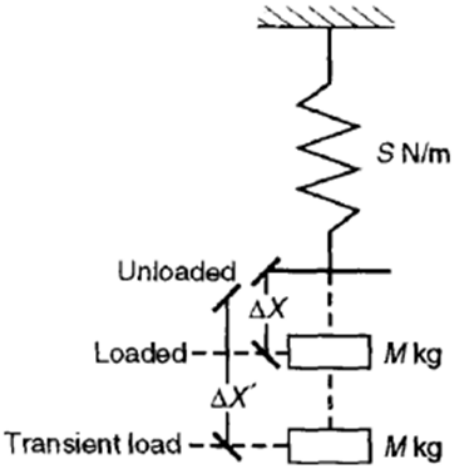

Figure 9.4: ***Illustrates*** **the Loaded spring machine stability analogy – overshoot.**

It can be seen how close the above analogy is by examining the equations of motion of the loaded spring and the synchronous machine as follows. For the spring:

$$M\frac{d^2x}{dt^2} + K\frac{dx}{dt} + Sx = \text{Force}$$

Where M is the applied mass, x is the extension, d2 x/dt 2 is the acceleration or deceleration of mass M, Kdx/dt is the velocity damping and S is the restoring force. For the synchronous machine:

$$M\frac{d^2\theta}{dt^2} + K\frac{d\theta}{dt} + Pe\sin\theta = P_m \text{ mechanical power}$$

Where M is the angular momentum and Pe sin is the electrical power. For small, sin tends to,

$$M\frac{d^2\theta}{dt^2} + K\frac{d\theta}{dt} + Pe\,\theta = P_m$$

And if we change power into torque by dividing by the synchronous speed, the analogy is exact:

$$J\frac{d^2\theta}{dt^2} + K'\frac{d\theta}{dt} + Te\,\theta = T_m \text{ the mechanical torque}$$

Varying load angles

The impact of a rapid shift in machine load may be shown visually using the power/load angle curve illustrated. Although either a synchronous generator or a synchronous motor may experience the reaction shown, it is simpler to picture a motor under abrupt load. Consider a synchronous motor that is initially running at point 'a' on its typical operating curve with mechanical power P1 and load angle 1.

$$\text{Power } P_e = \frac{EU}{x'_d}\sin\theta$$

Where xd is the transient reactance of the machine. If losses are ignored, operation at 'a' represents an equilibrium condition where the mechanical power P1 and the electrical power Pe are equal. Synchronous speed is the rate at which the machine runs. Let's say the mechanical load on the synchronous motor suddenly changes. The need for mechanical power rises to P2. The electrical system is unable to provide this rapid energy demand right away, so the motor must use its stored rotational energy, which causes it to slow down. The motor advances to point "c" on its power/load angle curve, where it is providing the new power demand P2, as it slows down, enabling more power to be extracted from the electrical supply. At 'c,' however, the motor is moving too slowly, which causes its load angle to keep rising. Beyond "c," the motor accelerates because the electrical power it receives is greater than the increased mechanical demand P2. The machine is once again operating at synchronous speed when the motor overswings to "d." Here, the motor continues to accelerate beyond synchronous speed and therefore begins to lessen its load angle since the electrical power is still larger than the mechanical power. The electrical and mechanical powers are once again equal at point "c," but since the machine is moving faster than synchronously, it backswings in the other direction, towards point "a." Although damping will prevent the machine from reaching 'a,' the damping effects force it to fluctuate about 'c' until it eventually stops at 'c.

REFERENCES

[1] J. H. Moon, H. N. Gwon, G. R. Jo, W. Y. Choi, en K. S. Kook, “Stochastic modeling method of plug-in electric vehicle charging demand for korean transmission system planning”, *Energies*, 2020, doi: 10.3390/en13174404.

[2] A. Sajadi, K. Clark, en K. A. Loparo, “Statistical Steady-State Stability Analysis for Transmission System Planning for Offshore Wind Power Plant Integration”, *Clean Technol.*, 2020, doi: 10.3390/cleantechnol2030020.

[3] H. Ranjbar, S. H. Hosseini, en H. Zareipour, “A robust optimization method for co-planning of transmission systems and merchant distributed energy resources”, *Int. J. Electr. Power Energy Syst.*, 2020, doi: 10.1016/j.ijepes.2020.105845.

[4] M. A. Al-Gabalawy, M. A. Mostafa, A. S. Hamza, en S. A. Hussien, “Modeling of the KOH-Polarization cells for mitigating the induced AC voltage in the metallic pipelines”, *Heliyon*, 2020, doi: 10.1016/j.heliyon.2020.e03417.

[5] V. H. Hinojosa en J. Sepúlveda, "Solving the Stochastic Generation and Transmission Capacity Planning Problem Applied to Large-Scale Power Systems Using Generalized Shift-Factors", *Energies*, 2020, doi: 10.3390/en13133327.

[6] M. Navidi, S. M. M. Tafreshi, en A. Anvari-Moghaddam, "A game theoretical approach for sub-transmission and generation expansion planning utilizing multi-regional energy systems", *Int. J. Electr. Power Energy Syst.*, 2020, doi: 10.1016/j.ijepes.2019.105758.

[7] M. L. Kloubert, "Probabilistic load flow approach considering dependencies of wind speed, solar irradiance, electrical load and energy exchange with a joint probability distribution model", *Energies*, 2020, doi: 10.3390/en13071727.

[8] P. P. C. Alzate, A. H. E. Zuluaga, en C. A. E. Salcedo, "Long-term transmission system expansion planning using valid inequalities", *Allergy, Asthma Immunol. Res.*, 2020.

[9] D. B. Nusantara, L. M. Putranto, Sarjiya, S. Isnandar, en T. K. Yudhantomo, "Analysis of Performance Index in Transmission Expansion Planning of Sulawesi's Electricity System", 2020. doi: 10.1109/ISRITI51436.2020.9315480.

[10] Z. Chen, Y. Hu, N. Tai, X. Tang, en G. You, "Transmission grid expansion planning of a high proportion renewable energy power system based on flexibility and economy", *Electron.*, 2020, doi: 10.3390/electronics9060966.

CHAPTER 10

THE PER-UNIT SYSTEM

Dr. Hannah Jessie Rani R, Assistant Professor
Faculty of Engineering and Technology, Jain (Deemed-To-Be University), Bengaluru, Karnataka, India
Email Id- jr.hannah@jainuniversity.ac.in

Power system analysis calculations often employ per-unit values of impedances, currents, voltages, and powers (which are scaled or normalized values) rather than physical values of ohms, amperes, kilovolts, and megavolt amperes due to the many benefits involved (or megadarra, or megawatts). A per-unit system is a way to represent quantities such that they are easier to compare. Any quantity's per-unit value is determined by comparing it to a base value (also known as a reference value) with the same dimensions. Consequently, every quantity's per-unit value may be described as,

$$\text{Quantity in per unit} = \frac{\text{physical quantity}}{\text{base value of quantity}}$$

The value in ohms, amperes, volts, etc. is referred to as the "physical quantity" in this context. Because it has a value of 1, or unity, in the per-unit system, the base value is also known as the unit value. A base current is thus also known as a unit current. The resultant per-unit value stated as a decimal has no dimension and is simply denoted by the subscript pu since the dimensions of the physical quantity and base quantity are the same[1], [2]. A B subscript denotes the basic amount. Pu, or 0/1, is the sign for per unit. The per-unit value is multiplied by 100 to get the percent system. Therefore,

$$\text{Quantity in percent} = \frac{\text{physical quantity}}{\text{base value of quantity}} \times 100$$

However, since it is always important to keep in mind that the amounts have been multiplied by 100, the percent approach is a little more challenging to use and more prone to mistake. As a result, the factor 100 must constantly be added or subtracted for reasons that may not be apparent at the time. For instance, 40% reactance multiplied by 100% current results in a voltage of 4000%, which must of course be reduced to 40% voltage. In power system calculations, the per-unit system is favoured. The following are some benefits of employing the per-unit: Since all impedances of a particular equivalent circuit may be immediately combined together independently of the system voltages, network analysis is substantially facilitated. It does away with the V5 divisions and multiplications that are necessary to express balanced three-phase systems using per-phase systems. Therefore, the base quantities in a balanced three-phase system immediately take into account the components V3 and related with delta and wye quantities. The impedance of an electrical device is often provided by its manufacturer in percent or per unit based on its nameplate ratings (e.g., its rated volt-amperes and rated voltage). A comparison of the constants reported in per units of various electrical devices may be used to assess differences in operational characteristics. Since the characteristics of identical pieces of equipment often lie within a very small range and are thus comparable when represented as per units based on rated capacity, average machine constants are simple to calculate. When using digital computers, it is more practical to employ per-unit amounts[3], [4].

Component symmetry and fault analysis

Overall, it may be claimed that three-phase systems that are properly balanced only exist in principle. Many systems are really quite close to being balanced, making it possible to evaluate them almost as if they were. The degree of imbalance cannot be ignored in certain emergency situations, such as unsymmetrical defects, unbalanced loads, open conductors, or unsymmetrical circumstances emerging in spinning equipment. It is required to size protection devices, including fuses and circuit breakers, and configure the protective relays in order to safeguard the system from such situations. Therefore, in order to do this, the system's currents and voltages must be known (and therefore computed) in advance while operating under such imbalanced circumstances. A technique to resolve an unbalanced set of n linked phasors into n sets of balanced phasors known as the symmetrical components of the original unbalanced set was put out by in 1918. Each set's phasors are equally spaced and of identical amplitude, either 120° or 0° apart. Although the approach is applicable to systems with any number of phases, only three-phase systems will be covered in this book. In researching unbalanced systems nowadays, the symmetrical component theory is often applied. Furthermore, the idea of symmetrical components has been used to create and operate a large number of electrical gadgets. Examples include the negative-sequence relay, which is used to identify system faults, the positive-sequence filter, which causes generator voltage regulators to react to voltage changes in all three phases as opposed to just one, and the Westinghouse type HCB pilot wire relay, which uses both positive and zero-sequence niters to identify faults[5], [6].

Equilateral Components

Any unbalanced three-phase system of phasors may be converted into one of three balanced systems of phasors: positive-sequence system, negative-sequence system, or zero-sequence system. A balanced system of phasors with the same phase sequence (and thus positive phase rotation) as the original unbalanced system serves as the representation for the positive-sequence system. The phasors of the positive sequence system are 120 degrees apart and of identical amplitude (b). A balanced system of phasors with the opposite phase sequence (and thus negative phase rotation) from the original system serves as the representation for the negative-sequence system. The phasors of the negative-sequence system are likewise identical in magnitude and separated from one another by 120 degrees (c). When compared to the zero-sequence system, which has three single phasors with identical magnitudes and angular displacements, the subscripts 0, 1, and 2 in the book, respectively, stand for the zero sequence, the positive sequence, and the negative sequence. As a result, three voltage phasors from an imbalanced set, Vfl, Vb, and Vc, may be written as follows using their symmetrical components,

$$\mathbf{V}_a = \mathbf{V}_{a1} + \mathbf{V}_{a2} + \mathbf{V}_{a0}$$

$$\mathbf{V}_b = \mathbf{V}_{b1} + \mathbf{V}_{b2} + \mathbf{V}_{b0}$$

$$\mathbf{V}_c = \mathbf{V}_{c1} + \mathbf{V}_{c2} + \mathbf{V}_{c0}$$

Operator

A v,=val + vfl2 + vfl0 v6 =vM +vM + vM v, = vcl + vc2 + vc0 (3.1) (3.2) (3.3) The need for a unit phasor (or operator) that will rotate some other phasor by 120° in the anticlockwise direction (i.e., add 120° to the phase angle of the phasor) but leave its amplitude largely

untouched when it is amplified by the phasor results from the application of the symmetrical components theory to three phase systems. Such an operator is defined by, and is a complex number of unit magnitude with an angle of 120°.

$$\begin{aligned}\mathbf{a} &= 1\angle 120^\circ \\ &= 1e^{j(2\pi/3)} \\ &= 1(\cos 120^\circ + j \sin 120^\circ) \\ &= -0.5 + j0.866\end{aligned}$$

$$j = \sqrt{-1}$$

It is clear that if the operator a is designated as,

$$a = 1\angle 120^\circ$$

Then,

$$\mathbf{a}^2 = \mathbf{a} \times \mathbf{a} = (1\angle 120^\circ)(1\angle 120^\circ) = 1\angle 240^\circ = 1\angle -120^\circ$$

Power in Symmetrical Components

The three-phase complex power at any point of a three-phase system can be expressed as the sum of the individual complex powers of each phase so that,

$$\begin{aligned}\mathbf{S}_{3\Phi} &= P_{3\Phi} + jQ_{3\Phi} \\ &= \mathbf{S}_a + \mathbf{S}_b + \mathbf{S}_c \\ &= \mathbf{V}_a\mathbf{I}_a^* + \mathbf{V}_b\mathbf{I}_b^* + \mathbf{V}_c\mathbf{I}_c^*\end{aligned}$$

or, in matrix notation,

$$\mathbf{S}_{3\Phi} = [\mathbf{V}_a \quad \mathbf{V}_b \quad \mathbf{V}_c]\begin{bmatrix}\mathbf{I}_a \\ \mathbf{I}_b \\ \mathbf{I}_c\end{bmatrix}^* = \begin{bmatrix}\mathbf{V}_a \\ \mathbf{V}_b \\ \mathbf{V}_c\end{bmatrix}^t\begin{bmatrix}\mathbf{I}_a \\ \mathbf{I}_b \\ \mathbf{I}_c\end{bmatrix}^*$$

Or,

$$\mathbf{S}_{3\Phi} = [\mathbf{V}_{abc}]^t[\mathbf{I}_{abc}]^*$$

Where,

$$[\mathbf{V}_{abc}] = [\mathbf{A}][\mathbf{V}_{012}]$$
$$[\mathbf{I}_{abc}] = [\mathbf{A}][\mathbf{I}_{012}]$$

And therefore,

$$[\mathbf{V}_{abc}]^t = [\mathbf{V}_{012}]^t[\mathbf{A}]^t$$

$$[\mathbf{I}_{abc}]^* = [\mathbf{A}]^*[\mathbf{I}_{012}]^*$$

Substituting equations,

$$\mathbf{S}_{3\Phi} = [\mathbf{V}_{012}]^t[\mathbf{A}]^t[\mathbf{A}]^*[\mathbf{I}_{012}]^*$$

Where,

$$[\mathbf{A}]^t[\mathbf{A}]^* = \begin{bmatrix} 1 & 1 & 1 \\ 1 & \mathbf{a}^2 & \mathbf{a} \\ 1 & \mathbf{a} & \mathbf{a}^2 \end{bmatrix}\begin{bmatrix} 1 & 1 & 1 \\ 1 & \mathbf{a} & \mathbf{a}^2 \\ 1 & \mathbf{a}^2 & \mathbf{a} \end{bmatrix} = \begin{bmatrix} 3 & 0 & 0 \\ 0 & 3 & 0 \\ 0 & 0 & 3 \end{bmatrix} = 3\begin{bmatrix} 1 & 0 & 0 \\ 0 & 1 & 0 \\ 0 & 0 & 1 \end{bmatrix}$$

Therefore,

$$\mathbf{S}_{3\Phi} = 3[\mathbf{V}_{012}]^t[\mathbf{I}_{012}]^* = 3[\mathbf{V}_{a0} \quad \mathbf{V}_{a1} \quad \mathbf{V}_{a2}]\begin{bmatrix} \mathbf{I}_{a0} \\ \mathbf{I}_{a1} \\ \mathbf{I}_{a2} \end{bmatrix}^*$$

$$\mathbf{S}_{3\Phi} = 3[\mathbf{V}_{a0}\mathbf{I}_{a0}^* + \mathbf{V}_{a1}\mathbf{I}_{a1}^* + \mathbf{V}_{a2}\mathbf{I}_{a2}^*]$$

There are no cross terms in this equation, such as Va0 I*1 or Vol I*0, indicating that the power of the three sequences is not coupled. Also take notice of the fact that the symmetric voltage and current components are of the same phase[7], [8].

Sequence un-Transposed lines' Impedances

An untransposed transmission line with uneven self- and mutual-impedances is represented by a circuit. Here

$$[\mathbf{V}_{abc}] = [\mathbf{Z}_{abc}][\mathbf{I}_{abc}]$$

Where,

$$[\mathbf{Z}_{abc}] = \begin{bmatrix} \mathbf{Z}_{aa} & \mathbf{Z}_{ab} & \mathbf{Z}_{ac} \\ \mathbf{Z}_{ba} & \mathbf{Z}_{bb} & \mathbf{Z}_{bc} \\ \mathbf{Z}_{ca} & \mathbf{Z}_{cb} & \mathbf{Z}_{cc} \end{bmatrix}$$

In which the self-impedances are,

$$\mathbf{Z}_{aa} \neq \mathbf{Z}_{bb} \neq \mathbf{Z}_{cc}$$

And the mutual impedances are,

$$\mathbf{Z}_{ab} \neq \mathbf{Z}_{ba} \neq \mathbf{Z}_{ca}$$

Multiplying both sides of equation,

$$[\mathbf{A}]^{-1}[\mathbf{V}_{abc}] = [\mathbf{A}]^{-1}[\mathbf{Z}_{abc}][\mathbf{A}][\mathbf{I}_{012}]$$

Where the similarity transformation is denned as,

$$[\mathbf{Z}_{012}] \triangleq [\mathbf{A}]^{-1}[\mathbf{Z}_{abc}][\mathbf{A}]$$

Therefore, the sequence impedance matrix of an un-transposed transmission line can be calculated using equation and can be expressed as,

$$[\mathbf{Z}_{012}] = \begin{bmatrix} \mathbf{Z}_{00} & \mathbf{Z}_{01} & \mathbf{Z}_{02} \\ \mathbf{Z}_{10} & \mathbf{Z}_{11} & \mathbf{Z}_{12} \\ \mathbf{Z}_{20} & \mathbf{Z}_{21} & \mathbf{Z}_{22} \end{bmatrix}$$

$$[\mathbf{Z}_{012}] = \begin{bmatrix} (\mathbf{Z}_{s0} + 2\mathbf{Z}_{m0}) & (\mathbf{Z}_{s2} - \mathbf{Z}_{m2}) & (\mathbf{Z}_{s1} - \mathbf{Z}_{m1}) \\ (\mathbf{Z}_{s1} - \mathbf{Z}_{m1}) & (\mathbf{Z}_{s0} - \mathbf{Z}_{m0}) & (\mathbf{Z}_{s2} + 2\mathbf{Z}_{m2}) \\ (\mathbf{Z}_{s2} - \mathbf{Z}_{m2}) & (\mathbf{Z}_{s1} + 2\mathbf{Z}_{m1}) & (\mathbf{Z}_{s0} - \mathbf{Z}_{m0}) \end{bmatrix}$$

Where, by definition,

$\mathbf{Z}_{s0}$ = zero-sequence self-impedance

$$\triangleq \tfrac{1}{3}(\mathbf{Z}_{aa} + \mathbf{Z}_{bb} + \mathbf{Z}_{cc})$$

$\mathbf{Z}_{s1}$ = positive-sequence self-impedance

$$\triangleq \tfrac{1}{3}(\mathbf{Z}_{aa} + \mathbf{a}\mathbf{Z}_{bb} + \mathbf{a}^2\mathbf{Z}_{cc})$$

$\mathbf{Z}_{s2}$ = negative-sequence self-impedance

$$\triangleq \tfrac{1}{3}(\mathbf{Z}_{aa} + \mathbf{a}^2\mathbf{Z}_{bb} + \mathbf{a}\mathbf{Z}_{cc})$$

$\mathbf{Z}_{m0}$ = zero-sequence mutual impedance

$$\triangleq \tfrac{1}{3}(\mathbf{Z}_{bc} + \mathbf{Z}_{ca} + \mathbf{Z}_{ab})$$

$\mathbf{Z}_{m1}$ = positive-sequence mutual impedance

$$\triangleq \tfrac{1}{3}(\mathbf{Z}_{bc} + \mathbf{a}\mathbf{Z}_{ca} + \mathbf{a}^2\mathbf{Z}_{ab})$$

$\mathbf{Z}_{m2}$ = negative-sequence mutual impedance

$$\triangleq \tfrac{1}{3}(\mathbf{Z}_{bc} + \mathbf{a}^2\mathbf{Z}_{ca} + \mathbf{a}\mathbf{Z}_{ab})$$

Therefore,

$$[\mathbf{V}_{012}] = [\mathbf{Z}_{012}][\mathbf{I}_{012}]$$

Due to the fact that equation's matrix is not symmetrical, the application of the equation will reveal that the three sequences are mutually coupled, which is an undesirable outcome[9], [10].

Capacitance and inductance of Transposed Lines in Sequence

The solution is to either entirely transpose the line or arrange the conductors with equilateral spacing between them such that the resultant mutual impedances1 are identical to one another, i.e., Zab = Zbc = Zca = Zm (b). Additionally, the equation may be written as follows if the self-impedances of the conductors are equivalent to one another: Zaa — Zbb = Zcc — Zs,

In passive networks $\mathbf{Z}_{ab} = \mathbf{Z}_{ba}$, $\mathbf{Z}_{bc} = \mathbf{Z}_{cb}$, etc.

$$[\mathbf{Z}_{abc}] = \begin{bmatrix} \mathbf{Z}_s & \mathbf{Z}_m & \mathbf{Z}_m \\ \mathbf{Z}_m & \mathbf{Z}_s & \mathbf{Z}_m \\ \mathbf{Z}_m & \mathbf{Z}_m & \mathbf{Z}_s \end{bmatrix}$$

$$\mathbf{Z}_s = \left[(r_a + r_e) + j0.1213 \ln \frac{D_e}{D_s} \right] l \quad \Omega$$

$$\mathbf{Z}_m = \left[r_e + j0.1213 \ln \frac{D_e}{D_{eq}} \right] l \quad \Omega$$

$$D_{eq} \triangleq D_m = (D_{ab} \times D_{bc} \times D_{ca})^{1/3}$$

r_a = resistance of a single conductor a

There is the resistance of Carson's equivalent (and fictitious) earth return conductor. It is a function of frequency and can be expressed as,

$$r_e = 1.588 \times 10^{-3} f \quad \Omega/\text{mi}$$

$$r_e = 9.869 \times 10^{-4} f \quad \Omega/\text{km}$$

At 60 Hz, re = 0.09528 O/mi. The quantity D€ is a function of both the earth resistivity p and the frequency / and can be expressed as,

$$D_e = 2160 \left(\frac{\rho}{f} \right)^{1/2} \quad \text{ft}$$

Where, for different earth types, p is the earth resistivity and is shown in Table 3.2. It is usual to use a value of 100 fl-m for p if the actual earth resistivity is unknown. De thus equals 2788.55 feet at 60 Hz. The GMR of the phase conductor is still the Ds.

Magnetic Discordances Because of Misplaced Lines

Equation cannot be utilised if the line is neither transposed nor its conductors are evenly spaced. Use the following equation as a substitute,

$$[\mathbf{Z}_{abc}] = \begin{bmatrix} \mathbf{Z}_{aa} & \mathbf{Z}_{ab} & \mathbf{Z}_{ac} \\ \mathbf{Z}_{ba} & \mathbf{Z}_{bb} & \mathbf{Z}_{bc} \\ \mathbf{Z}_{ca} & \mathbf{Z}_{cb} & \mathbf{Z}_{cc} \end{bmatrix}$$

Where,

$$\mathbf{Z}_{aa} = \mathbf{Z}_{bb} = \mathbf{Z}_{cc} = \left[(r_a + r_e) + j0.1213 \ln \frac{D_e}{D_s} \right]$$

$$\mathbf{Z}_{ab} = \mathbf{Z}_{ba} = \left[r_e + j0.1213 \ln \frac{D_e}{D_{ab}} \right]$$

$$\mathbf{Z}_{ac} = \mathbf{Z}_{ca} = \left[r_e + j0.1213 \ln \frac{D_e}{D_{ac}} \right]$$

$$\mathbf{Z}_{bc} = \mathbf{Z}_{cb} = \left[r_e + j0.1213 \ln \frac{D_e}{D_{bc}} \right]$$

The corresponding sequence impedance matrix can be found from equation as before. Therefore, the associated sequence admittance matrix can be found as,

$$[\mathbf{Y}_{012}] = [\mathbf{Z}_{012}]^{-1}$$

$$= \begin{bmatrix} \mathbf{Y}_{00} & \mathbf{Y}_{01} & \mathbf{Y}_{02} \\ \mathbf{Y}_{10} & \mathbf{Y}_{11} & \mathbf{Y}_{12} \\ \mathbf{Y}_{20} & \mathbf{Y}_{21} & \mathbf{Y}_{22} \end{bmatrix}$$

$$[\mathbf{I}_{012}] = [\mathbf{Y}_{012}][\mathbf{V}_{012}]$$

Since the line is neither transposed nor its conductors equilaterally spaced, there is an electromagnetic unbalance in the system. Such unbalance is determined from equation with only positive-sequence voltage applied. Therefore,

$$\begin{bmatrix} \mathbf{I}_{a0} \\ \mathbf{I}_{a1} \\ \mathbf{I}_{a2} \end{bmatrix} = \begin{bmatrix} \mathbf{Y}_{00} & \mathbf{Y}_{01} & \mathbf{Y}_{02} \\ \mathbf{Y}_{10} & \mathbf{Y}_{11} & \mathbf{Y}_{12} \\ \mathbf{Y}_{20} & \mathbf{Y}_{21} & \mathbf{Y}_{22} \end{bmatrix} \begin{bmatrix} 0 \\ \mathbf{V}_{a1} \\ 0 \end{bmatrix}$$

$$= \begin{bmatrix} \mathbf{Y}_{01} \\ \mathbf{Y}_{11} \\ \mathbf{Y}_{21} \end{bmatrix} \mathbf{V}_{a1}$$

According to Gross and Hesse, the per-unit unbalances for zero sequence and negative sequence can be expressed, respectively, as

$$\mathbf{m}_0 \triangleq \frac{\mathbf{I}_{a0}}{\mathbf{I}_{a1}} \quad \text{pu}$$

$$= \frac{\mathbf{Y}_{01}}{\mathbf{Y}_{11}} \quad \text{pu}$$

$$\mathbf{m}_2 \triangleq \frac{\mathbf{I}_{a2}}{\mathbf{I}_{a1}} \quad \text{pu}$$

$$= \frac{\mathbf{Y}_{21}}{\mathbf{Y}_{11}} \quad \text{pu}$$

Since, in physical systems,

$$\mathbf{Z}_{22} \gg \mathbf{Z}_{02} \text{ or } \mathbf{Z}_{21}$$

$$\mathbf{Z}_{00} \gg \mathbf{Z}_{20} \text{ or } \mathbf{Z}_{01}$$

The approximate values of the per-unit unbalances for zero and negative sequences can be expressed respectively, as

$$\mathbf{m}_0 \cong -\frac{\mathbf{Z}_{01}}{\mathbf{Z}_{00}} \quad \text{pu}$$

$$\mathbf{m}_2 \cong -\frac{\mathbf{Z}_{21}}{\mathbf{Z}_{22}} \quad \text{pu}$$

Capacitance and inductance of Synchronous Machines in Sequence

In synchronous machines (as well as other rotating machines), the impedances to positive-, negative-, and zero-sequence currents often have distinct values. Depending on the amount of time that is assumed to pass between the instant of the fault initiation and the instant at which values are desired, the positive-sequence impedance of the synchronous machine can be chosen to be either its sub transient (A), transient (X'd), or synchronous* (Xd) reactance (e.g., for relay response, breaker opening, or sustained fault conditions). However, the sub transient reactance is often interpreted as the positive sequence reactance of the synchronous machine in fault investigations. A synchronous machine's negative-sequence impedance is often calculated from,

$$\mathbf{Z}_2 = jX_2 = j\left(\frac{X''_d + X''_q}{2}\right)$$

The negative sequence reactance and sub transient reactance in a cylindrical-rotor synchronous motor are identical. A synchronous machine's zero-sequence impedance varies greatly and is influenced by the coil pitch. It is much less than the comparable reactances for positive and negative sequences. By connecting the three armature windings together in

series and applying a single-phase voltage, it may be monitored. The zero-sequence reactance is defined as the ratio of the voltage level of one phase winding to the current. It roughly corresponds to the zero-sequence reactance. It provides typical three-phase synchronous machine reactance values. Because they are substantially less than the comparable reactance values, the resistance values in the explanation above are disregarded. The analogous circuit of a synchronous machine with a cylindrical rotor and constant field current. The three-phase stator armature windings' coil groups are 120 electrical degrees apart from one another, which induces balanced three-phase sinusoidal voltages in the stator in Figure 10.1.

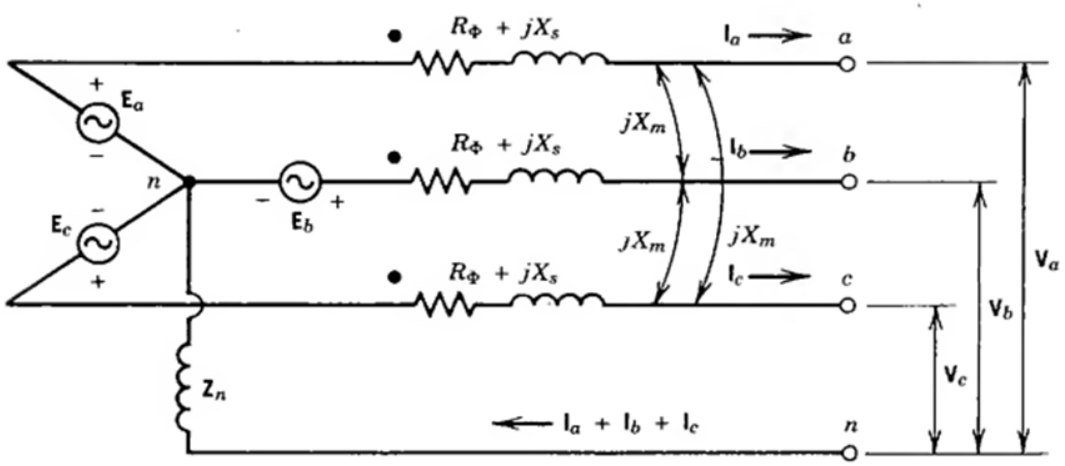

Figure 10.1: ***Illustrates*** **the Equivalent circuit of cylindrical-rotor synchronous machine.**

Windings. Additionally, due to machine symmetry, each of the three identity and mutual impedances is equivalent to the other three. In light of the neutral impedance Zn and using Kirchhoff's voltage law (KVL), it is possible to demonstrate that,

$$\mathbf{E}_a = (R_\Phi + jX_s + \mathbf{Z}_n)\mathbf{I}_a + (jX_m + \mathbf{Z}_n)\mathbf{I}_b + (jX_m + \mathbf{Z}_n)\mathbf{I}_c + \mathbf{V}_a$$

$$\mathbf{E}_b = (jX_m + \mathbf{Z}_n)\mathbf{I}_a + (R_\Phi + jX_s + \mathbf{Z}_n)\mathbf{I}_b + (jX_m + \mathbf{Z}_n)\mathbf{I}_c + \mathbf{V}_b$$

$$\mathbf{E}_c = (jX_m + \mathbf{Z}_n)\mathbf{I}_a + (jX_m + \mathbf{Z}_n)\mathbf{I}_b + (R_\Phi + jX_s + \mathbf{Z}_n)\mathbf{I}_c + \mathbf{V}_c$$

Or, in matrix form,

$$\begin{bmatrix} \mathbf{E}_a \\ \mathbf{E}_b \\ \mathbf{E}_c \end{bmatrix} = \begin{bmatrix} \mathbf{Z}_s & \mathbf{Z}_m & \mathbf{Z}_m \\ \mathbf{Z}_m & \mathbf{Z}_s & \mathbf{Z}_m \\ \mathbf{Z}_m & \mathbf{Z}_m & \mathbf{Z}_s \end{bmatrix} \begin{bmatrix} \mathbf{I}_a \\ \mathbf{I}_b \\ \mathbf{I}_c \end{bmatrix} + \begin{bmatrix} \mathbf{V}_a \\ \mathbf{V}_b \\ \mathbf{V}_c \end{bmatrix}$$

Where,

$$\mathbf{Z}_s = R_\Phi + jX_s + \mathbf{Z}_n$$
$$\mathbf{Z}_m = jX_m + \mathbf{Z}_n$$
$$\mathbf{E}_a = \mathbf{E}_a$$
$$\mathbf{E}_b = \mathbf{a}^2\mathbf{E}_a$$
$$\mathbf{E}_c = \mathbf{a}\mathbf{E}_a$$

Alternatively, equation can be written in shorthand matrix notation as,

$$[\mathbf{E}_{abc}] = [\mathbf{Z}_{abc}][\mathbf{I}_{abc}] + [\mathbf{V}_{abc}]$$

Multiplying both sides of this equation by [A] 1 and also substituting equation into it,

$$[\mathbf{A}]^{-1}[\mathbf{E}_{abc}] = [\mathbf{A}]^{-1}[\mathbf{Z}_{abc}][\mathbf{A}][\mathbf{I}_{012}] + [\mathbf{A}]^{-1}[\mathbf{V}_{abc}]$$

Where,

$$[\mathbf{A}]^{-1}[\mathbf{E}_{abc}] = \frac{1}{3}\begin{bmatrix}1 & 1 & 1\\ 1 & \mathbf{a} & \mathbf{a}^2\\ 1 & \mathbf{a}^2 & \mathbf{a}\end{bmatrix}\begin{bmatrix}\mathbf{E}\\ \mathbf{a}^2\mathbf{E}\\ \mathbf{a}\mathbf{E}\end{bmatrix} = \begin{bmatrix}0\\ \mathbf{E}\\ 0\end{bmatrix}$$
$$[\mathbf{A}]^{-1}[\mathbf{Z}_{abc}][\mathbf{A}] \triangleq [\mathbf{Z}_{012}]$$
$$[\mathbf{A}]^{-1}[\mathbf{V}_{abc}] = [\mathbf{V}_{012}]$$

Also, due to the symmetry of the machine,

$$[\mathbf{Z}_{012}] = \begin{bmatrix}\mathbf{Z}_s + 2\mathbf{Z}_m & 0 & 0\\ 0 & \mathbf{Z}_s - \mathbf{Z}_m & 0\\ 0 & 0 & \mathbf{Z}_s - \mathbf{Z}_m\end{bmatrix}$$

Or,

$$[\mathbf{Z}_{012}] = \begin{bmatrix}\mathbf{Z}_{00} & 0 & 0\\ 0 & \mathbf{Z}_{11} & 0\\ 0 & 0 & \mathbf{Z}_{22}\end{bmatrix}$$

Where,

$$\mathbf{Z}_{00} = \mathbf{Z}_s + 2\mathbf{Z}_m = R_\Phi + j(X_s + 2X_m) + 3\mathbf{Z}_n$$
$$\mathbf{Z}_{11} = \mathbf{Z}_s - \mathbf{Z}_m = R_\Phi + j(X_s - X_m)$$
$$\mathbf{Z}_{22} = \mathbf{Z}_m - \mathbf{Z}_m = R_\Phi + j(X_s - X_m)$$

Therefore, equation in terms of the symmetrical components can be expressed as,

$$\begin{bmatrix} 0 \\ \mathbf{E}_a \\ 0 \end{bmatrix} = \begin{bmatrix} \mathbf{Z}_{00} & 0 & 0 \\ 0 & \mathbf{Z}_{11} & 0 \\ 0 & 0 & \mathbf{Z}_{22} \end{bmatrix} \begin{bmatrix} \mathbf{I}_{a0} \\ \mathbf{I}_{a1} \\ \mathbf{I}_{a2} \end{bmatrix} + \begin{bmatrix} \mathbf{V}_{a0} \\ \mathbf{V}_{a1} \\ \mathbf{V}_{a2} \end{bmatrix}$$

or, in shorthand matrix notation,

$$[\mathbf{E}] = [\mathbf{Z}_{012}][\mathbf{I}_{012}] + [\mathbf{V}_{012}]$$

Similarly,

$$\begin{bmatrix} \mathbf{V}_{a0} \\ \mathbf{V}_{a1} \\ \mathbf{V}_{a2} \end{bmatrix} = \begin{bmatrix} 0 \\ \mathbf{E}_a \\ 0 \end{bmatrix} - \begin{bmatrix} \mathbf{Z}_{00} & 0 & 0 \\ 0 & \mathbf{Z}_{11} & 0 \\ 0 & 0 & \mathbf{Z}_{22} \end{bmatrix} \begin{bmatrix} \mathbf{I}_{a0} \\ \mathbf{I}_{a1} \\ \mathbf{I}_{a2} \end{bmatrix}$$

$$[\mathbf{V}_{012}] = [\mathbf{E}] - [\mathbf{Z}_{012}][\mathbf{I}_{012}]$$

Note that the machine sequence impedances in the above equations are,

$$\mathbf{Z}_0 \triangleq \mathbf{Z}_{00} - 3\mathbf{Z}_n$$

$$\mathbf{Z}_1 \triangleq \mathbf{Z}_{11}$$

$$\mathbf{Z}_2 \triangleq \mathbf{Z}_{22}$$

The impedance Z,, is external to the machine, which causes the expression provided in the equation. The networks of a synchronous machine's sequences.

REFERENCES

[1] P. K. Sadhu en S. Das, "▪ Per-Unit Systems", in *Elements of Power Systems*, 2020. doi: 10.1201/b19119-9.

[2] Z. Fang, Y. Lin, S. Song, C. Song, X. Lin, en G. Cheng, "Active distribution system state estimation incorporating photovoltaic generation system model", *Electr. Power Syst. Res.*, 2020, doi: 10.1016/j.epsr.2020.106247.

[3] S. J. Kassinger en M. L. van Hoek, "Biofilm architecture: An emerging synthetic biology target", *Synthetic and Systems Biotechnology*. 2020. doi: 10.1016/j.synbio.2020.01.001.

[4] V. M. Fernández-Cabanás, L. Pérez-Urrestarazu, A. Juárez, N. T. Kaufman, en J. A. Gross, "Comparative analysis of horizontal and vertical decoupled aquaponic systems for basil production and effect of light supplementation by LED", *Agronomy*, 2020, doi: 10.3390/agronomy10091414.

[5] S. J. Bedoya-Pacheco, R. F. Emygdio, J. A. Sena Do Nascimento, J. A. M. Bravo, en F. A. Bozza, "Intensive care inequity in Rio de Janeiro: The effect of spatial distribution of health services on severe acute respiratory infection", *Rev. Bras. Ter. Intensiva*, 2020, doi: 10.5935/0103-507X.20200012.

[6] S. Sadeghi, S. Ghandehariun, en G. F. Naterer, "Exergoeconomic and multi-objective optimization of a solar thermochemical hydrogen production plant with heat recovery", *Energy Convers. Manag.*, 2020, doi: 10.1016/j.enconman.2020.113441.

[7] R. P. Lazo en J. Q. Gonzabay, "Economic analysis of hydroponic lettuce under floating root system in semi-arid climate", *Granja*, 2020, doi: 10.17163/lgr.n31.2020.09.

[8] K. Ardon-Dryer, Y. Dryer, J. N. Williams, en N. Moghimi, "Measurements of PM2.5 with PurpleAir under atmospheric conditions", *Atmos. Meas. Tech.*, 2020, doi: 10.5194/amt-13-5441-2020.

[9] A. Fecher, T. Robbert, en S. Roth, "Per piece or per kilogram? Default-unit effects in retailing", *J. Retail. Consum. Serv.*, 2020, doi: 10.1016/j.jretconser.2019.101956.

[10] A. Naranjo, A. Johnson, H. Rossow, en E. Kebreab, "Greenhouse gas, water, and land footprint per unit of production of the California dairy industry over 50 years", *J. Dairy Sci.*, 2020, doi: 10.3168/jds.2019-16576.

CHAPTER 11

ZERO SECTION NETWORKS

Mr. Harsh Shrivastava, Assistant Professor,
Department of Electrical Engineering, Jaipur National University, Jaipur India
Email Id- ershrivastava@jnujaipur.ac.in

It's crucial to understand that the zero-sequence system is, in a sense, a single-phase system rather than a three-phase system. This is due to the fact that at any moment throughout all of the system's phases, the zero-sequence currents and voltages are both identical in magnitude and phase. But the presence of zero-sequence currents in a circuit depends on the existence of a clear channel for their passage. Therefore, the zero-sequence impedance in a circuit is infinite if there is no full channel for zero-sequence currents. This infinite impedance is represented in a zero-sequence network representation as an open circuit. In displays zero-sequence networks for three-phase loads linked by wye and delta. An ungrounded neutral on a wye-connected load has infinite resistance to zero-sequence currents because there is no return channel via the neutral conductor or the ground. The zero-sequence currents flowing through the three phases and their total, 3Ifl0, flowing through the ground, on the other hand, have a return route when they are coupled to a load through a wye and have a securely grounded neutral. In the zero-sequence network, an impedance of 3Z,, should be added between the neutral point n and the zero-potential bus N0 if the neutral is grounded via some impedance Z. This occurs because a current of 3Ia0 results in a 3Ia0 Z,, voltage drop between the neutral point n and the ground. Therefore, the neutral impedance should be 3Zn in order to represent this voltage drop in the zero-sequence network where the zero-sequence current Ifl0 flows. Zero-sequence currents flowing in the line have no route when the load is connected in a delta configuration. Therefore, as viewed from its terminals, its zero-sequence impedance is infinite. Nevertheless, there is a chance that the delta circuit will experience zero-sequence currents. However, they need to be generated in the delta by induction from an external source or zero-sequence voltages[1], [2].

Impedances of transformers in section

Three identical single-phase transformers might be combined to create a three-phase transformer. A three-phase transformer bank is what is referred to in this situation. It might also be constructed as a three-phase transformer with a tank and a single common core (either with a shell-type or core-type construction). Here, just the three-phase transformer banks will be examined for the purpose of simplicity. A transformer has the same resistance to currents in both the positive and negative sequences. In practise, it is frequently assumed that series impedances of all sequences are the same without taking the transformer type into consideration, despite the fact that the zero-sequence series impedances of three-phase units are only slightly different from the positive- and negative-sequence series impedances:

$$\mathbf{Z}_0 = \mathbf{Z}_1 = \mathbf{Z}_2 = \mathbf{Z}_{trf}$$

Naturally, Z0 is infinite if the transformer connection prevents the passage of zero-sequence current. Equivalents of three identical single-phase transformer banks with two windings in zero-sequence networks that do not account for excitation currents. On the connection diagrams, the potential routes for zero-sequence current flow are shown. If no route is shown on the connection diagram, this indicates that the transformer connection does not provide a

channel for the zero-sequence current, which prohibits it from flowing. Although the delta-delta bank may have zero-sequence currents flowing through its delta windings, it also precludes the zero-sequence current from flowing through any other parts of the bank since there isn't a return route for it. Also take notice that Z0 + 3Zn should be used instead of Z0 + 3Zn if the neutral point n of the wye winding is grounded via Z„. Naturally, the Zn is zero if the wye winding is completely grounded, therefore 3Zn should be substituted by a short circuit. The Z„ is unlimited, on the other hand, if the connection is unground, hence an open circuit should be used in lieu of 3Zn. It's noteworthy to note that only the zero-sequence network is impacted by the kind of grounding; neither the positive nor negative sequence networks are affected. It's noteworthy to observe that a wye-grounded-wye-connected three-phase transformer bank has no way for zero-sequence current to pass. This is due to the transformer bank's ungrounded wye connection, which prevents zero-sequence current from flowing in any particular winding on the wye side. Therefore, apart from a negligibly tiny magnetising current, there cannot be any zero-sequence current in the equivalent winding on the wye grounded side of the transformer due to the absence of equal and opposite ampere turns in the wye side of the transformer bank[3], [4].

Unbalanced Fault Analysis

The majority of power system faults are unbalanced (i.e., asymmetrical) three-phase faults, particularly single line-to-ground failures, as opposed to balanced (i.e., symmetrical) three-phase faults. According to reference 5, for instance, the three-phase, single line-to-ground, line-to-line, and double line-to-ground faults often occur at rates of 5, 70, 15, and 10%, respectively. The three-phase fault is often regarded as the most serious. The single line-to-ground fault, however, can be more severe than the three-phase fault in two situations: it occurs on the wye-grounded side of the delta-wye-grounded transformer banks and the related generators have firmly grounded neutrals or low impedance neutral impedances. About 86.6 percent of the three-phase fault current is present in the line-to-line fault current. The defects may be divided into three categories: simultaneous faults, series faults, and shunt faults (short circuits) (having more than one fault occurring at the same time). By exploiting the symmetrical elements of an imbalanced system of currents or voltages, the unbalanced defects may be simply fixed. The three imaginary networks that may be used to model an imbalanced system are the positive-sequence (the only one with a driving voltage), the negative-sequence, and the zero-sequence networks, which are each linked to the other in a specific way depending on the fault type. Only shunt faults are discussed in this book[5], [6].

Shunt Errors

Phase a's voltage to ground at fault point F prior to the fault occurring is VF, and it is often chosen to be 1.0/CTpu. However, a F value that is not 1.0/0pu is theoretically feasible. If so, it provides formulae to figure out how to compute the fault currents and voltages at the fault point F and their related symmetrical components for different sorts of defects. Note that the fault point views the positive, negative, and zero-sequence impedances as Zt, Z2, and Z0, respectively. In the table, Zeq, the equivalent impedance to replace the fault in the positive-sequence network, replaces T f, the fault impedance.

Unidirectional Line-to-Ground Fault

A transmission system's single line-to-ground (SLG) problem often happens when one conductor touches the neutral wire or falls to the ground. A generic illustration of an SLG fault with a fault impedance Zf at a fault location F. In fault studies, the fault impedance Zf is often disregarded. The networks that link the generated sequences. The faulty phase is often taken for granted to be phase for the purpose of simplicity in fault computations. The phases

of the system may simply be renamed if the faulty phase in actuality isn't phase a (for example, phase b) (i.e., a, b, c becomes c, a, b). The "generalised fault diagram" is used in a second technique. The zero-, positive-, and negative sequence currents may all be shown to be equal to one another[7], [8]. Therefore,

$$\mathbf{I}_{a0} = \mathbf{I}_{a1} = \mathbf{I}_{a2} = \frac{1.0 \angle 0^\circ}{\mathbf{Z}_0 + \mathbf{Z}_1 + \mathbf{Z}_2 + 3\mathbf{Z}_f}$$

Since,

$$\begin{bmatrix} \mathbf{I}_{af} \\ \mathbf{I}_{bf} \\ \mathbf{I}_{cf} \end{bmatrix} = \begin{bmatrix} 1 & 1 & 1 \\ 1 & \mathbf{a}^2 & \mathbf{a} \\ 1 & \mathbf{a} & \mathbf{a}^2 \end{bmatrix} \begin{bmatrix} \mathbf{I}_{a0} \\ \mathbf{I}_{a1} \\ \mathbf{I}_{a2} \end{bmatrix}$$

The fault current for phase a can be found as,

$$\mathbf{I}_{af} = \mathbf{I}_{a0} + \mathbf{I}_{a1} + \mathbf{I}_{a2}$$

$$\mathbf{I}_{af} = 3\mathbf{I}_{a0} = 3\mathbf{I}_{a1} = 3\mathbf{I}_{a2}$$

$$\mathbf{V}_{af} = \mathbf{Z}_f \mathbf{I}_{af}$$

Substituting equation into equation, the voltage at faulted phase a can be expressed as,

$$\mathbf{V}_{af} = 3\mathbf{Z}_f \mathbf{I}_{a1}$$

$$\mathbf{V}_{af} = \mathbf{V}_{a0} + \mathbf{V}_{a1} + \mathbf{V}_{a2}$$

The fault impedance Zf may be thought of as the impedances in the arc (in the event of having a flashover between the line and a tower), the tower, and the tower footing.

Therefore,

$$\mathbf{V}_{a0} + \mathbf{V}_{a1} + \mathbf{V}_{a2} = 3\mathbf{Z}_f \mathbf{I}_{a1}$$

Which justifies the interconnection of sequence networks in series. Once the sequence currents are found, the zero-, positive-, and negative sequence voltages can be found from.

$$\begin{bmatrix} \mathbf{V}_{a0} \\ \mathbf{V}_{a1} \\ \mathbf{V}_{a2} \end{bmatrix} = \begin{bmatrix} 0 \\ 1.0 \angle 0^\circ \\ 0 \end{bmatrix} - \begin{bmatrix} \mathbf{Z}_0 & 0 & 0 \\ 0 & \mathbf{Z}_1 & 0 \\ 0 & 0 & \mathbf{Z}_2 \end{bmatrix} \begin{bmatrix} \mathbf{I}_{a0} \\ \mathbf{I}_{a1} \\ \mathbf{I}_{a2} \end{bmatrix}$$

$$\mathbf{V}_{a0} = -\mathbf{Z}_0\mathbf{I}_{a0}$$
$$\mathbf{V}_{a1} = 1.0 - \mathbf{Z}_1\mathbf{I}_{a1}$$
$$\mathbf{V}_{a2} = -\mathbf{Z}_2\mathbf{I}_{a2}$$

In the event of having a SLG fault on phase b or c, the voltages related to the known phase a voltage components can be found from,

$$\begin{bmatrix}\mathbf{V}_{af}\\ \mathbf{V}_{bf}\\ \mathbf{V}_{cf}\end{bmatrix} = \begin{bmatrix}1 & 1 & 1\\ 1 & \mathbf{a}^2 & \mathbf{a}\\ 1 & \mathbf{a} & \mathbf{a}^2\end{bmatrix}\begin{bmatrix}\mathbf{V}_{a0}\\ \mathbf{V}_{a1}\\ \mathbf{V}_{a2}\end{bmatrix}$$

$$\mathbf{V}_{bf} = \mathbf{V}_{a0} + \mathbf{a}^2\mathbf{V}_{a1} + \mathbf{a}\mathbf{V}_{a2}$$

$$\mathbf{V}_{cf} = \mathbf{V}_{a0} + \mathbf{a}\mathbf{V}_{a1} + \mathbf{a}^2\mathbf{V}_{a2}$$

Underground Cables

Within a protective coating, underground cables may include one or more conductors. Lead is often used as the impenetrable protective layer that covers insulation. Insulating materials keep the conductors apart from one another and the sheath. Rubber and rubber-like compounds, varnished cambric, and oil-impregnated paper are the three insulating materials employed. Cables rated 600 V-35 kV utilise rubber, whereas cables rated 600 V-138 kV use polyethylene (PE), propylene (PP), and polyvinyl chloride (PVC). Rubber is the best material for underwater cables because of its great moisture resistance. Cables with voltage ratings of 600V to 28kV employ varnished cambric. Solid-type cables up to 69 kV and pressurised cables up to 345 kV both employ oil-impregnated paper. The pressure within the oil-impregnated cable is not elevated above atmospheric pressure in solid-type cables. Gas in gas pressure cables or oil in oil-filled cables keep the pressure in pressurised cables above atmospheric pressure. Because of its reduced dielectric losses and affordable price, impregnated paper is employed for higher voltages. For voltages 59 kV and below, cables are either (1) low pressure (not exceeding 15 psi) or (2) medium pressure (not exceeding 45 psi). For voltages of 69 kV and below, high-pressure cables with installed pipes are not cost-effective (up to 200 psi). While a product is defective or when the cable is operating under variable loads, voids or cavities may emerge. Voids in the insulation of cable not under pressure are caused by the cable being bent during handling and installation, as well as by the differing thermal expansion coefficients of the insulating paper, the impregnating agent, and the lead sheath. The insulation is destroyed as a result of greater electrical field strength ionisation that develops in the dielectric spaces. The power factor shift that occurs when a test voltage is applied may be used to identify the existence of ionisation. With the oil-filled cable, void formation is prevented. With the help of the gas-filled cable, the insulation's pressure is raised to a point where any gaps or cavities that may already present are ionization-free. Ionization rises as the temperature rises and falls as the pressure rises[9], [10].

Conductors

Aluminum or copper conductors may be utilised in subterranean cables. For aluminium to transport the same current as copper, bigger conductor diameters are required. Stranded conductors must be employed because of the need for mechanical flexibility. In compared to copper wire, similar aluminium cable is lighter in weight and has a greater diameter. Stranded conductors may be arranged in a number of ways, including rope, concentric, compressed, and compact.

Types of Underground Cable

There are several different categories for cables. For instance, depending on where they are, they may be categorised as (1) subterranean, (2) undersea, and (3) airborne. According to the kind of insulation, they may be divided into three categories: (1) rubber and rubber-like compounds, (2) varnished cambric, and (3) oil-impregnated paper.

Depending on the number of conductors in a particular cable, they may be categorised as (1) single conductor, (2) two conductor duplex, (3) three conductor, etc. Based on the presence or lack of metallic shields above the insulation, they may be categorised as shielded (like the Hochstadter or type H cable) or nonshielded (belted). Solid, lubricant- or gas-filled shielded cables are all options.

Their protective coating may be categorised as either (1) metallic (like a lead sheath) or (2) nonmetallic (e.g., plastic). Insulation shields support the following functions: limiting electromagnetic or electrostatic interference, improving cable protection from induced potentials, equalising voltage stress inside the insulation, decreasing surface discharges, and reducing shock danger (when grounded correctly). Shielding should generally be taken into account for nonmetallic covered cables running at a circuit voltage greater than 2 kV and in the event that any of the following circumstances present:

1. Conduit changes from conducting to non-conducting.
2. Change from wet to dry ground.
3. In arid environments with dry soil.
4. Within moist conduits.
5. Aerial line connections.
6. Locations that use conductive pulling chemicals.
7. Where cement deposits, soot, salt, or other conducting elements gather on the cable's surface.
8. In locations where electrostatic discharges are strong enough to interfere with radio or television reception but not strong enough to destroy cable.

Cables are often hauled into subterranean ducts. However, if they must be buried underground, armour must be used to mechanically protect the lead sheath, which is the covering over the insulation. The armour is constructed from thick steel wires or two steel tapes coiled in an overhand pattern. Since single-conductor cables may be produced with conductor diameters up to 3.5 kill or greater, they are helpful for handling high weights. They are also employed when balanced single-phase transformer loads are provided or when phase isolation is necessary. They are often used to give training in tiny manholes by terminating three-conductor cables in single-conductor potheads, such as at pole risers. Three single-

conductor wires may be installed in a single duct by using them in triplexes or wrapped three in parallel on a reel. a power cable with a single conductor and paper insulation. The belted cable architecture is often utilised for three-phase low voltage operation, up to 5 kV, or in the 10-15 kV voltage range with the addition of conductor and belt shielding. In order to create a smooth "cushion" for the lead sheath, a portion of the total insulation is put over partly insulated conductors in the shape of an insulating belt, giving this method its name.

Statistics on world energy

Additionally, the carbon dioxide emissions prevent the transfer of heat from the Earth's surface to space, which has an impact on climate (see following chapters). These statistics have been known since the early 1970s (Meadows et al. 1972), yet in 2004 human energy consumption (and associated CO emissions) increased to 429.4 EJ (429.41018 J). The Sun's radiation on Earth is 14,000 times more than what the whole world uses in terms of energy. The energy of solar irradiance on Earth, accumulated over a year, is substantially more than all of the known fossil fuel resources in Figure 11.1.

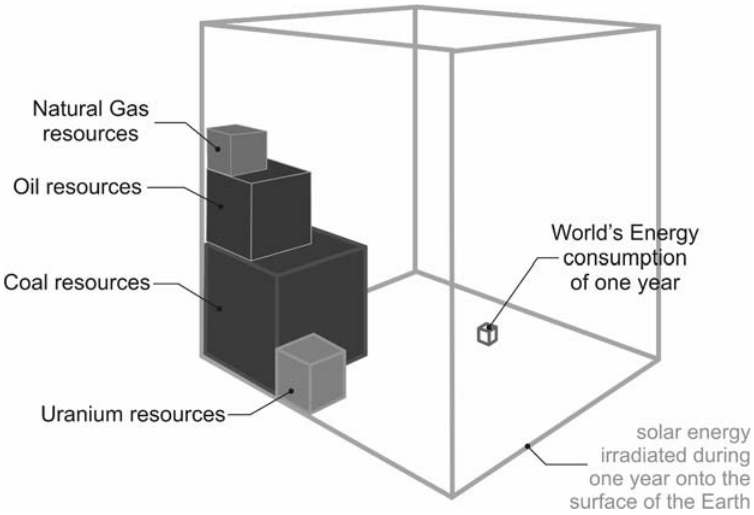

Figure 11.1: ***Illustrates*** **the World'senergyconsumptionincomparisontoallitsfossilresourcesanditsannualsolarenergy potential(adaptedfromGreenpeace).**

Emissions of CO_2 by Humanity

Burning fossil fuels like coal, oil, and gas to meet human energy needs has resulted in increased CO_2 emissions, especially since the start of industrialization, as shown in Figure 11.2. Since there are not enough plants (biomass) at the moment to fully complete the conversion of CO_2 to O_2, an accumulation of CO_2 in the atmosphere is seen (see Figure 11.3). An increase in this impact comes from fewer plants (e.g., due to deforestation) in Figure 11.4.

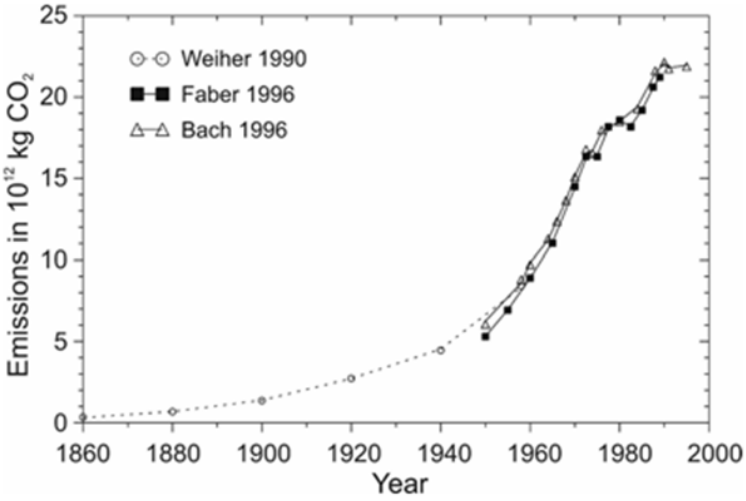

Figure 11.2: ***Illustrates*** **an accumulation of CO 2 in the atmosphere is observed.**

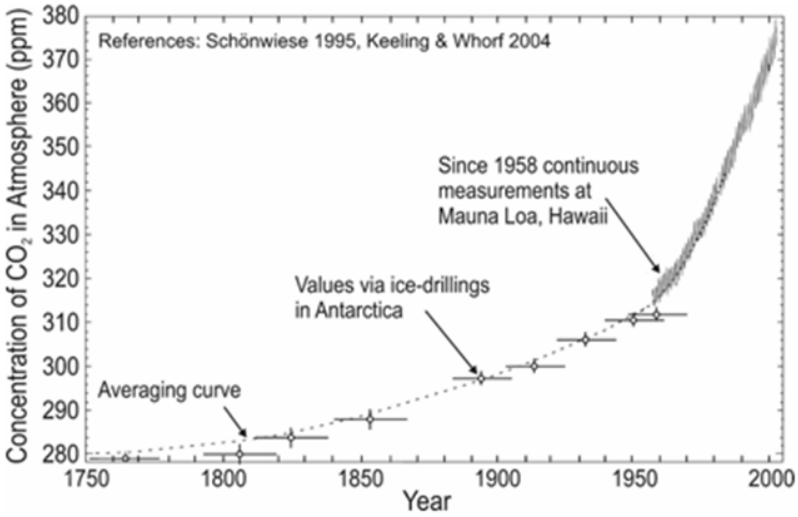

Figure 11.3: ***Illustrates*** **the CO_2 -contents oftheEarth'satmosphereinppm("partsper million) asafunctionoftime.Before1958detectionbydrillingsintheAntarctica:rangeofconfidenceind icated;from1958onwardscontinuousmeasurementsatMaunaLoa(Hawaii).Graphicsbased onSchönwiese1995,Keeling&Whorf2004.**

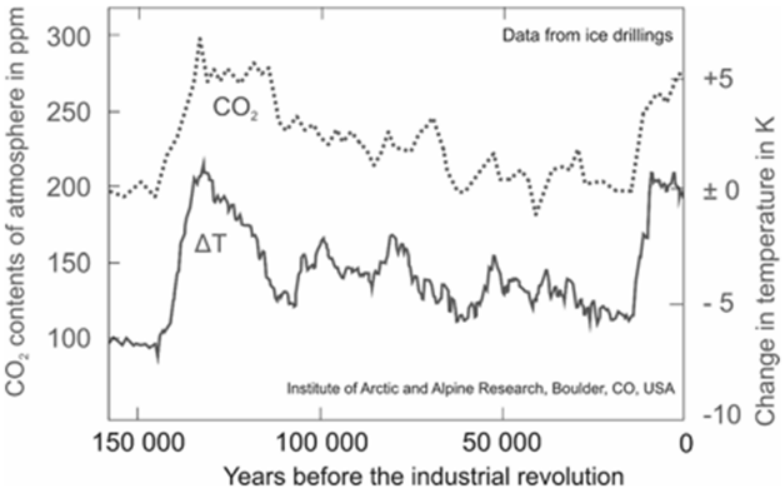

Figure 11.4: ***Illustrates*** **the Correlation of CO_2-contents of the Earth's atmosphere and its temperature change from 150,000 B.C to 1750 A.D according to the Institute of Alpine and Alpine Research, Boulder, Colorado, USA.**

CO_2-induced global warming

The gases important for the greenhouse effect, such as water vapour, methane, N2O, and ozone, show a good transmittance only for the visible part of the radiation (= 350-800 nm), but hinder the emission of infrared heat radiation (> 10,000 nm) from the earth to space. This is in contrast to the main components of the atmosphere, N 2 and O2, which allow the same good optical transmittance of incoming solar irradiation as when the earth's surface is emitting more, but doing so at a greater surface temperature, an equilibrium of incoming and outgoing energy fluxes ensues. This is known as the greenhouse effect. The earth's surface would be 30 K cooler without this natural greenhouse effect. Table provides a summary of the potential consequences of natural greenhouse gases in Table 11.1.

Table 11.1: ***Illustrates*** **the** Components of natural greenhouse effect.

Gas, chemical formula	**Share of natural increase of temperature**	**Relative share**
Watervapor, H_2O	20.6K	62%
Carbondioxide, CO_2	7.2K	22%
Ozone near ground, O_3	2.4K	7%
Nitrous oxide, N_2O	1.4K	4%
Methane, CH_4	0.8K	3%
Others	ca.0.6K	2%
Sums of shares	33K[1)]	100%

Alternative estimates only indicate a total influence of 15-20 K, but the Intergovernmental Panel on Climate Change (IPCC) 1994 findings suggest a total effect of 30 K. (incl. clouds).

Since the start of the industrial period, human activity has increased emissions of greenhouse gases, both natural and man-made. As a consequence, more infrared heat radiation is trapped in the atmosphere, raising the ground surface temperature. Since 1850, the atmosphere's ability to reflect infrared light from the ground has risen by around 1%. Svante Arrhenius, a Swedish scientist, first proposed that increased carbon dioxide levels in the atmosphere may cause climate change in 1896. Surprisingly, he precisely projected the greenhouse effect's size by 5 K at a doubling of the CO2 level. The British scientist Callendar's 1938 demonstration of a rise in atmospheric carbon dioxide during the preceding decades sparked interest in climatology. However, it wasn't until 1971–1972 that the world began to pay attention to carbon dioxide since it was realised that its consequences may be just as bad as the general air pollution that was the topic of concern at the time.

A group of specialists was convened in 1977 by the World Meteorological Organization and the UN organisation in Geneva, Switzerland, who concluded that a global climate congress was necessary. The 1970 conference was the catalyst for worldwide research that greatly increased our understanding of the climate, particularly the processes behind climatic change and the greenhouse effect. Recent findings on the impact of emissions on the climate are provided.By taking air temperature readings, it is possible to verify the greenhouse effect's effectiveness in terms of climate. Despite variations, Figure shows that there has been a noticeable rise in the worldwide air temperature at sea level of 0.5–1.0 K since the turn of the century. Along with meteorological consequences (ocean winds and currents, sea and groundwater levels), this rise also affects biological activity 1, which might have a significant impact on the human habitat in Figure 11.5.

.

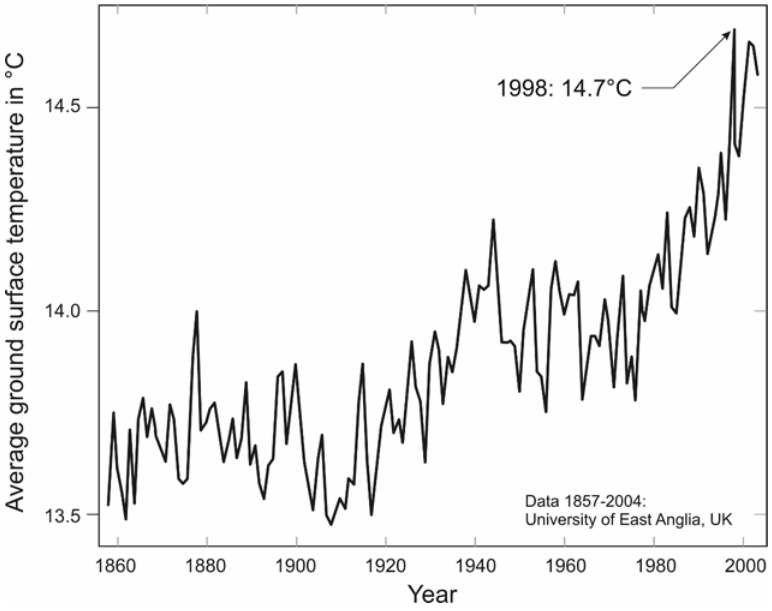

Figure 11.5: The Observedairtemperatureneartheground(mediatedoverthenorthernhemisphere)from1858to2004.

The fact that the actual temperature increase is less than what would be expected given the rise in atmospheric CO_2 must also be taken into account. This happens as a result of a brief

drop in temperature brought on by anthropogenic sulphur dioxide in the atmosphere. The effects of an increase in atmospheric temperature are not only limited to an increase in the frequency of natural disasters like floods and hurricanes, as shown in Figure 11.6, but also enhanced chemical and biological activities like faster bacterial growth and a doubling of the speed of chemical- biological reactions (RGT-rule), up to an upper limiting temperature (ca. 60°C for enzymes). To prevent these events, man-made CO_2-emissions should be lowered, either by using less energy or by switching to energy sources that generate less CO_2.

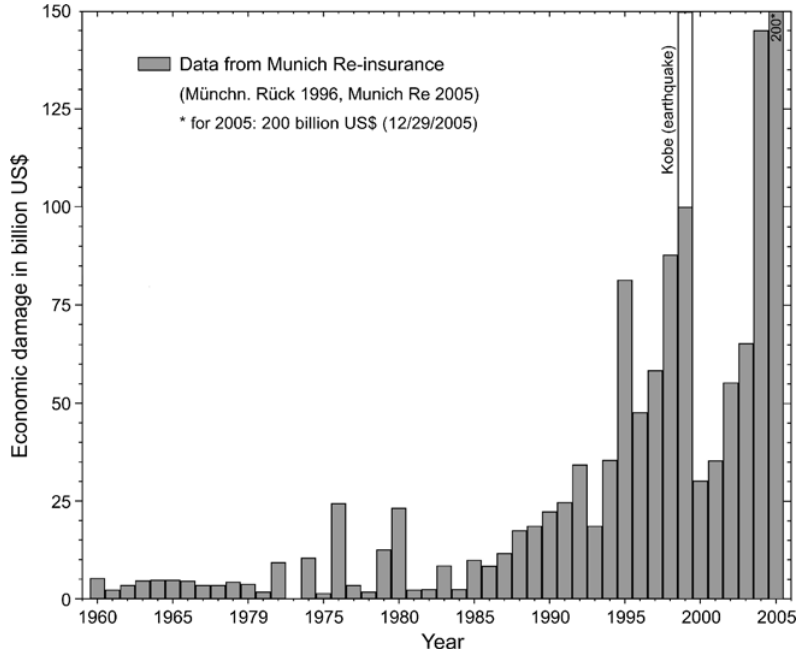

Figure 11.6: The Worldwidedamage(inbillions US$) causedbynatural disastersasafunctionoftime.

However, combining both of these approaches energy conservation and the replacement of traditional energy sources will result in the optimum outcome. Current estimates of human climate change suggest that without the implementation of such measures, global mean temperatures would rise by 1-2.5 K over pre-industrial levels by the decade 2036–2046. As long as these inaccuracies are sustained over time, this range is very susceptible to mistakes in the model's sensitivity to climate change, rates of oceanic heat absorption, or global reaction to sulphate aerosols.

Quantification of CO_2 Diminution

As a result of the dangers associated with a buildup of CO_2 in the atmosphere, the German government and several other countries committed to cut CO_2 emissions by 50% by the year 2020. This doesn't appear like it can be done using the methods being utilised (i.e., merely by an increase of efficiency of power generation). Even when the demand for a set amount of crude energy to produce a certain gross domestic product was effectively decreased, this action by itself will not achieve the target of a 50% reduction to be attained by 2020. This goal can only be achieved if a significant quantity of energy can be produced with reduced CO2 emission. Long-term, this entails replacing fossil fuel power plants with renewable energy generators.Future power plants must be renewable in order to meet the goals listed above. The public generally accepts renewable energy sources favourably as they offer practically infinite supply, minimal secondary costs, a declining cost trend, and no emissions.

As a key illustration of the conversion of renewable energy, the use of photovoltaics for electrical energy production is explored in Figure 11.7.

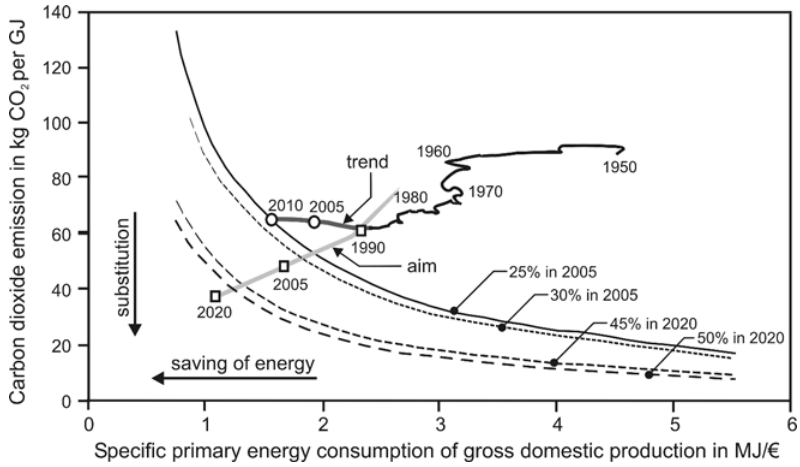

Figure 11.7: *Illustrates* the Reduction of CO_2-emissions by depletion of energy consumption and by substitution of CO_2-intense energy generation. Also displayed are goals for CO_2 reductions.

REFERENCES

[1] X. Wang *et al.*, "Location of Single Phase to Ground Faults in Distribution Networks Based on Synchronous Transients Energy Analysis", *IEEE Trans. Smart Grid*, 2020, doi: 10.1109/TSG.2019.2938667.

[2] K. Polychronopoulou, A. Lois, en D. Draganov, "Body-wave passive seismic interferometry revisited: mining exploration using the body waves of local microearthquakes", *Geophys. Prospect.*, 2020, doi: 10.1111/1365-2478.12884.

[3] Z. Li *et al.*, "Single-phase-to-ground fault section location in flexible resonant grounding distribution networks using soft open points", *Int. J. Electr. Power Energy Syst.*, 2020, doi: 10.1016/j.ijepes.2020.106198.

[4] H. Shi, J. Gong, A. R. Simpson, A. C. Zecchin, en M. F. Lambert, "Leak detection in virtually isolated pipe sections within a complex pipe system using a two-source-four-sensor transient testing configuration", *J. Hydroinformatics*, 2020, doi: 10.2166/hydro.2020.170.

[5] W. Li, W. Xu, Z. Qiao, en X. Wang, "Fault section location method for a distribution network based on concave and convex characteristics of transient zero sequence current", *Dianli Xitong Baohu yu Kongzhi/Power Syst. Prot. Control*, 2020, doi: 10.19783/j.cnki.pspc.190710.

[6] H. Wu, Y. Wu, Z. Lai, W. Wang, en Q. Yang, "A hybrid film-bulk-acoustic-resonator/coupled-line/transmission-line high selectivity wideband bandpass FBAR filter", *IEEE Trans. Microw. Theory Tech.*, 2020, doi: 10.1109/TMTT.2020.2989264.

[7] S. Yildiz, A. Aksen, en B. S. Yarman, “Design of multiband matching ladders without mutual coupling using parametric representation of Brune functions”, *Int. J. RF Microw. Comput. Eng.*, 2020, doi: 10.1002/mmce.22358.

[8] S. R. Ola *et al.*, “Alienation coefficient and Wigner distribution function based protection scheme for hybrid power system network with renewable energy penetration”, *Energies*, 2020, doi: 10.3390/en13051120.

[9] N. H. Chan, S. K. C. Cheung, en S. P. S. Wong, “Inference for the degree distributions of preferential attachment networks with zero-degree nodes”, *J. Econom.*, 2020, doi: 10.1016/j.jeconom.2020.01.015.

[10] A. Kulshrestha *et al.*, “A hybrid fault recognition algorithm using stockwell transform and wigner distribution function for power system network with solar energy penetration”, *Energies*, 2020, doi: 10.3390/en13143519.

CHAPTER 12

TRADITIONAL AND RENEWABLE ENERGY SOURCES

Mr. M.Sashilal, Associate Professor,
Department of Electrical Engineering, Jaipur National University, Jaipur India
Email Id- msashilal@jnujaipur.ac.in

The carbon-based fossil fuels (coal, gas, and oil) and nuclear power shall be referred to as "conventional sources of energy" in the section that follows.The photo-synthetic process, which took place many millions of years ago, produced fossil fuels. Simply explained, they are nothing more than solar energy or solar radiation storage. Fossil fuels have existed in their current forms for more than 100 million years, making their production a geological one-time event with a very poor conversion efficiency (see Table 12.1). Fossil resources must be seen as finite from a human standpoint. They scarcely qualify as "renewable," in this context.

Table 12.1: the Energyconversiontimescaleandconversionefficienciesofsolarenergyintodifferentenergycarriers.

Energycarrier	Timefor"production" ofenergyinyears	Solarconversionefficiency	Literature
Coal,lignite	>150,000,000	<0.001%	Bennewitz1991
Oil,gas	>100,000,000	<0.001%	Bennewitz1991
		1%	Kaltschmitt2003
Wood	1–30	0.55%	Kleemann1993
		0.1%	Spreng1995

The current pricing advantage of fossil fuels is justified by politically advantageous factors including the price war of the OPEC nations, their "terms of trade" with the main consumer nations, and the direct and indirect subsidies of conventional fuels. Giving subsidies for exploration, mining, and transportation, such as for coal and nuclear power in Germany and diesel in Brazil, is a kind of direct subsidization. By imposing costs for subsequent actions on the populace and the government, indirect subsidization is accomplished (e.g., air and water pollution control, security of supply for oil, security for nuclear waste). Examples of efforts to ensure the supply of oil include military presence (for instance, in Saudi Arabia) or even storage in dry mass above ground of 570,000 kg of beech wood, which has an irradiance of 3.7 PJ/(km 2 a) (240,000 kg below the ground as roots and humus). Based on the energy density and average irradiance of forest growth in temperate climates[1], [2].

For sugar beets, the maximum solar yield is 5.4% (for all cropland, it is 0.3%). photosynthesis in relation to the average world level. direct action (for instance, in Iraq, where the previous war cost US taxpayers over $300 billion US). Another illustration: A 24-hour surveillance by only one guard would cost 900 million US dollars over the course of 12,500 years, even if Plutonium only loses 50% of its activity. The price trend of

conventional fuels changed significantly during the medium term (Figure in 12.2), but since it is a limited resource with constant (or even rising) demand, its price may rise over the long run in Figure 12.1.

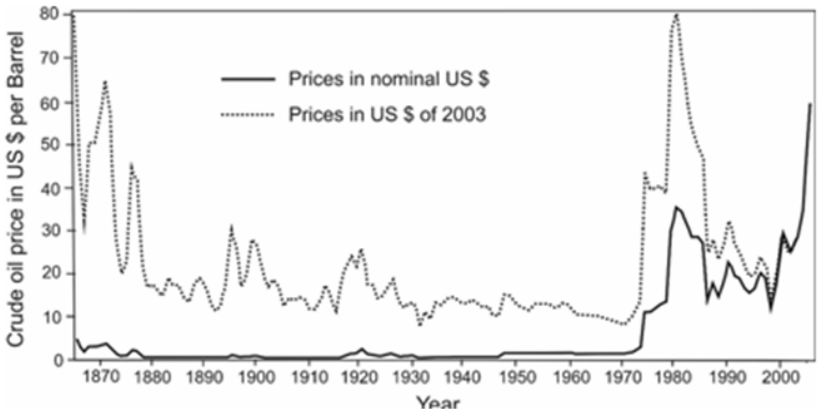

Figure 12.1: The DevelopmentinpriceofcrudeoilinUS$(actualand2003value)duringthelast150years.

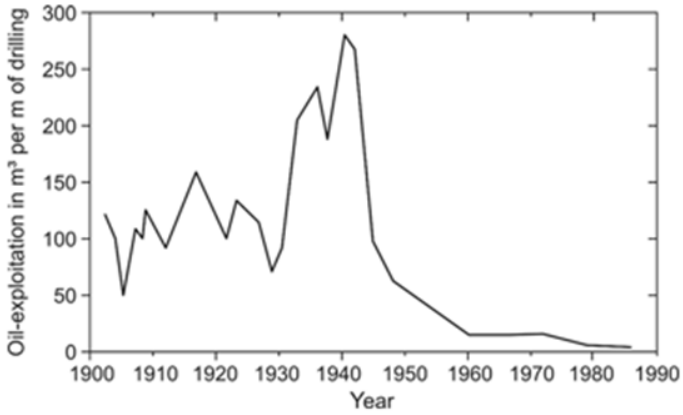

Figure 12.2: The ExploitationrateofUSoil-welldrillingssince1900.

The price development is also important because it shows that a similar (though less severe) impact could be seen in the mid-forties, at the same time when the pace of oil drilling in the US reduced (to almost nil) and the price of oil surged globally. Utilizing these energy sources has social consequences as well, including an increase in health problems (allergies, respiratory tract disorders, etc.) and the deterioration of cultural artefacts and the environment (acid rain). The destruction brought on by air pollution to historical structures and monuments in Munich serves as an illustration: According to estimates, it took more than 300 years for air pollution harm to grow by one grade from 1700 to 1850. However, between 1930 and 1955, this time abruptly shrunk to less than 50 years. Depending on when the structure was built, it takes between 70 and 120 years for deterioration to progress by one grade nowadays. Despite the fact that the contaminants have already been much decreased from 150 years ago, this implies that the expenses of restoration will double.

For the year 2000, the total estimated expenses for further cultural monument repairs in Germany were over US$ 70 billion[3], [4]. According to a study by the Federal Institute of Material Research, the costs for additional maintenance due to damage by air pollutants for

buildings without cultural value (structures, bridges, industrial plants, high voltage transmission towers) are approximately US $ 4.1 billion every year in Germany (BAM 1990).

Utilizing nuclear energy leads to irreversible technological, administrative, political, and social institutions that are in opposition to democratic culture in Figure 12.3. According to a researchby the University of Münster, a serious catastrophe involving a "Biblis" type reactor in Germany would have cost US $ 2.35 trillion. Highly radioactive nuclear waste must be consistently monitored and guarded throughout a number of such half-lives since it has half-lives of several thousand years (for example, Plutonium has a half-life of 12,500 years). Even with public pressure, the resulting technological, administrative, and military system cannot be changed. Consequently, this complex will be exempt from democratic laws.

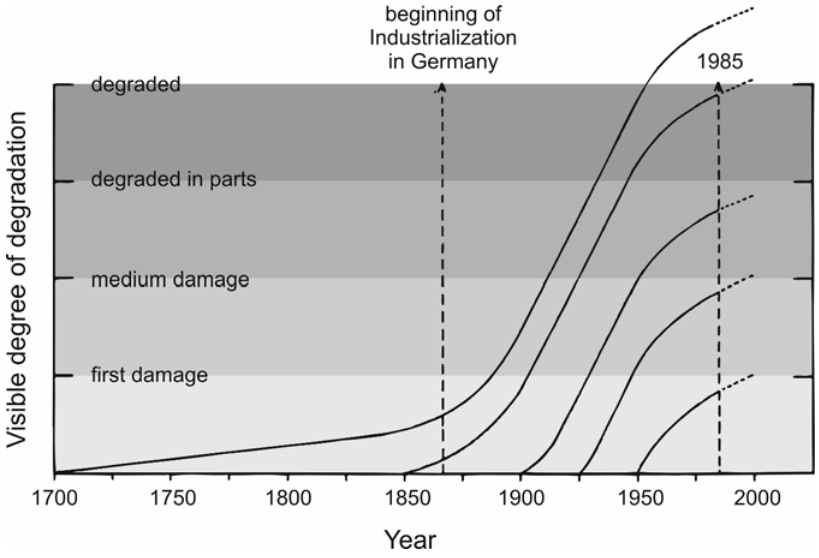

Figure 12.3: ***Illustrates*** **the DamageofhistoricalbuildingsinMunich(Germany)asafunctionoftimeaccordingtothePreservationOfficeforHistoricalMonumentsoftheStateGovernmentofBavaria.**

The cost of insurance is overestimated by at least 8,000 times since the real insurance for such an incident is just $294 million USD. The usage of nuclear power will not be further explored at this point since it differs fundamentally from all other kinds of energy consumption and is not immediately measurable and compared[5], [6].

Conversion of energy

Various analyses of the energy needs of power plant infrastructure and the financial requirements for the operation with fossil and renewable energy sources have previously been published. It is evident that owing to significant advancements in manufacturing technology and material utilisation, relative emissions for solar power generated by photovoltaics over the last ten years decreased from 230-318 g/kWh to 26-41 g/kWh. According to the most recent development, typical wafer thicknesses will decrease from 0.3 mm to 0.2 mm as a result of a shortfall in silicon supply; as a result, the numbers from the most recent publication by Alsema et al. (2005) will likely be off by 25–30%.This book should retain its relevance even if the precise energy needs and greenhouse gas emissions of PV technology may vary in absolute terms over time since the accounting approach it presents will always be appropriate. Later chapters and the Annex include more information.

Inaccuracies with regard to energy amortization periods have been found in the past. Frequently, the necessary operational fuels—like combustibles—have not been taken into account in the considerations. For instance, a straightforward coal power plant achieved an "energy amortisation time" of one year as opposed to a PV power plant's four years. However, under the higher definition, a simple ground campfire would have the shortest amortisation period of any power plant. Renewable energy sources have been unfairly criticised in this manner for a while now, either on purpose or out of ignorance. Any combustible fuel-powered energy conversion plant has an indefinite energy amortisation time! It is unnecessary to include any facilities that convert renewable energy since they all use renewable fuels. The primary concern with regard to the greenhouse effect is not only energy consumption, but also the actual CO2 emissions that occur throughout the course of a power plant's whole lifecycle, including recycling of its parts and materials. For instance, even though the production of aluminium requires ten times more energy than that of stainless steel, this may still be acceptable if the energy is produced using renewable energy sources (as it is for the production of aluminium in the Scandinavian countries) and the aluminium is recycled later, allowing recovery of 90% of the energy used and reducing effective CO_2 emissions. (For instance, in Brazil, almost 90% of aluminium cans are recycled[7], [8].

Approach

The purpose of this account is to investigate how the widespread usage of PV generators impacts the population's overall net CO_2 emissions. The whole life cycle of the PV generator must be taken into account in order to do so, taking into account things like manufacture, transport, installation, usage, electrical yield, and dismantling operations.

Production

Other steps that are leading to a more ecologically friendly manufacture of PV systems are investigated in addition to the current state-of-the-art production techniques. Particularly important in this case are the reductions in energy use (at the same yields) and CO_2 emissions. We will evaluate the electrical energy produced by a solar power plant while taking into account all pertinent factors, including the environment (irradiance, reflective losses, microclimates), and any potential interactions between these factors.

Balance

The Life Cycle Analysis will assess the precise reduction of CO achieved by using a PV system (LCA). The system must not only be an effective means of production (minimising cycles of matter and energy), but it should also, if at all feasible, boost yields without exerting too much effort. The method by an integrated analysis of a whole system, taking into account the origin of its components under inclusion of the capacity to recycle and the operating circumstances, is new in this book.

Optimization

The goal is the improvement of PV systems while taking into account the actual environment, its effects on operation (irradiation, reflection, outside temperature, wind speed), and the interaction parameter of the individual components with a view to optimising the energetically weighted effectiveness. The assertions presented will be verified by building up a prototype. We'll look at the potential for mass manufacturing and how it may affect the CO_2 balance.

Photovoltaics

The direct conversion of photons into electricity is known as photovoltaics (PV). While photovoltaics will play a significant part in the area of renewable energies, electricity will continue to be utilised as a source of energy in growing amounts. PV technology has a long lifespan, is quiet and emission-free while in operation, and is modular. Due to existing semiconductor technology, there is a considerable possibility for cost reduction. In addition, existing manufacturing methods may be made more effective and affordable by using mass production techniques. Although owing to a shortage of silicon as a raw material, prices at the plants are now stabilising at 3 €/Wp. Prices are predicted to drop once further in 2006 once new silicon manufacturing facilities go into service. According to the most recent data, manufacturing costs of 1-1.6 €/Wp are doable[9], [10].

Short History

Solar cells were created as a result of some of the most significant scientific discoveries of the 20th century, which combined the efforts of multiple Nobel Prize–winning scientists of the time. Max Planck, a German physicist, spent the first part of the century seeking to understand the nature of the light produced by hot things like the sun. In order to make theory and observations fit, he had to assume that energy was constrained to discrete levels. This inspired Albert Einstein to theorise that light was composed of microscopic "particles," subsequently known as photons, each of which had a little amount of energy that varied depending on the colour of the photon, in his "miraculous year" of 1905. The energy of blue photons is about double that of red photons.

Even less energy exists in infrared photons, which are undetectable to the eye. Although they are invisible, ultraviolet photons—the culprits behind sunburn and skin cancer—carry significantly more energy than blue photons, which explains the harm they may inflict. Erwin Schrödinger's wave equation, which was developed in 1926 as a result of Einstein's original idea, is the pinnacle of quantum mechanics. In 1930, Wilson found the solution to this equation for a solid substance. This gave him the opportunity to explain the distinction between insulators and excellent conductors of electricity, as well as the characteristics of semiconductors and their intermediate electrical properties. Electrical currents may easily pass through metals because electrons, which carry electrical charge, are free to roam around. Electrons in insulators are bound by the bonds that keep their atoms together. They need a surge of energy to break these ties and enable them to move. Similar principles apply to semiconductors, however a smaller shock is required in this case; even the red photons from sunlight have sufficient energy to release one electron in silicon, the prototypical semiconductor. In 1940, Russell Ohl made the accidental discovery of the first silicon solar cell. When he shined a flashlight on what he believed to be a pure rod of silicon, he was shocked to find that it had a significant electrical potential. A closer look revealed that modest amounts of impurities were imparting certain silicon "negative" qualities (n-type). It is now understood that these characteristics result from an excess of mobile electrons having a negative charge. Other sections exhibited "positive" (p-type) characteristics, which are now understood to be caused by a lack of electrons and had the effect of having an excess of positive charge (something close to a physical demonstration of the mathematical adage that two negatives make a positive).

In 1949, William Shockley developed the p-n junction theory, which he utilised to construct the first functional transistors. P-n junctions are devices that are created by junctions between "positive" and "negative" areas. Following the 1950s semiconductor revolution, the first effective solar cells appeared in 1954. At the time, this generated a great deal of excitement

and front-page attention.In 1958, spacecraft became the new solar cells' first commercial use. Up until the early 1970s, this was the main commercial use. However, oil embargoes at that time period sparked a new interest in the possibilities of cells closer to home. A terrestrial solar cell business began to emerge at this time, and it has expanded quickly ever since, especially in recent years. The industry is positioned to have an increasingly significant influence throughout the first two decades of the new century due to growing worldwide commitment to reducing carbon dioxide emissions as a first step in containing the "Greenhouse Effect" and falling cell prices.

Effect of Photovoltaic

A large-area semiconductor diode is a solar cell. It is made up of a p-n junction produced by doping impurities into the semiconductor crystal (consisting of four covalent bonds to the neighboring atoms for the most commonly used silicon solar cells). With five outside electrons on phosphorus atoms, which are impurities, only four outer electrons are necessary to fit the atom into the silicon crystal structure. The fifth electron is free and movable. As a result, this area of the crystal is known as the n-region because it contains a large percentage of free negative charges. The p-region is the opposite: One outside electron is always absent for a full binding into the crystal structure when the crystal is doped with boron atoms, which contain only three outer electrons. The location of the missing electron is moved because this electron could be "stolen" from nearby atoms. Another way to think of this missing electron is as a positive-charged "hole" that is roving and movable. In the p-regions, where free holes outnumber free electrons by a large margin, electrons are referred to be minority charge carriers. Electrons diffuse into the p-areas and "holes" into the n-regions due to concentration differences at the "border" between the two regions, creating an electrical field at the once electrical neutral junction (see Figure 12.4): the zone of space charge building up. It grows until it successfully prevents a further dissemination of carriers.

When light (or solar radiation) strikes a semiconductor, it creates electron-hole pairs, increasing the minority charge carriers' concentration by many orders of magnitude. The electric field in the space charge zone divides these charge carriers as they diffuse there. A tension V could be seen between the n-side and p-side contacts, as seen in Figure 12.5. A current I travels through a load resistor R when it is applied, dissipating electrical power.

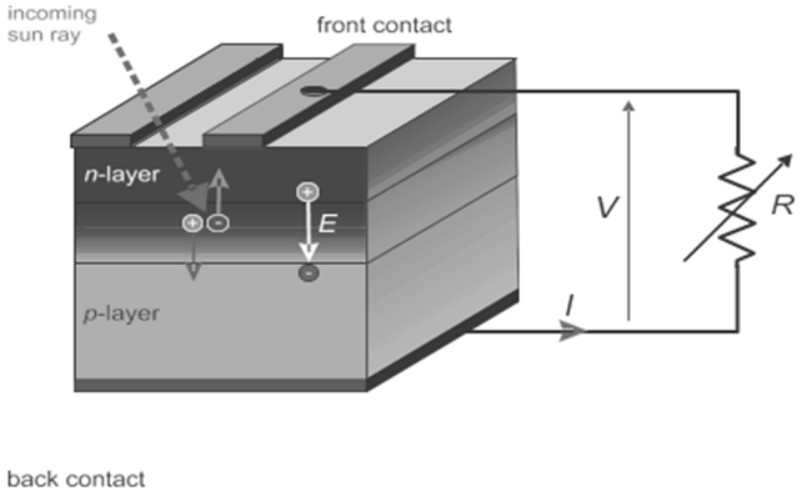

Figure 12.4: ThePrincipleofphotovoltaicenergyconversioninan*n-p*-dopedsemiconductor.Generatedpowerissuppliedtoanohmicload R(scheme).

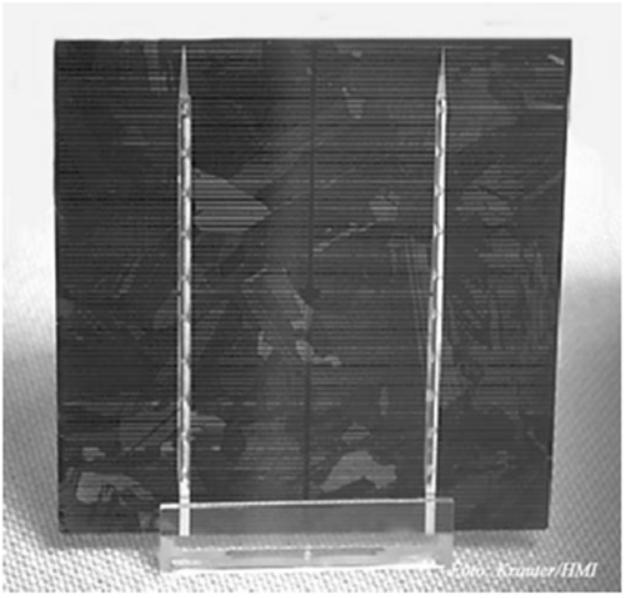

Figure 12.5: The Frontviewofasquaremulti-crystallinesilicon(mc-Si)solarcellatasizeof10cmx10cm.

According to Figure 12.6 below, the characteristic of a solar cell with no irradiance (dark characteristic) corresponds to diode characteristic 8. This feature changes with the quantity of the photo current Iphot in the blocking direction when the solar cell is lit (light characteristic). Plotting the resultant currents and voltages at various loads when connected to a variable load resistor (see Figure 2.1) will reveal this solar cell feature.

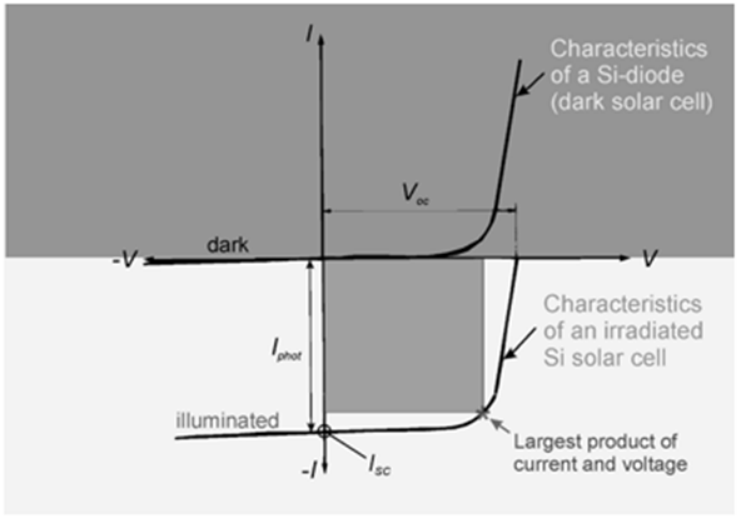

Figure 12.6: The Current-voltagecharacteristicsofadiode(darksolarcell)andairradiatedsolarcellwithashortcircuitcurrentI_{SC}andopencircuitvoltageV_{OC}.

The current in a short circuit one of a solar cell's most crucial properties is its isc. It happens in a short-circuited, lit solar cell. Circuit-opening voltage Voc: If no current is applied, the tension between the contacts is described (open circuit). The sum of the open-circuit voltage Voc and the short-circuit current Isc yields the theoretically possible (optimal) power that

might be drawn from the terminal, Popt, or the "rectangular-ness" of the trace of the characteristic. Figure 12.7 *Illustrates* the relationship between the power P and the tension V as well as the related I-V characteristic.

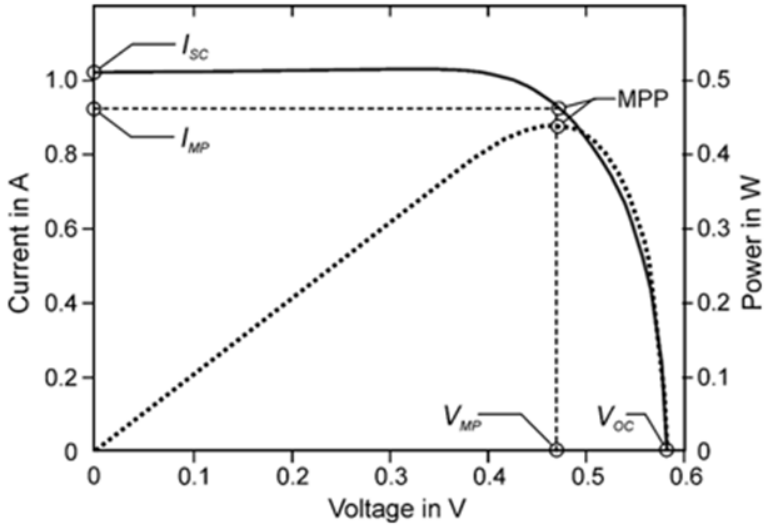

Figure 12.7: TheCurrent-VoltagecharacteristicsandPower-Voltagecharacteristicsof asiliconsolarcell.AlsoshownistheMaximumPowerPoint(MPP)atVmp and Imp.

The effectiveness of photovoltaic conversion PV is defined as the electrical power output divided by the solar cell's irradiation power. PV is reliant on spectrum and irradiance. Standard test conditions (STC) are used to determine the conversion efficiency. These conditions include an irradiance of 1,000 W/m 2 perpendicular to the front surface, a cell temperature of 25°C, and a spectral distribution based on solar irradiance passing through the atmosphere at an elevation angle of 41.8°. The theoretical maximum photovoltaic conversion efficiency exists due to physical limitations. For crystalline silicon, this amounts to around 28% and has three primary causes:

A so-called indirect semiconductor is silicon. As a result, the presence of a phonon (lattice vibration), which occurs very seldom and has a relatively low absorption coefficient, determines whether a photon will be absorbed.With a band gap of 1.1 eV, silicon allows for the transfer of energy from higher energy photons to lower energy photons as heat rather than being completely absorbed. The so-called "spectral sensitivity" or "spectral response" of a solar cell is defined by this loss as well as other losses (see below).

1. The maximum voltage (open-circuit voltage), Voc, for silicon is around 0.7 V and relies on the difference between the potentials produced by the p-n transition.
2. Various loss processes in practise diminish this theoretical conversion efficiency:
3. Optical losses, such as reflection and shadowing losses brought on by the front contacts as well as losses from irradiance that is not absorbed (transmitted).
4. Ohmic losses from parallel resistors and parasitic series resistors (via connections and sheet resistance).

Losses in recombination

Quantum efficiency refers to a solar cell's capacity to transform an incoming photon of a certain wavelength into an electron-hole pair. Reflection losses on the solar cell's surface are

not taken into account by "internal quantum efficiency," but they are by "external quantum efficiency." Despite the fact that, in accordance with Max Planck's equation, the energy of photons (or "quanta" of energy) grows with frequency, each typically only generates one electron-hole pair with a fixed energy potential. As a result, spectral efficiency—the ratio of electrical energy produced to radiation—declines as wavelengths become shorter. When the energy of the incoming photon is just enough to produce one electron-hole pair, the spectral efficiency is at its peak. The photovoltaic effect is nonexistent if the photon's energy is insufficient to produce an electron-hole pair; for silicon solar cells, this occurs at wavelengths higher than 1,100 nm. The actual spectral characteristic must be measured since it deviates somewhat from the ideal due to imperfections in the silicon crystal. As seen in Figures12.8 and 12.9, the so-called "spectral sensivity" or "spectral response" S () is determined by dividing the photon density (jphot()) by the intensity of incoming radiation (irradiance) E() or G(). The response of a solar cell to modulation at a certain wavelength is used to calculate spectral efficiency. To counteract the distracting effects of the irradiance level, the measurement is conducted by irradiating a bias spectrum (such as AM 1.5).

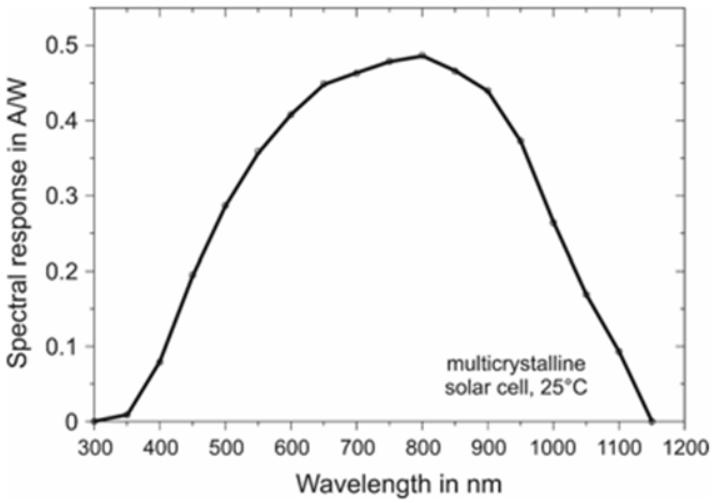

Figure 12.8: the Actual spectral response of a multi-crystalline silicon solar cell (ASE).

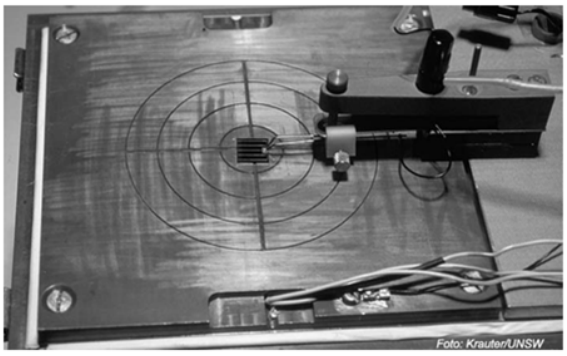

Figure 12.9: the Device to measure I-V characteristics, efficiency and spectral response. Shown with a high efficiency solar cell at UNSW.

The thickness and state of the atmosphere through which the Sun's radiation must travel determine the precise spectral distribution on the surface of the Earth. These factors also affect the efficiency and power production of solar cells to some extent (see Figure 12.10; further details are available in the chapter on irradiance modelling).

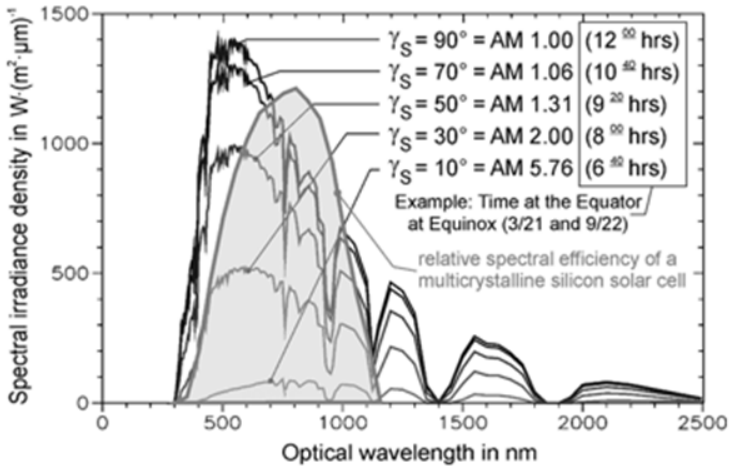

Figure 12.10: ***Illustrates*** **the Actual spectral response of a multi-crystalline (mc) silicon solar cell (ASE) together with the solar spectra for different elevation angles of the sun, equivalent air masses (AM), and time at the equator for Equinox.**

REFERENCES

[1] I. Siksnelyte-Butkiene, E. K. Zavadskas, en D. Streimikiene, "Multi-criteria decision-making (MCDM) for the assessment of renewable energy technologies in a household: A review", *Energies*. 2020. doi: 10.3390/en13051164.

[2] S. Tishkov, A. Shcherbak, V. Karginova-Gubinova, A. Volkov, A. Tleppayev, en A. Pakhomova, "Assessment the role of renewable energy in socio-economic development of rural and arctic regions", *Entrep. Sustain. Issues*, 2020, doi: 10.9770/jesi.2020.7.4(51).

[3] X. Álvarez, E. Valero, N. de la Torre-Rodríguez, en C. Acuña-Alonso, "Influence of small hydroelectric power stations on river water quality", *Water (Switzerland)*, 2020, doi: 10.3390/w12020312.

[4] A. P. Barčić *et al.*, "Possibilities of increasing renewable energy in Croatia, Slovenia and Slovakia – wood pellets", *Drv. Ind.*, 2020, doi: 10.5552/drvind.2020.2024.

[5] H. Yasmeen, Y. Wang, H. Zameer, en Y. A. Solangi, "Decomposing factors affecting CO2 emissions in Pakistan: insights from LMDI decomposition approach", *Environ. Sci. Pollut. Res.*, 2020, doi: 10.1007/s11356-019-07187-3.

[6] J. Mammadov, "THE IMPACT OF ALTERNATIVE AND RENEWABLE ENERGY ON GLOBAL CLIMATE CHANGE", *EurasianUnionScientists*, 2020, doi: 10.31618/esu.2413-9335.2020.5.71.604.

[7] G. Zimon, M. Sobolewski, en G. Lew, "An influence of group purchasing organizations on financial security of SMEs operating in the renewable energy sector-case for Poland", *Energies*, 2020, doi: 10.3390/en13112926.

[8] A. J. Al-Yasiri, M. A. Ali, R. S. Ali, en H. N. Bekheet, "Renewable energy sources in international energy markets: Reality and prospects", *Int. J. Innov. Creat. Chang.*, 2020.

[9] E. Lisin, G. Kurdiukova, P. Okley, en V. Chernova, "Efficient methods of market pricing in power industry within the context of system integration of renewable energy sources", *Energies*, 2019, doi: 10.3390/en12173250.

[10] W. S. W. Abdullah, M. Osman, M. Z. A. A. Kadir, en R. Verayiah, "The potential and status of renewable energy development in Malaysia", *Energies*, 2019, doi: 10.3390/en12122437.

CHAPTER 13

PHOTOVOLTAIC SYSTEM

Mr. Vivek Jain, Associate Professor,
Department of Electrical Engineering, Jaipur National University, Jaipur India
Email Id- vivekkumar@jnujaipur.ac.in

Only little variations in electrical potential may be obtained because the internal electrical field in a solar cell is rather weak (0.3 V for germanium and 0.7 V for silicon). The open circuit voltage that could really be reached is a little lower than these numbers. Solar cells are joined in series to produce so-called "strings" of solar cells, which provide larger voltages.Due to their extreme fragility, these threads are often sandwiched between two sheets of soft plastic and glass to form what is known as a "solar module" or "PV module." The translucent soft plastic used above and below the cell strings is often the copolymer EVA (ethylene-vinyl-acetate), although other choices include PVB, silicones, and TPU (thermoplastic polyurethane, a relatively new material). A tempered front glass is added to the composite in order to strengthen it and increase its durability. It is referred to as a "laminated module" if the backside is a composite foil (a mixture of layers such as PVF-aluminum-PVF or PVF-polyester-PVF), and as a "encapsulated module" if the backside is glass (see Figure 13.1), 36 to 72 cells are needed in a series connection since the output voltage of such a PV module is often adjusted to 17 to 35 V for off-grid applications, which enables to completely charge a 12 V (or a 24 V) battery. A tiny terminal box containing the electrical terminals and a metal or plastic frame that aids in mounting the module and adds extra rigidity to it are attached to complete the module in Figure 13.2.

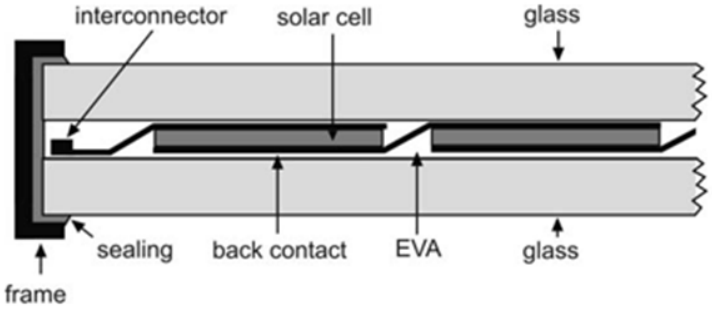

Figure 13.1: The Cross section of an encapsulated PV-module.

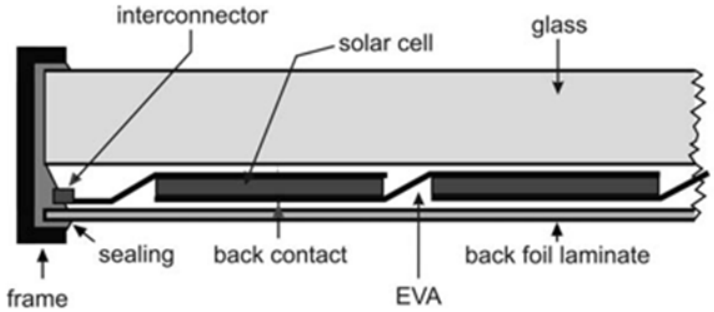

Figure 13.2: *Illustrates* the Cross section of a laminated PV-module.

Powerful Qualities

Some current-voltage characteristics, similar to those of solar cells, are used to describe the electrical properties of a PV module (see Figure 13.3 and 13.4). You may record combinations of current and voltage that, when the load is altered, produce an I-V curve by attaching a variable ohmic load to the terminals of the exposed PV module.The so-called "Maximum Power Point" is when output power, which is produced by multiplying the I-V pairs, reaches its maximum value (MPP). "Standard Test Conditions" (STC) have been established in order to make the data comparable: The cell operating temperature is set to 25°C, the irradiance is 1,000 W/m 2, and the spectrum is fixed and corresponds to a solar spectrum at Air Mass 1.5. (See also Annex for references to IEC 904-1 and IEC 891, respectively, DIN EN 60904-1 and DIN EN 60891). In the range of 350 to 1,000 W/m2, the fluctuation of the irradiance E (or G) has very little impact on the open-circuit voltage of a PV module. The voltage declines logarithmically with decreasing irradiance levels. Because the short-circuit current is equal to the quantity of electron-hole pairs produced by the absorbed photons, it is directly proportional to the irradiance. As a result, a PV generator's potential output power is proportional to the irradiance from 350 to 1,000 W/m 2. (Constant conversion efficiency)[1], [2].

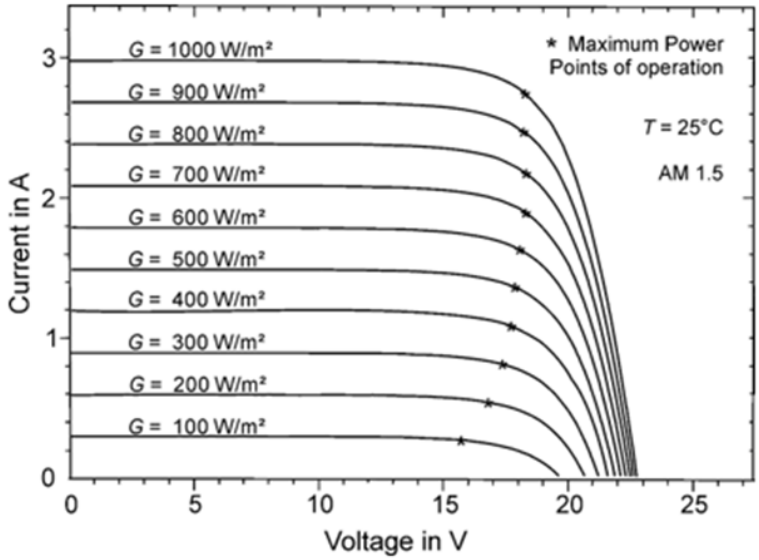

Figure 13.3: *Illustrates* the Current-voltage characteristics of a multi-crystalline silicon PV- module for variations of irradiance (temperature and spectrum are kept constant at 25°C resp. AM 1.5).

The conversion efficiency declines at lower irradiance levels as a result of voltage losses, which are dependent on the internal shunt resistance. Low irradiation levels need solar cells with higher shunt resistance than those with lower shunt resistance (mainly caused by impurities in the cell material).

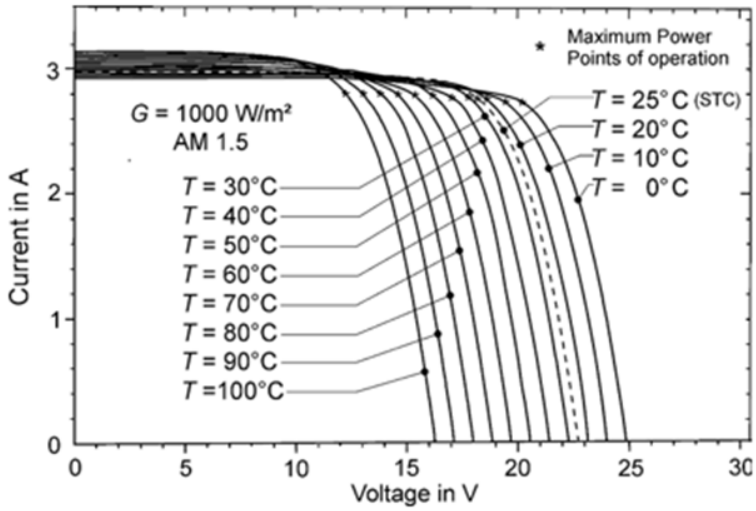

Figure 13.4: *Illustrates* the Current-voltage characteristics of a multi-crystalline silicon PV module at variations of temperature (irradiance and spectrum kept constant at 1,000 W/m² resp. AM 1.5)

An increasing cell temperature at constant irradiance causes a reduction of the open-circuit voltage and consequentlyoftheoutputpowerby-0.4%/Kto -0.5%/Kforcrystallinesiliconsolarcells(seeFigure 13.5)

EquivalentElectricalCircuit

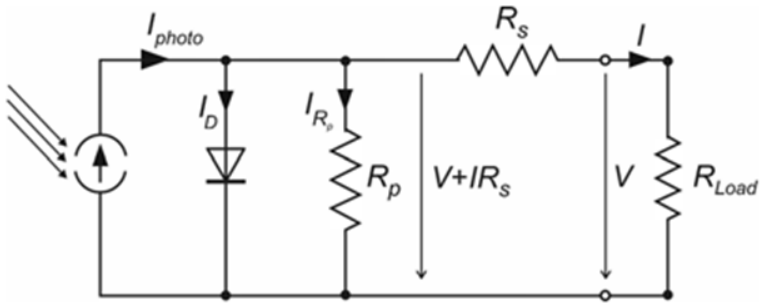

Figure 13.5: theEquivalent electrical networkdiagramofasolarcellaccordingtothe"onediodemodel".

The current-voltage characteristic of a solar cell approached by a "one diodemodel"(equivalentelectricalnetworkdiagram)couldbedescribedasfollows:

$$I = I_{photo} - I_0\left(\exp\frac{q(V+IR_s)}{kT} - 1\right) - I_{R_p}$$

$$R_p = R_{p,dark} \cdot e^{-\alpha E}$$

$$I_{R_p} = \frac{V + I R_s}{R_p}\left(1 + a\left(1 - \frac{V + I R_s}{V_{br}}\right)^{-m}\right)$$

Thecurrent-voltage-characteristicsofaPVmodulecouldbedescribedas:

$$I = I_{photo} - I_0\left(\exp\frac{q\left(\sum V + I R_s\right)}{kT} - 1\right) - I_{R_p}$$

The parallel resistor is often thought of being constant. However, according to Zimmermann (1995), a typical value for a = 1.6910-3 m2 W-1, the parallel resistor R is 350 M in the dark and drops to 70 M at 1,000 W m-2 of irradiance.

Bypass Diodes

The element with the lowest current determines the total current, as is the case with all series connections (such as those at batteries or solar panels). Only cells with an equivalent current at the operating voltage are chosen for series connection in order to prevent losses. Additionally, a cell's current may be decreased by local shadowing (caused, for example, by dirt on the surface of the module), which reduces the overall current and power production. The (reverse) voltage at the shadowed cell may exceed the negative breakthrough voltage if the string is long enough, which may cause a local power dissipation that might potentially cause the cell to explode. To solve this issue, "bypass diodes" are switched in parallel (or, more often, "antiparallel," with the direction of the solar cell diode) to the solar cells or a short string of solar cells (see Figure 13.6). When a cell's current is decreased by shadowing, a reverse voltage develops inside the cell (assuming a load is connected) until it exceeds the breakthrough voltage of the bypass diode. As a result, some of the total current flows through the bypass diode while the remaining current continues to flow through the cell.A low reverse breakthrough voltage of the solar cell diodes (for example, at multi-crystalline solar cells) or a cell integrated bypass-diode (Green 1980: "Integrated Solar Cells and Shunting Diodes," Australian Patent 524,519; U.S. Patent 4,323,719) are other solutions to this issue[3], [4].

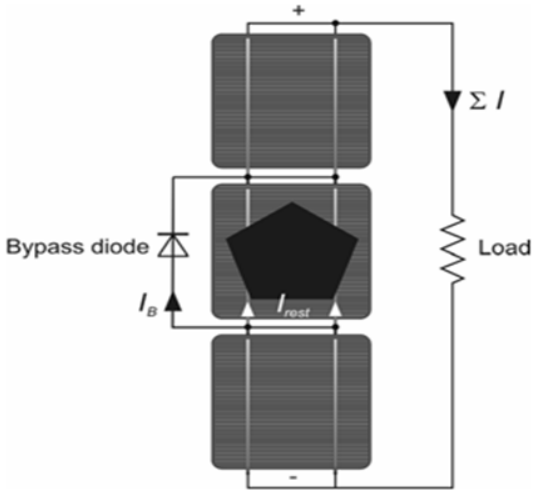

Figure 13.6: The Schemeof operationof abypass diode: solar cell withpartial shadinginastringof3cellsinseriesconnection.

Electrical connectors

The cell string wires travel through the lamination of the module and are secured by a pull relief. The wires are then attached to a plastic box with a plug- or screw-able termination that serves as an extension or end. In order to speed up installation, the most recent modules come pre-configured with external connections and waterproof connectors for module connecting. Bypass diodes are located in the terminal box or incorporated into the frame.

Multiple Strings

Modules are switched in series because the efficiency of the power conditioning parts (such as inverters) rises with voltage. Safety regulations in certain nations (like the US) restrict the maximum voltage to 600 V. (500 V incl. a security factor). The maximum power output for the most popular cell sizes (10 cm by 10 cm to 15 cm by 15 cm) is thus 2 to 3 kWp.Modules (or strings of modules) are switched in parallel to increase power outputs without exceeding the maximum voltage of 600 V (or to increase currents). The other strings may damage the defective string when they attempt to "feed" it in the event of a failure, such as a voltage decrease in a string brought on by, for example, a greater temperature or a shadowed cell (voltage is also lower when a bypass diode is applied). As a result, "string"-diodes are linked in series to each string of solar cells in order to safeguard the string by preventing reverse currents (Figure 13.7). If a failure lowers the voltage of a string, the "string" diode enters a blocking condition while the other strings continue to provide power to the intended load. Voltage loss at the string diode is permanent in this design, which is a drawback. However, voltage loss may be decreased by using a germanium or Schottky barrier type 9 low breakthrough voltage diode. Additionally, reverse currents may be detected by magnetic field sensors, which would then activate an off-switch[5], [6].

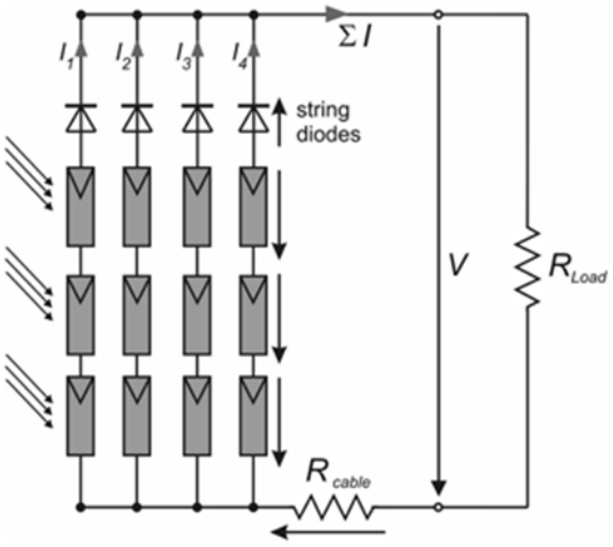

Figure 13.7: the ParallelconnectionofPVstringsviastringdiodesforprotection.

At silicon diodes, voltage loss is 0.3 V instead of 0.7 V. Utilizing relatively tiny "string" inverters on the power conditioning side is another technique. The output of each string's (synchronized) AC power is then paralleled.

Technical Features

Wraparound Lamination

An "encapsulated" PV module is one that is made of glass, plastic, solar cell, plastic, and glass, while a "laminated" PV module is made of glass, plastic, solar cell, plastic, and glass. In a vacuum laminator at 150 °C, an EVA (ethylene-vinyl-acetate) foil with a thickness of 0.5 to 0.7 mm is used as the primary component of the plastic: At that temperature, the copolymer EVA "cure" and makes the lamination process irreversible. Air bubbles within the laminate are avoided by the suction. A particular UV absorber is put to the sign to prevent damage caused by ultraviolet solar radiation (also known as "yellowing" or "browning"). Tedlar-Polyester-Tedlar® or Tedlar®-Aluminum-Tedlar foils with a thickness of 0.5 mm are often employed as the "laminated PV modulebackside "'s foil in place of glass. A polyvinyl fluoride film is called Tedlar® (PVF). To obtain a high optical transmission and to comply with ISO 203 requirements, both kinds of glass sheets are produced of thermally tempered, iron-free glass that is 2 to 4 mm thick. Additional material characteristics are included in the Annex.

Aluminum profiles are primarily used to construct the framing of PV module frames, which secure the lamination to the frame. Saw tooth inlays or stainless steel screws are used to hold the frame's corners in place. Silicon rubber small tube profiles that are pressed between laminate and aluminium frame maintain the laminate in place while also being resilient to mechanical stress and thermal expansion. A second, "cleaner" alternative is to apply a self-adhesive seal tape (such as Butyl) on the laminate's rim before tightening the frame. Frameless modules are being utilised more often to save costs, as well as for a better self-cleaning effect and reduced energy use during manufacturing. Fixture compounds are used to install such modules to the structure.PV module torsion stability for wind speeds up to 200 km/h, resistance to hail up to a diameter of 25 mm[7], [8].

Mounting and Fixing

Modules with frames come with screw threads or mounting holes in Figure 13.8. All screws and threads must be made of stainless steel of V2A to V4A standard due to the needed resistance to corrosion (for maritime applications) in Figure 13.9. Fixing is accomplished for frameless PV modules using fixture compounds.

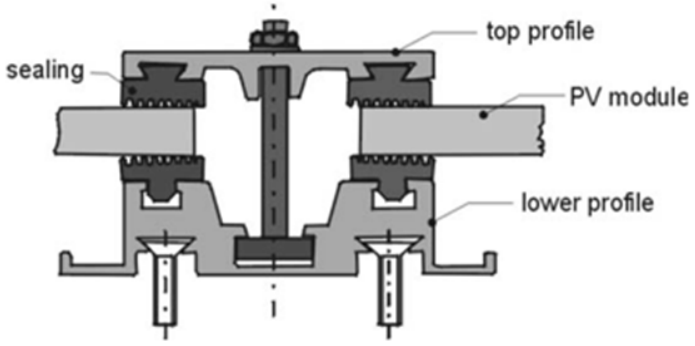

Figure 13.8: the Cross-sectionofafixture-compoundforframelessPVmodules.

Figure 13.9: The Roof-mountedPVgeneratorwithframelessmodulesandfixturecompounds.

In addition to using less material, handling is improved since screwing and fastening are now done at the front of the panel. The edges of the module accumulate less dust and filth as a result, which is a benefit. While framed modules tend to generate a buildup of dirt that accumulates from the edges (at the frame boundary) to the centre of the front surface of the module, layers of dirt are washed away during rains. The more uniform aesthetic appearance that the frameless PV modules provide is also valued by architects. The adhesive technique is a relatively recent advancement towards the affordable and aesthetically pleasing installation of PV modules. Early results, such as the PHALK-Mont Soleil 560 kWp in Switzerland, show great promise. The installation was quicker, and corrosion issues in the mounting compound, which consists of aluminium frames, stainless steel fasteners, and steel support structures, were removed. On the other hand, nondestructive module disassembly is not feasible; however, given the long lifespan and high dependability of PV modules, this feature is not as important. Future increases in the cost of labour and falling module prices will make this strategy even more advantageous. Despite the fact that the thermal expansion coefficient of the relevant polymers is higher than that of glass, module size is limited by the tendency for bending during processing to significantly stress the module[9], [10].

The characteristics of PV generators during operation

Due to voltage losses, the electrical power production of silicon solar cells diminishes as cell temperature rises. When the temperature is raised by 30 K, the voltage and power losses for commonly used single- and multi-crystalline silicon solar cells range between 12% and 15%. (see Table 13.1). On a bright day, cell temperatures of 30 K or higher above ambient temperatures may be attained with standard installation or roof integration of the PV generators. The temperature impact causes the solar cells' conversion efficiency to be at its lowest, especially around midday when irradiance is at its highest level.

Table 13.1: the measured temperature coefficients (*TC*) for Silicon PV modules

Type of PV	$TC\,(V_{OC})$	$TC\,(I_{SC})$	$TC\,(FF)$	$TC\,(P_{mp})$
module	in%/K	in%/K	in%/K	in%/K
Single-Si#1	-0.2817	0.0411	-0.1265	-0.3619
Single-Si#2	-0.3413	0.0130	-0.1642	-0.5035

Multi-Si#1	-0.2632	0.0435	-0.1172	-0.3318
Multi-Si#2	-0.3675	0.0675	-0.1732	-0.4690
Multi-Si#3	-0.2925	0.0407	-0.1556	-0.3996
ASE300-DG/50 (multi-Si)	-0.3726	0.1097	$TC(V_{mp})$=-0.4752 $TC(I_{mp})$=+0.0372	-0.4397
a-Si_{min}				-0.0393
a-Si_{max}				-0.2045

As of right present, the reference criteria for classifying PV modules (STC: Standard Test Conditions 11, SOC: Standard Operating Conditions) STC: cell temperature of 25 °C, irradiation of 1000 watts per square metre (perpendicular), and solar spectrum of 1.5 air masses (see also IEC 60904-1, IEC 62145 and IEC 61215). SOC is the same as STC, except it uses actual measured cell temperature that occurs at 800 W/m2 of solar radiation, 20°C of ambient air temperature, and 1 m/s of wind speed. Common temperatures range from around 42°C to 57°C. SOC is making greater progress. Present only demonstrations for a single operating point (specific spectrum, perpendicular incidence, constant cell temperature and constant air speed). The user's understanding of the yield over a certain time period, including all actual operating circumstances, is more crucial. For this reason, it is essential to examine and anticipate the real daily temperature, efficiency profile, and actual energy output, particularly when doing an economic assessment of a PV power plant. There might be significant discrepancies between estimates based on SOC, and particularly STC. This is brought on by optical reflection losses as well as high temperatures.

REFERENCES

[1] L. Hernández-Callejo, S. Gallardo-Saavedra, en V. Alonso-Gómez, "A review of photovoltaic systems: Design, operation and maintenance", *Solar Energy*. 2019. doi: 10.1016/j.solener.2019.06.017.

[2] S. Seme, K. Sredenšek, B. Štumberger, en M. Hadžiselimović, "Analysis of the performance of photovoltaic systems in Slovenia", *Sol. Energy*, 2019, doi: 10.1016/j.solener.2019.01.062.

[3] W. Van Sark, "Photovoltaic system design and performance", *Energies*, 2019, doi: 10.3390/en12101826.

[4] M. Chaabane, W. Charfi, H. Mhiri, en P. Bournot, "Performance evaluation of solar photovoltaic systems", *Int. J. Green Energy*, 2019, doi: 10.1080/15435075.2019.1671405.

[5] O. F. C. Atalaya, D. Y. A. Santillan, en M. D. Choque, "Comparative analysis between a photovoltaic system with Two-Axis Solar Tracker and one with a fixed base", *Int. J. Adv. Comput. Sci. Appl.*, 2019, doi: 10.14569/ijacsa.2019.0101018.

[6] D. T. Cotfas en P. A. Cotfas, "Multiconcept Methods to Enhance Photovoltaic System Efficiency", *International Journal of Photoenergy*. 2019. doi: 10.1155/2019/1905041.

[7] S. Shittu, G. Li, Y. G. Akhlaghi, X. Ma, X. Zhao, en E. Ayodele, "Advancements in thermoelectric generators for enhanced hybrid photovoltaic system performance", *Renewable and Sustainable Energy Reviews*. 2019. doi: 10.1016/j.rser.2019.04.023.

[8] X. Li, Q. Wang, H. Wen, en W. Xiao, "Comprehensive Studies on Operational Principles for Maximum Power Point Tracking in Photovoltaic Systems", *IEEE Access*, 2019, doi: 10.1109/ACCESS.2019.2937100.

[9] G. Jiménez-Castillo, F. J. Muñoz-Rodríguez, C. Rus-Casas, en P. Gómez-Vidal, "Improvements in performance analysis of photovoltaic systems: Array power monitoring in pulse width modulation charge controllers", *Sensors (Switzerland)*, 2019, doi: 10.3390/s19092150.

[10] Y. Zhang, H. Chen, en Y. Du, "Lightning protection design of solar photovoltaic systems: Methodology and guidelines", *Electr. Power Syst. Res.*, 2019, doi: 10.1016/j.epsr.2019.105877.

CHAPTER 14

INSTALLATION OF PV MODULES

Mr. Sunil Dubey, Associate Professor,
Department of Electrical Engineering, Jaipur National University, Jaipur India
Email Id- sunildubey@jnujaipur.ac.in

While ongoing research and development into more sophisticated manufacturing techniques led to reduced prices for solar cells and PV modules, costs for installation and mounting remained constant or even rose as a consequence of high labour costs. Already, 21%-53% of the installation costs are covered. A concrete base and metal tubes or profiles that are often even custom-made to meet the size of the modules make up traditional installation in the open field. Due of the sensitivity to corrosion, such a specialised structure entails expensive material and labour expenses as well as significant maintenance expenditures. Aluminum and other materials that need a lot of energy to create result in longer energy payback periods for PV producing systems. Innovations at the support-structure and the foundation may also take place, leading to quicker installation via screw-less and foundation-less construction, in addition to enhanced module fastening techniques like the glue technology, which allows for mounting cost savings in Figure 14.1.

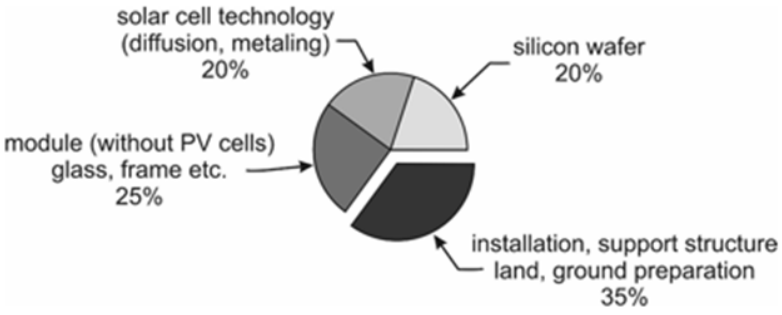

Figure 14.1: The Distribution of costs at a small PV power plant installation without powerconditioning.

Currently, distant settings like alpine regions are where photovoltaics are most economical to use. However, there may be issues with the shipping of equipment like as concrete mixers and steel bearers. Conventionally powered generators, such as diesel generators, need extra transportation expenses for gasoline, oil, and replacement parts in distant places where electrical grid access is costly. Even in the current economic climate, renewable energy producing units are often the most economical in these distant places [1], [2].

Future Photovoltaic Development

Significant progress has been achieved in the last several decades in both reducing manufacturing costs and improving photovoltaic conversion efficiencies in the lab (Green 1995). However, solar energy production is only economically viable in off-grid applications if the societal costs of fossil fuels are ignored. The potential for individual system components to evolve is not too far from the theoretical ideal. Although materials other than silicon may be used to make solar cells with better efficiency, these materials are less common, more costly, and often less environmentally friendly than silicon. Additional

research is required in the fields of installation, PV system composition, and cost-effective manufacture (thin film technology, integrated power conditioning, applications). Details used on laboratory samples could not be extended to mass production in order to preserve cheap manufacturing costs. As a consequence, commercially available solar cells have maximum conversion efficiencies of 20% to 21% (for example, Sunpower), whereas test samples in laboratories have up to 25%. (e.g., UNSW, ISE). Additional ohmic losses result from the cells' required series connection, and the poorest cell acts as a limiter on the amount of current that may flow. Additionally, owing to space requirements for electrical insulation and the thermal expansion of the cells, the whole module area cannot be covered by solar cells. Due to this need, the amount of module space that can be covered by solar cells is limited, and as a result, the total efficiency only reaches 15% to 17%. The following additional losses might be seen under actual operational circumstances:

1. Losses in optical reflection caused by irradiance that is not perpendicular.
2. Losses brought caused by low irradiance (reduction of form factor and voltage).
3. Voltage decrease caused by thermal losses as a result of high cell temperatures.

Shadowing: If a cell in a serial string is shaded, the output current is constrained by the lowered current of the shadowed cell. Reduction of output current for irradiance sun spectra with an air mass lower than AM 1.5. Somewhat avoiding this impact is possible using bypass diodes. Bypass diodes' leakage current might potentially result in certain performance losses. In a solar generator with parallel strings, low voltage strings caused by shadowing would function as a load. In order to prevent a load situation on the string, serial diodes are utilised. However, voltage losses at the serial diodes range from 0.3 to 0.7 V, depending on the kind of diode [3], [4].

Frequently, power conditioning devices are put in a tiny structure far from the generator. The literature states that for the majority of applications, the wire losses from the generator to the converters are in the neighbourhood of 3%. The inverters often have a high conversion efficiency at the rated power input, but the efficiency drops at low irradiance levels and low power input. As a result, the actual conversion efficiency may differ much from the rating over the course of a single day. In light of all these losses, the ratio of annual electrical energy output to annual irradiance is just 10:1 to 12:1. The literature utilises a nebulous adjustment factor, "Performance Ratio", to make up the discrepancy between the projected power output rating and actual performance in order to account for these losses and the ensuing disparities with the expected yields. Recently, inverters have also been referred to using this phrase. Both thorough investigations into the root causes of performance losses and proactive steps to prevent them are uncommon. In this article, a few strategies for making up for these inadequacies are described. The yields obtained under actual working settings are 23–45% lower than those obtained in labs or under standard test conditions (STC). Within I-MAP, inquiries into such impact have been made (Intensive Monitoring and Analysis Program).

An increase of electrical yield of 12% might be attained under actual working circumstances by enhancing the optical and thermal characteristics of PV module installation, which would bring operational efficiency a lot closer to nominal efficiency. The significance of installation and mounting challenges is increasing as a consequence of higher efficiencies and reduced prices of PV system components (solar modules and inverters). As may be observed, costs are disproportionately large, particularly for attaching the module. However, there is a significant opportunity to lower these cost sectors' prices, which would subsequently speed the adoption of photovoltaics in the energy industry. Efficiency improvements that are greater

than those possible with solar cell technology may be anticipated by increasing our understanding of how the PV module interacts with the natural environment [5], [6].

Autonomous Operation of Inverters

Even if the irradiance levels affect how electrical power is generated, energy storage is still necessary, particularly when the time of demand and the time of production are not the same—which is often the case. As a result, the system must be expanded to include storage, which consists of a battery and a suitable charge/discharge controller (see Figure 14.2). In order to convert the DC from the PV panel and storage to the AC needed, an inverter must be constructed since alternating voltage is often needed.

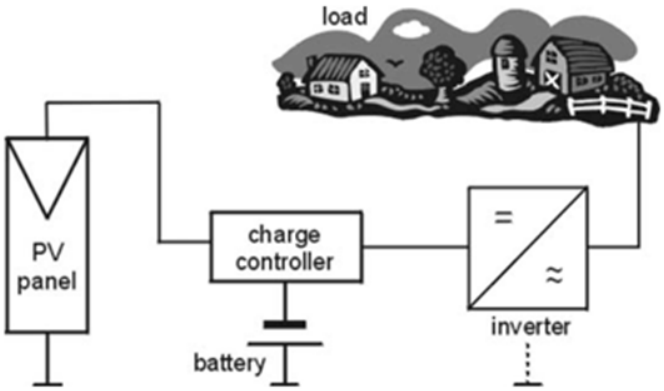

Figure 14.2: The Block diagram of an auto nomous PV system with storage and an inverter for A Cloads.

The simplest method to do this is to use devices known as rectangular inverters to swap the polarity of the DC with the frequency required for AC (50 Hz or 60 Hz). However, this kind of AC conversion results in significant degrees of distortion and higher frequency aberrations, which might harm delicate loads and obstruct radio signals. To more closely approximate the necessary sine-form, utilise switches with a brief interval of zero voltage (so called trapezoid inverters). Although this form of inverter exhibits higher distortion levels than rectangular inverters, they are still high.

Previously, "rotating inverters" were used. At those, an AC generator is connected to a DC motor. Although the efficiency of this approach is rather low and the frequency changes as the load changes, it does provide a very smooth sinusoidal output. PWM is the most recent technology used in inverters (pulse width modulation). Here, DC is briefly turned on and off (a pulse) in a way that the integral of the pulse is comparable to the real level at the desired sinus profile. So that the integral is comparable to the next real level of the sinus signal provided by the controller, the next pulse width is likewise modified in this manner. Such an inverter has a pretty high efficiency (up to 96%) output that is extremely near to a perfect sinus after filtering [7], [8].

The energy production of autonomous photovoltaic systems fluctuates as a result of daily and seasonal variations Electrical grid injection inverters

in sun irradiation. In Central Europe, summertime irradiance is often five to six times greater than wintertime irradiance. These PV systems must thus have sufficient energy storage devices to power loads during times of low or absent radiation. Storage drives up the cost of a system (particularly seasonal storage) and raises the price of produced energy. As a result,

energy is supplied into the public grid during times of excess production and similarly removed during times of insufficient solar power creation. 14. DC electricity from the PV generator must be transformed into AC in accordance with the specifications of the public grid to enable grid injection.

Contrary to inverters in autonomous systems, the controller does not provide the reference sinus for the PWM; rather, the grid does. Despite the fact that the grid's impedance is often relatively low, the inverters still need to be synchronised before operation and customised to the specific voltage and frequency of every given grid. As a result, inverters used for grid connections and those for autonomous systems are different. Utilities establish guidelines in order to keep distortion levels and voltage and current synchronisation within a certain range in the event of any connection to the grid. Although there have been many documented failures in the past with grid-connected inverters, the technology today has been shown to be quite reliable. Just an According to several studies, the public grid in many nations, including Germany, can accommodate PV grid injection in an area of at least 15% of its nominal grid power in Figure 14.3. However, only a few kinds of inverters are capable of operating in both grid-connected and autonomous modes. Small loads may often be powered by DC, but most appliances need AC at 115 or 230 volts at 50 or 60 hertz. It is often recommended to use a three-phase AC system for power needs more than 3 to 10 Kw [9], [10].

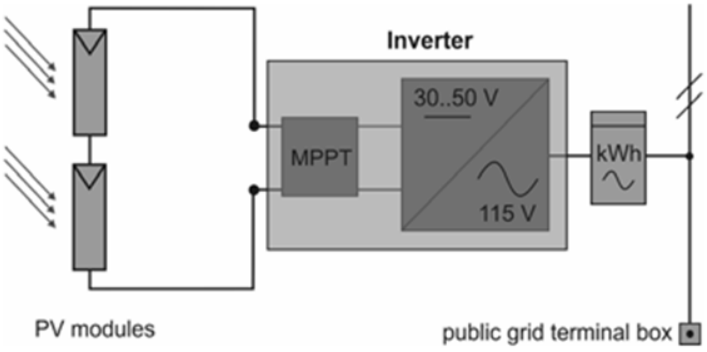

Figure 14.3: The Scheme of a typical single-phase PVgrid injection systemequipped with aMaximum-Power-Point-Tracker(MPPT)andanenergycounter(kWh).

There are several kinds of PV grid injectors. Their methods of commutation, such as whether they use transformers to provide galvanic isolation from the grid, and the kind of power electronics they use are different (thyristor, GTO, bipolar-transistor, MOS-FET or IGBT). The majority of these grid injectors are offered in a power range of 0.6 to 5 kW thanks to substantial financing schemes for PV power plants of these proportions (for example, the German 1,000 and 100,000 PV Roofs Program). The pulse-width-modulation idea is a commonly used concept (PWM). The first step is to get a rectangular current by altering the polarity of the DC output from the PV power station (every 10 ms for 50 Hz or every 8.33 ms for 60 Hz) in order for PWM to produce a 50 or 60 Hz sinus for an AC grid. The rectangular current is then alternately turned on and off (referred to as "pulsing") in order to produce an integral of the pulses that is as near as feasible to the desired corresponding sinus value. A lowpass filter is used to "smooth" the pulses after the rather high frequency (10 to 100 kHz) pulsing in order to do the integration. If the "guiding" grid fails, the inverter must likewise be instantly turned off. The frequency and phase must be adjusted to the real grid state. A grid inverter should generally meet the following criteria:

A current source's output current synchronously tracks the grid voltage.

The regulations (e.g., VDE 0838, EN 60555) do not let the distortion and ensuing spectrum harmonics of the grid frequency to exceed specified thresholds, which necessitates a suitable adaptation of the output current to the sinus form.

In order to prevent reactive power from bouncing back and forth between the grid and the inverter, which would result in further losses and ultimately an overcharge, the injected current and the grid voltage should not have any phase difference (cos p = 1).

The grid injector has to be immediately disengaged from the grid in case of failure (missing grid voltage, significant frequency changes, short circuits, or isolation failures). The grid injector shouldn't interfere with or have an effect on the functioning of the control signals in the grid, which are often utilised by energy providers. The input terminal resistance should be properly adjusted to the solar generator's real operating characteristics, such as via "Maximum Power Point Tracking" (MPPT). Low (3%) input voltage fluctuations are necessary to enable solar generator operating near to its Maximum-Power-Point (for example, at 100 Hz induced by a single phase injector device). Overvoltage shouldn't result in faults, such as when a solar generator operates at low temperatures close to open circuit circumstances.

By changing the PV generator's point of operation towards open circuit voltage, the input power is restricted for overload circumstances to a specific amount. This may occur if the inverter's nominal power is less than the nominal power coming from the PV generator. At extremely high irradiance, such an uncommon event results in an input overflow of the grid injector. To prevent grid use, the grid inverter should be powered by the solar generator (e.g., at nighttime). The inverter should start operating as soon as there is low irradiance and should run steadily. At irradiance levels of 50 W/m2, modern PV systems are already injecting electricity into the grid, and up to this point, 10% of the nominal inverter power has allowed for efficiency of 90%.

Terminals at the input and output should be shielded against transient overvoltages (such as surges brought on by lightning strikes). This is mostly accomplished via the use of overvoltage or surge arrester devices. The "electromagnetic compatibility" (EMC) rules, such as EN 55014, must be followed. The devices' noise emissions should be minimal to enable use within occupied buildings.

The utilities are also concerned about the quality of electricity coming from a PV system into the utility grid. If the inverter output contains an excessive amount of harmonics, they may interfere with loads at other sites (which may need sinusoidal power) or with utility equipment (e.g., for data transmission over the transmission line). Electrical equipment that uses a lot of harmonic distortion in the power supply, such as motors, heats up and experiences vibrations that shorten the bearing lives. The limitations for harmonics are established by rules in IEEE 929 and IEEE 519, as stated in Table 14.1. Limitations for harmonic distortion for grid-connected PV systems are shown in Tables.

Table 14.1: *Illustrates* the limitations for harmonics are established by rules in IEEE 929 and IEEE 519.

Oddharmonics	Distortionlimitation
3^{rd}through9^{th}	4.0%
11^{th}through15^{th}	2.0%

17ththrough21st	1.5%
23rdthrough 33rd	0.6%
above33rd	0.3%

Voltage disturbances: The voltage at the inverter's output shouldn't be more than 5% greater than the voltage at the utility connection point. As a result, the inverter should detect anomalies in the grid's voltage and turn the inverter off as necessary. If the utility voltage either falls below 50% of its nominal value or rises over 110% of its nominal value, disconnection should take place within 10 cycles. The utility line voltage should switch off the inverter within two seconds if it is between 50% and 92% of its nominal value. Disturbances in frequency: In 60 Hz systems, the inverter should be unplugged if the line frequency drops below 59.5 Hz or rises over 60.5 Hz.

Power elements the power factor, which is brought on by a phase change in the voltage and current, shouldn't be less than 0.85. DC current injection into the AC grid: DC current cannot exceed 0.5% of the rated inverter output current. Additionally, that standard presupposes rules for islanding protection, reconnecting after grid failure and restoration, grounding surge protection, and DC and AC disconnecting. There are sometimes other standards set out by the neighbourhood energy providers. The Annex contains a list of additional international and European rules. An example of a single phase PV injection system's usual setup (with a maximum-power-point-tracker and an energy counter).

Various inverter types

Commutated external inverters

The "commutation-voltage" required by external commutated inverters during the commutation period must be provided by an external AC voltage source (which is not a component of the inverter). This AC voltage is provided by the grid to inverters that are controlled by it. "Natural commutation" is used to run externally controlled inverters. One of its key characteristics is that, following ignition, a "current rectifier valve" with a greater voltage potential takes over the current from a previous rectifier valve. For high power applications, the externally commutated, grid-controlled inverter is often utilised. Self-commuted inverters are cutting edge for low power applications (1 MW), which are most typical for PV power supply systems.

Inverters that self-commutate

Self-commutated inverters may commutate without an external source of AC power. The energy storage that is a component of the inverter (often by a "delete" capacity) or a rise in resistance of the current rectifier valve that will be turned off provide the commutation voltage, respectively (e.g., a MOS-FET power transistor or an IGBT). Self-commutated inverters are intended for all types of electrical energy conversion for energy flows in either direction or both directions. Today, only self-commutated inverters are employed in the power range necessary for PV applications (1 MW).

Inverters using PWM

A pulse-inverter is a self-commutated inverter whose output voltage (or current, as the case may be) is pulse-controlled. Frequent on-and-off switching at the pulse frequency fp within this period increases the number of commutations per period at this sort of inverter, which may be utilised to minimise harmonics of current and voltage since it is comparable to an

increment of pulse numbers. Grid-controlled inverters can only increase their pulse counts by appropriately boosting their inverter rectification bracing. Figure 14.4 *Illustrates* how a single phase bridge circuit couples a DC voltage source (PV generator) with an AC voltage source using a pulse inverter.

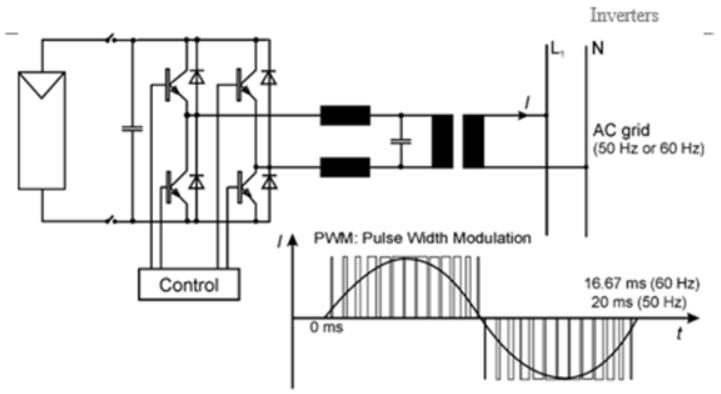

Figure 14.4: the Schemeofcircuitofasinglephasesinusinverterbasedonpulsewidthmodulationforphotovoltaicgridinjection.

The inductances on the AC side determine the current's harmonics. In order to comply with the utilities' requirements for grid-feeding (EN 60 555), a certain minimum inductance should be maintained. The low pass filter and isolation transformer on the inverter in Fig. 3.3 Supplementary remove all harmonics up to the order of n-1, where n is the number of pulses in each cycle of the AC current. The switching losses in power electronic equipment are enhanced with high switching frequencies. The cost of the low pass filter rises with low switching frequencies. The DC from the PV generator is overlaid by a sinusoidal current with double the grid frequency, whilst the power entering the single-phase grid pulses with twice the frequency for the sinusoidal current.

Connection to the electrical grid

Grid voltages in electrical systems Voltage requirements for grid-feeding into public electrical networks (VDE/IEC guidelines, in square brackets: the actual practise in Europe) in Table 14.2:

Table 14.2: The Voltage requirements for grid-feeding into public electrical networks (VDE/IEC guidelines.

Lowvoltage:	230/400V	Supplyofsmallconsumersin households,agricultureandindustry
Mediumvoltage:	10kV[12kV]	Publicandindustrygridsystems
Highvoltage:	110kV[123kV] 220kV[245kV] 380kV[420kV]	Forcountrywidegridsystem dependingonspaceandcapacity

Veryhighvoltage:	756kV	Countrywidegridsystems, transmissionofhighpoweroverlargedistances

PV grid-feeding has only been used up to now in the low- and medium-voltage range.

Values at Electrical Grid Boundaries

The used inverters must meet the specifications set out by the utilities (mostly with regard to the maximum number of harmonics) and be able to resist any potential effects of the grid's overvoltage (surge) on the inverter.

For AC-grids intended for the connection of inverters, short- and long-term voltage tolerances are required. Additionally controlled is the bankable departure from the desired sinusoidal form. It is also necessary to take into account how the inverter's operation affects the grid voltage's form, particularly when the inverter is switching on and off. A variation of the root mean square of the AC voltage between 90% and 110% of the nominal grid voltage is allowed for the long-term grid voltage tolerance (according to VDE 160, part two and international norms). Along with long-term voltage variations, short-term, non-periodic overvoltages may also happen; the amount of these overvoltages depends on their temporal development. For discharged (released, unloaded) generators, their value may vary from 1.5 to 2 times the normal voltage to 10 to 100 times for statics. By using suitable surge-arresters at least in high- and medium-voltage grids, elevated surges must be kept to a maximum of 2.5 times the normal voltage.

Electricity Long-Distance Transportation

High voltage DC transmission (HVDC) is often preferable to AC transmission over stretches of more than 1,500 km. It also has the following advantages: Lower peak voltages allow for smaller insulators and safety distances, which reduces the environmental effect (landscape-aisles) for a given amount of transmitted power. Additionally, there are no issues with EMS (EMV) and reactance. Electrical energy technology has used HVDC technology for 25 years and may now be said to be mature. Transmission lines totaling 11,000 km are now in use, and 4,500 km more are being built.

For instance, an HVDC system of 1.2 MV (around 600 kV) has been used in Brazil since 1994 to transport electrical electricity totaling 6,300 MW across an 805-kilometer distance from the 12.6 GW hydroelectric facility Itaipu in Foz de Iguaçu to the So Paulo area (Ibiuna). The generator's output of 18 kV, 50 Hz, three phase AC is first changed to 525 kV and then rectified at the rectifier plant near Foz de Aegis. The HVDC is reversed at Ibiuna to the typical 60 Hz 15 before being eventually injected into the public electrical network of So Paulo, the second-largest city in the world, after being transported over a long distance via a 600 kV positive and a 600 kV negative line. In the IKARUS 16 project, an HVDC transmission line of 2 GW at 400 kV was described using the import of solar power to Germany as a reference. Using HVDC has the following extra benefits in this scenario: In addition to transport, nine of the eighteen 715 MW producing units convert their 50 Hz frequency to 60 Hz. Because the power plant is situated on the border between Paraguay and Brazil, which uses a 50 Hz public grid, half of the generators had to be constructed at a 50 Hz frequency for political reasons. However, Paraguay only consumes 2% of the energy produced, with Brazil using the remainder.

The HVDC transmission line connecting the terminal stations is 2,000 km long to link a PV power plant in Southern Spain to the customers in Germany. A length of 1,200 km of

transmission lines on the African continent were projected to reach places with very high solar irradiation for the link from Northern Africa to Germany. A 200 kilometre sea cable connects Tunisia and Sicily, while a final 1,900 km overland transmission carries the power to Germany. The link from Spain has an annual efficiency of 88%, whereas the connection from Africa has an efficiency of 84%. This indicates that the transport losses range from 12% to 16%, or 0.5% for transmission losses per 100 km and 1.5% for terminal station losses. The cost of the terminal stations is 84.4 €/kW, the cost of the overland transmission lines is 30,675 €/km, and the cost of the cable is 1.02 €/km. Therefore, the overall investment costs are somewhat less than 1.02 billion euros for the connection from southern Spain to Germany and 1.53 billion euros for the connection from Northern Africa, which represent just approximately 30% of the expenditures for the annual subsidy to carbon mining in Western Germany in Table 14.3.

Table 14.3: *Illustrates* the HVDCTransmissiontoCentralEuropefromdifferentlocations.

Location	SouthernSpain	NorthAfrica	Jamal	NEAfrica
Power (total)	2,000MW	2,000MW	26,500MW	72,414MW
Power (Net)	1,760MW	1,679MW	24,644MW	67,055MW
Voltage	400kV	400kV		
Current	2x2.5kA	2x2.5kA		
Trans mission line (overland)	2,000km	3,100km		
Trans mission line (seacable)	0km	200km	4,100km	5,100km
Efficiency Duringa year	88%	84%	93.1%	92.6%

The total cost of imported PV power distributed via the public grid in Germany with current technology ranges from 0.22 to 0.34 euros per kilowatt hour (kWh). These expenses are less than half of what local PV energy production would cost in Germany. Additional benefits of solar energy importation include: Although overall irradiance is larger, seasonal variations in irradiance have less of an impact than short-term fluctuations in electrical production caused by irradiance.

Storage

Electrical energy is often required at times other than those in which it is created. If connecting to the electrical grid is not an option, energy must be stored for use between production and consumption. In theory, a wide range of storage options are feasible:

Battery storage recently utilized for short-term storage, capacitors (expensive, self-discharge is rather high, e.g., "Gold-Caps®," "Ultra-Caps®") Inductors (small storage capacity, high voltage, virtually not utilised) (little storage capacity, high voltage, practically not used). Mechanical holding Kinetic power (flywheel, sometimes used for mid-size, short-term power storage) Powerful potential (water storage in high altitudes, e.g., mountain lakes, pumps in

combination with hydro-electrical power generation). Chemical holding Electrolysis (electrolysis of water to hydrogen and oxygen as storage medium, later burning or transformation into energy using fuel cells) (electrolysis of water to hydrogen and oxygen as storage medium, later burning or transformation into electricity by fuel cells) Alessandro Volta was the first person to realise that an electrical potential could be created electrochemically, which is where the word "voltage" comes from. Applying a voltage to the electrodes reverses this process ("charging"). The lead battery using sulphuric acid as an electrolyte is the most typical method of electrochemical storage for solar energy systems. Consequently, a more thorough discussion of this strategy will follow. The remaining procedures are less frequent, thus they are only addressed in general terms in Figure 14.5.

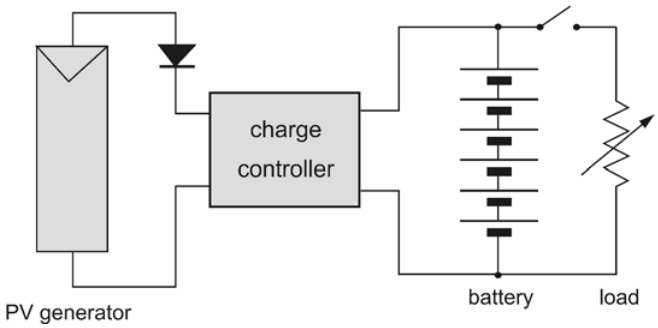

Figure 14.5: The SchemeofaPVsystemwithachemicalbatterystorage.

Acid Battery with Lead Sulfide

At least for large capacity needs, lead sulphide acid batteries, generally known as "lead-acid" batteries, were created in 1859 by French scientist Gaston Planté and are still the most widely used rechargeable batteries today. The energy-to-weight ratio is somewhat low when compared to other battery types, even if the energy-to-volume ratio is adequate. They have a large surge current capacity and are quite inexpensive. A series connection of battery cells may enhance each cell's nominal voltage of 2 V.

Principle

Two electrode plates, one made of pure lead and the other having a surface covered in lead oxide, are submerged in an electrolyte of diluted sulfuric acid (usually 37% H2SO4). Lead-acid batteries that have been discharged may freeze because during the process of discharging both electrodes transform into lead sulphate (PbSO4) and the electrolyte into water. Lead sulphate is transformed back into lead dioxide (PbO2 at the positive electrode) and sponge lead (Pb at the negative electrode) during charging, and sulphate ions (SO_2) are forced back into the electrolyte solution to create sulfuric acid (see equation of chemical reaction below).

$$PbO_2+Pb+2H_2SO_4-2PbSO_4+2H_2O$$

Gassing

When the battery is given more current than it can utilise, gassing happens. Gases such as hydrogen and oxygen are created by the surplus current. Gassing to some extent is typical, however severe gassing may be a sign of overcharging the batteries. Ample ventilation must be provided since the gases emitted are explosive if they come into contact with a spark or flame. Batteries often begin to gas about 80–90% of their full charge. To cease charging as soon as the battery begins to gas is a widespread misconception. If the charge is stopped at

the point of gassing in most batteries, which happens at 80% SOC, the battery will never achieve full charge. When the battery hits this position, the majority of better chargers reduce the current in order to avoid excessive gassing.

At sealed gel cells, gassing occurs: Gelled cells are substantially more sensitive to gassing than flooded batteries are. Large bubbles or "pockets" in the gel may form, which lowers battery capacity because they make poor contact with the plates. Additionally, the gel may become permanently dehydrated due to water loss, creating these pockets. To prevent over-gassing, gelled batteries are charged at 0.1 to 0.3 V less voltage than flooded batteries. Some product brochures and marketing claim that gelled cells have a "large" capacity for accepting a charge, however this is untrue since they can only handle around half to a quarter of the maximum current that flooded batteries can.

SG: Specific Gravity

The unit of measurement for electrolyte strength. The weight of the electrolyte is compared to water using specific gravity (SG; 1.000 kg/l). The majority of hydrometers come with a correction chart since SG fluctuates with temperature. At 25°C, a complete charge should be about 1.265, however this value varies with temperature. In sealed batteries, SG is impossible to measure. SG for pure acid is 1.835 kg/l. The SG of a completely depleted battery will be about 1.120 kg/l. As soon as water is introduced, SG should not be measured since the electrolyte must completely mix before the measurement is correct. An equalisation charge would significantly speed up the process, which may otherwise take hours or even days. There is no practical method to quantify the SG, which may be as high as 1.365 in certain AGM (absorption glass mat) batteries. If you purchase new batteries, you should completely charge them, balance them, and then measure their specific gravity (SG) for future reference. This is because not all manufacturers utilise the same SG, and SG may also vary depending on the location where a battery is purchased. A device called a hydrometer is used to measure the electrolyte in a battery's specific gravity. The majority of lead-acid batteries have a specific gravity of between 1.1 and 1.3 kg/l, with most fully charged batteries having a specific gravity of between 1.23 and 1.30 kg/l. Hydrometers are affordable and are available at any shop that sells auto accessories. There are batteries with stronger or weaker acid that were designed for usage in very hot or extremely cold areas. If so, the battery will often be labelled. A battery's energy effectiveness depends on its discharge current (see Figure 14.6). Avoid using high discharge currents since they reduce efficiency and reduce battery life.

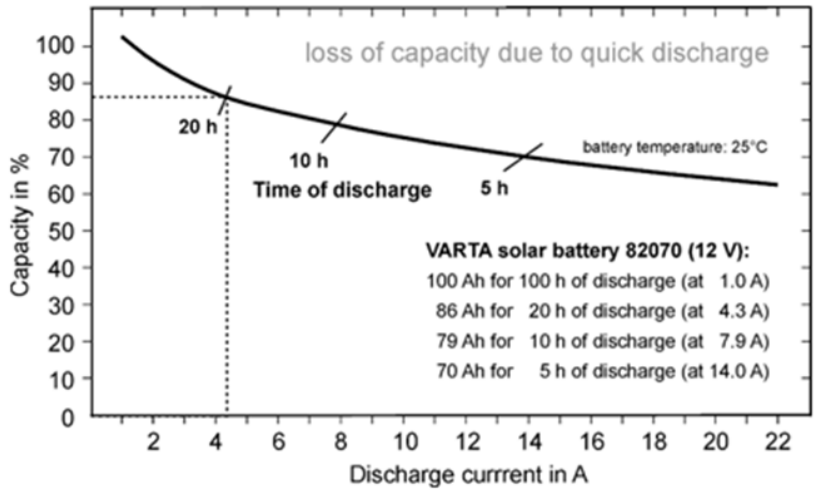

Figure 14.6: The Use able capacity as a function of discharge current for a12 V lead acid solar battery with a rated capacity of 100 Ah (for100 hrs of discharge).

Temperature of Operation

For every 10 K over 25°C, lead acid batteries' lives are lowered by 50%. Peak operating temperatures of the battery are lower than maximum ambient temperatures because of the battery's high heat capacity. In situations where the temperature fluctuates continuously by more than 5 K, temperature correction for the charging regime is necessary. It is advised that the temperature sensor for the battery's operating temperature be located at the positive pole and thermally shielded from the surrounding environment.

Self-Discharge

When a battery is in an open circuit, self-discharge happens, mostly because the electrodes and electrolyte are interacting. The negative electrode's lead changes into lead sulphide:

$$Pb+H_2SO_4 \Longrightarrow PbSO_4+H_2$$

$$At the positive electrode lead dioxide is reduced to lead sulfide also:$$

$$2PbO_2+2H_2SO_4 \Longrightarrow 2PbSO_4+2H_2O+O_2$$

$$Additionally a corrosion reaction with the grid of the positive electrode occurs and builds up a sulfatati on layer:$$

$$Pb+PbO_2+2H_2SO_4 \Longrightarrow 2PbSO_4+2H_2O$$

Gas evolution results from this self-discharge process, which also lowers the capacity of the sulphuric acid concentration. Figure 14.7 shows that when temperatures rise and there are more charging/discharging cycles, the rate of self-discharge accelerates. This is especially true for batteries with antimony-containing grids. When just enough current is given to offset the batteries self-discharge, the battery is said to be "floated" or operating at its float voltage. For a 12 V battery, this is normally between 14.2 and 14.5 volts.

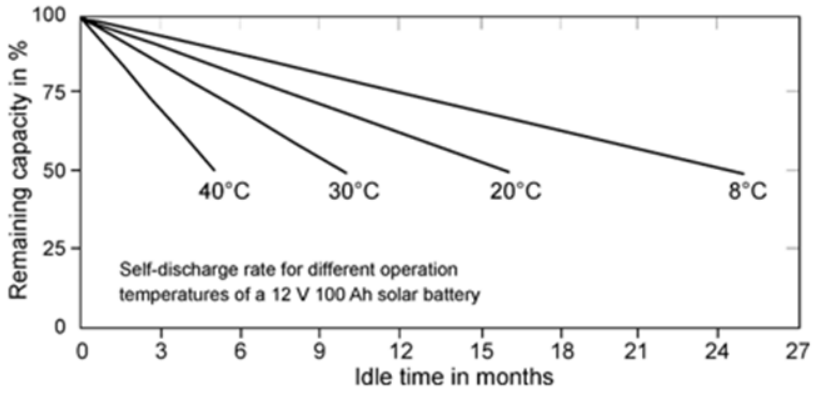

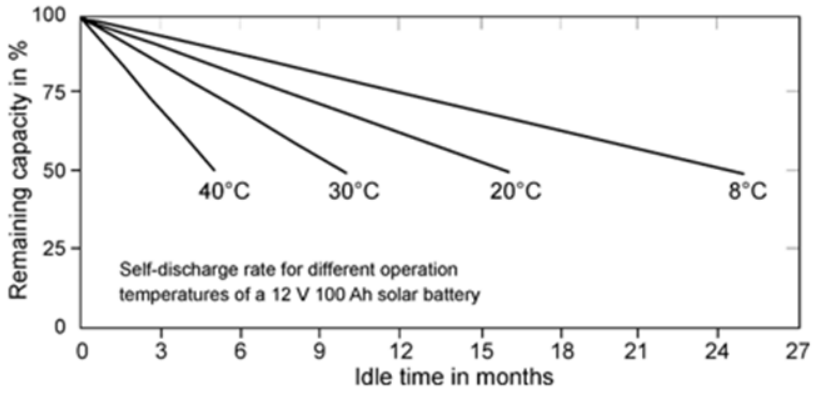

Figure 14.7: *Illustrates* the Relative self-discharge of a 12 V 100 Ah lead-acid solar battery as a function of idle time and operation temperature.

Deep Discharge

Lead acid batteries shouldn't be utilised to their maximum potential, unlike other battery types (such NiCd batteries) in Figure 14.8. The battery's lifespan in Figure decreases with increasing "depth of discharge" (DOD).

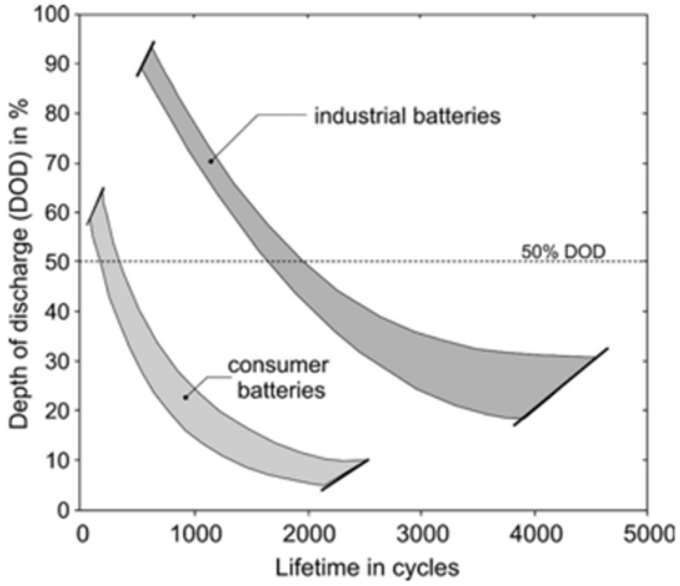

Figure 14.8: the Decreaseof useablelifetimefor different typesof lead-acidbatteriesasafunctionofincreasingdepthofdischarge(DOD).

This is because when DOD increases, the concentration of sulfuric acid decreases. $PbSO_4$ (the major discharge product) is extremely soluble in diluted H_2SO_4. The electrode sulphates, which results in short circuiting and severe corrosion. Batteries used for starting, lighting, and ignition (SLI- or automotive batteries) and industrial batteries are both allowed to drain down to 80% DOD in order to lessen these issues. It is, nonetheless, quite challenging to ascertain this final DOD. A set discharge voltage (cutoff voltage), which is roughly comparable to the critical DOD, is where the majority of modern solar controllers intervene to shut off the charge current. Only a few solar I-I chargers, like the German company Steca's "Solarix" solar controller, can account for the fact that the cutoff voltage is load-dependent.

If the critical DOD is reached, a diesel generator is turned on in big PV systems (hybrid PV-Diesel system). A backup system is not necessary for smaller battery units, however oversizing the battery may be an efficient technique to prevent severe drain. Large lead acid solar batteries are hard to come by and highly costly. For this reason, certain brand-new solar batteries are now being created, such as one built by the German company Akku Gesellschaft with a capacity of 260 Ah at 1.28 kg/l of sulfuric acid and a rated capacity of 240 Ah at 12 V. The lifespan of this battery is estimated to be between five and six years, or 800 cycles (50% DOD).

Sulfation

As a result of the lead-acid battery's discharge, massive $PbSO_4$ crystals grow, which is known as sulfation. Even while lead sulphate is produced in the materials of the plates during typical discharging, the phrase "big crystal" refers to the formation of a distinct type of lead sulphate that does not easily transform back into regular material when the battery is charged. When these big crystals are there, it is extremely hard to charge both electrodes. Sulfation often occurs as a consequence of acid stratification and crystallisation following discharge at low currents (i.e., self-discharge currents). The process also happens if a battery is kept too long in a drained state, if it is never completely charged, or if the electrolyte content has dropped excessively as a result of overcharging and/or significant water loss via evaporation. Sulfation is often remedied by charging slowly (at low current) and at a higher voltage than usual; typically, this is done at 2.4 to 2.5 V per cell at 0.5 to 8 A. (depending on battery size). In many instances, this will progressively eliminate the sulfation.

Charger Types

There is no battery that can fully satisfy all the features, however lead acid batteries are utilised for a wide range of applications, including long-term storage, short-term high current output applications, high energy efficiency, long lifespan, low weight, low maintenance, cheap cost, etc. The following list of product kinds on the market is not exhaustive. Although the materials and technology utilised primarily determine prices, other factors, like as manufacturing capacity, rivals, and the popularity of certain battery sizes, may also be considered.

Vehicle Batteries

For starting autos, SLI (starting, lighting, and ignition) batteries were developed. The battery is not intended for extensive cycling but rather for short duration, high power output. However, because to its affordability and accessibility, this kind is often employed for solar applications. The lifespan is not very long (one to four years). The DOD shouldn't be allowed to get over 50%. This battery type should be maintained under a trickle charge current or, alternatively, recharged every two months if it must be out of use for extended periods of time. If there is only access to solar energy, it is impossible to store seasonal energy using this kind of battery. The battery may be directly charged by the PV generator for 2 to 5 minutes twice a week for up to 2 minutes without a solar controller in order to prevent acid stratification and, therefore, salvation. Mechanically shaking the battery does not assist since there is insufficient room between the plates to facilitate remixing.

Agricultural Batteries

Industrial batteries are mostly utilised for cyclic applications, however they may also be used for stationary purposes. Tubular electrodes and thicker flat plates may be used to achieve this. To prevent mass shedding, the active mass of the tubular version is equipped with a plastic

shield. Due to its low specific kWh costs, the tubular form is commonly used in solar applications.

Batteries solar

By enhancing their cycle behaviour, these unique kinds are created from both the SLI battery and the industrial battery. Since the underlying technology is quite affordable, many battery firms choose to use modified SLI batteries. By using thicker electrodes, using electrodes enclosed in special pocket separators to prevent short circuits, shedding the active mass, using an excess of electrolyte to lessen the drop in acid concentration during discharge, and using grids made of low-antimony or antimony-free alloys to lessen gassing and self-discharge, the main drawbacks of the typical SLI battery can be reduced.

REFERENCES

[1] W. Zhang *et al.*, "Evaluation of the photovoltaic potential in built environment using spatial data captured by unmanned aerial vehicles", *Energy Sci. Eng.*, 2019, doi: 10.1002/ese3.408.

[2] S. Mahmoudi, N. Huda, en M. Behnia, "Photovoltaic waste assessment: Forecasting and screening of emerging waste in Australia", *Resour. Conserv. Recycl.*, 2019, doi: 10.1016/j.resconrec.2019.03.039.

[3] V. Gupta, M. Sharma, R. K. Pachauri, en K. N. Dinesh Babu, "Comprehensive review on effect of dust on solar photovoltaic system and mitigation techniques", *Solar Energy*. 2019. doi: 10.1016/j.solener.2019.08.079.

[4] S. Mishra, H. Ziar, O. Isabella, en M. Zeman, "Selection Map for PV Module Installation Based on Shading Tolerability and Temperature Coefficient", *IEEE J. Photovoltaics*, 2019, doi: 10.1109/JPHOTOV.2019.2900695.

[5] C. Xu, B. Li, X. Yuan, C. Liu, en C. Shen, "Recycling of waste crystalline silicon photovoltaic modules", *Chinese J. Environ. Eng.*, 2019, doi: 10.12030/j.cjee.201901113.

[6] J. M. Paredes-Parra, A. J. García-Sánchez, A. Mateo-Aroca, en Á. Molina-García, "An alternative internet-of-things solution based on LOra for PV power plants: Data monitoring and management", *Energies*, 2019, doi: 10.3390/en12050881.

[7] M. Dhimish, P. Mather, V. Holmes, en M. Sibley, "CDF modelling for the optimum tilt and azimuth angle for PV installations: Case study based on 26 different locations in region of the Yorkshire UK", *IET Renew. Power Gener.*, 2019, doi: 10.1049/iet-rpg.2018.5301.

[8] A. Ajitha *et al.*, "Underwater performance of thin-film photovoltaic module immersed in shallow and deep waters along with possible applications", *Results Phys.*, 2019, doi: 10.1016/j.rinp.2019.102768.

[9] M. Kumar en A. Kumar, "Experimental validation of performance and degradation study of canal-top photovoltaic system", *Appl. Energy*, 2019, doi: 10.1016/j.apenergy.2019.03.168.

[10] K. Ilse *et al.*, "Techno-Economic Assessment of Soiling Losses and Mitigation Strategies for Solar Power Generation", *Joule*. 2019. doi: 10.1016/j.joule.2019.08.019.

CHAPTER 15

VARIATIONS OF INDUSTRIAL BATTERIES

Mr. Harsh Shrivastava, Assistant Professor,
Department of Electrical Engineering, Jaipur National University, Jaipur India
Email Id- ershrivastava@jnujaipur.ac.in

The fundamental structure of upgraded industrial batteries remains the same, but the electrolyte volume and lead percentage of the grid alloy alter. To prevent acid stratification, these batteries are equipped with an automated water-refilling system and/or an air pump in big installations in Figure 15.1

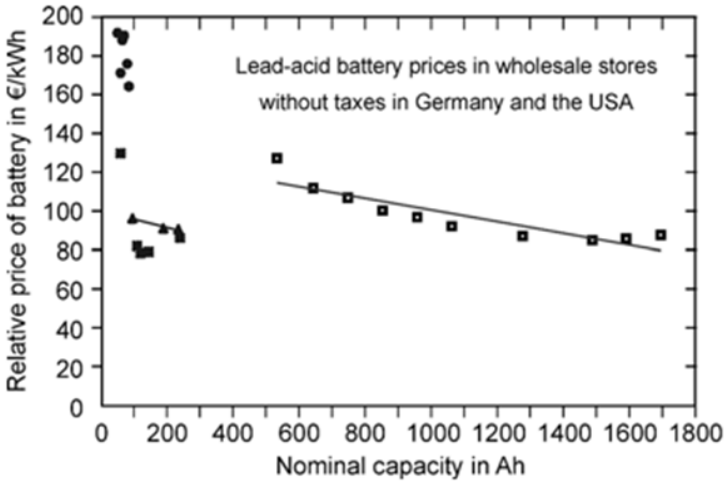

Figure 15.1: ***Illustrates*** **the Relativepricesoflead-acidbatteriesasafunctionofnominalstoragecapacity(ISET)**

VRLA(“Maintenance-Free”)Batteries

Batteries that have been overcharged emit hydrogen and oxygen while also losing water as a result. In open batteries, this loss must sometimes be compensated up by adding fresh distilled water to the battery. When used correctly, sealed units reduce this loss, which is why they are sometimes referred to as "maintenance-free" batteries or VRLA (Valve Regulated Lead-Acid) batteries. Since water cannot be added to these devices, if they are overcharged, a valve will allow the battery to vent, which results in a permanent loss of capacity.In an effort to lessen this impact, recovering Transported to the negative electrode, where it is reduced back to water, the oxygen produced at the positive electrode. Through gas holes created in silica or glass fibre employed to trap the acid, oxygen is transported through sulfuric acid. The amount of immobilised electrolyte means that the acid stratification and sulphation are reduced. Although they weren't intended specifically for solar applications, VRLA batteries may be utilised in this way. A well cared for open battery, however, lasts longer than a VRLA battery[1], [2].

Alternative Batteries

Nickel-Cadmium Batteries

Nickel-cadmium batteries may work well for standalone PV systems and are often used as rechargeable batteries for home appliances. Compared to lead-acid batteries, they offer a

variety of benefits:

They are more durable, operate better in low temperatures, have low internal resistance that allows for large currents, and have a greater energy density than lead-acid batteries. They can also be charged and discharged at a considerably faster rate (up to 30 minutes) They are minimal maintenance and maintain a very consistent voltage during discharge, however they also have several drawbacks: They are often twice as costly, have poorer energy efficiency (75%) and, in contrast to lead acid batteries, will lose capacity if the battery is not regularly fully drained and utilised to its DOD (so-called "memory effect"). Because cadmium is a toxic substance, it's essential to recycle the battery when it has served its purpose[3], [4].

Batteries made with nickel hydride

These batteries resemble nickel-cadmium batteries, except instead of using a cadmium electrode, they use a metal hydride electrode. This offers the following notable benefits: In comparison to nickel cadmium cells, they feature a 50% greater specific capacity, an electrode material that is far less dangerous, and a lower memory effect. Previously, these cells had a high rate of self-discharge, but new manufacturing techniques have mitigated this issue. This kind of battery may eventually replace the nickel cadmium battery due to its tremendous benefits.

Battery Types: Lithium-Ion

Although these batteries are relatively pricey, they provide the following significant benefits:

Low self-discharge rates of 2-4%/month between 25°C and 60°C, High energy density, High efficiency (energy efficiency 95% at room temperature up to 60°C, Even at -10°C energy efficiency stays 90%),

Even at very low temperatures, function.

Integrated control circuits in the battery casings are able to regulate how sensitive Lithium-Ion batteries are to under- and over-voltage.

Battery Types: Nickel-Iron

Anodes made of steel wool substrates with active iron material and cathodes made of nickel-plated steel wool substrates with active nickel material are used in alkaline-type electric cells, together with potassium hydroxide as the electrolyte. The first "Edison Cell" was this.

Low expenses and much extended lifespan are benefits (3,000 cycles).Low energy efficiency (usually 55%), very high self-discharge rates (usually 40%/month), high water consumption, a small temperature range (0 to 40°C), a high specific weight/volume, and a high internal resistance are all disadvantages.A series connection of battery cells results in a significant voltage drop due to high internal resistance. Additionally, it implies that compared to other batteries, the output voltage changes much more with load and charge.

This voltage fluctuation has to be supported by the power conditioning components. When connected directly to the battery, several typical DC equipment (like a refrigerator) must also withstand similar voltage fluctuations without being damaged. The substantial losses while charging and discharging will increase the size of the solar panels you require by an additional 25–40% for the same amount of energy use[5], [6].

Fuel cells: Basics

In theory, a hydrogen-oxygen fuel cell is just reversing electrolysis; given enough hydrogen and oxygen, the fuel cell will generate energy. Two electrodes are sandwiched around an electrolyte in a fuel cell. Electricity, water, and heat are produced when oxygen flows over one electrode and hydrogen flows over the other. The fuel cell's anode receives hydrogen fuel. Through the cathode, oxygen (or air) enters the fuel cell. The hydrogen atom divides into a proton and an electron, which travel in separate directions to the cathode with the aid of a catalyst. The electrolyte is traversed by the proton. Before returning to the cathode to join the hydrogen and oxygen in a water molecule, the electrons generate a distinct current that may be used. Any hydrocarbon fuel, including gasoline, methanol, and natural gas, may provide hydrogen for a fuel cell system using a "fuel reformer." Emissions from this kind of system would still be far lower than emissions from the cleanest fuel combustion processes since the fuel cell depends on chemistry rather than combustion[5], [6].

Many fuel cell types

Acid Phosphoric

This kind of fuel cell is the most advanced in terms of commerce. Hospitals, nursing homes, hotels, commercial buildings, schools, utility power plants, and airport terminals are just a few of the varied areas where it is already in use. Phosphoric acid fuel cells have an energy production efficiency of over 40%, and if the steam produced by this specific fuel cell is utilised for co-generation, it achieves a roughly 85% efficiency, as opposed to 30% for the most efficient internal combustion engine. The typical operating temperature is 204°C. Larger vehicles like buses and trains may also utilise these fuel cells.

Membrane for proton exchange (PEM)

These cells are suitable for applications, such as in vehicles, where rapid starting is needed since they run at relatively low temperatures (around 93°C), have a high power density, and can quickly change their output to match fluctuations in power demand. They are the best prospects for light-duty cars, buildings, and maybe even smaller applications like the replacement of rechargeable batteries in video cameras, according to the U.S. Department of Energy.

Burning carbonate

High fuel-to-electricity efficiency and the flexibility to use coal-based fuels are promised by molten carbonate fuel cells. At roughly 649 °C, this cell is in operation. Demonstration units are getting ready for testing in California in 1996 after the first full-scale molten carbonate stacks have been tested.

Strong Oxide

The solid oxide fuel cell is another very promising fuel cell that might be employed in huge, high-power applications, such as industrial and massive central energy producing plants. Some researchers anticipate using solid oxide in automobiles. In Europe, a 100 kW test is getting ready. In Japan, there are already two 25 kW small units online.

The typical hard ceramic material used in a solid oxide system, which allows operating temperatures to exceed 1,000°C, replaces the liquid electrolyte. The efficiency of producing electricity might approach 60%. A solid oxide fuel cell design employs a collection of meters-long tubes. A compressed disc that resembles the top of a soup can is one of the additional possibilities[7], [8].

Alkaline

These cells have been around for a while on space missions and can generate electricity at up to 70% efficiency. The electrolyte is alkaline potassium hydroxide. They were previously too expensive for commercial use, but now a number of businesses are looking at methods to save expenses and increase operating flexibility.

Various Fuel Cells

The fuel cell family includes the relatively new direct methanol fuel cells (DMFC). These cells are similar to PEM cells in that their electrolyte is a polymer membrane. However, the DMFC does not need a fuel reformer since the anode catalyst itself pulls the hydrogen from the liquid methanol. With this kind of fuel cell, which normally operates at a temperature between 48.9°C and 87.8°C, efficiency levels of approximately 40% are anticipated. Higher temperatures result in greater efficiency.

Generate Your Own Fuel Cells

Regenerative fuel cells, a still-young member of the fuel cell family, might be appealing as a closed-loop method of power production. A solar-powered electrolyzer separates water into hydrogen and oxygen. The fuel cell, which produces electricity, heat, and water, is supplied with hydrogen and oxygen. The procedure then restarts with the water being cycled back to the solar-powered electrolyzer.

Solar Power in the Tropics

The greatest "natural" markets for PV are off-grid applications inside the current "sunbelt" around the equator, even though the majority of PV capacity is being installed grid-connected in mild temperatures owing to advantageous laws in several nations there. The fundamental components of a typical PV system for off-grid applications are quite straightforward: a PV generator (consisting of a number of PV modules), energy storage (most often a lead-acid battery), and power conditioning equipment (grid connection only plays a small part in the tropics) (consisting of a charge regulator and, optionally, an inverter). Around a million of these systems have been deployed globally in total. However, countless failures have been observed in reality; many of them are not technical in character. This chapter emphasises key crucial factors and best-practice examples of how to establish a dependable, efficient, long-lasting, and cost-effective PV power supply based on 10 years of real-world experience in Brazil. Even at large-scale rural electrification schemes, it seems that many system plans and installs in the past did not take certain suggestions into account[9], [10].

Issues with Installation Before

Additional Planning Considerations

Calculating the Required Load

While the cost of a PV installation rises approximately in proportion to the amount of power used, customers often underestimate design loads during the planning stage in an effort to save expenses, leading to a sub-dimensioned and unstable system. The most effective approach is to track power and energy use over time. An analysis of consumption frequently reveals that it is significantly less expensive to replace older, high-energy-consumption devices with new, energy-efficient ones (such as light bulbs, refrigerators, and freezers) than to size the PV generator and the batteries in accordance with the energy requirements of the old devices.

Project development dynamics and time constraints

Years may pass between project conceptualization, planning, finance, purchasing, and shipping before "turn-key" installation (considering bureaucracy for project legislation, import taxation and liberation). Importation is sometimes quite time-consuming, hence it is recommended to employ expensive external services provided by so-called "despachos." There have been reports of waiting durations between one and one and a half years, so equipment may "disappear" and packaging may deteriorate.

The project's side conditions could have changed throughout the entire process, including the relocation of the people to whom the power plant was assigned, the installation of electrical grid lines, the purchase of diesel generating units, and even the flooding or conversion of the site where the installation would take place.Rarely does simple planning from beginning result in a turnkey energy supply system; instead, the design often has to be reevaluated and materially altered. Continuous preparedness, monitoring, and control are necessary to achieve this.

Financing

The work of procuring project support packages is crucial yet time-consuming. Such aids frequently come with a lot of restrictions, including short installation times, the requirement to use national equipment (like batteries), collaboration with local businesses and utilities, long-term grid power guarantees, certification by government municipalities, and intense bidding competition. Although financial compensation is provided in local currency and is subject to local interest rates, there are risks that must be considered, such as exchange rate fluctuations. Because wages, rent, and raw materials are paid in local currency, a localised component manufacturing or assembly line might lower these risks. In most circumstances, this strategy will avoid excessive import tariffs.

Importation

Equipment and material import is a challenging and time-consuming issue: Import tariffs may be steep and have a significant financial effect in order to shield certain local industries from competing with imported items that are less expensive (import taxes may double the price of some goods, principally electronics). Authorities frequently exempt goods of strategic interest, such as renewable energy technology, from high taxation, but this requires knowledge, extensive paperwork, and the declared goods have to precisely fit into the exemption categories. Authorities are aware that these regulations are not economically sustainable and may eventually paralyse a country's economy. Recommended phrases: Ensure that each part of your system is well explained (in the native tongue!).

Along with correct records of the equipment, the project partners' backgrounds must also be carefully recorded (e.g., a company's establishment certificate, evidence of their financial and technical competence). Units indicated in the paperwork (per piece, per volume, per kilogramme, British/American/local measurements) and currencies and their conversion rates, as well as which one is to be used (for example, Brazil has six distinct official exchange rates for R$ vs. US$), are crucial issues. Sub-components, such as general electronics, processing units, memory, transformers, terminals, instruments, displays, and PV units, may need to be separated into independent sections with various import tax rates and certification requirements. Often, importation is taxed on the whole transaction, including freight charges, rather than just the value of the imported items.

Language Issues

Within Administrative Phases

Applications for funds and credit, certification documents, and importation paperwork all demand a thorough understanding of the local tongue. Particularly legal and technical terminology may be challenging. Even among speakers of the "same" language, terminology might vary. (For instance, Portuguese from Portugal vs Portuguese from Brazil or British/American/Indian/African English). When it comes to the "proper" usage of their phrases and when it comes to their position, authorities and officials are often highly sensitive. If they are upset, they may purposefully slow down procedures. On the other hand, if you persistently inquire (in a kind way) about the real project status, they won't bother (a situation where usually European officials would become annoyed). The best approach is to "involve" the authorities in your project, i.e., highlight the significance of the initiative for their nation so they feel happy to be a part of it.

In the Installation Location

Aside from inherent language hurdles, those who work remotely sometimes lack a basic understanding of technical vocabulary. Even though interactive training takes a lot of time, it is necessary. It's crucial to employ training materials that are adequately illustrated. Illiteracy is pervasive (often worse than official statistics suggest), particularly in rural areas where young workers are required. You shouldn't count on running across somebody who speaks a foreign tongue there.

Mounting technical issues

The use of the finest materials on hand is necessary due to the harsh climatic conditions, which include high temperatures, high humidity, high irradiance, strong winds (in regions near the sea associated with salty air), and limited accessibility for repair. Frequently, stainless steel parts must be imported since they are not readily accessible locally.

Affixing PV Modules

In order to prevent becoming loose and discourage theft, mounting and securing should ideally be done using rivets rather than screws. Additionally, it could be difficult to get stainless steel screws and they might even be stolen (see below).

The PV generator's wiring

Since local electricians (outside of those who work on cars) seldom use high current, low voltage DC wiring, it might be challenging to find flexible UV-resistant wires with the right diameter and colour. The same is true for terminals, switches, and fuses. These components often have to be imported since they cannot be found locally.

Theft Avoidance

In tropical regions, notably in Africa, PV panel theft is becoming an increasingly important problem. To make it easier to identify PV panels that have been stolen, South African Telecom made the decision to only purchase orange PV modules. To prevent theft, components may be attached using rivets rather than screws (see above). Even minor parts, including instruments, terminals, plugs, cables, or even water tabs, are often targets of theft since they have such high value to the impoverished. To prevent this problem, a community adaption of the system and the designation of a responsible local person in charge are most beneficial.

Considerations for Safety

Batteries should be kept in a secure position, away from the living area, in addition to safe installation with isolation of terminals and wiring. Serious mishaps might be caused by metallic items that have been left on the battery contacts.

PV Generator Non-MPP Operation

Due to the usual I-V properties of solar cells and PV modules, electrical power production declines essentially linearly when operating voltages are decreased when the load curve intersects the PV generator's I-V curve on the "left" side of the Maximum-Power-Point (MPP). On the other hand, power decreases exponentially as operating voltages increase when the load curve cuts the I-V producing curve on the "right" side of the MPP. The latter happens when the generator's voltage is decreased, such as when operating single- or multi-crystalline silicon solar cells at high temperatures (these solar cells generally have a voltage-temperature coefficient of -0.4%/K to -0.5%/K). It is therefore advised to either purchase charge controllers with an integrated step-up DC-DC converter and an MPP tracker to enable full battery charge even when a generator's voltage levels are reduced, or to purchase PV modules that contain a greater number of solar cells connected in series to increase the generator's voltage level. Unfortunately, such equipment is not offered by the industry as a regular item.

Energy Reserves

Charger Types

Despite the fact that there are many distinct battery kinds, lead-acid batteries have the greatest cost-benefit ratio. There are three types of lead-acid batteries available: traditional ("open" - enabling replenishment of lost water), "maintenance free" (surplus of electrolyte, decreased gassing), and "sealed gel" (absorbed electrolyte). Maintenance-free batteries are favoured since maintenance procedures are often subpar or water replenishment is done with polluted water. In hotter areas, fully sealed batteries are less durable and have shown shorter lifetimes compared to maintenance-free batteries, particularly when charge-control is not adequately implemented.

Voltage Nominal Level

Solar batteries are often only available in 12 V blocks in tropical nations since they are made from automobile or truck batteries. The batteries must be paralleled in order to increase storage capacity at a given voltage since the most storage capacity that can be found in Brazil is 220 Ah. Inconsistencies in electrical properties like internal resistance are likely to happen as a result of tolerances in the battery manufacturing process (such as at the electrode plate treatment or within a battery's acid concentration). In this scenario, paralleled batteries will experience high internal currents, which will diminish their capacity for storage and shorten the battery bank's lifespan. Even with more costly, large capacity batteries, we saw considerable voltage discrepancies. This impact might be brought on by subpar manufacturing techniques and a lack of quality control, potentially as a result of the limited volume of high capacity batteries produced. On the installation site, test procedures are often challenging to carry out. Non-homogeneous storage conditions may also create issues with batteries. For instance, exposure to heat (such as from sunshine) can increase internal currents and harm batteries. Because battery import tariffs are often too costly, using domestic goods with greater voltage levels is typically the only option, which eliminates the requirement for battery paralleling. For every 1.3 kWh of storage needed, a 12 V, 220 Ah battery must have

its voltage level raised by 12 V using a 50% maximum depth of discharge. Additional safety problems must be addressed for voltages exceeding 50 V. During a PV system's lifespan, conventional lead-acid batteries need to be replaced roughly four times. A replacement plan must be devised in order to have the resources for both the financial purchase of a new battery and the labour to replace it. Old batteries may be sold to certain refurbishment businesses for a pittance, but these businesses are often situated outside of the major cities and only work with automobile batteries.

Devices for Power Conditioning

Local equipment may have a cos f as low as 0.6, but most electrical gear utilised as a load in industrialised nations has a cos p between 0.9 and 1. As a result, inverters must be able to manage such inductive loads. Additionally, friction losses have a tendency to be larger, which raises the inverter's beginning currents.

Changing Devices

MOSFETs power a large number of inverters. MOSFETs can be easily paralleled because of the positive temperature coefficient of their on-resistance, but when the device operates at high temperatures, this could create a vicious cycle. High temperatures increase the internal on-resistance and cause more heat to be dissipated, which heats up other paralleled MOSFETs mounted on the same heat-dissipating device.Ventilation many inverters employ temperature-controlled fans to provide forced ventilation. On-demand fans sometimes fail to start because they are blocked by leaves or bug remnants. To prevent that, "cool" operation is advised, utilising oversized switching devices with low on-resistances and high current reserves that just need natural ventilation. Thermal plan must be created for operating temperatures of 70°C and beyond since it must be taken into account that the ambient air temperature within a container might easily surpass 60°C. The typical maximum operating temperature for power conditioning equipment is 55°C, which reduces lifespan and increases failure rates (e.g. capacitor de-lamination, display degradation, terminal melting and eventually short-circuiting).

Charge-Controllers

At high operating temperatures, non-temperature-controlled charge controllers may result in excessive gassing. As a result, electrolyte is lost and has to be supplied. The capacity and longevity of "maintenance-free" and sealed batteries will be decreased since this is not achievable.

Operations and Upkeep

Pollution and system component deterioration

Bird droppings, seeds, pollen, leaves, branches, dust, and dirt spots may build on the PV panel and cause considerable performance losses, even though the fauna and flora are often more abundant in topical places. Typically, the solar cells within a PV module are wired in series, causing the output current of the circuit to be dominated by the cell that receives the greatest shade. If bypass diodes are not used correctly, "hot spots" may result in long-term cell damage. The self-cleaning effect requires a sufficient inclination angle of the panel, yet in tropical climates, the PV-panel is set almost horizontally to catch the greatest irradiance, thus restricting self-cleaning. Birds, mice, rats, snakes, spiders, cockroaches, termites, anion, scorpions, frogs, lizards, and bats may live in battery and power conditioning equipment shelters, which can quickly corrode wires, terminals, and relays (Fig. 1.5). Additionally, the psychological impact must be considered: if the area is unclean and smells bad, maintenance

activities will not be undertaken.

Recommendations: The hut should have sufficient ventilation on one side to maintain a manageable temperature and enable battery gases to escape, while on the other hand, the invasion of insects and animals should be avoided (e.g. grids, solid nets). Remain neat and orderly.

Monitoring Local people may struggle to recognise and describe the status of the system (or feel scared to do so) and are scarcely able to take the necessary steps. Thus, it is crucial to educate local staff members and enhance their ability. Long-term supply of replacement parts and sufficient tools are also important, as are enough, simple-to-read instruments and logical, simple-to-explain, fail-save switches with optical and/or auditory feedback - preferably inside a flow diagram of the system. This requirement also serves to deter theft and damage by requiring the nomination and payment of a local responsible person to oversee the plant (see above). To spot issues or start preventive maintenance, a remote monitoring system (by cellular phone line or through satellite) might be quite beneficial.

The manufacture of solar cells

The following considerations are concentrated on silicon solar cells as they constitute the foundation of the majority of terrestrial PV applications. Since silicon is the second most common element in the crust of the Earth, its supply is almost limitless. Cells made of silicon have an extremely long lifespan (more than 25 years), because to their solid crystalline structure. The Sun's spectrum can be converted to electrical energy quite successfully thanks to silicon's wide band gap. The disposal of silicon is straightforward and comparable to that of glass. The key difficulty in manufacturing is the purifying process, which must provide silicon that is extremely pure to enable effective solar cells while using the least amount of energy feasible.

The manufacture of technical silicon (MG-Si)

For the needs of the aluminium and steel industries, metallurgical silicon (MG-Si), also known as technical silicon, is manufactured on a massive scale. Global production amounts to one million metric tonnes annually. Carbon reduces the raw material silicon oxide (SiO2), which is present in quartz or sand, to silicon while exhaling CO or CO2. In order to create silicon, carbon (in the form of a blend of wood chips, coke, and coal) reduces silicon in huge arc furnaces. Periodically, the 1,500°C liquid silicon is poured out of the furnace (with a purity of 98–99%) and further purified (up to 99.5%) by being blasted with oxygen or oxygen/chlorine combinations. It is then poured into small troughs, where it is allowed to solidify before being broken into pieces. A typical furnace has a production rate of one tonne of MG-Si per hour. The electrical power consumption might be lowered to 13 kWh/kg by using a unique feeding technique (mixing quartz and sand briquettes). By 1.6 kWh/kg, transportation, feed mixture manufacturing, feeding, and grinding are taken into account. When it comes to energy usage, the primary combustibles utilised to make sand briquettes are coke and coal. Emissions account for more than 50% of all energy losses. This presents a big chance for savings but also carries a significant risk on the technical and financial fronts, thus it has not yet been taken into consideration.

Silicon of Metallurgical Grade (MG-Si) to Polysilicon of Semiconductor Grade (EG-Si)

Silicon must be considerably purer than metallurgical grade silicon in order to be used in solar cells and other semiconductor devices. The "Siemens C-process" is the commonly used purification method. The metallurgical silicon is fluidized in a reactor at 300°C to 400°C with

HCl in the presence of a Cu catalyst after grinding (grain size 0.5 mm), producing $SiHCl_3$ and H_2. A condenser is used to process the gases. Trichlorosilane $(SiHCl)_3$ is created from the resultant liquid by successive fractional distillations. In a reactor, the $SiHCl_3$ is reduced by hydrogen to extract the pure silicon, which then deposits on electrically heated silicon rods at 1,000°C in the form of a fine-grained polycrystalline structure. The last phase used to have a poor yield, and it also consumes a lot of energy.In complex chemical manufacturing facilities, semiconductor-grade silicon is produced on a big scale (about 3,000 metric tons/a), therefore it must be taken into account in an energy and material relationship with the plant's whole product line. For instance, it is necessary to take into account the utilisation of waste tetrachlorsilane ($SiCl_4$), which lowers the quantity of trichlorsilane ($SiHCl_3$). The manufacturing plant's vapour pipe grid receives heat from the reactors during the cooling phases, which is then utilised to produce other goods. As a result, there is a fuel substitution that results in a 29.8 kWh/kg energy advantage for combustibles. The method uses 114.3 kWh of electricity per kilogramme. Despite the fact that the procedure still has room for technological and energetic development, big advancements are not anticipated given the current state of the economy.

Single-Crystalline Silicon Production

Silicon must not only be very pure but also exist as a single crystal with no structural flaws in the semiconductor devices sector. The 'Czochralski' technique is the main way that such material is produced commercially. In a crucible, molten semiconductor-grade silicon is combined with minute amounts of a dopant. Boron is a common p-type dopant used in solar cells. By gradually drawing a seed crystal from a silicon melt, a huge cylindrical single crystal may be produced. The resultant single-crystalline rods are typically between 1.5 and 2 metres long and 125 to 130 mm in diameter. The melt must be kept at 1,450°C for several hours since the pulling is done at a pace of 1 mm/min. High energy losses have been documented even with extremely excellent thermal isolation because of heat transfer from the melt's surface's thermal radiation. Only by increasing the rod's diameter, which can be done industrially to diameters up to 212 mm (eight inches), could the yield be increased; for further information, see Aulich 1986. To improve the fill of the PV module area, the round rods are often sawn to columns with a quasi-quadratic cross section (quadrats with round corners).

The floating zone (FZ) technique, in addition to the Czochralski method, enables the manufacture of very effective solar cells: The column is locally melted when polycrystalline ingots are passed through an inductive heating ring. Even though most contaminants are more soluble in melt than in solid body, they nonetheless spread into the molten zone. The impurities may be removed from the central section and gathered at the ends by advancing the molten zone down the whole column towards the crystal's ends (which are sliced off later). Without contacting the silicon, heating and crystallisation are performed. The purest silicon is created by carrying out this procedure repeatedly. FZ-Si-based cells are very costly as a result of the time and energy required by this process, and as a result, their usage is mostly restricted to space applications.

Semiconductor-Grade Silicon to Multi-Crystalline Silicon

EG-Si is likewise heated to a molten state in a protective environment with low pressure, but it is then poured directly into a crucible. Temperature controls the cooling and crystallisation process. Although this cast silicon is not as high-quality as the material made by CZ or FZ, it is still sufficient to create solar cells that are extremely effective 17. The ingot is composed of several smaller crystals, or "grains," as opposed to having a single, big crystal. A

crystallisation rate of 0.5 kg/min is common. The ingots are sliced after being chopped into columns with a square base. The traditional Silan production technique for multi-crystalline wafers, according to Wagemann 1994, has a specific energy need of 2,300 kWh/kg. Cucible casting and multi-wire slurry slicing only need 200 kWh/kg using lye bath processing with solar grade silicon (at a yield of 35%). The usual energy needs for silicon growth and potential efficiencies for solar cells made of that material are summarised. Industrial multi-crystalline silicon cells with a surface area of 100 cm2 have a conversion efficiency of 15.8%. (Sharp). For a 4 cm2 cell, the laboratory record is 17.8%. (UNSW). Commercial multi-crystalline cells have an efficiency of about 15%. (e.g., Q- cells).

The manufacture of silicon wafers (Single- and Multi-Crystalline)

For photovoltaic applications, silicon solar cells only need to be around 0.1 mm thick to absorb the majority of the suitable solar radiation wavelengths. Therefore, wafers (slices) of the same thickness may be made from the big single crystal column (ingot). In-hole saws, which are often employed, have 50% cutting losses at the thinnest wafer thicknesses of 0.45 mm.

The fabrication of thinner wafers (0.2 mm) with a much better cut (cutting losses of 0.1 mm only) and less crystalline distortions is made possible by the employment of slurry-wire-saw technology. By doing this, silicon depletion and the ensuing energy use are reduced. In addition, hundreds of wafers may be cut at once; the whole ingot (up to a length of 1.6 m) can be divided into wafers. Only one wafer may be produced at a time using in-hole saws. A wire with a thickness of 0.18 mm and a length of up to 200 km is stretched to a square by four guide rollers at the slurry-wire-saw as it is stripped from a spool at a speed of 5 m/s. A silicon carbide with a grain size of 12 m that is suspended in cutting oil is used for the machining. The oil transfers heat while also acting as a carrier for the silicon-carbine. Thinner silicon wafers are more fragile and need special handling because of this in Figure 15.2.

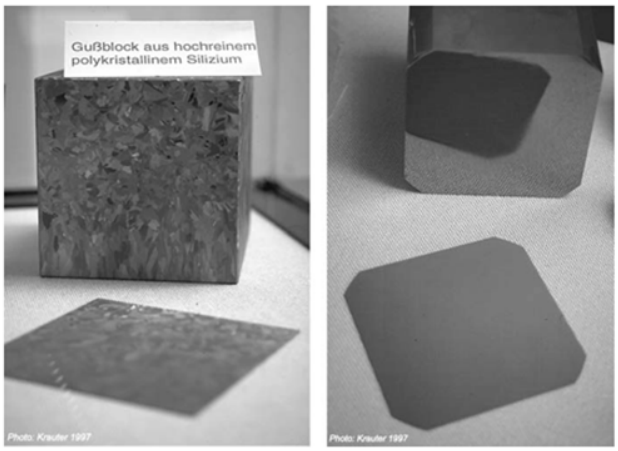

Figure 15.2: Independently whether the wafers are single- or multi-crystalline.Single-Crystalline Solar Cells from Single-Crystall Wafers.

The single-crystalline wafers go through the following procedure before they are able to produce a functional solar cell:

To repair damage from the wafer slicing process, utilise "lap" (fine polishing using Al_2O_3 with a grain size of 10 m as abrasive medium).After depositing the contacts, texture may be created by damage-etching (wet chemical with KOH as cauterant) to create a pyramid-shaped

structure that serves as an optical anti-reflective layer, or by sputtering TiO_2 or Ta_2O_5 in vacuum and sintered at 400°C.Doping: As was noted in the part above, boron was typically added to the Si-melt in order to produce p-type wafers in conventional solar cell technology. N-type impurities are added to create a p-n junction, which is needed to create a solar cell. The most common impurity (dopant) is phosphorus. The procedure that is used the most often involves bubbling a carrier gas through phosphorous oxychloride ($POCl_3$), mixing it with a little quantity of oxygen, and then passing it down a heated furnace tube where wafers are stacked. This causes the surface of the phosphorous-containing wafers to develop an oxide layer (phosphorus glass). Phosphorus diffuses from the oxide into the silicon at temperatures between 800°C and 900°C. After 20 minutes, the boron impurities in the wafer's surface area are overwhelmed by the phosphorous impurities, creating a narrow, strongly doped n-type zone. Removal of the phosphorus oxide ("phosphorous glass") via wet-chemical process at 20°C to 60°C, if necessary, etches away the junctions at the side and back of the cell. Additional boron-implantation is occasionally performed to generate a back-surface-field (BSF) by "emitter-diffusion" (gas phase diffusion at 900°C).

Electrical contact attachment: The technique utilised is referred to as "vacuum evaporation" in conventional technology. In a vacuum, the metal that has to be depositedmostly Alis heated till evaporation. The contact will subsequently be established when the metal vapour condenses in the colder solar cells. Metal is often placed across the full back surface for the back contact. The characteristic grid pattern on the top surface of solar cells is produced using a shadow mask for the front contacts ("screen printing technique"). Ti/Pd/Ag is the primary material used. The contacts are then sintered at 400 degrees Celsius in an IR oven.

Testing: visual control of the cells to ensure that the anti-reflective coating is uniform. Contact bonding durability tested mechanically. Opto-electrical test: recording current-voltage characteristics at an irradiance corresponding to an AM 1.5 spectrum, grouping the cells according to form factor and equivalent short-circuit current.In the first model example, the operations need 216 kWh of electrical energy per m^2 of cell area, 116 kWh of fuel per m^2, and 12 kWh of non-energetic fuel per m^2. In the second scenario, fuel consumption is 39 kWh/m^2, electrical energy consumption is 102 kWh/m^2, and non-energetic fuel consumption stays the same at 12 kWh/m^2. The appendix has a more thorough derivation of this estimate.

While many processes, like gas phase diffusion, have a high base load, the amount of energy used during processing depends on how much production capacity is actually used. Simply switching from a one shift to a four shift operating mode may cut processing energy usage to 30% of the original scenario (Hagedorn 1989). The additional energy used for climate control, ventilation, lighting, etc. is close to the energy required for processing.

Multiple Crystalline Solar Cells from Multiple Crystalline Wafers

Multi-crystalline solar cell manufacturing is comparable to single-crystalline solar cell manufacturing, but there is an additional phase involved: "Passivation" by hydrogen of the multi-crystalline material's grain boundaries.

Cleaning by KOH-based oxide etching

Doping (diffusion of emitter): Traditionally, this was done using a phosphorus emulsion screen printing method, followed by diffusion in an IR oven at 900°C for a maximum of 30 minutes (resulting depth of diffusion: 0.3-0.5 m). Nowadays, gas diffusion is often favoured,

Discarding phosphorous glass (wet-chemical)

Wafers are processed in a hydrogen plasma at 300°C for 30 minutes to passivate grain boundaries.Using contacts: screen printing (backside Ag/Al paste, front side Ag paste), sintering in an IR oven for 20 minutes at the highest temperature possible,screen printing a TiOx-emulsion to create an anti-reflective layer that is then sintered at room temperature (20°C).

Testing: Opto-electrical cell test: recording current-voltage characteristics at an irradiance equivalent to a spectrum of AM 1.5, classification of the cells into groups of equivalent short-circuit current, and visual cell test: verifying homogeneity of the anti-reflective coating on the cell. Mechanical cell test: contact bonding.

The energy consumption of these processes is similar to that of single-crystalline solar cells: in the first mode example, electrical energy consumption is 213 kWh/m^2, fuel consumption is 107 kWh/m^2, and non-energetic fuel consumption is 8 kWh/m2.Electrical energy usage for the second mode example is 89 kWh/m2, while fuel consumption is 34 kWh/m^2. 10 kWh/m^2 is the non-energetic fuel usage (Hagedorn 1989). By switching to a four-shift manufacturing operation and using wafers with a 0.2 mm thickness, primary energy consumption and carbon dioxide emissions would be cut in half.

Amorphous silicon solar cell manufacturing

Amorphous silicon thin sheets containing a little amount of hydrogen are used to create these cells. This significantly lowers the material's electrical resistance and enables n- or p-type doping. A very thin n-layer and players with intrinsic I layers thick enough to absorb virtually all incoming light combine to create a p-i-n structure, which improves current collection. The p-n junction generates an electric field that permeates the whole i-layer and significantly facilitates the collecting of photogenerated charge carriers. Unfortunately, light absorption degrades i-electrical layer's characteristics, and cells operate worse when exposed to sunlight. Careful management of the deposition conditions and the use of several junctions, each with a thinner i-layer, may lessen the impact but not completely remove it. On a triple junction stack, an amorphous silicon cell's greatest efficiency to date is 13.6%.

REFERENCES

[1] H. F. Andersen *et al.*, “Silicon-Carbon composite anodes from industrial battery grade silicon”, *Sci. Rep.*, 2019, doi: 10.1038/s41598-019-51324-4.

[2] H. Jouhara *et al.*, “Applications and thermal management of rechargeable batteries for industrial applications”, *Energy*, 2019, doi: 10.1016/j.energy.2018.12.218.

[3] A. Porvali *et al.*, “Mechanical and hydrometallurgical processes in HCl media for the recycling of valuable metals from Li-ion battery waste”, *Resour. Conserv. Recycl.*, 2019, doi: 10.1016/j.resconrec.2018.11.023.

[4] A. Ulvestad, C. E. L. Foss, H. F. Andersen, P. E. Vullum, J. Voje, en J. P. Maehlen, “Degradation Phenomena in Silicon-Carbon Composite Anodes from Industrial Battery Grade Silicon”, *ECS Meet. Abstr.*, 2019, doi: 10.1149/ma2019-03/2/168.

[5] C. K. Chang, “Factors affecting capacity design of lithium-ion stationary batteries”, *Batteries*. 2019. doi: 10.3390/batteries5030058.

[6] B. Bereczki, B. Hartmann, en S. Kertesz, “Industrial Application of Battery Energy Storage Systems: Peak shaving”, 2019. doi: 10.1109/IYCE45807.2019.8991594.

[7] V. Papadopoulos, J. Knockaert, C. Develder, en J. Desmet, "Investigating the need for real time measurements in industrial wind power systems combined with battery storage", *Appl. Energy*, 2019, doi: 10.1016/j.apenergy.2019.04.051.

[8] Y. Liu, S. Lu, S. Chen, H. Wang, J. Zhang, en Y. Xiang, "A Sustainable Redox Flow Battery with Alizarin-Based Aqueous Organic Electrolyte", *ACS Appl. Energy Mater.*, 2019, doi: 10.1021/acsaem.8b01512.

[9] J. de la Peña Llerandi, C. S. de Mingo, en J. C. Ibáñez, "Continuous battery health diagnosis by on-line internal resistance measuring", *Energies*, 2019, doi: 10.3390/en12142836.

[10] L. S. Roselin *et al.*, "Recent advances and perspectives of carbon-based nanostructures as anode materials for Li-ion batteries", *Materials*. 2019. doi: 10.3390/ma12081229.

CHAPTER 16

PRODUCTION OF SOLAR CELLS

Mr. M.Sashilal, Associate Professor,
Department of Electrical Engineering, Jaipur National University, Jaipur India
Email Id- msashilal@jnujaipur.ac.in

The development of the technology for gallium arsenide (GaAs), which is used to make semiconducting lasers and blue light-emitting diodes, is dependent on market demand. The most effective solar cells have been built using GaAs due to its almost perfect band-gap and associated spectrum efficiency. GaAs will always be a costly solar cell material due to the scarcity of gallium resources (production is only 30 tons/a). The quantity of material needed for a particular power output may be decreased using concentrator systems. GaAs' straight band gap also implies that light is absorbed extremely fast after entering, requiring just a few microns of layering. Arsenic's toxicity is a major drawback, therefore any environmental effects of using massive GaAs solar energy systems would need to be carefully considered[1], [2].

Copper Sulfide – cadmium Sulfide Cells (Cu_2S – CdS)

Cells made of copper sulphide and cadmium sulphide (Cu_2S - CdS) CdS solar cells have been developed since 1954. Since then, several efforts to create a commercial solar cell based on this material have been made. The simplicity with which these cells may be created is what stands out about them. There are several ways to create such substrates since fine-grained multi-crystalline CdS is also suitable as a substrate material. The spraying approach and vacuum evaporation seem to be the most promising. These cells' poor efficiency and lack of the inherent stability that silicon solar cells have are their main drawbacks. Low efficiencies increase the space needed for a given output, which raises the price of other system components. Even if the cells were free, it would still be less expensive to utilise higher-efficiency cells that are more expensive since balance-of-system expenses, such as those associated with site preparation, support structures, and wiring, may dominate PV system prices to such a degree. As a general rule, 10% module efficiency is the lowest that can probably be allowed for PV power production on a broad scale that is both affordable and effective[3], [4].

Making of PV Modules

A so-called "string" is created by connecting six to twelve solar cells in series. Traditional cell connection tabs are made of flat silver wires. Then, welding with a point or an infrared beam is used to contact. Currently, cooper flat-wire tabs (diameter 100-200 m) coated with an alloy made of 60% Sn, 38% Pb, and 2% Ag are in use. These tabs may be purchased by eddy current, IR, hot air, laser, or flame. A coating alloy of 96.5% and 3.5% Ag is being used more often to prevent the dangerous lead, although its fusion temperature is 40 K higher. A solar module (also known as a PV module) is built from three to twelve of these strings and shields the PV generator from the elements. To do this, a front sheet of glass, transparent plastic, and a rear sheet of glass or foil are fused together with the cell matrix. Ethylene-vinyl-acetate is the copolymer used most often for this kind of plastic (EVA)[5], [6].

Lamination Technique

Using pressure and heat, the module's compound (glass - EVA - solar cell matrix - EVA - glass, or of glass - EVA - solar cell matrix - EVA - backside laminate) is produced. Vacuum-laminators are often used throughout the whole lamination process (heating, curing of the co-polymer EVA, and cooling). Other approaches, such employing a separate oven for regular pressure curing, are being explored. In mass production, "curing" at normal pressure shortens the cycle time and enables rapid laminator reloading. Because the laminator does not need to be cooled down, energy loss is decreased. The benefit of separate or "equalised" processing is diminished by the use of current "quick cure" EVA as an encapsulation, which enables the curing period to be cut from 22 minutes to 4 minutes. A vacuum laminator with a built-in heating and cooling system is used, as will be covered later in the book. The new independent processing is also discussed inside a proposal for a "passing through" laminator made by the Austrian business Isovolta AG because of its relevance for energy efficiency and potential reduction of CO_2 emissions.

The "constant temperature" approach, regulated laying down and raising up of the modules from the heating plates in the vacuum oven, is now employed more and more. This process significantly boosts production throughput. Two-stage processing is the preferred technique in Japan. It is possible to prevent "fast-curing" EVA at the expense of more handling by pre-laminating in a vacuum laminator and then curing in a circulating air oven. TPU (thermoplastic polyurethane), which does not need any curing time, may be important in the future; Bayer is working on a suitable roller-laminator. TPU prices are still twice as much as regular EVA, however. The brand names and values shown in the tables below are only representative samples for the calculation of the unique energy needs for PV modules since the equipment for the lamination process develops quickly[7], [8].

Built-in Laminator

By applying ambient pressure to the laminate's top side while it is heated by a heating plate below, a flexible membrane in the vacuum laminator's cover plate (which forms a separate chamber) builds up the appropriate pressure on the laminate (release of vacuum). Isovolta's recommended lamination procedure for traditional EVA is as follows:

1. Vacuum up to around 10 mbar, load laminate at 90 mbar
2. Heat from 90 degrees Celsius to 155 degrees Celsius in 10 minutes (a 6,5 K/min);
3. The top plate is subjected to ambient pressure to generate membrane pressure at 120 °C.
4. Maintain temperature for 15 minutes after reaching 155°C.
5. Cool down from 155 °C to 90 °C in 10 minutes (a -6.5 K/min),
6. When the laminator reaches 100°C, open it.

The steps in the lamination process using traditional and "quick cure" EVA in accordance with the "Spring born" technique (see Photo cap, 1996):

1. Pre-heat the laminator's heating plates to 75°C.

2. Load the laminator with two silicon or Teflon® separator foil.

3. Establish a vacuum in the laminator's bottom (1.3 mbar, attained after 3 minutes).

4. Once the laminate achieves a temperature of 60°C (also after three minutes), increase pressure (1 bar) in the laminator's cover plate.

5. Set the following cycle's temperature to 75°C.

A steeper time-temperature ramp of 15 K/min (instead of 6.5 K/min) and pressurization at 60°C (instead of 120°C), before the melting point of EVA at 80°C, are two significant deviations from the Isovolta method. Electrical energy production for the heating plates is thought to be carried out at a 35% efficiency in order to compare primary energy consumption of heating. Neglect is given to heat losses from convection and heat conduction to the evacuated laminate's containment. Due to the heating mattress' excellent thermal insulation, the electrical heating mattress itself and the heat transfer from the heater into the laminate account for the majority of its power usage. To heat a large (3 m2), thin (5 mm) glass, EVA, and solar cell laminate from 25°C to 150°C, about 1 kWh is required:

In order to attain the final temperature in 8 minutes, a heating output of 8.73 kW is required. A further 0.547 kWh must be added in order to power the heated mattress, which weighs 37.5 kg and has a copper conductivity of 0.108 Wh/(kg K). This results in a total power need of 12.83 kW. The laminate may be removed at 90°C, while cooling power is similar to or less. When using a tube-based cooling system (instead of air ventilation), its heat capacity must also be taken into account. It is assumed that maintaining the temperature at 155°C will need 10% of total power usage[9], [10].

Laminator with "Passing-Through"

The "passing-through" procedure uses the same temperature cycles as the technique using the integrated laminator. Through the vacuum laminator, curing oven, and cooling zone, the laminate is moved by a conveyor belt. Ten minutes pass between cycles. The vacuum laminator (which can produce laminates up to 1.2 m2 in size here) requires 9 kW, the double-sized curing oven requires 12 kW, and the remaining power is used for cooling, ventilation, process control, and handling. When the temperature hits 60°C, the laminate may be pressured and takes three minutes of pumping to be bubble-free. At the same time, the power for heating is raised and held at 155°C. The information in Tables 17 and 18 demonstrates how the simultaneous lamination of many modules greatly saves energy usage (comparison of ICOLAM II from Isovolta with SPI 460 from Spire). The energy consumption per cycle for all kinds of laminators was estimated for an eight-minute heating time at maximum power. Using 10% of the maximum power value, power usage to maintain the temperature for 4 or 22 minutes was taken into consideration. If an extra "curing oven" is utilised, the cycle duration of the laminator for conventional EVA may be adjusted to "rapid cure" EVA, however this will need an additional 10 kW of electricity. The integrated laminator utilising "rapid cure" EVA provides the lowest energy usage thanks to its quick cycle duration of about 4 minutes. The separation of the lamination, curing, and cooling processes at the ICOLAM II does not have a favourable impact on the decrease of energy flows, according to data provided by the manufacturer and estimates shown above in tables. Primary is caused by lamination using traditional laminators. Two manufacturers of laminators since 1996 (NPC and S.E. Project: 26 kW for four 83.6 W p modules) maintain the temperature of the hearing plates constant at 155°C at the start of the cooling process by lifting the laminate off the hearing plate in an effort to reduce energy losses by changing the temperature of the heating plate. Manufacturers claim that traditional laminators only use 20% as much energy as these machines. According to the relationship between the heat capacity of the laminate and the heat capacity of the hearing plate, a saving of 30% is more logical. 3 kWh/m2 is the energy usage. 5 kWh/m2 are a reasonable amount when using active cooling.

"Encapsulated" PV module manufacturing

A PV module that has been "encapsulated" is made of the following substance: plastic, glass sheet, solar cell matrix, plastic, and glass sheet. EVA (ethylene vinyl acetate) is often utilised as the plastic layer, allowing the glass sheets and cell matrix to fit tightly together. A vacuum laminator is used to pressurise the compound during the laminating process at 145°C to 200°C in order to prevent air bubbles in the laminate. When the co-polymer EVA, which is provided in foils with a thickness of 0.5 to 0.7 mm, is laminated, it "cure[s],]" making the melting process irreversible. UV absorbers are added to the EVA to stop the plastic from degrading from UV light (also known as "yellowing" or "browning"). Iron-free ("white") glass that has been thermally tempered and is 2-3 mm thick makes up the glass sheets.

Conditioning for Electrical Power

Depending on the kind of system, several converters may be required to match the PV generator's current and voltage to the load needs. A charge controller, deep discharge protection, and electrochemical storage are required for an autonomous system. A Maximum-Power-Point-Tracker (MPPT) and a DC-AC converter (inverter), which enable the use of AC loads, are also advantageous for adjusting the load to the PV generator's real current-voltage characteristics optimally.PV systems for grid injection need an inverter with grid synchronisation capabilities; a Maximum-Power-Point-Tracker is also advantageous. These two gadgets are often used in tandem. Table 6.12 lists the energy needs for the units, including wiring, at various power plant sizes. Table A16 in the Annex provides a comprehensive inventory of all materials used in power conditioning components. The mix of power generation and particular emissions of raw material-producing nations.

Power Yield

A thorough operational model was created as part of a Ph.D. thesis (Krauter 1993c) in order to quantify losses brought on by inadequate optical and thermal adaptation of solar-electrical converters to actual operating circumstances. This model was utilised as a platform and tool to calculate, as precisely as feasible, the yield of PV systems, together with well-known electrical performance modelling. All factors that have an impact on the electrical yield (and therefore on the specific CO 2 output) of more than 1% were taken into account while simulating the PV system.

A Model for Calculating Cell Reaching Irradiance

The spectrum that actually reaches the cell is extracted along the route of irradiance from the Sun, via the Earth's atmosphere, and through the photovoltaic power conversion mechanism of the solar panel.

Position of Sun with Regard to Earth's Surface

The equations from 1978 were utilised in earlier iterations of the model (Krauter 1993c, Strauß 1994), which took into account updates and enhancements from Archer 1980, Wilkinson 1983, and Kambezidis 1990. These models are inapplicable for sites between the Tropic of Capricorn and the Tropic of Cancer, or between 23.5° South and 23.5° north of the Equator, when the Sun's height is more than 90°. In place of these equation components, similar formulae from DIN 5034 part 2 have been used. In accordance with DIN 5034 part 2, the actual location of the Sun may be computed using the Sun's azimuth and elevation angles as follows in Figure 16.1:

Latitude (positive number for areas North of the equator, negative value for sites south of the Equator) (positive value for locations North of the equator, negative value for locations south of the Equator). Declination, or the Sun's position in relation to the Equator at solar noon (the greatest height of the day).

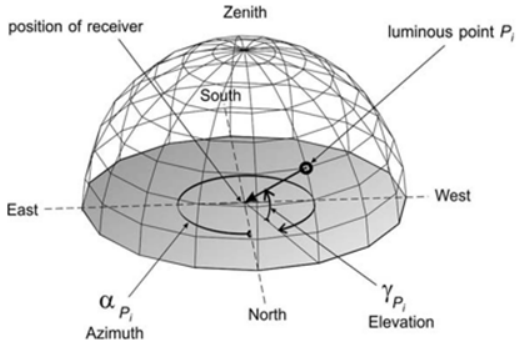

Figure 16.1: The Definition of the elevation angle α_S and the azimuth angle a_S of aluminous point P_i according to DIN 5034 part 2.

The formulae have been changed to account for the Earth's surface's bow as well as the refractive qualities of the atmosphere, which vary with air pressure and temperature. The following adjustments are suggested by The Astronomical Almanac 1996:

The two functions and their derivations only slightly diverge at the transition point at an elevation angle of 15°, which causes the overall function that takes atmospheric refraction into account to progress smoothly and steadily in Figure 16.3. For S 15°, the precision is around 0.0017°. The Sun's location (S, aS), the module elevation (M), and the module azimuth (M) all play a role in determining the incidence angle (in) onto the PV module surface in Figure 16.2:

$$\theta_{in} = \arccos(\sin\gamma_S \cdot \cos\gamma_M \quad \cos\gamma_S \cdot \sin\gamma_M \cdot (\alpha_S - \alpha_M))$$

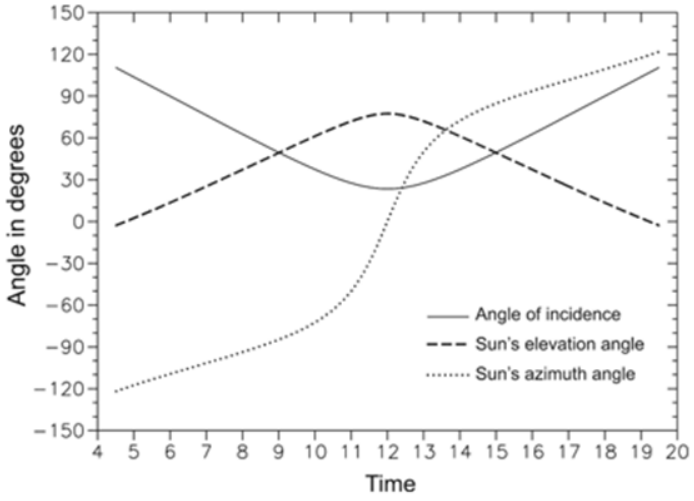

Figure 16.2: *Illustrates* the Sun' selevationα_S ,Sun'sazimutha$_S$,and incidence angle θ_{in}on to module surface during a day (6/21,lat=ϕ=36°N,α_M=36°directed towards South).

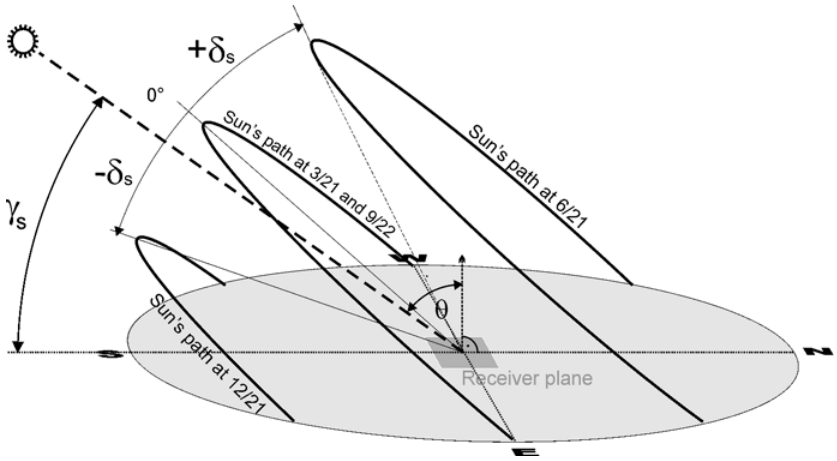

Figure 16.3: Shows the sun's path across the northern hemisphere during the equinoxes (March 21 and September 22), summer (6/21) and winter (December 21). The maximum deviations from the midday points S are also shown, together with the real sun's elevation angle S and the associated incidence angle S on a receiver (following Ertürk 1997).

Method of the Sun's Radiance Through the atmosphere of the Earth

Sunlight constant

The Sun emits 1,353 7 W/m2 of radiation directly above the Earth's atmosphere. This amount is known as the "Solar Constant" E. Due to the Sun's somewhat elliptic trajectory, the distance between the Earth and the Sun does not stay exactly constant. As a result, the solar constant varies slightly (1%).

Global Radiation

A portion of the irradiance is absorbed and scattered by the atmosphere of Earth in Figure 16.4. Angle of incidence and wavelength of solar irradiation both affect absorption and the likelihood of scattering in Figure 16.5. Not all of the dispersed component is lost; some of it will manifest as diffuse irradiance and reach the Earth's surface in Figure 16.6. Global irradiance is the total of direct and diffuse irradiance in Figure 16.7. Typical values for the global irradiation under clear skies as a function of the sun's elevation angle, S.

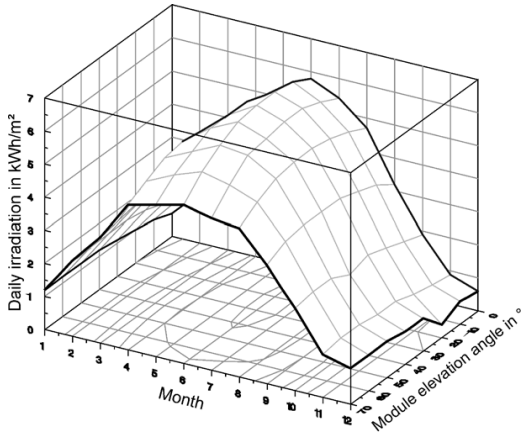

Figure 16.4: shows the Daily Global Irradiation throughout a Year as a Function of Elevation Angle of the Receiver Plane For a location in Central Europe (51° N, 11.5° E).

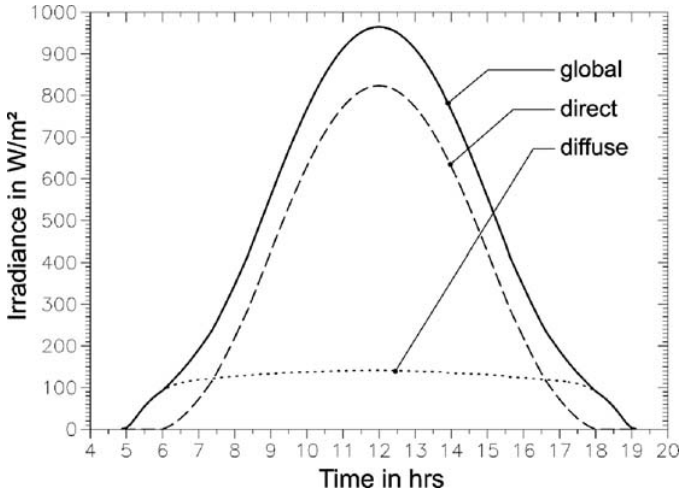

Figure 16.5: shows the Direct and Diffuse components of global irradiance under clear sky circumstances on March 21 (respectively, September 22) with a receiver plane with the same elevation angle as the latitude angle (for example, 36°), so the sun will incident perpendicularly at midday.

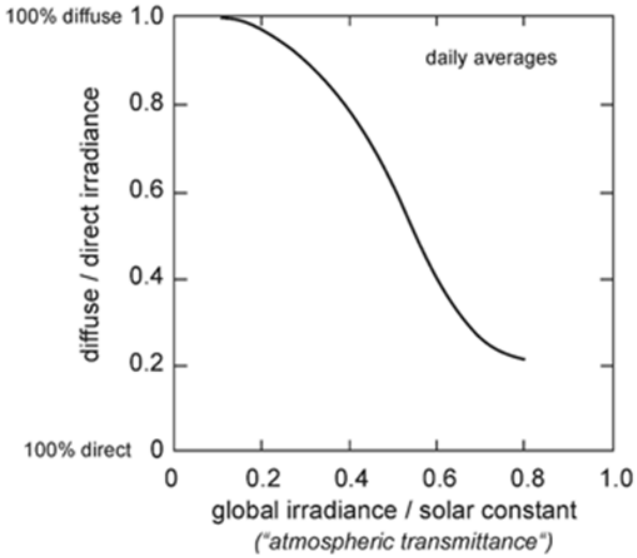

Figure 16.6: *Illustrates* the Relative diffuse irradiance component as a function of the relative global irradiance.

Direct Radiation

Position of the sun, air mass, atmospheric conditions (temperature, humidity, clouds, aerosols), and angle of incidence of the sun's radiation towards the receiver plane all affect direct irradiance (e.g., a solar module).The solar generator's photovoltaic capacity factor fluctuates as a result of changes in spectral composition in addition to variations in irradiance because of its spectral selective sensivity. Just lately, considerations for these variations in the

days and seasons were made (Krauter 1993c etc.).

As the most up-to-date approximation of actual circumstances, the CIE spectrum publication No. 85 (1990) was chosen as a guide for modelling since it contains information on various air masses (see in Figure 16.8) and turbidity parameters. Also provided were spectra for various H_2O-, CO_2-, and O_3-contents.

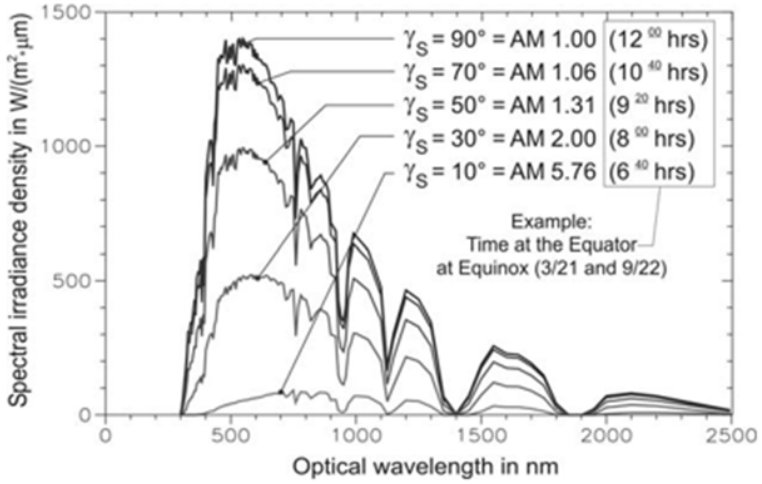

Figure 16.7: *Illustrates* the Direct terrestrial irradiance spectra of the sun (AM 1-5.6) according to tables of CIE publication No. 85 (1990) for AM 1, AM 2 and 5.6, other values by interpolation.

Diminished Radiance

Even under clear sky circumstances, there is always a sizable diffuse component of the solar irradiance for terrestrial applications. The diffuse component makes about 30% to 60% of the total irradiance during the course of a year (global irradiance). The diffuse or dispersed radiation's spatial distribution throughout the hemisphere of the sky is not uniform. The likelihood that a scattered solar ray will strike an air molecule or aerosol and be reflected depends on the air density and thickness of the atmosphere it is travelling through. According to Fresnel's Law, the reflected component is a function of the angle of incidence and the optical refractive indices of the medium involved. A multiple dispersion must also be taken into account. The model DIN 5034 part 2 is used to calculate the angular sky irradiance as a function of the location of the sun. Figure 54 shows a contour plot (projection of the sky's hemisphere to the plane) as an illustration of the distribution of the sky's illumination at an elevation angle of the sun of S = 30°. Table 16.1 provides examples for the average monthly turbidity factors TL in Germany.

Table 16.1: depicts the Average monthly turbidity factors TL in Germany.

Month	**Highest**	**Monthly average of TL Average**	**lowest**
January	4.80	3.8 ± 1.0	3.20
February	4.60	4.2 ± 1.1	3.60
March	5.40	4.8 ± 1.5	4.30

April	5.70	5.2 ± 1.8	4.80
May	5.80	5.4 ± 1.7	4.90
June	7.40	6.4 ± 1.9	5.60
July	6.90	6.3 ± 2.0	5.70
August	6.90	6.1 ± 1.9	5.70
September	6.00	5.5 ± 1.6	5.20
October	4.90	4.3 ± 1.3	4.00
November	4.20	3.7 ± 0.8	3.30
December	4.10	3.6 ± 0.9	3.30
Yearly 5.40		4.9 ± 1.5	4.70

Angle of Annual Irradiance Distribution in Central Europe

Clear skies are a must for the observations shown above. The sky is often clouded in many places, including central Europe, in reality. Preu et al. 1995 carried out calculations of the angular distribution for Freiburg, Germany (48° N) based on a diffuse-direct distribution of the so-called "Typical Meteorological Year" (TMY) using an albedo of 0.2. For various module orientations (horizontal and tilted south with module elevation angles of 30°, 48°, and 90°), the global irradiance is shown in Figure 16.8 as a function of the incidence angle. The cumulative irradiance took into account an angular range of one degree for all incidence angles other than zero. Because the angular range examined is indefinitely tiny and consequently the cumulative irradiance, the number zero was selected for an incidence angle of precisely 0°.

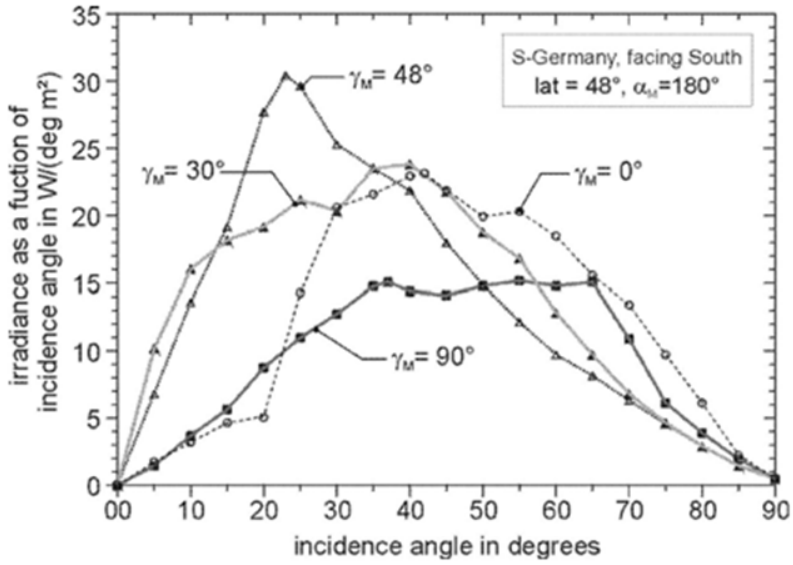

Figure 16.8: ***Illustrates*** **the Irradiance as a function of incidence angle for different elevation angles uM of the PV module at Freiburg, Germany (48° N).**

REFERENCES

[1] M. Mrinalini, N. Islavath, S. Prasanthkumar, en L. Giribabu, "Stipulating Low Production Cost Solar Cells All Set to Retail…!", *Chemical Record*. 2019. doi: 10.1002/tcr.201800106.

[2] Y. H. Chiu, T. H. Lai, M. Y. Kuo, P. Y. Hsieh, en Y. J. Hsu, "Photoelectrochemical cells for solar hydrogen production: Challenges and opportunities", *APL Mater.*, 2019, doi: 10.1063/1.5109785.

[3] A. Blakers, "Development of the PERC Solar Cell", *IEEE J. Photovoltaics*, 2019, doi: 10.1109/JPHOTOV.2019.2899460.

[4] M. M. Taniguchi *et al.*, "Glass engineering to enhance Si solar cells: A case study of Pr3+−Yb3+ codoped tellurite-tungstate as spectral converter", *J. Non. Cryst. Solids*, 2019, doi: 10.1016/j.jnoncrysol.2019.119717.

[5] L. C. Andreani, A. Bozzola, P. Kowalczewski, M. Liscidini, en L. Redorici, "Silicon solar cells: Toward the efficiency limits", *Advances in Physics: X*. 2019. doi: 10.1080/23746149.2018.1548305.

[6] M. J. García-Salinas en M. J. Ariza, "Optimizing a simple natural dye production method for dye-sensitized solar cells: Examples for betalain (bougainvillea and beetroot extracts) and anthocyanin dyes", *Appl. Sci.*, 2019, doi: 10.3390/app9122515.

[7] Y. C. Huang, C. F. Li, Z. H. Huang, P. H. Liu, en C. S. Tsao, "Rapid and sheet-to-sheet slot-die coating manufacture of highly efficient perovskite solar cells processed under ambient air", *Sol. Energy*, 2019, doi: 10.1016/j.solener.2018.11.020.

[8] X. Xiao *et al.*, "Highly Efficient Hydrogen Production Using a Reformed Electrolysis System Driven by a Single Perovskite Solar Cell", *ChemSusChem*, 2019, doi: 10.1002/cssc.201802512.

[9] M. H. Kang *et al.*, "Fabrication of Spray-Coated Semitransparent Organic Solar Cells", *IEEE J. Electron Devices Soc.*, 2019, doi: 10.1109/JEDS.2019.2949685.

[10] Y. Qin, Z. H. Lin, J. J. Chang, en Y. Hao, "Research progress of printed perovskite solar cells", *Chinese Optics*. 2019. doi: 10.3788/CO.20191205.1015.

CHAPTER 17

MODEL OF MODULE ENCAPSULATION BY OPTICS

Mr. Vivek Jain, Associate Professor,
Department of Electrical Engineering, Jaipur National University, Jaipur India
Email Id-vivekkumar@jnujaipur.ac.in

For slabs thicker than the wavelength of the irradiance, the optical model presented here is mathematically precise since all potential internal and external reflections are taken into account. Any optical system made up of a variety of distinct homogeneous plane slabs with refractive indices, absorption coefficients, and thicknesses may use it. Additionally covered are optical dispersion and complicated refractive indices. The thicknesses might range from infinity to the irradiance's wavelength range. An irradiance model was constructed to take into account the spatial distribution of direct and diffuse irradiance under clear sky circumstances in order to determine the solar reflection performance of an optical system during daytime.

Reflective losses in practical circumstances

Estimates of reflecting losses at the surface of PV modules, which range between 2 and 4 percent of the incoming irradiance, have been made in previous contributions using perpendicular incidence. This only applies to tracking systems without diffuse insolation portions (like in space). Direct insolation only really strikes the surface of the module twice a year for non-tracking terrestrial systems. Occasionally, the reflected portion grows in accordance with FRESNEL laws1 (see below). Even on particularly clear days, there is always a diffuse portion of insolation for terrestrial applications, which, depending on the geographic circumstances, ranges from 30% to 60% of the total insolation on an annual average. Figure 17.1 provides an illustration of the polarisation distribution of diffuse radiation at the sky hemisphere. In the future, a more sophisticated model developed by Perez et al. (1993) will be utilised instead of the diffuse radiation in anisotropic that was previously taken from DIN 5034[1], [2].

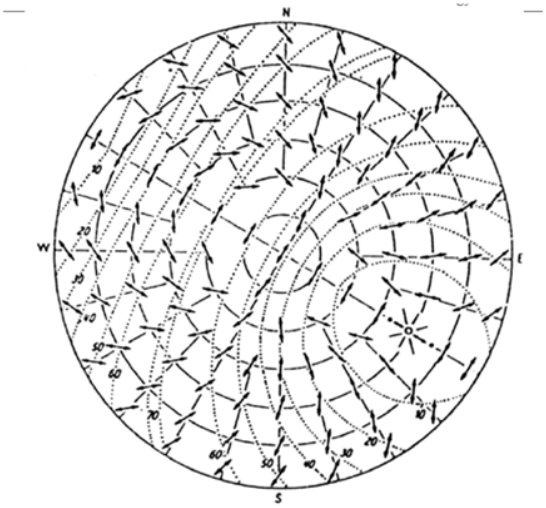

Figure 17.1: ***Illustrates*** **the Polarization pattern of the sky hemisphere for a clear day for an elevation angle of the sun of 30° (after von Frisch 1965).**

A model for the encapsulation of the cell that separates the insolation accessing the cell from sun and sky irradiance was created in order to produce an accurate depiction of the real optical conditions in the module. This was achieved by simulating the optical processes occurring both outside and within the encapsulation (see also in Figure 17.2). Diffuse irradiance is polarised because it is dispersed. As a result, reflectance is polarization-dependent, as previously discussed (Krauter et al. 1991; Krauter 1993): Polarization caused a 0.5% to 5% increase in reflection loss across the diffuse region. The annual average for reflection losses is in the 20% range (Krauter et al. 1994, Krauter and Hanitsch 1996). The improvement of PV module encapsulation layers' transmittance via the reduction of reflecting losses is crucial for the optimization of PV systems[3], [4].

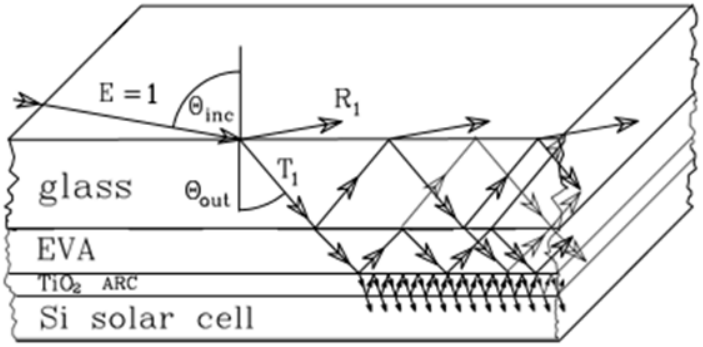

Figure 17.2: ***Illustrates*** **the Ray-tracing through a PV module encapsulation.**

The optical contact at the boundary layers

Perpendicular incidences: At the transitions when radiation from a material of a particular optical density (n0) enters into another (n1), the radiation is broken up into a reflecting component (R) and a transmission one (T) at the optical interface in 17.3.

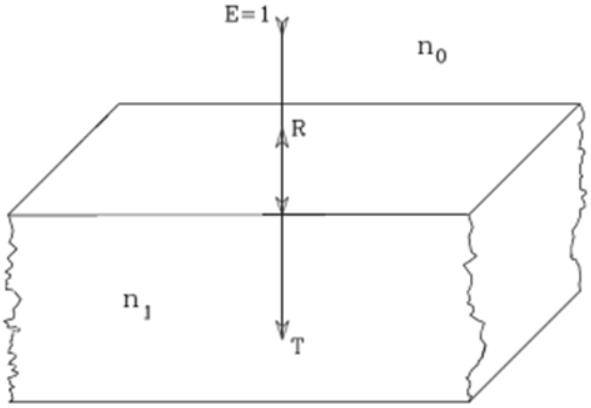

Figure 17.3: ***Illustrates*** **the Perpendicular incidence on a plane surface (θin = 0°).**

R is also called “reflectance” and T, “transmittance” (see, e.g., Dietz 1991). Irradiance (E) of the incoming radiation is normalized to E = 1.

$$R = \frac{(n_1 - n_0)^2}{(n_0 + n_1)^2}$$

$$T = 1 - R$$

N on-perpendicular incidences: More realistic is the case of non- perpendicular incidences of insolation (see Figure 17.4). Here the reflectance could be calculated by the FRESNEL formula (see, e.g., Born and Wolf 1975) for a certain angle of incidence θin.

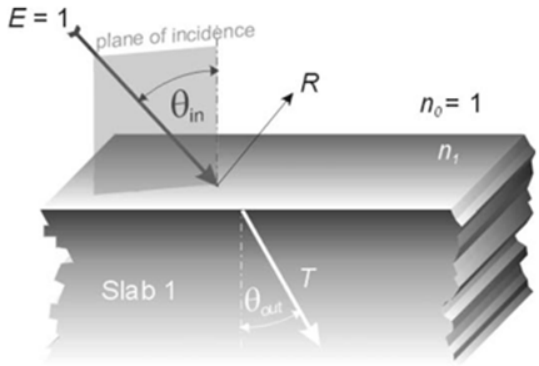

Figure 17.4: ***Illustrates*** **the Transmittance and reflectance at an optical boundary for non-perpendicular incidence (θin › 0°).**

Plane-slab optical transmittance

Incident insolation must cross two optical boundary layers and be attenuated by internal material absorption. Though not fully lost, reflection at the bottom border bounces up and forth through the slab at a diminishing intensity (see Figure 17.5).

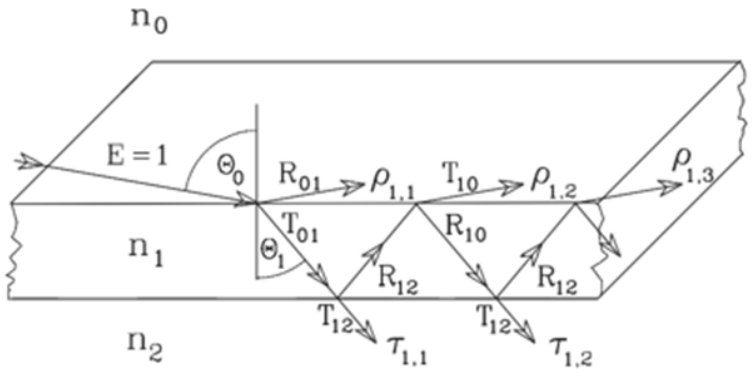

Figure 17.5: ***Illustrates*** **the Transmittance through a plane optical slab.**

A layer is identified by the index "k," the upper medium by the index "k-1," and the lower medium by the index "k+1" in order to provide a uniform nomenclature. The angles of refraction and incidence at the change from medium "k-1" to medium "k" are denoted by the symbols k and k+1, respectively. The media indices in the order of the radiation travelling through them, k,k1, are used to identify optical transitions (e.g. T01). The transmitted portions of the irradiance on slab k are denoted by the symbols k,i and pk,i, respectively. In order to make the formulae simple, a difference between the polarisation planes is no longer made. Therefore, the particular components R, R and T, T have to be entered for the often used variables R and T. In addition, the incident irradiance is adjusted to E=1. For instance, the coefficient of absorption a1() of the material, its thickness d1, and the incidence angle 1

on the examined slab 1 all contribute to the absorptive attenuation of an incident ray after it passes through the slab 1:

$$\frac{\Delta E_1}{E_1} = \exp\left(-\alpha_l \frac{d_1}{\cos\theta_l}\right)$$

It is also possible to determine a from a() = 4 v k -1 if the imaginary portion of the complex refractive index n = n - j k is known. As a result, slab 1's incident boundary surface experiences reflection loss R01, while its lower surface experiences reflection loss R12[5], [6]. The remaining transmitted component is made up of:

$$\tau_{l,1} = T_{01} T_{1,} \exp\left(-\alpha_l \frac{d_1}{\cos\theta_l}\right)$$

Internal reflection at the boundary 2–1 travels through layer 1 once again and is diminished as a result. This beam is refracted once again at the boundary 0-1, but a component, T10, enters medium 0. Under attenuation, the reflected component R10 reaches boundary 1-2, where another component T12 enters layer 2.

$$\tau_{l,2} = T_0 \; R_{12} R_{10} T_{12} \exp\left(\frac{-3\alpha_l d_1}{\cos\theta_l}\right)$$

In general: Summing up all transmitted fractions of the layer 1:

τ_l

$$= T_{01} T_{12} \exp\left(\frac{-\alpha_l d_1}{\cos\theta_l}\right) \sum_{i-1}\left[R_{12} R_{10} \exp\left(\frac{2\alpha_l d_1}{\cos\theta_l}\right)\right]^{i-1}$$

$$\tau_{l,i} = T_{01} T_{12} R_{12}^{i-1} R_{10}^{i-1} \exp\left(\frac{-(2i-1)\alpha_l d_1}{\cos\theta_l}\right)$$

This infinite series is a geometrical one and can be summarized as follows:

τ_l

$$= \frac{T_{01} T_{12} \exp\left(\frac{-\alpha_l d_1}{\cos\theta_l}\right)}{1 - R_{12} R_{10} \exp\left(\frac{-2\alpha_l d_1}{\cos\theta_l}\right)}$$

Because radiation is being absorbed in the slab, the reflectivity p of a slab has to be computed explicitly, because p › 1 - τ. The reflected components p1,i of a slab 1 are to be calculated as follows:

$$\rho_{l,1} = R_{01}$$

$$\rho_{l,2} = T_{01} R_{12} T_{10} \exp\left(\frac{-2\alpha_l d_1}{\cos\theta_l} \right)$$

$$\rho_{l,3} = T_{01} R_{12}^2 R_{10} T_{10} \exp\left(\frac{-4\alpha_l d_1}{\cos\theta_l} \right)$$

$$\rho_{l,i>1} = T_{01} R_{12}^{i-1} R_{10}^{i-2} T_{10} \left(\exp\left(\frac{-2\alpha_l d_1}{\cos\theta_l} \right) \right)^{i-1}$$

The sum of all reflected components p1 of the layer 1:

$$\rho_1 = R_{01} + T_{01} R_{12} T_{10} \exp\left(\frac{-2\alpha_l d_1}{\cos\theta_l} \right) \sum_{m=1}^{\infty} \left[R_{10} R_{12} \exp\left(\frac{2\alpha_l d_1}{\cos\theta_l} \right) \right]^{m-1}$$

This infinite series is again a geometrical series and can be summarized:

$$\rho_l = R_{01} + \frac{T_{01} R_{12} T_{10} \exp\left(\frac{-2\alpha_l d_1}{\cos\theta_l} \right)}{1 - R_{10} R_{12} \exp\left(\frac{-2\alpha_l d_1}{\cos\theta_l} \right)}$$

Internal Transmission and Reflection

Knowledge of the internal transmission τ^- is necessary to determine the transmission of multiple layer systems, for example τ^- 1: the transmittance of slab 1, when it is illuminated from reflections coming out of slab 2. To distinguish internal transmittance and internal reflectance from the external ones, a bar over the variable is used.

$$\bar{\tau}_l = T_{10} \exp\left(\frac{-\alpha_l d_1}{\cos\theta_l} \right) \sum_{i=1}^{\infty} \left[R_{10} R_{12} \exp\left(\frac{-2\alpha_l d_1}{\cos\theta_l} \right) \right]^{i-1}$$

$$\bar{\tau}_l = \frac{T_{10} \exp\left(\frac{-\alpha_l d_1}{\cos\theta_l} \right)}{1 - R_{10} R_{12} \exp\left(\frac{-2\alpha_l d_1}{\cos\theta_l} \right)}$$

At the boundary between slab 2 and slab 1, T21 is neglected because it has been already accounted for by the net reflectivity of the lower slabs[7], [8]. The internal reflectivity p⁻ 1 is set up the same way:

$$\bar{\rho}_i = R_{10}T_{12}\exp\left(\frac{-2\alpha_i d_1}{\cos\theta_i}\right)\sum_{i=1}\left|R_{12}R_{10}\exp\left(\frac{-2\alpha_i d_\cdot}{\cos\theta_i}\right)\right|^{i=1}$$

$$\bar{\rho}_i = \frac{R_{10}T_{12}\exp\left(\frac{-2\alpha_i d_1}{\cos\theta_i}\right)}{1 - R_{12}R_{10}\exp\left(\frac{-2\alpha_i d_1}{\cos\theta_i}\right)}$$

The transition from slab 2 to slab 1 (T21) is also neglected.

Transmission over Two Slabs

We'll now look at an optical system made up of slabs 1 and 2. There are reflections across two slabs (between the top border of one slab and the lower boundary of the other) in addition to the internal reflections inside each slab that need to be taken into account. The rays and their infinite series are summed up as slab transmittances and slab reflectances p to keep the illustration simple. Bold arrows in Figure 17.6 indicate how to achieve this. The most direct entrance into slab 3 is shown in the accompanying fraction:

$$\tau_{12,1} = \frac{\tau_1 \tau_2}{T_{12}}$$

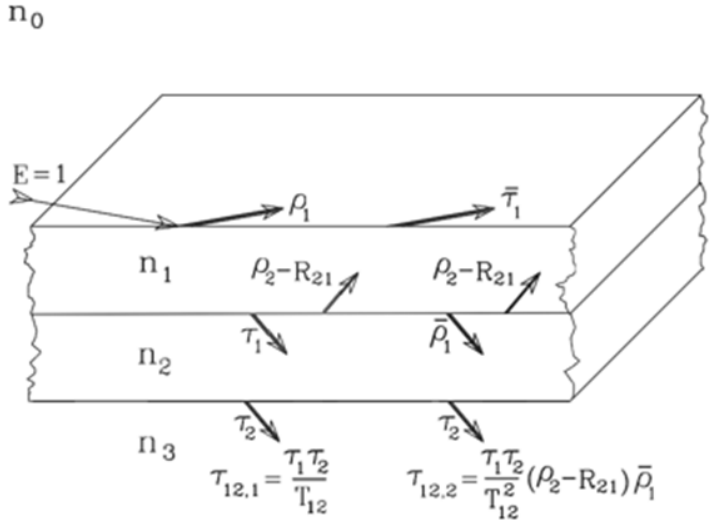

Figure 17.6: ***Illustrates*** **the Transmittance of an optical system consisting of two optical slabs.**

It should be noted that the reflection at the boundary 1-2 has been considered in both 1 and 2 for the combination of the slab transmittances 1 and 2. T12 must thus be adjusted by 12 once. As a result, this must be done for each further slab combinations up to k+1.

Transmission through three slabs

Now, the module encapsulation is seen as three slabs with various optical characteristics (see in Figure 17.7). As determined in the higher chapter, the two upper slabs 1 and 2 are now regarded as a system with a shared transmittance and common reflectance. Therefore, only interactions between slab system 12 and the new slab 3 need to be taken into account, such as transmittances and internal reflections[9], [10].

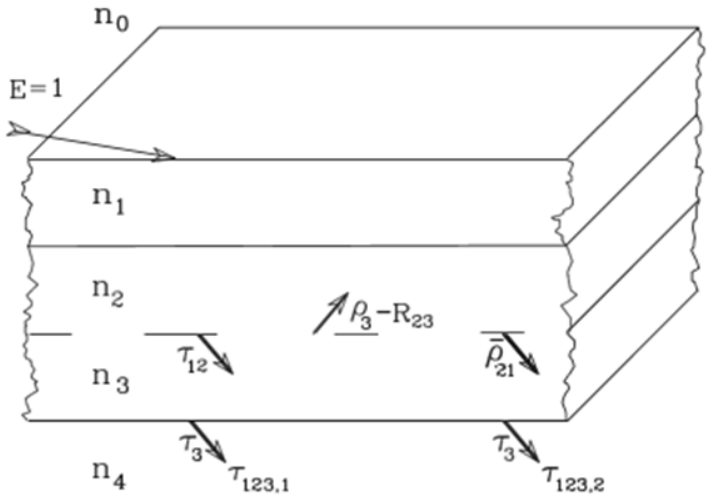

Figure 17.7: ***Illustrates*** **the transmittance of an optical system consisting of three optical slabs**.

The ray is divided into a transmitted and a reflected portion at the module surface (i.e., slab 1), and the latter merges with the fractions reflected at the inner borders at absorptive attenuation to travel towards the boundary layer of slab 2. In light of this, the transmission of slabs 2 and 3 follows the same pattern. Due to their shared transmittance and shared reflectance, the two higher slabs 1 and 2 are now regarded as a system. The findings for the fraction entering slab 4 are as follows:

Transformer

Electricity is transferred from one circuit to another through electrical transformers, which modify the voltage level but don't change the frequency. They were designed to use an AC supply, therefore differences in the supply voltage must effect variations throughout the current. As a consequence, an increase in voltage and vice versa will happen as current increases. Transformers contribute to the reliability and efficiency of energy networks by altering voltage levels as needed. Although they are used in a variety of domestic and professional contexts, the long-distance distribution and regulation of electricity may be their most significant usage. Transformer: Transformer functioning is based on the idea of mutual induction. An iron core connects the transformer's windings. A voltage is produced in the windings as a result of the permeability in the core, which links the primary and secondary windings. The workings of the transformer are explained in the paragraphs that follow. An alternating voltage is applied to the main winding, where causes magnetizing potential to flow through it. As a result, magnetizing flux is generated and concentrated in the contained

low reluctance permanent magnets path. This flux links the primary and secondary windings together. Voltage is self-induced throughout the main winding and the secondary winding, accordingly. Each turn, the voltage output is the same in the primary and the secondary windings. The temperature throughout the windings is influenced by the winding's number of turns. Depending on the voltage level, there are two different kinds of transformers: step up transformers and step down transformers. Its electrical voltage is increased by using step-up transformers. Transformers called step downs are used to reduce electrical voltage. Instrumentation transformers, distribution lines, and power generating equipment make up the three types of transformers.

REFERENCES

[1] S. H. Tan en P. P. Rohde, "The resurgence of the linear optics quantum interferometer — recent advances & applications", *Reviews in Physics*. 2019. doi: 10.1016/j.revip.2019.100030.

[2] P. S. Salter en M. J. Booth, "Adaptive optics in laser processing", *Light: Science and Applications*. 2019. doi: 10.1038/s41377-019-0215-1.

[3] A. Zolfaghari, T. Chen, en A. Y. Yi, "Additive manufacturing of precision optics at micro and nanoscale", *International Journal of Extreme Manufacturing*. 2019. doi: 10.1088/2631-7990/ab0fa5.

[4] M. Hahsler, M. Piekenbrock, en D. Doran, "Dbscan: Fast density-based clustering with R", *J. Stat. Softw.*, 2019, doi: 10.18637/jss.v091.i01.

[5] S. Hippler, "Adaptive Optics for Extremely Large Telescopes", *J. Astron. Instrum.*, 2019, doi: 10.1142/S2251171719500016.

[6] J. M. Dudley, G. Genty, A. Mussot, A. Chabchoub, en F. Dias, "Rogue waves and analogies in optics and oceanography", *Nature Reviews Physics*. 2019. doi: 10.1038/s42254-019-0100-0.

[7] M. J. Townson, O. J. D. Farley, G. Orban de Xivry, J. Osborn, en A. P. Reeves, "AOtools: a Python package for adaptive optics modelling and analysis", *Opt. Express*, 2019, doi: 10.1364/oe.27.031316.

[8] I. D'Amico *et al.*, "Nanoscale quantum optics", *Riv. del Nuovo Cim.*, 2019, doi: 10.1393/ncr/i2019-10158-0.

[9] G. W. Burr, "A role for optics in AI hardware", *Nature*. 2019. doi: 10.1038/d41586-019-01406-0.

[10] K. Wang *et al.*, "Graphene transistor based on tunable Dirac fermion optics", *Proc. Natl. Acad. Sci. U. S. A.*, 2019, doi: 10.1073/pnas.1816119116.

CHAPTER 18

TRANSFORMER WORKING PRINCIPLE OF TRANSFORMER

Mr. Sunil Dubey, Associate Professor,
Department of Electrical Engineering, Jaipur National University, Jaipur India
Email Id- sunildubey@jnujaipur.ac.in

A transformer is made up of a laminated steel core and two inductive windings. The coils and steel core are separated from one another. An oil regulator that can provide oil to cool its transformer tank, suitable bushings for connecting terminals, a tank-like container for both the winding and cores assembly, and other parts may also be found in a transformer. Figure 18.1 on the left depicts a transformer's basic structure. The cores of all types of transformers are constructed by stacking or combining laminated steel sheets with little to no gap separating them (to achieve continuous magnetic path). The steel used does have a high silicon content and is occasionally heat treated to provide high permeability and minimum hysteresis loss. Eddy current losses are minimized by using laminated steel sheets. E, I, while L are formed from the sheets. To avoid excessive impedance at joints, laminations are layered by flipping the sides of joints. In those other words, if the joints of the first sheet construction are located on the front face, the joints of the next assembly will be located on the back face [1], [2].

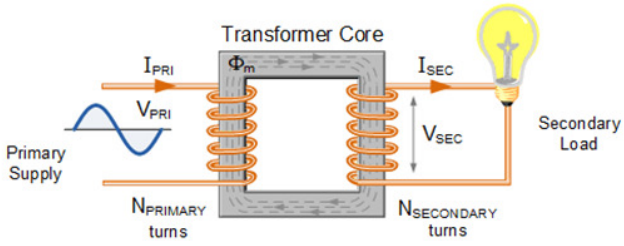

Figure 18.1: *Illustrates* the circuit diagram of transformer.

Transformer Construction (single-phase):

Keep in mind that perhaps the two coil windings are just magnetically coupled and not electrically connected. A single-phase transformer may be used to alter the voltage provided to the primary winding shown Figure 18.2by either raising or lowering it.

When a transformer is used to "increase" the voltage within its own secondary winding in relation to the primary, it is referenced to as a step-up transformer. To "decrease" the voltage on a certain secondary winding in relation to the main, step-down transformers were utilized[3], [4].

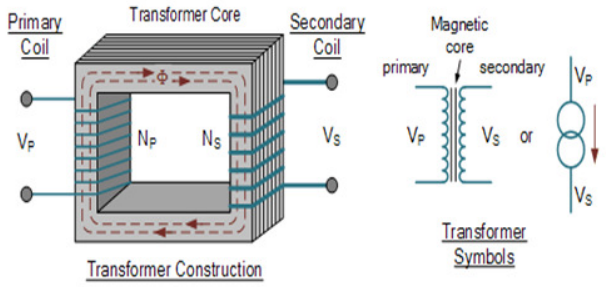

Figure 18.2: ***Illustrates*** **the circuit diagram of single phase transformer.**

Where:

VP is equal to the Primary Voltage

VS is equal to the Secondary Voltage

NP is equal to the Number of Primary Windings

NS is equal to the Number of Secondary Windings

Φ (phase) is equal to the Flux Linkage.

Remember that the two coil windings really aren't electrically linked, but merely magnetically related. A single-phase transformer could alter the voltage provided to the main winding while it is in operation. When a transformer is used to "increase" the voltage its own secondary winding in relation to the primary, it is called to as a step-up transformer. To "decrease" the voltage upon that secondary coil in relation to the main, step-down transformers are utilized. Furthermore, there is a third situation that takes place whenever a transformer's secondary voltage is equal to the main winding's voltage differential. In other terms, the output's voltages, current, and power are exactly the same. These transformers, also known as impedance transformers, are often used for resonant frequency or even when separating neighboring electrical circuits[5], [6].

A Transformers Turns Ratio

By adjusting the number of coil rounds in the primary winding (NP) in relation to the number of coils turns upon that secondary winding, the voltage differential between both the primary and secondary windings may be produced (NS). There is now a ratio between the main coil's turns divided by that of the secondary coil's turns since the transformer is essentially a linear device. This ratio, sometimes known as a transformer's "turns ratio" or the ratio of transformation (TR). The transformer's functioning and the accompanying voltage present just on secondary winding are determined by the ratio value of the turn. The proportion of wire turns on the main winding to those on the secondary winding must be understood. The turn's ratio, which compares both two windings in sequence and has no measures, is expressed with a colon, for example, 3:1. (3-to-1). According to this example, 3 volts on the main winding will result in 1 volt here on secondary winding, or a 3 volts-to-1 volt ratio. The resultant voltages must vary in the same ratio if the proportion between the numbers of turns varies, and this is true. The theme of Transformers is "ratios." Any particular transformer's primary to secondary ratio, inputs to ratio of output, and turn ratio will all be equal to that transformer's reference voltage. In other terms, "turns ratio = voltage ratio" for something like a transformer. Just the turn’s ratio matters, not really the actual number of cable turns on any particular winding, and this correlation is represented as: Formula for ratio transformation.

$$\frac{N_P}{N_S} = \frac{V_P}{V_S} = n = \text{turn ratio}$$

Considering the phase angles and a perfect transformer: ΦP ≡ ΦS Because the turns ratio 3:1 represents a completely different transformer relationships and output voltage from a situation in which the turns ratio is presented as: 1:3, it is vital to note that perhaps the order of the numbers is crucial when describing a transformer's turns ratio value[7], [8].

Transformer Action

As people've seen, the turn ratio, or the ratio of secondary winding to primary winding coils turns, influences the voltage output of the secondary coil. However, how does this secondary voltage created if the two windings remain electronically insulated from one another. A transformer, as shown in Figure 18.3, essentially consists of two coils twisted around a single soft iron core.

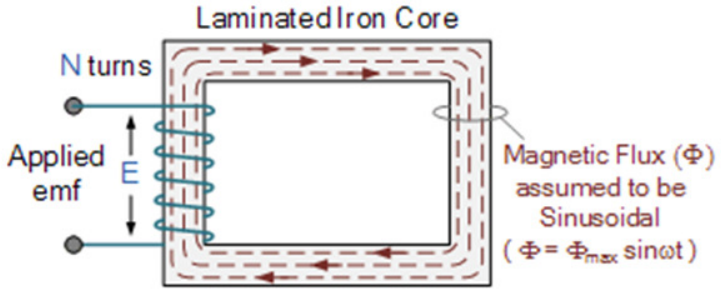

Figure 18.3: *Illustrates* the inner surface component of transformer.

The main coil receives current whenever an alternating voltage (VP) is provided, which causes the coil to create a magnetism around itself. Faraday's Law of electromagnetic induction refers to this phenomenon as mutual inductance. As even the current flow increases from zero to its optimum amount, denoted as d/dt, the magnetic field becomes stronger. The soft inner core of the this electromagnet creates a route for and focuses the magnetic flux as that of the magnetic field and the direction it has created extend outward from the coil. Under the effect of the AC supply, that magnetic flux rises and decreases in opposing directions, connecting the turns of the both windings. The amount of current as well as the number of turns throughout the winding, however, determine the intensity of the magnetic field that is induced into to the soft core of iron. The magnetic field intensity decreases when current is decreased. A voltage is induced into in the secondary coil whenever the magnetic streams of flux travel around the core and pass through to the turns of a secondary winding. N*d/dt (Faraday's Law), where N represents the number many coil turns, will determine how much voltage is generated. Additionally, the main winding voltage and this induced voltage have the same frequency. As a result of the identical magnetic flux connecting the turns of both windings, we can observe that the same potential is generated in each coils turn of both windings[9], [10]. As a consequence, each winding's overall induced voltage is inversely proportional to the number of revolutions in that winding. However, if the magnetic inefficiencies of the core are considerable, the peak magnitude of the output voltage accessible upon that secondary winding will indeed be decreased.

They may either transmit more current through the primary coil or maintain the same flow of current while enhancing the number the coil turns (NP) of the wrapping in order to boost the

primary coil's ability to generate a magnetic field strong enough to overcome the core's magnetic losses. The "ampere-turns," a product of amperes and turns, is what defines the coil's magnetizing power. So let's assume we have a transformer with something like a single main turn and a single secondary turn. If there are no losses and one volt is delivered to the primary coil's one turn, enough power must flow and magnetic flux must be produced to induce one voltage in the secondary coil's one turn. In other words, each winding can handle the same amount of volts every turn. The fundamental connection between the induced emf, (E) in a coil winding with N turns being given by when the magnetic flux fluctuates sinusoid ally = max, sint:

Emf = turns x rate of change:

$$E = N\frac{d\emptyset}{dt}$$

$$E = N * \omega * \emptyset_{max} * \cos \omega t$$

$$E_{max} = N\omega\emptyset_{max}$$

$$E_{rms} = \frac{N\omega}{\sqrt{2}}\emptyset_{max} = \frac{2\pi}{\sqrt{2}} * f * N * \emptyset_{max}$$

Where:

f= is the flux frequency in Hertz, = ω/2π

N= is the number of coil windings.

Φ=is the amount of flux in Webbers$E_{rms} = 4.44\ fN\emptyset_{max}$

Electrical Power in a Transformer

The power rating of the transformer is yet another of its fundamental characteristics. Simply calculating the current even by voltage to get a rating in Volt-amperes gives you the power rating of a transformer (VA). Larger power transformers were rated in Kilo volt-amperes (kVA), where 1 kilo volt-ampere is equivalent to 1,000 volt-amperes, or Mega volt-amperes (MVA), wherein 1 mega volt-ampere is equivalent to 1 million volt-amperes. Single small component transformers may simply be measured in volt-amperes. Since transformers are constant-wattage devices and only vary the voltages to current ratio, the power available inside the secondary coil and the primary winding will be equal in a perfect transformer (again, disregarding any losses). In a perfect transformer, total voltage, V, multiplied by that of the current, I, will always stay constant, making the Power Ratio equal to just one (unity). In other words, electricity generation on the primary side place at a single voltage/current level is "converted" into electric power on the secondary side using the same frequency and voltage/current level. The transformer may increase (or decrease) voltage, but it cannot increase power. The output current always seems to be equal to the input power since a transformer steps up a voltages while stepping down a current and vice versa. When primary power matches secondary power, we may say that (PP = PS).

Power in a Transformer

$$Power_{Primary} = Power_{Secondary}$$

$$Power_{Primary} = Power_{Secondary} = V_P I_P \cos \emptyset_P = V_S I_S \cos \emptyset_S$$

The main phase angle is P, while the secondary phase angle is S.Keep in mind that because

power loss is inversely proportional to the square of both the transmitted current, that is: I2R, doubling the voltage, for example, would reduce the current by exactly the same amount while providing the same quantity of electricity to the load, resulting in a 4x reduction in losses. The total losses would be decreased by an amount of 100 if the voltage were raised by a ratio of 10, and the current would fall by the same amount.

Transformer Basics – Efficiency

A transformer may transmit energy without the need of any moving components. This indicates that no losses due to friction and wind age are present in other electrical equipment. Transformers do experience additional kinds of losses, referred to as "copper losses" and "iron losses," although these are often fairly minor. The electrical power that is lost in heat as a consequence of the currents flowing through the copper windings of a transformers is known as copper losses, also known simply I2R loss. The biggest loss in a transformer's functioning is due to copper losses. By square the amperes then multiplying by the winding's resistance in ohms, it is possible to calculate the actual watts of power lost (in each winding) (I2R). The lagging of the magnetic molecules throughout the core in proportion to the switching magnetic flux is known called iron losses, also referred as hysteresis. The reason for this trailing (or out-of-phase) state is because magnetic molecules need power to reverse; they don't do so until the flux has enough force to do so. Their reversal causes friction, and heat is created in the core as a consequence of friction, which is a sort of power loss. By using particular steel alloys for the core, hysteresis within in the transformers may be reduced. The amount of electricity lost by a transformer affects how efficient it is. Power (wattage) loss between both the main (input) and secondary (output) field winding of a transformers is a measure of its efficiency. As a consequence, a transformer's efficiency is high and equal towards the proportion of the input power toward the primary winding (PP) and output (PS) of both the secondary winding.

An ideal transformer should transfer all of the electricity generated it receives on one of its primary side to its own secondary side with a 100% efficiency rate. Real transformers, however, are not always as effective. Their greatest efficiency while working at full maximum load is closer to 94% and 96%, which is nonetheless pretty respectable for an electrical equipment. A transformer's efficiency may reach up to 98% when it is running at a steady AC voltage and frequency. A transformer's efficiency is stated as:

Transformer Efficiency

Where: Power units are used to represent input, output, and losses.

$$Efficiency, \eta = \frac{output\ power}{input\ power} * 100\%$$

$$= \frac{input\ power - Losses}{input\ power} * 100\%$$

$$= \frac{1 - Losses}{input\ power} * 100\%$$

When discussing transformers, the main watts are often referred to as "volt-amps," or VA, to distinguish them from either the secondary watts. The efficiency equation may then be changed to:

$$Efficiency, \eta = \frac{secondary\ watts\ (output)}{Primary\ VA\ (Input)}$$

When studying about the fundamentals of transformers, utilizing images may help students retain the connection between the input, output, and efficiency of the transformer. Here, the three values of VA, W, and have been stacked to form a triangle, with the top representing power in megawatts and the bottom representing volt-amps and efficiency. This configuration accurately reflects where each number really sits in the efficiency formulae. I'll then wrap up my primer on transformer fundamentals. A magnetic field is used by a transformer to convert one value on its own output winding to a different amount of voltage (or current) on its input winding. A transformer is made up of two electrically separate coils and works on the Faraday principle of "faraday's law of induction," according to which the magnetic flux produced by the currents and voltages passing in the main coil winding induces an EMF in the transformer's second winding.

To minimize eddy current and power inefficiencies, the main and secondary coil secondary winding are both wrapped around a single, individually laminated soft iron core. The secondary winding of the transformer distributes electricity to the load, whereas the stator windings of the transformer is linked to the AC power source that must be sinusoidal in nature. However, if the voltage and current ratings are followed, a transformer may be utilized in reversal with both the slightly greater to the secondary coil.

Transformer Construction

A magnetic circuit, more generally referred to as the "transformer core," is part of the architecture of a transformer and is intended to provide a channel for the magnetic field to travel around. The voltage induction between both the two input and output windings requires this magnetic route. However, because the primary and secondary windings are so far apart from one another, this style of transformer design, in which the two windings are coiled on different limbs, is not particularly effective. Low magnetic connection between both the two windings and significant magnetic flux leakage from either the transformer itself are the effects of this. But in addition to this "O" shape structure, there are many "transformer construction" kinds and designs that may be employed to get around these shortcomings and create a smaller, more condensed transformer. By putting the two windings into close proximity to one another and enhancing the magnetic coupling, it is possible to increase the efficiency of a straightforward transformer design. The magnetic coupling between the secondary winding may be improved by enlarging and intensifying the magnetic circuit surrounding the coils, but doing so also results in an increase in the magnetic cores of the transformer core.

The cores is designed to avoid flowing electric currents only within iron core itself in addition to providing a low resistance route for the magnetic field. Eddy currents, which circulate and produce energy losses and core heating, reduce the transformer's effectiveness. The iron circuit, which would be continually exposed to the opposing magnetic fields created by the external sinusoidal voltage supply, is the principal cause of these losses. Voltages produced in the iron circuit are what cause these voltages. Making the transformer core out of thin steel laminations is one technique to cut down on these undesired power losses. The center iron core of the majority of transformer designs is formed of a high permeability material, often from thin silicon strong materials. These thin reinforcements are put together in an assembly to provide the necessary magnetic route with the least amount of magnetic loss. Because the steel sheet itself has a high resistivity, potential eddy current loss may be minimized by using thin laminations. Those steel transformer couplers range in thickness

from 0.25 mm to 0.5 mm, and since steel conducts electricity, they are electrically isolated from any fastening studs, rivets, or bolts by a very thin layer of insulating varnishes or through the application of a corrosion products to the surface.

Transformer Construction of the Core

Generally, the name associated with the construction of a transformer is dependent upon how the primary and secondary windings are wound around the central laminated steel core. The two most common and basic designs of transformer construction are the Closed-core Transformer and the Shell-core Transformer. In the "closed-core" type (core form) transformer, the primary and secondary windings are wound outside and surround the core ring. In the "shell type" (shell form) transformer, the primary and secondary windings pass inside the steel magnetic circuit (core) which forms a shell around the windings as shown in Figure18.4.

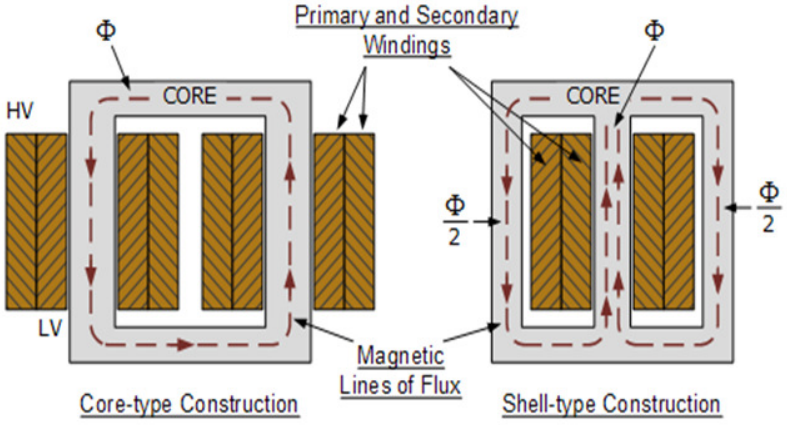

Figure 18.4: ***Illustrates*** **the core and shell type construction of transformer.**

The magnetic flux between the main and secondary windings flows wholly inside the core in both kinds of transformer core designs, with no dissipation of magnetic flux via air. Approximately half of the winding is wrapped around every leg (or limb) of a transformer's magnetic circuit when it is constructed using a core type transformer. In order to increase permanent magnets and allow virtually all magnetic lines of force to pass across both the primary and secondary windings while simultaneously time, the coils are not set up with the primary winding on one leg as well as the secondary winding on the opposite. Instead, half of a primary winding as well as half of both the secondary winding are stacked circumferentially on each leg. The term "leakage flux" refers to the tiny amount of magnetic force lines that flow beyond the core of this kind of transformer.The primary and secondary windings of shell type power transformers are wrapped on the same central leg, which has double the cross-sectional surface of the two outer limbs, therefore preventing leakage flux. The magnetic flux maintains two intense magnetic routes outside the coils upon that left and right without recovering to the core coils, which is advantageous in this situation. As a result, the magnetic flux flowing from around outer extremities of this particular transformer design is equal to /2. Due to the closed route that the magnetic flux takes around the coils, core losses are reduced and overall efficiency is improved.

Transformer Laminations

However, one may be asking how the main and secondary windings for these sorts of transformer structures are twisted around these laminated iron or stainless steel cores. The coils are initially coiled on a former with a cross section of a kind that is cylinder, rectangular, or oval to fit the construction of both the laminated core. Within both the shell and core type transformers designs, the individual reinforcements are punched out or pressed from larger steel sheets forming thin steel strips that resemble the characters "E"s, "L"s, "U"s, and "I" as needed to install the coil field winding.

Transformer Core Types

When joined, these lamination stampings provide the necessary core shape. One component of a typical shell-type transformer core shown Figure 18.5 is an E-I core, which is made up of two "E" stampings and two end closing "I" stampings. In order to decrease the resistance of the air gap there at connections during construction, these separate laminations are closely butted together, creating a highly saturated density of magnetic flux. In order to create an overlapped junction and the proper core thickness, equipment and other facilities laminations are often stacked alternatively one on top of the other. Reduced flux leakage reduced demagnetization are further advantages of this alternative stacking of something like the laminate again for transformer. Most isolation transformers, step-up and step-down transformers, in addition to auto transformers, employ an E-I core laminated transformer architecture.

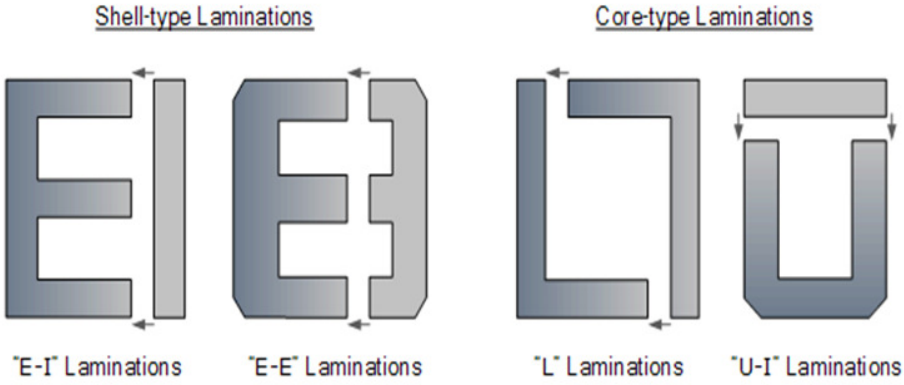

Figure 18.5: *Illustrates* the circuitry of shell and core type's laminations.

Transformer Winding Arrangements

Transformer windings, which are the primary current-carrying conductors coiled around the laminated portions of the core, are another crucial component of a transformer's design. Two windings would be included in a single-phase, two-winding transformer, as depicted. The main winding is the one that is linked to the voltage source, generates the magnetic flux, and induces a voltage by mutual induction throughout the secondary winding. A transformer is referred to as a "Step-down Transformer" if indeed the secondary output voltage is less than the main input power. A "Step-up Transformer" is referred to as such if this same secondary output voltage is higher than that of the main input voltage.

Either copper or aluminum wire is utilized as the primary current-carrying component in some kind of a transformer winding. Although aluminum wire is lighter and often less costly than copper wire, it is primarily employed in bigger power transformer operations because a

higher cross-sectional area of conductors is required to convey the same amount of electricity as with copper. Copper conductors are often utilized in low voltage electronic and electronic circuits because they have a better mechanical strength as well as a smaller connector size than corresponding aluminum kinds. This is especially true for tiny kVA acceptable voltage transformers. The drawback is that these transformers may be rather heavy when they are fully assembled with their cores.

Concentric coils and sandwiched circuits are two major categories for transformer windings and circuits. The windings are often placed concentrically around at the core limbs in core-type method is implemented, as illustrated above, with both the higher voltage secondary conducting being coiled above the lower voltage secondary winding. Sandwiched or "pancake" coils are made out of flat conductors twisted in a spiral shape; the term comes from the way the conductors are arranged into discs. Individual coils are piled together and kept apart by insulation material like paper or plastic sheet, while alternate discs are designed to spiral around the outside towards to the center in an interleaved manner. With a core architecture of the shell type, sandwich coils intermediate windings are much more prevalent.

Figure 18.6 shows another typical cylindrical coil configuration used in low voltage, high current transformer applications: helical windings, commonly known as screw windings. Large cross-section rectangular conductors are used to make the windings, which are then wound on their sides with insulated strands running continuously parallel along the duration of the cylinder. Appropriate spacers are implanted between adjacent did turn or diskettes to reduce turbulent flows between both the parallel strands. The coil advances in the shape of a corkscrew as it spirals outward. In an air-cooled transformers, a thin coating of varnish or enamel serves as the insulation to preventing the conductors from short - circuiting to one another. The wire is coated with this thin coat of varnish or enameled painting before being looped around the core. Larger transmission and distribution equipment use oil-impregnated sheets or cloth to insulation the conductors from one another. The whole cores and field winding are submerged and enclosed in a tank of transformer oil for protection. The transformer oil functions as a coolant as well as an insulator.

Figure 18.6: *Illustrates* the diagram of transformer core.

Transformer Dot Orientation

A laminated core cannot simply include one of the coil configurations wrapped around it. The secondary current and voltage may not be in phase with the main voltage and current, however that is a possibility. The orientation of each of the two current coil in relation to the other is unique. To maintain track of their respective orientations and since each coil might be coiled around the core in either the clockwise or an anticlockwise direction, "dots" are employed to designate a specific end of the each winding. The "dot convention" is the name

given to this technique for determining a transformer's orientation or winding direction. The transformer's polarity is then defined by the relative polarity of something like the secondary winding with regard to the primary voltage, after which the windings of a transformers were wound such that the right phase relationships exist between the winding energies.

Transformer Construction using Dot Orientation

In Figure 18.7, the first transformer's two "dots" are shown next to one another on its two windings. The current approaching the main side dot and the current exiting the secondary dot are "in-phase." Because of this, the polarities of something like the voltages there at dotted ends are also in phase, however when the voltage is positive there at dotted end of the main coil, it is likewise positive there at dotted extremity of the secondary coil.

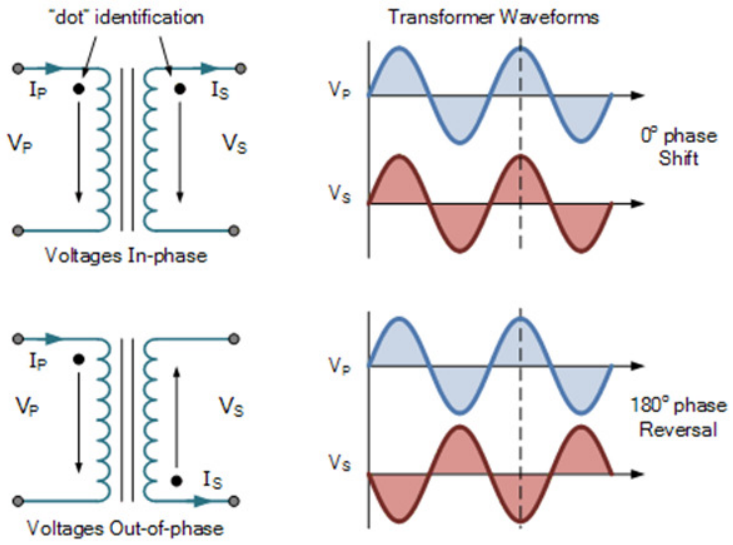

Figure 18.7: ***Illustrates*** **the construction of transformer by using dot orientation.**

The secondary and primary coil secondary winding of a second transformer are coiled in the opposite directions, as shown by the two dots at the windings' opposing ends. Because of this, the current approaching the main dot and the current exiting the secondary dot are 180o "out-of-phase." As a result, the polarity of the energies at the dotted endpoints are also out of phase, thus while the main coil's dotted end is positive, the voltage from across corresponding second winding will be negative. The power transfer may then be built into a transformer in such a way that it is either "in-phase" with the main voltage or "out-of-phase" with that as well. To communicate transformers throughout series-aiding (secondary voltage is summed) or series-opposing (secondary voltage is the difference) configurations, which require a number of distinct secondary windings that were already electrically separated from one another, it is crucial to understand the dot polarity of each secondary winding. It is often useful to have the option of adjusting a transformer's turn ratio to counteract the impacts of changes in the main supply voltage, the transformer's regulation, or shifting load circumstances. The transformer's voltage is often controlled by adjusting the turn ratio, which affects the voltage ratio. To facilitate this modification, a portion of the main winding here on high voltage side usually tapped off. Due to the lower voltages per revolution upon that high voltage side compared to the low frequency secondary side, tapping is favored there.

Transformer Primary Tap Changes

In this simple example, the principal tap changes are computed for a 5% change in supply voltage, although any value may be used. As shown in Figure 18.8, certain transformers with a single core may include two or even more secondary windings or multiple or more main windings to be utilized in various applications.

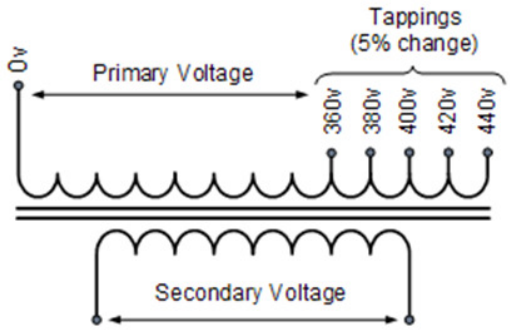

Figure 18.8: *Illustrates* the circuit diagram of Primary Tap Changes.

REFERENCES

[1] J. Cui, L. Qu, en W. Qiao, "A single-phase electromagnetic transformer with an adjustable output voltage", 2019. doi: 10.1109/ECCE.2019.8912933.

[2] J. Wang, Q. Zhou, Z. Lu, Z. Wei, en W. Zeng, "Gas sensing performances and mechanism at atomic level of Au-MoS2 microspheres", *Appl. Surf. Sci.*, 2019, doi: 10.1016/j.apsusc.2019.06.075.

[3] A. Suresh Kumar, R. K. Pongiannan, C. Bharatiraja, A. Yusuf, en N. Yadaiah, "A magnetically coupled converter connected three phase voltage source inverter for EV applications", *Int. J. Power Electron. Drive Syst.*, 2019, doi: 10.11591/ijpeds.v10.i2.pp645-652.

[4] W. Deng, Y. Yang, Y. Guo, en L. Li, "Research on predictive control about TSMC hybrid transformer", *Dianli Xitong Baohu yu Kongzhi/Power Syst. Prot. Control*, 2019, doi: 10.19783/j.cnki.pspc.180728.

[5] X. Hu, P. Ma, B. Gao, en M. Zhang, "An Integrated Step-Up Inverter Without Transformer and Leakage Current for Grid-Connected Photovoltaic System", *IEEE Trans. Power Electron.*, 2019, doi: 10.1109/TPEL.2019.2895324.

[6] X. Xinze *et al.*, "DC transformer requirements and fault operation analysis in PV medium voltage DC power collection system", *J. Eng.*, 2019, doi: 10.1049/joe.2019.0798.

[7] F. Pang, Y. Liu, J. Ji, Q. Bu, en C. Zhang, "On-site transient performance calibration of DC current transformer for HVDC transmission project", *Dianli Xitong Baohu yu Kongzhi/Power Syst. Prot. Control*, 2019, doi: 10.19783/j.cnki.pspc.180947.

[8] J. X. Yuan, C. S. Wang, Y. Zhu, J. P. Dong, C. H. Tian, en B. C. Chen, "Soft start method of super large capacity and high voltage motor", *Dianji yu Kongzhi Xuebao/Electric Mach. Control*, 2019, doi: 10.15938/j.emc.2019.04.008.

[9] J. Alammar, "The Illustrated Transformer", *Blog*, 2019.

[10] T. Shao, Y. Guo, H. Chen, en Z. Hao, "Transformer-Based Neural Network for Answer Selection in Question Answering", *IEEE Access*, 2019, doi: 10.1109/ACCESS.2019.2900753.

CHAPTER 19

TRANSFORMER CONSTRUCTION – CORE LOSSES

Mr. Harsh Shrivastava, Assistant Professor,
Department of Electrical Engineering, Jaipur National University, Jaipur India
Email Id- ershrivastava@jnujaipur.ac.in

The capacity to enable magnetic flux to circulate is known as permeability, and it is significantly larger in steel or iron compared to that of air. The majority of transformer cores are made of low carbon steel, which has a susceptibility of up to 1500 as opposed to merely 1.0 for air. This indicates that a steel laminated cores is capable of carrying a magnetic flux 1500 percent stronger than air. Nevertheless, two different forms of losses throughout the steel happen when a magnetic flux runs in the core material of a transformers. Eddy current losses on the one hand, and hysteresis effects on the other hand".

Hysteresis Losses

Hysteresis of the Transformer Because to such sinusoidal supply voltage's impact, magnetic lines of force that are necessary to magnetize the core regularly change in value and direction, first in one direction before switching to the other, therefore results in losses. Heat is produced as a result of this molecular friction, which costs the transformer energy. The lifespan of the insulating materials used for the construction of the windings and structures might be shortened over time by extreme heat loss. As a result, a transformer's cooling is crucial. Transformers are also built to function at a certain supply frequency. Decreasing the supply frequency will enhance hysteresis and raise the iron core's temperature. Therefore, dropping the supply frequency between 60 Hertz to 50 Hertz will elevate the amount of hysteresis occurring and lower the transformer's VA capacity[1], [2].

Eddy Current Losses

On the other hand, circulating currents that are induced into steel as a result of the passage of the magnetic flux from around core are what lead to transformer eddy current losses. Continuous circulating currents are produced as a result of the core behaving like a single wire loop throughout the magnetic flux. The eddy currents produced by a solid iron core will have to be substantial since iron is an excellent conductor. Instead of enhancing the utility of the transformer, eddy currents serve as a negative force that causes the core of the transformer to heat up and lose power as they fight the flow of induced emf[3], [4].

Laminating the Iron Core

Although eddy current losses inside a transformer core can indeed be totally avoided, they may be significantly decreased and managed by reducing this same steel core's thickness. The magnetic path of the transformers or coil is divided up into several thin pressed steel forms known as "laminations" rather than having one large solid iron core in Figure 19.1.

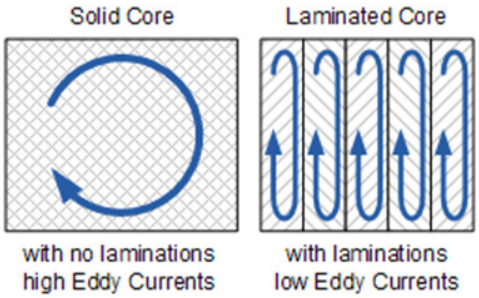

Figure 19.1: ***Illustrates*** **the laminating the iron core of transformer.**

As we saw above, the laminations employed in the building of a transformer are made of very small slices of insulated metal linked together to create a solid yet laminated core. To improve the effective resistivity of a core and hence raise the overall resistance to restrict the passage of the eddy currents, those laminations are separated from one another by a layer of varnish of paper. All of this insulation has the effect of significantly reducing the unwelcome generated eddy current power loss in the core, which is why every magnetic iron circuit in every transformers as well as other electro-magnetic equipment is laminated. Eddy current inefficiencies in method is implemented are decreased by using reinforcement bars[5], [6].

Transformer Construction – Copper Losses

The term "transformer core losses" refers to the energy losses, which manifest as heat owing to hysteresis as well as eddy currents throughout the magnetic path. Because alternating magnetic fields cause these losses throughout all magnetic materials, Even if there is no load attached to the secondary winding, a transformers will always have core losses anytime the main winding is activated. As the magnetic flux generating these losses was constant at any and all loads, the conjunction of hysteresis and electrical resistance losses is sometimes known to as "transformer iron losses.

Copper Losses

However, the transformer is also responsible for a different kind of energy loss known as "copper losses." Transformer The resistance value of the secondary and primary windings is the major cause of copper losses. The majority of transformer coils are wrapped using copper wire, which has a resistance value in Ohms (). According to Ohms Law, any magnetic currents passing through copper wire will be resisted by the copper string's resistance. Large electrical currents begin to flow between the main and secondary windings of a transformer when an excess electricity is attached to the secondary winding, and electrical power and energy losses (the I2 R) happen as heat. Copper losses often change with both the load current, ranging from practically nil at no load to a maximum during full load whenever current flow is at it's greatest. To decrease these core and copper losses, a transformer's volt-amperes (VA) rating may be raised by improved design and construction. Conductors having a wide cross-section are needed for a transformer having high rating of voltage and current in order to reduce copper losses. By enhancing its insulation to tolerate greater temperatures or by boosting the rate at which heat drainage (better cooling) using pressurized air or oil, the transformer's VA rating may be raised. Thus, a perfect transformer would have the following characteristics:

1. Hysteresis losses and loops are both zero.
2. Zero Electromotive Force Losses due to Core Material's Infinite Resistivity 0
3. Zero winding impedance results in zero I2*R copper losses, which equals zero.

Transformer Loading

In the earlier lessons on transformers, they used the assumption that the transformer was perfect, meaning it had no core losses and no copper losses inside the transformer's windings. However, losses related to transformer overloading will always occur when a transformer is placed "on-load" in the actual world. Let's first examine what happened to a transformers when it is in this "no-load" state, which is in which there is no electrical load attached to the transformer's secondary winding and no secondary current will flow as a result. When a transformer's secondary side winding completely open circuited, meaning that nothing is connected as well as the transformer loading is zero, such transformer is described as being "on no-load." A minor current, IOPEN, will flow through into the primary coil winding of a transformer whenever an AC sinusoidal power source is connected to the primary winding because the standard power voltage is present. This primary current's flow is limited by a back EMF and the primary winding impedance while the secondary circuit is unconnected and open. Clearly, this no-load primary current (Io) should be enough to sustain a sufficient gravitational flux in order to generate the necessary back emf[7], [8].

Transformer "No-load" Condition

Despite the fact that secondary circuit in Figure 19.2 is open circuited, the ammeter above should show a modest current that flows through the primary winding. The following two elements make up this no-load main current:

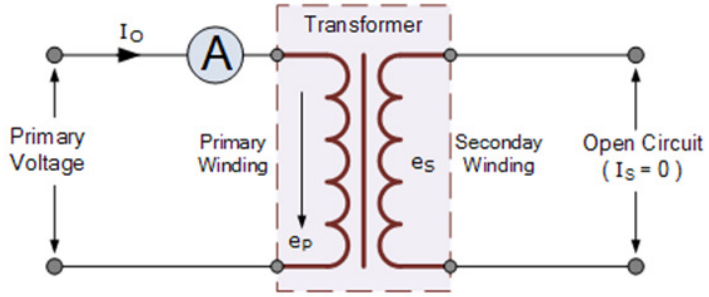

Figure 19.2: *Illustrates* the circuit diagram of Transformer "No-load" Condition.

1. A current that is in phase and provides the core losses (eddy current and hysteresis).
2. A little current, IM at 90 degrees to the voltage that creates the magnetic flux.

Transformer "On-load"

A current flows throughout the secondary winding and to the load whenever an excess electricity is attached to a transformer's secondary winding and the transformer overloading is therefore higher than zero. The magnetic flux generated in the core by the main current is what causes the carried out effectively, which is caused by the induced voltage supply.

In the transformer core, the secondary winding, IS, which depends on the load's characteristic, induces a secondary magnetic field, S, which moves in the absolute reverse direction of the main primary field, P. Due to the opposition between these two

electromagnetic fields, the combined magnetic field is less than the single magnetic field generated by that of the primary winding by itself when the supplementary circuit is open circuited in Figure 19.3.

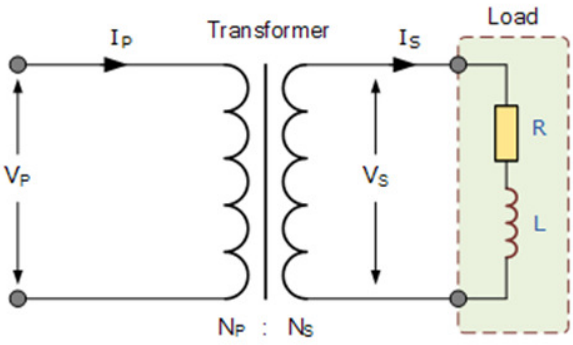

Figure 19.3: ***Illustrates*** **the circuit diagram of Transformer On-load Condition.**

The primary current, IP, marginally increases as a result of the combined magnetic field's reduction of the primary winding's inductances. A balanced situation between the main and secondary earth's magnetic field must constantly be present for a transformers to function properly. The primary current increases until the magnetic field of the core is returned to its original intensity. As a consequence, both the main and secondary sides of the power are equal and balanced. Users are aware that a transformer's turns ratios specifies that each winding's total electromotive force is proportional to the number of turns in the that winding that a transformer's energy input and output are equal to volts equals amperes (V x I). Therefore:

$$power_{prim} = power_{sec}$$

$$V_P * I_P = V_s * I_S$$

Then $\frac{V_P * I_P}{V_s} = I_S$

$$\frac{V_P * I_P}{V_s} = \frac{I_S}{I_P}$$

But as previously stated, "voltage ratio = turns ratio" means that a transformer's amperage ratio is equal to its turn ratio. So that they may be connected, the connection between a transformer's voltage, current, and the number of turns is provided as:

Transformer Ratio

Keep in mind that the relationship between the current and the voltage and the number of rotations is inverse. This indicates that when a transformer is loaded here on secondary winding, if somehow the voltage is increased, the current must decrease, and vice versa, in in order to keep a balanced power rating throughout the transformer's windings. Or, "lower voltage, greater current" or "higher voltage, lower current".

1. When the voltage ratio is represented by NP/NS = VP/VS.
2. The current ratio is represented as NP/NS = IS/IP.

Combining Transformer Impedances

One must multiply or reduce by the square root of the turn ratio to relate a resistance or characteristic impedance through one side of the transformer to the other (Turns Ratio2). In order to refer (or reflect) the impedances (resistivity and characteristic impedance) from the secondary towards the primary aspect of the transformer, one must multiply by both the turns ratio square, N2, and we need to divide by the turns ratio squared while referring electrical primary characteristic impedance towards the secondary winding. Therefore, primary to secondary reflection decreases R and X by an amount defined by N2, but secondary to primary sources raises R and X. The linked load impedance and characteristic impedance are also subject to this referring to or reflection of both the impedances in Figure 19.4.

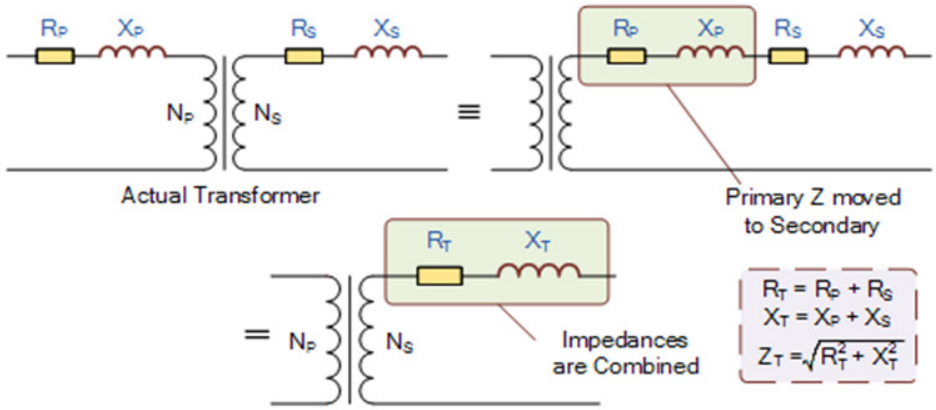

Figure 19.4: *Illustrates* the circuit diagram of Combining Transformer Impedances.

For instance, if a secondary resistant of 2 ohms is referred to the primary side with an 8:1 turns ratio, the second permanent resistive value will be 2 x 82 = 128 ohms, whereas a primary resistance of 2 ohms will produce a secondary resistance value of 0.03125 ohms.

Transformer Voltage Regulation

The variation in secondary voltage magnitude during full load, or when the main supply voltage is kept constant, whereas the transformer loading is reaching its maximum, is referred to as voltage regulation. Regulation controls the voltage decrease (or rise) that takes place within the transformers when the voltage output drops too low due to the overloading, which impacts the transformer's efficiency and performance. A voltage regulation's proportion (or per unit) of the no-load potential is used to represent it. The percentage regulating of a transformers is thus provided if E symbolizes the secondary voltage at no loading while V represents this same secondary voltage at full load:

$$\frac{no\ load - full\ load}{no\ load} = \frac{E - V}{E} \%100$$

Therefore, the regulation would've been 5% if, for instance, a transformer produces 100 volts when it is not loaded but only 95 volts when it is fully loaded. The internal impedance of a winding, which comprises its resistance, R, and more critically its AC reactance, X, the current, as well as the phase angle, will determine the value of E-V. Additionally, voltage regulation often rises as the load's maximum power gets more lagging (inductive). When it comes to transformer loading, voltage regulation can be either positively or negatively in value, using the no-load voltage as both a reference and changing down in regulatory

oversight as the loads are applied, or using the full-load voltage as a reference and changing up in regulation even as load is decreased or eliminated. In general, the core type transformer does not regulate as effectively as the shell type transformer whenever the transformer consumption is large. This happens because the frame interpolation of the armature winding in the shells type transformer results in improved flux distribution.

Multiple Winding Transformers

Various combinations of current and voltages are possible with multiple main or secondary windings in multiple winding transformers. Transformers with multiple main windings often have two or even more secondary windings. The main or secondary side of the transformer may contain more than one winding, which is one of its wonderful features. Transformers with many windings are often referred to as multiple wrapping transformers. A transformer with numerous windings operates on the same principles as a regular transformer. The calculations for primary and secondary voltages, current flow, and turns ratios are identical this time; however, we must pay close attention to the voltage magnetic poles of each winding because once connecting them together because the dot convention indicates the winding's favorable (or negative) polarization.

Transformers with multiple windings, sometimes referred to as multi-coils or numerous winding transformers, have much more than one secondary or primary coil on such a single laminated core, thus their name. The functioning is the same whether they are multi-winding, multi-phase single-phase transformers or three-phase transformers. In order to give a step-up, step-down, or a mix of the two between the different windings, multiple winding transformers may also be employed. In actuality, a multiple winding transformer is capable of having numerous secondary field winding within the same core, each of which may produce a different degree of voltage or current. The volt-ampere merchandise in each winding of a multiple winding transmitter is the same because transformers work on the mutual induction principle and each individual twisty can support the same number of volts per turn. Accordingly, NP/NS = VP/VS, if any turns ratio between both the individual armature winding becoming relative towards the primary supply. Single transformer is frequently employed in electronic circuits to give a range of lower voltages for various components. Power supply and triac switching conversions are two common applications for multiple winding transformers. Therefore, a transformer may contain a variety of secondary windings that are all electrically separated from one another and from the primary, just as they are from each other. The voltage produced by every one of the secondary coils will thus be proportionate to the number of coil spins, for instance.

Multiple Winding Transformer

An illustration of a typical "many winding transformer in Figure 19.5" is shown above. This transformer contains several separate secondary windings that provide different voltage levels. To run the transformer from greater supply voltages, these primary windings may be utilized alone or coupled together.

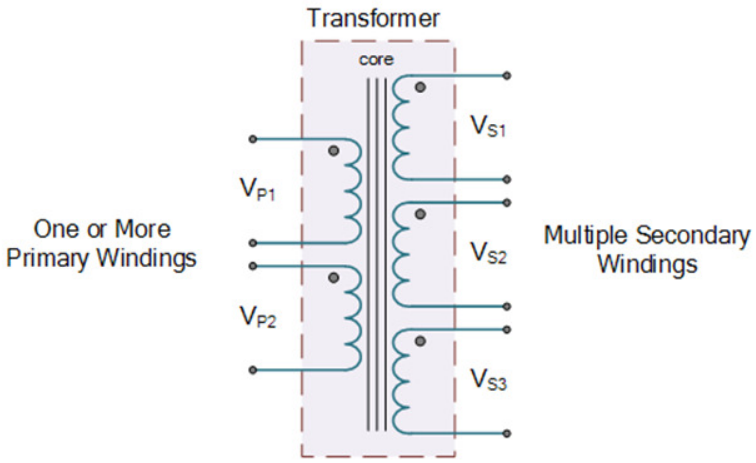

Figure 19.5: *Illustrates* the circuit diagram of Multiple Winding Transformer.

Different connections between the secondary windings might provide a greater voltage and current supply. It should be noted that electrical equivalence between the two power transformers is a requirement for connecting them in parallel. They have identical current and voltage ratings.

Dual Voltage Transformers

There are a variety of transformers with multiple windings that feature two main windings with similar ratings for voltage and current and two secondary field winding with the same specifications. With the windings coupled together either in a parallel or series arrangement configuration for larger primary voltage or secondary current flow, these transformer are made to be employed in a number of applications. Dual Converts the mechanical energy is a more popular name for these double winding transformers.

Dual Primary & Dual Secondary Transformer

The transformer comprises 4 windings in total—two primary and two secondary. With dual distribution transformer, as shown in Figure 19.6, the connections to the main or secondary windings must always be done appropriately. When a transformer is powered, a dead short that's been caused by faulty connection will often cause the transformer to fail. Dual voltage transformers, as we previously said, may be linked to run from power supply of several voltage levels, therefore their name. Let's take an example where the primary winding has a voltage rating of 12/24V on the secondary as well as 240/120V on the primary. This is accomplished by rating each of the two main windings at 120V so each secondary winding at 12V. It is necessary to connect the transformer to ensure that every primary winding gets the appropriate voltage.

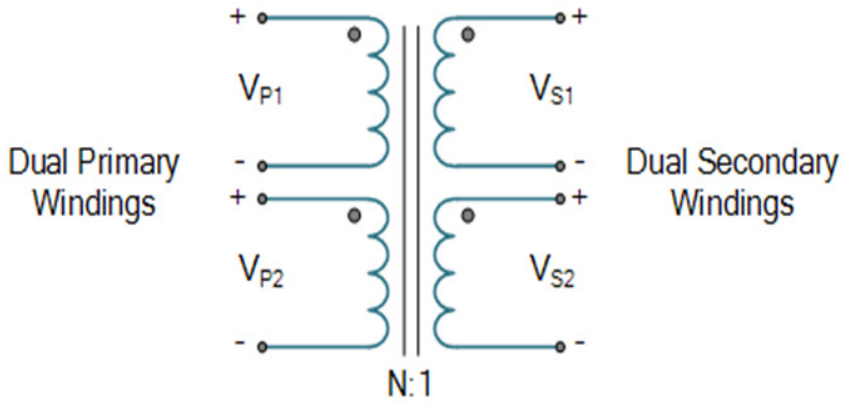

Figure 19.6: *Illustrates* the circuit diagram of Dual Secondary Transformer.

Series Connected Secondary Transformer

Due to the fact that the two primary windings, each rated at 120V, are similar, half of the 240V supply voltage, or 120V, is dropped throughout each winding, ensuring that the same primary current can flow through both when the two windings are connected in parallel across the 240V supply. The secondary voltage output in Figure 19.7 is equal to the total of the voltages of a two secondary windings, each of which has a rating of 12V and 2.5A.

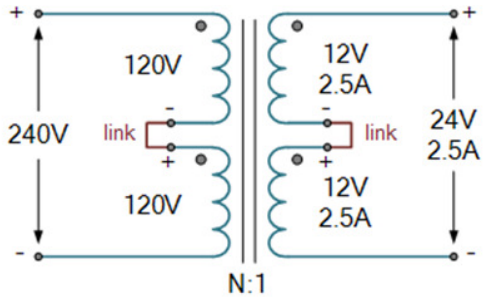

Figure 19.7: *Illustrates* the circuit diagram of Series Connected Secondary Transformer.

The secondary current is exactly the same at 2.5 Amps because the two windings are linked in series, causing the same amount of electricity to flow throughout every winding. Therefore, the output in our example above is regulated at 24 Volts, 2.5 Amps for just a secondary connected in series. Take the parallel-connected transformers, for example.

Parallel Connected Secondary Transformer

The two primary windings have remained unchanged in this instance, but really the two secondary windings have been combined in a parallel manner with regard to respective dot orientation. The secondary terminal voltage would remain the same at 12 Volts, but the current increases since the two secondary field winding, as previously, are each rated at 12V, 2.5A. In our previous example, the output is thus rated at 12 Volts, 5.0 Audio amplifiers for a secondary that is connected in parallel. Although the secondary and current voltages produced by various dual voltage transformers may vary, the basic idea remains the same. For coils to output the necessary voltage or current, their connections must be right.

On the windings, the terminals with the same phase shift are shown by dots. For instance, connecting two secondary field winding in opposite dot orientation will result in minimum waste or destruction to the transformers in Figure 19.8 because the two magnetic fluxes will cancel each other out.

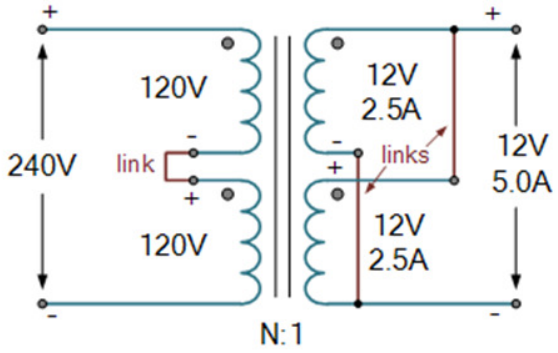

Figure 19.8: *Illustrates* the circuit diagram of Parallel Connected Secondary Transformer.

The Center-tap Transformer is a different kind of dual voltage transformer that has just one stator winding that is "tapped" at its electromagnetic center point. Two or even more transformers may well be linked in parallel with both the existing transformer to deliver a load greater than the rating of a existing converter. Whenever the load on any of the transformers exceeds its capacity, the other transformers are linked in parallel. Parallel operation is more reliable than using a single, bigger unit. Whenever two transformers are linked in parallel, the expense of maintaining the replacements is reduced. Instead of upgrading the present transformer with a single, bigger unit, it is often more cost-effective to install a second transformer in parallel. In the event of two simultaneous transformers with identical ratings, the cost of a replacement unit is likewise less expensive than the cost of a single transformer.

Center Tapped Multi Winding Transformers

A center-tap transformer is made to link two different secondary voltages, VA and VB, via a single point. This particular transformer set-up results in a two-phase, three-wire supply. The energy in each winding remains the same because the secondary voltages were same and proportionate to the supply voltage, VP. The turn's ratio, as indicated in Figure 19.9, determines the voltages generated across each secondary winding.

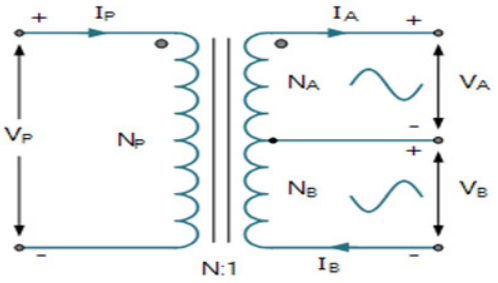

Figure 19.9: *Illustrates* the circuit diagram ofCenter Tapped Multi Winding

Transformers.

A typical center-tap transformer is seen above. The secondary winding's precise center, where the tapping point is located, provides a common connection between two secondary voltages that are equal but opposing. The output VA will be positively charged with regard to the ground when the center-tap is grounding, however the voltage at the additional secondary, VB, will be negatives and opposed in nature, meaning they are 180o electrically out of phase with one another. The usage of an unsubstantiated center tapped transformer does have one drawback, however, that is the possibility of unbalanced voltages in the two secondary windings as a result of asymmetrical currents flowing in the common middle connector due to unbalanced loads. Using the dual power electronics converters mentioned before, we can also create a center-tap transformer. One may utilize the middle link as the tap as indicated by stringing together the secondary windings. The secondary winding's overall output voltage will equal 2V if indeed the output from each supplementary is V, as illustrated.

Center-tap Transformer using Multiple Winding Transformers

Several Windings In electrical and electronic circuits, transformers are used in a variety of ways. They may be used to provide various secondary voltages to various loads. Having their secondary windings linked together in succession to create a center-tapped transformer in Figure 19.10, or have their field winding coupled together within series or parallel configurations to generate larger voltages or currents.

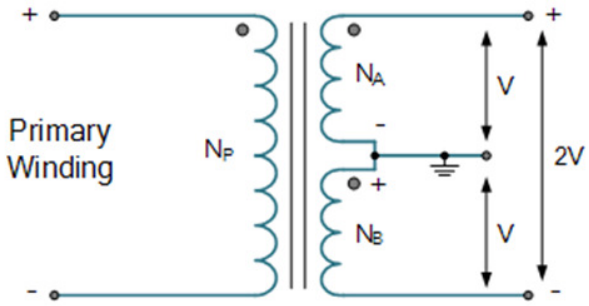

Figure 19.10: ***Illustrates*** **the circuit diagram of Center-tap Transformer using Multiple Winding Transformers.**

REFERENCES

[1] A. Eddiai, M. Meddad, M. Rguiti, A. Chérif, en C. Courtois, “Design and construction of a multifunction piezoelectric transformer”, *J. Aust. Ceram. Soc.*, 2019, doi: 10.1007/s41779-018-0206-3.

[2] Y. Wang, X. Zhang, H. Yu, X. Li, en Y. Xu, “Investigation on the compatibility of transformer construction materials with natural ester”, 2019. doi: 10.1109/ICDL.2019.8796536.

[3] S. A. M. Saleh *et al.*, “Solid-State Transformers for Distribution Systems-Part I: Technology and Construction”, *IEEE Trans. Ind. Appl.*, 2019, doi: 10.1109/TIA.2019.2923163.

[4] G. L. Ma, Q. Xie, en A. Whittaker, “Seismic performance assessment of an ultra-high–voltage power transformer”, *Earthq. Spectra*, 2019, doi: 10.1193/111217EQS234M.

[5] A. Acakpovi, "Transformer Wireless Monitoring System Using Arduino/XBEE", *Am. J. Electr. Power Energy Syst.*, 2019, doi: 10.11648/j.epes.20190801.11.

[6] S. E. Bankov, "Synthesis of Impedance Transformers for Super-Wideband Two-Section Antenna Arrays", *J. Commun. Technol. Electron.*, 2019, doi: 10.1134/S1064226919070027.

[7] Y. H. H. Tsai, S. Bai, M. Yamada, L. P. Morency, en R. Salakhutdinov, "Transformer dissection: An unified understanding for transformer's attention via the lens of kernel", 2019. doi: 10.18653/v1/d19-1443.

[8] M. Chirca, M. A. Drancă, D. C. Popa, S. Breban, en M. Iusep, "Design Analysis of a Toroidal Transformer for Traction Application", 2019. doi: 10.1109/MPS.2019.8759721.

CHAPTER 20

CONCEPT OF AUTOTRANSFORMER

Mr. Harsh Shrivastava, Assistant Professor,
Department of Electrical Engineering, Jaipur National University, Jaipur India
Email Id- ershrivastava@jnujaipur.ac.in

An autotransformer costs less than conventional transformers because its primary and secondary windings seem to be electrically and magnetically connected. In contrast to a previous voltage transformer, which had two electrically separate windings called the primary and secondary, an automatic transfer switch has only had one single voltage winding that is shared by both sides. At different places along its length, this single wrapping is "tapped" to deliver a portion of the main voltage supply throughout its secondary load. Additionally, the autotransformer has a single winding that is shared by both the main and secondary circuits, although it still has the standard magnetic core.As a result, the main and secondary windings of an autotransformer are connected magnetically and electronically. An autotransformer lacks the primary/secondary winding separation of a typical double wound transformer, which is its largest drawback. The main benefit of this kind of transformer architecture is that it can be produced much more cheaply for the same VA rating. The secondary is a portion of the section of the winding referred to as the main part of the winding, which is linked to the AC power source. By flipping the connections, an autotransformer can also be employed to scale the supply voltage up or down. The secondary voltage is "stepped-down" as illustrated if the primary is the whole winding, is linked to a source, as well as the secondary circuits is attached across just a piece of the winding. The secondary winding, IS, travels throughout the opposite direction while the main current, IP, is moving through into the single wrapping as shown by the arrow. As a result, the current flowing through the winding at the section of the winding that produces the secondary voltage, VS, seems to be the difference between IP and IS[1], [2].

Additionally, the Autotransformer may be built using several tapping points. Auto-transformers may be used to raise supply voltage relative to supply voltage VP or to give various voltage points along a winding, as illustrated. A single winding of an autotransformer has two end terminals one and or more endpoints at the intermediate tap points. It is a transformers with shared turns between the main and secondary coils. The common part of the winding is the area that both the main and secondary share. The series part of the winding is the area that is not shared by the main and secondary. Two of something like the terminals get the principal voltage. Two terminals are used to provide the voltage level, one of which is often shared with a main voltage terminal.

Since both windings have the same volts-per-turn, each produces a voltage proportional to the number of turns. It is possible to utilize a smaller, smaller, simpler core and only one winding in an autotransformer because some of the outgoing current travels directly from the source to destination (via the series section) and only some of it is transmitted inductively (through into the common section). However, autotransformers' the voltage and current proportion may be calculated using the same method as conventional two-winding transformer[3], [4].

Multiple Tapping Points of autotransformer

An auto-transformer winding is often marked by using capital (upper case) characters on the label. For instance, to designate the supply end, use A, B, Z, etc. Commonly, the common neutral connector is denoted by the letters N or n. All tapping locations along the main winding of the auto-transformer are designated with suffix numbers for the secondary tapings. As seen in Figure 20.1, these numbers typically begin at "1" and continue in order of increasing for any and all tapping locations.

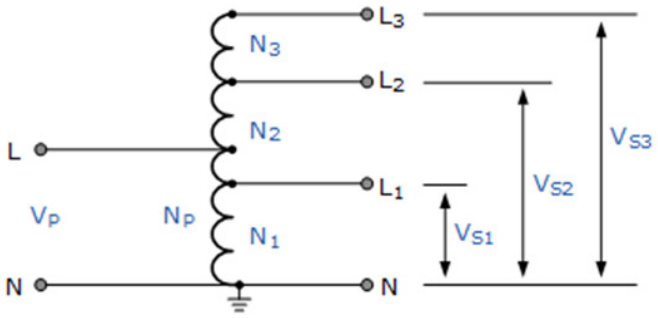

Figure 20.1: ***Illustrates*** **the circuit diagram of Multiple Tapping Points of autotransformer.**

Autotransformer Terminal Markings

An autotransformer is mostly used to modify line voltages in order to either change or maintain their value. The transformer proportion is modest if the voltage change is quite little, whether up or down, since VP and VS are virtually equal. IS and IP at this time are almost equal. Since the currents are significantly lower, the section of the winding that transports the difference between the currents may be produced from a substantially smaller conductor size, saving money compared to a double wrapped transformers of equal size. However, for a given VA or KVA ratings, an autotransformer's regulating, leakage inductance, and physical size because there is no second winding) are lower than for a twin wound transformers. In comparison to traditional double wound transformers with the same VA rating, autotransformers are obviously far less expensive. It is customary to weigh an autotransformer's price against a comparable double wound kind when selecting whether to use one. Comparing the quantity of silver saved in the unwinding allows for this. It is possible to demonstrate that the reduction in copper is equal to n*100% if the ratio "n" is defined as the proportion of the dropout wattage to the greater voltage[5], [6]. As an example, consider the copper savings for the four autotransformers in Figure 20.2.

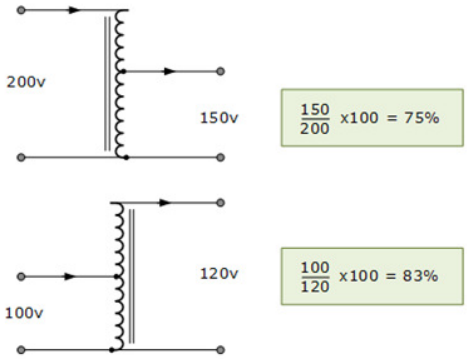

Figure 20.2: ***Illustrates*** **the saving in copper for the two autotransformers.**

Disadvantages of an Autotransformer

An autotransformer's principal drawback is that it lacks the primary to secondary coil isolation seen in a typical double wound transformer. In such case, stepping down larger energies to much lower voltage levels appropriate for lesser loads cannot be done safely using an autotransformer.

The primary winding's load current ceases flowing through it, terminating the transformer's activity, and the whole primary voltage is supplied to the output terminal if the equivalent circuit winding becomes open-circuited.Because of the increased current flowing harming the autotransformer, if the secondary circuit experiences a short-circuit situation, the ensuing main current would be much higher than a comparable double wound transformer.

Since there is no isolation between both the primary and secondary windings as well as the neutral connector is shared by both, earthling the secondary winding also continents the primary. Equipment isolation from the ground occasionally involves the use of double wound transformers.The autotransformer can be employed to transform energies whenever the primary to secondary proportion is near to unity, as well as for starting electromagnetic induction, controlling transmission line voltage, and beginning electromagnetic induction.The main and secondary windings of a typical two-winding transformer may also be connected in series to create an autotransformer; however, depending on the way the interconnection is made, the secondary current may either add to or remove from the primary voltage[7], [8].

Variac

Another important application of the auto transformer type of configuration is to create a variable AC voltage from either a fixed voltage AC source in addition to having a permanent or tapped secondary that delivers a voltage output at a set level. The Variac is the more popular name for this sort of variable autotransformer, which is often used in laboratory and science laboratories in schools and universities. A variable autotransformer, often known as a variac, is built similarly to a fixed type. The auto transformer has a solitary primary winding wound around a lamination magnetic core, but the secondary voltage dynamically tapped using a carbon brush as opposed to being set at a predefined tapping point.

The main winding is exposed, and this carbon brush is spun or allowed to glide along it, coming into contact with it as it travels and producing the necessary voltage level.The secondary voltage output of a variable autotransformer is entirely changeable from the main supply reference voltage to zero volts because it has a variable tap inside the form of a charcoal brush that glides upward and downward the primary winding to regulate the

secondary winding length. A substantial number of primary windings are often used in the construction of the variable autotransformer to provide a secondary voltage that may be varied from a few volts to a few hundredths of a volt per turn. This is made possible by the carbon brushes or slider's constant contact including one or more principal winding turns. Itself along the length, the main coil's turns are uniformly spaced. The output voltage then starts to follow the angular rotation[9], [10].

Variable Autotransformer

As people can see, the variac can smoothly change the voltage applied to the load from zero towards the recommended supply voltage. The output voltage gain may be more than the actual voltage supply if the power source was tapped anywhere along the main winding. Additionally, variable autotransformers may be used to lower lights, and when they are, devices are commonly referred to as "dimmer stats." Because they may be utilized to give a changeable AC supply, vacs are also particularly helpful in electronics and electrical workplaces and laboratories. However, care must be taken with appropriate fuse protection to make sure that, in the event of a breakdown, the greater supply voltages is not represented somewhere at secondary terminals in Figure 20.3.

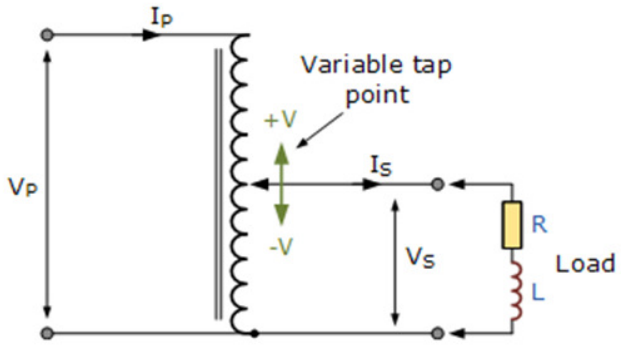

Figure 20.3: ***Illustrates*** **the circuit diagram of Variable Autotransformer.**

The Autotransformer is superior to traditional double wound transformers in very many ways. They are often smaller, better efficient for the identical VA rating, and less expensive than double wrapped transformers that have the same VA rating since they use less copper in their manufacture. Additionally, they have better voltage control than a comparable two winding transformers owing to their reduced resistance and permeability reactance, lower core plate copper inefficiencies, and lower I2R.

The Current Transformer

Due to a constant voltage on the main winding, current transformers provide an output proportional to the current that flows through it. A particular kind of "instrument transformer," the Current Transformer (C.T.), is made to create an alternating current through its secondary winding that is proportionate to the current being monitored in its primary. Current transformers therefore provide easy solution to securely monitor the real electrical current travelling in an AC transmission line. Using a normal ammeter while reducing high voltage currents to a considerably lower value. Figure 20.4 shows how the fundamental current transformer's operating principle differs somewhat from a conventional voltage transformers.

The main winding of a current transformer has one or a very small number of turns, unlike with the voltage or energy transformers we previously studied. One flat turn, a coil of sturdy wire wrapped all around core, or merely a conductor or dc power supply inserted through the center hole, as illustrated, may be used as the main winding. The main winding of the current transformer, which never has more beyond a few turns, seems to be in series with both the current carrying wire feeding a load, and as a result, the arrangement is what gives rise to the term "series transformer" for the device.

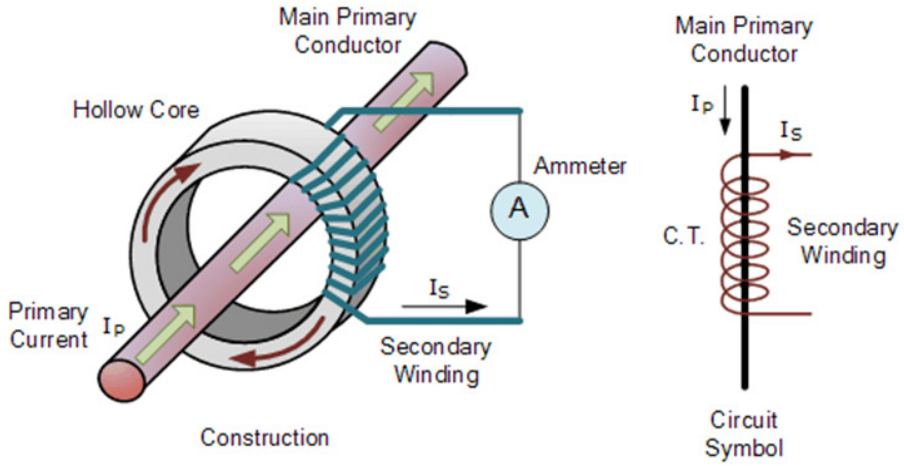

Figure 20.4: ***Illustrates*** **the circuit diagram of Current Transformer.**

However, a laminated cores of low-loss magnetic material may have a significant number of coil turns wrapped on it for the secondary winding. Depending on the amount that the current must always be stepped down as it attempts to generate a constant current, irrespective of the connected load, this core has a big cross-sectional area, which makes it such that the concentration of magnetic flux formed is low utilizing wire with much lower cross-sectional areas. Until the voltage produced in the supplementary is sufficient to saturate the core or result in failure from high voltage breakdown, this same secondary winding will feed current either through a short circuit, represented by an ammeter, or through a resistive load. In contrast to a voltage transformer, a current transformer's main current is not controlled by the secondary load present but rather by an external load. Typically, the secondary current has a rating of 1 Ampere or 5 Amperage for main currents with higher values. Current transformers come in three fundamental varieties: wound, toroidal, and bar.

Wound Current Transformer - The wire carrying the measured current flowing throughout the circuit is physically linked in series with the primary winding of the transformer. The transformer's turn ratio affects how large the secondary current.These Toroidal Current Transformers lack a main winding. Instead, the toroidal transformer's windows or hole is used to thread the line carrying the network's electricity through. Due to their "split core," certain current transformers may be opened, installed, and shut without interrupting the circuit to that they are connected.Current transformers with a bar-style primary winding—equivalent to one turn—use the cable or bus-bar of both the main circuit as that of the primary winding. They are typically fastened to the current carrying equipment and are completely insulated from either the system's high working voltage.

Current Transformer

For regular operation, current transformers may "step-down" or lower current levels between thousands of micro amp to an output device of a defined ratio either with 5 Amps or 1 Amp. Because CTs are shielded from just about any high-voltage power lines, they may thus be employed with tiny and precise instruments and control equipment. Current transformers may be used in a wide range of metering applications, including wattmeter's, power factor counters, watt-hour meters, protection devices, and trip circuits in ferromagnetic circuit breakers, or MCBs. Typically, current transformers and amperage are employed as a matched pair, with the current transformer's design providing a maximum secondary voltage that corresponds to an ammeter's full-scale displacement. The two currents throughout the main and secondary windings of the majority of current transformers have a roughly inverse turn ratio. For this reason, the CT is often calibrated for a certain kind of ammeter. The secondary capacity for most current transformers is typically 5 amps, and the main and secondary currents are stated as a ratio like 100/5.

Accordingly, when 100 amps are flowing in the main conductor, there will be 5 amps flowing throughout the secondary winding since the current flowing is 20 orders of magnitude larger than the secondary current. A current transformer with a ratio of, example, 500/5 will generate 5 amps throughout the secondary for a primary wire current of 500 amps, a 100-fold increase. The secondary current may be made considerably less than the main current being measured by increasing the number the secondary coil, Ns, since as Ns grows, is decreases proportionally. In other circumstances, the current in the main and secondary windings as well as the number of turns made are inversely proportional. The amp-turn equation applies to all transformers, including current transformers, as we learned in our course on double wrapped voltage transformers.

$$T.R. = n = \frac{N_P}{N_S} = \frac{I_S}{I_P}$$

from which it get:

secondary current, $I_S = I_P(\frac{N_P}{N_S})$

The turns ratio is determined by the current ratio, and since the primary typically has one or two bends while the secondary might have hundreds, the proportion between the two can be fairly high. Consider the main winding's 100A current rating as an example. The secondary winding is rated at the industry-standard 5A. Then, the main and secondary liquidity amount is 100A to 5A, or 20:1. In other words, the main current dominates the secondary current by a factor of 20. To be clear, a current transformer with a rating of 100/5 does not correspond to one with a rating of 20/1 or other subdivisions of 100/5. This is due to the fact that the ratio of 100/5 does not really represent the ratio of main to secondary currents, but rather the "input/output current rating." Also take notice of the inverse relationship between the number of revolutions as well as the current in the main and secondary windings. However, very considerable changes in the ratio of turns in a current transformer may be made by altering the primary turns via the CT's window, where first primary turn is equivalent with one pass and more around one pass through into the window alters the electrical ratio.

Handheld Current Transformers

Currently, a wide variety of specialized current transformer types are available. Clamp meters, as seen, are a common and portable variety that can be employed to measure circuit loading. Without interrupting or opening the circuit, clamp meters encircle a current-carrying wire and measure its current by calculating the magnetic field around it. The reading is often shown on a digital display. Split core current transformers are an alternative to portable clamp-style CTs; they include a detachable end that eliminates the need to disconnect the load conductor or bus bar in order to install them. These have square window diameters ranging from 1 inch to over 12 inch, and they can measure currents from 100 amps to 5000 amps (25-to-300mm).

In conclusion, a current transformer, also known as a CT, is an instrument transformer that transforms a primary current into a secondary winding using a magnetic medium. A significantly lower current is then produced by its secondary winding, which may be utilized to identify overcurrent, underneath, pulse duration, or average current circumstances. A current transformer is sometimes referred to as a series transformer because its primary coil is always wired in series with the main conductor. For convenience of measurement, the nominal secondary current is regulated at 1A or 5A. Construction may be one single election turn just like in Toroidal, Doughnut, or Bar types, or a several wrapped primary turns, generally for low current ratios. Transformers for current are designed to be utilized as proportional current equipment. Consequently, just as a voltage transformer should not be run into a short circuit, a current transformer's secondary coil should never be controlled into an open switch. If the digital multimeter is to be disconnected or when the CT is not in use, their connections must be short-circuited prior to actually charging up the system since opening the secondary circuit of an active current transformer would result in very operating voltage.

Three Phase Transformers

Three-phase Transformers, whether it's with Delta or Star linked windings, are the foundation of electrical power distribution. To create and transfer electric power over great distances for usage by businesses and industry, a three-phase electrical system is employed. Three phase transformers are used to increase or reduce three-phase voltages (including current flow) because the three phase transformer's windings may be linked in a variety of ways. We have examined the design and functioning of the single-phase, two-winding voltage transformer up to this point, which may be used to alter the secondary voltage's relationship to the primary voltage supply. However, voltage transformers may also be built to link to two, three, six, or even intricate combinations of up to 24 phases for certain DC rectification transformers, in addition to only one single phase. We can utilize three single-phase transformer on something like a three-phase supply if we fixably link their main windings to one another and respective secondary windings to one another. For the production, transmission, and distribution of electricity as well as for all industrial uses, three-phase supplies—also known as 3-phase or 3 supplies—are employed. While compared to single-phase power, three-phase supplies offer several electrical benefits. However, when thinking about three-phase transformers, we must deal with three opposing voltages and currents that vary by 120 degrees of phase-time.

REFERENCES

[1] A. Kumar, S. Kamal, M. Raghuram, D. Deepankar, S. K. Singh, en X. Xiong, "High Gain Quasi-Mutually Coupled Active Impedance Source Converter Utilizing Reduced Components Count", *IEEE Trans. Ind. Appl.*, 2019, doi: 10.1109/TIA.2019.2932696.

[2] C. Liu, Y. S. Ganebo, en D. Wang, "Optimal configuration method of capacitor isolation device against DC bias on improved niche GA algorithm", *J. Eng.*, 2019, doi: 10.1049/joe.2018.8883.

[3] M. Brenna, F. Foiadelli, H. J. Kaleybar, en S. S. Fazel, "Smart electric railway substation using local energy hub based multi-port railway power flow controller", 2019. doi: 10.1109/VPPC46532.2019.8952414.

[4] J. Bonet-Jara, J. Pons-Llinares, S. Bernal-Perez, en R. Sabater I Serra, "A VIRTUAL laboratory for an enhanced and safe understanding of the electric transformers operation", 2019. doi: 10.21125/inted.2019.2277.

[5] A. V. Mayorov, M. Y. L'vov, en Y. N. L'vov, "Methodology of Decision-Making when Assessing the Technical Condition of Power Transformers and Autotransformers of Power Networks Considering the Failure Risk Factor", *Power Technol. Eng.*, 2020, doi: 10.1007/s10749-020-01148-4.

[6] C. Li, D. Serrano, en J. A. Cobos, "Analysis of a 48V-12V Hybrid Switched Capacitor Converter with DC Winding Current Auto transformer", 2020. doi: 10.1109/COMPEL 49091. 2020. 9265816.

[7] W. Widianingsih, "Pengaruh opini audit tahun sebelumnya, ukuran perusahaan, dan kondisi keuangan terhadap opini going concern", *Ekon. dan Bisnis Islam*, 2020.

[8] N. Cahyani *et al.*, "Efektivitas pelayanan kesehatan pada Rumah Sakit Tk.III Dr. R. Soeharsono (TPT) Banjarmasin", *J. Chem. Inf. Model.*, 2020.

[9] M. Wang, X. Yang, T. Q. Zheng, en M. Ni, "DC Autotransformer-Based Traction Power Supply for Urban Transit Rail Potential and Stray Current Mitigation", *IEEE Trans. Transp. Electrif.*, 2020, doi: 10.1109/TTE.2020.2979020.

[10] B. Li, Z. Wang, S. Guo, en M. Li, "No Load Simulation and Downscaled Experiment of UHV Single-Phase Autotransformer under DC Bias", *IEEE Access*, 2020, doi: 10.1109/ACCESS.2020.2974247.